AD 273 806

RADC-TDR-61-303

School of Electrical Engineering
CORNELL UNIVERSITY
Ithaca, New York

RESEARCH REPORT EE 517

THEORETICAL AND EXPERIMENTAL INVESTIGATION OF LINEAR BEAM MICROWAVE TUBES

Final Report, Parts IV and V

1 April 1957 to 31 August 1961

Approved by

G. Conrad Dalman
Lester F. Eastman
Paul R. McIsaac

Published under Contract No. AF30(602)-1696
Rome Air Development Center, Griffiss Air Force Base, N. Y.

RADC-TDR-61-303

School of Electrical Engineering
CORNELL UNIVERSITY
Ithaca, New York

RESEARCH REPORT EE 517

THEORETICAL AND EXPERIMENTAL INVESTIGATION OF LINEAR-BEAM MICROWAVE TUBES

Final Report, Parts IV and V 1 April 1957 to 31 August 1961

Approved by

G. Conrad Dalman
Lester F. Eastman
Paul R. McIsaac

Published under Contract No. AF30(602)-1696
Rome Air Development Center, Griffiss Air Force Base, New York

CONTENTS OF FINAL REPORT

PART IV

BEAM ANALYZER

PART V

CATHODE STUDIES

FINAL REPORT

PART IV:

BEAM ANALYZER

A BEAM TESTER FOR STUDYING THE CHARACTERISTICS OF D-C AND VELOCITY-MODULATED ELECTRON BEAMS

A. S. Gilmour, Jr.

RADC-TN-61-188

School of Electrical Engineering
CORNELL UNIVERSITY
Ithaca, New York

RESEARCH REPORT EE 495

A BEAM TESTER FOR STUDYING THE CHARACTERISTICS OF D-C AND VELOCITY-MODULATED ELECTRON BEAMS

A. S. Gilmour, Jr.

LINEAR BEAM MICROWAVE TUBES

Technical Report No. 9 1 May 1961

Published under Contract No. AF30(602)-1696
Rome Air Development Center, Griffiss Air Force Base, New York

CONTENTS

ABSTRACT

This report describes, and gives the results of d-c measurements on a beam tester designed primarily for determining the characteristics of velocity-modulated electron beams. Some of the important features of the tester are: (1) a valve between the electron gun and the drift region, which makes it possible to keep the cathode at pressures below 1×10^{-7} mm Hg at all times, including periods when the drift tube is exposed to air and when changes are being made in the beam-scanning mechanism, etc.; (2) an aperture which may be positioned so as to make current measurements at any point in an electron beam; (3) a double vacuum system that permits aperture adjusting rods to be moved into and out of the drift-tube region without causing appreciable changes in pressure; and (4) an automatic scanning and recording device, which eliminates the necessity for taking point-by-point measurements in the beam.

The effect of the magnetic field of the filament of the gun, and of other stray magnetic fields, on the beam shape is shown by cross sections which were taken by the automatic recorder. Plots are given of the cyclotron wavelength, scallop wavelength, and beam diameter as functions of the magnetic focusing field and the beam voltage. The cyclotron wavelength is found to agree with the theoretical value to within 2 percent. The experimental scallop wavelengths are about 7 percent below the theoretical values. The reason for this discrepancy has not been determined, although the effects of the magnetic field in the gun

region and of the space-charge forces caused by positive ions and by reflected electrons have been investigated. The equilibrium beam diameter containing 93 percent of the beam is found to agree with the theoretical values to within 3 percent. The 95 percent diameter is greater than the theoretical value by about 6 percent and the 90 percent diameter is less by about 6 percent.

I. INTRODUCTION

This report describes, and gives the results of d-c measurements on a beam tester which was designed primarily for determining the characteristics of velocity-modulated electron beams focused by axial magnetic fields. Although many workers[1, 2, 3] have made measurements on velocity-modulated beams, no one has examined the state of the beam carefully before it was modulated. A knowledge of the state of the unperturbed beam to be velocity-modulated is important because most theories that describe the r-f behavior of a beam are based on an ideal beam; i. e., one that is laminar, free from scalloping or other variations in the axial direction, with a charge density that is constant in the radial and angular directions. Since one of the purposes of the linear-beam microwave-tube research program at Cornell University is to compare the predictions of existing theories to the actual beam behavior, it was necessary to produce a beam that approximated the ideal beam as closely as possible. In addition, it was desirable to produce a beam similar to those used in commercial linear beam tubes, so that the results obtained would have a direct bearing on the design and operation of commercial tubes.

The beam tester is described in Section II and many of the precautions taken to produce a reasonably good beam are pointed out. One of the important features is the valve between the electron gun and the drift tube, which made it possible to keep the cathode at pressures below 1×10^{-7} mm Hg at all times, including periods when the

drift tube region was opened to make changes inthe beam-measuring apparatus. This means, of course, that it will be possible to make r-f measurements on the same beam that is described in this report.

Section III gives a d-c beam theory similar to that of Wang[4] and Kleen[5] and the beam characteristics predicted by the theory are compared to those obtained experimentally. In general good agreement is found, and it is possible to produce a beam with practically no scalloping (less than 2 percent) and with a very small amount of detectable translaminar current.

II. DESCRIPTION OF EQUIPMENT

The beam tester to be described in this report is shown in Figure 2-1. The description of the tester is divided into four main parts: the vacuum systems, the electron gun and its associated apparatus, the magnetic focusing field, and the beam-scanning mechanism.

A. VACUUM SYSTEM

A schematic drawing of the vacuum system used on the beam tester is shown in Figure 2-2. This system was designed to meet the following major requirements: (1) low ultimate pressure, and (2) flexibility and cathode protection. A discussion of the reasons for these requirements and the manner in which they were satisfied follows:

1. Low Ultimate Pressure

During operation, the pressure in the parts of the system containing the cathode and the beam should be about 1×10^{-7} mm Hg. This pressure is desirable to prevent the poisoning of the cathode and the formation of a quantity of ions large enough to affect the shape of the electron beam. The desired pressure was produced by using a three-stage oil diffusion pump in conjunction with a zeolyte trap, which could be baked at 500° C while being evacuated. This combination consistently produced pressures lower than 2×10^{-7} mm Hg without bakeout when the tube was being operated.

Figure 2-1. Beam Tester.

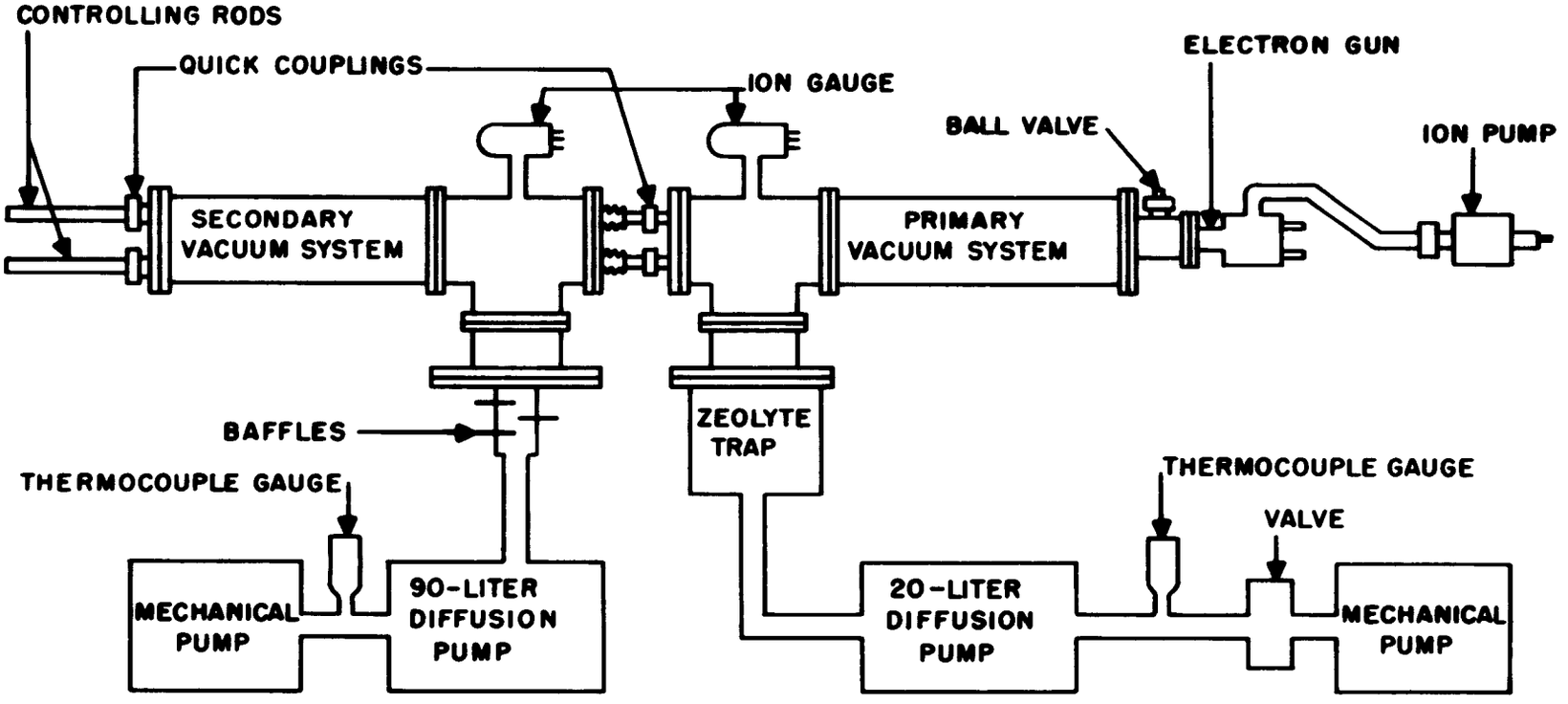

Figure 2-2. Beam Tester Vacuum System.

In order to move parts inside the vacuum system while the tube was being operated, polished stainless steel rods, which passed through Veeco quick couplings, were used. This arrangement is shown in Figure 2-3a. The rods could be moved through the couplings easily, and practically no leakage resulted when the rods were coated with a thin film of Dow-Corning high-vacuum grease. In an early test on the quick couplings, when rods were moved through them into the vacuum system, the pressure in the system increased from 1×10^{-7} mm Hg to nearly 1×10^{-5} mm Hg because of the gas being released from the rods, although little leakage resulted. This problem was eliminated by using the secondary vacuum system shown in Figure 2-2, which employed a high-speed diffusion pump and baffles, and maintained a pressure of about 1×10^{-6} mm Hg. The secondary system kept under vacuum those parts of the stainless steel rods that were to be moved into the primary system. The primary and secondary systems were separated by modified Veeco quick couplings similar to those shown in Figure 2-3b. As a result the pressure in the primary system rarely exceeded 5×10^{-7} mm Hg.

Figure 2-4 shows some of the components of the vacuum system. The demountable vacuum flanges were made from 3/8" thick Type 304 stainless-steel plate and were polished on the mating sides. Two types of gaskets were used. Where no insulation was required between parts of the vacuum system, lead "O" rings which have been found to make excellent seals, were clamped between the stainless steel flanges. Although over one-hundred rings were used on the beam tester, none was found to leak. There are two drawbacks to using lead: (1) that, in

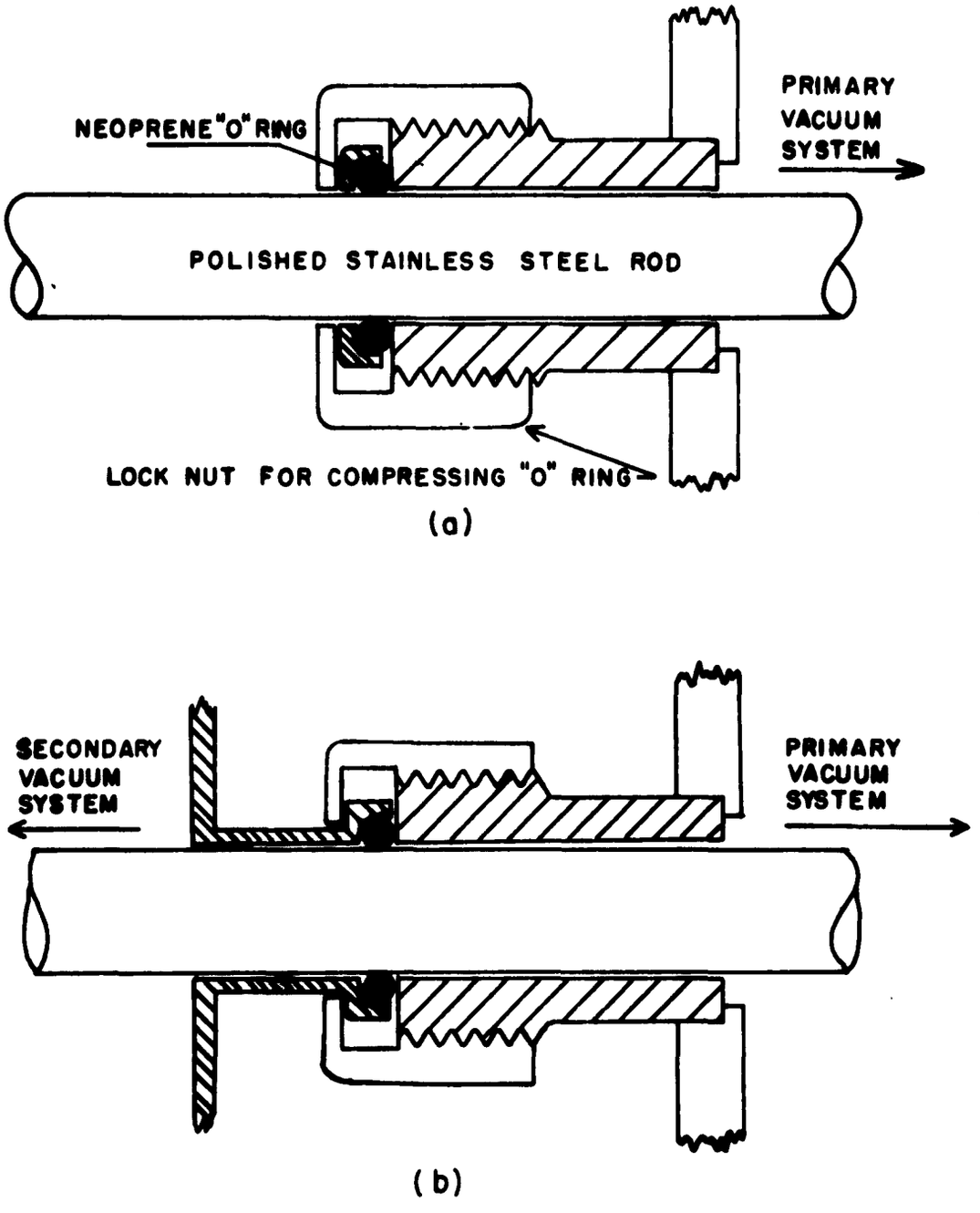

Figure 2-3. Veeco Quick Coupling: (a) Standard; (b) Modified Coupling Used between Vacuum Systems.

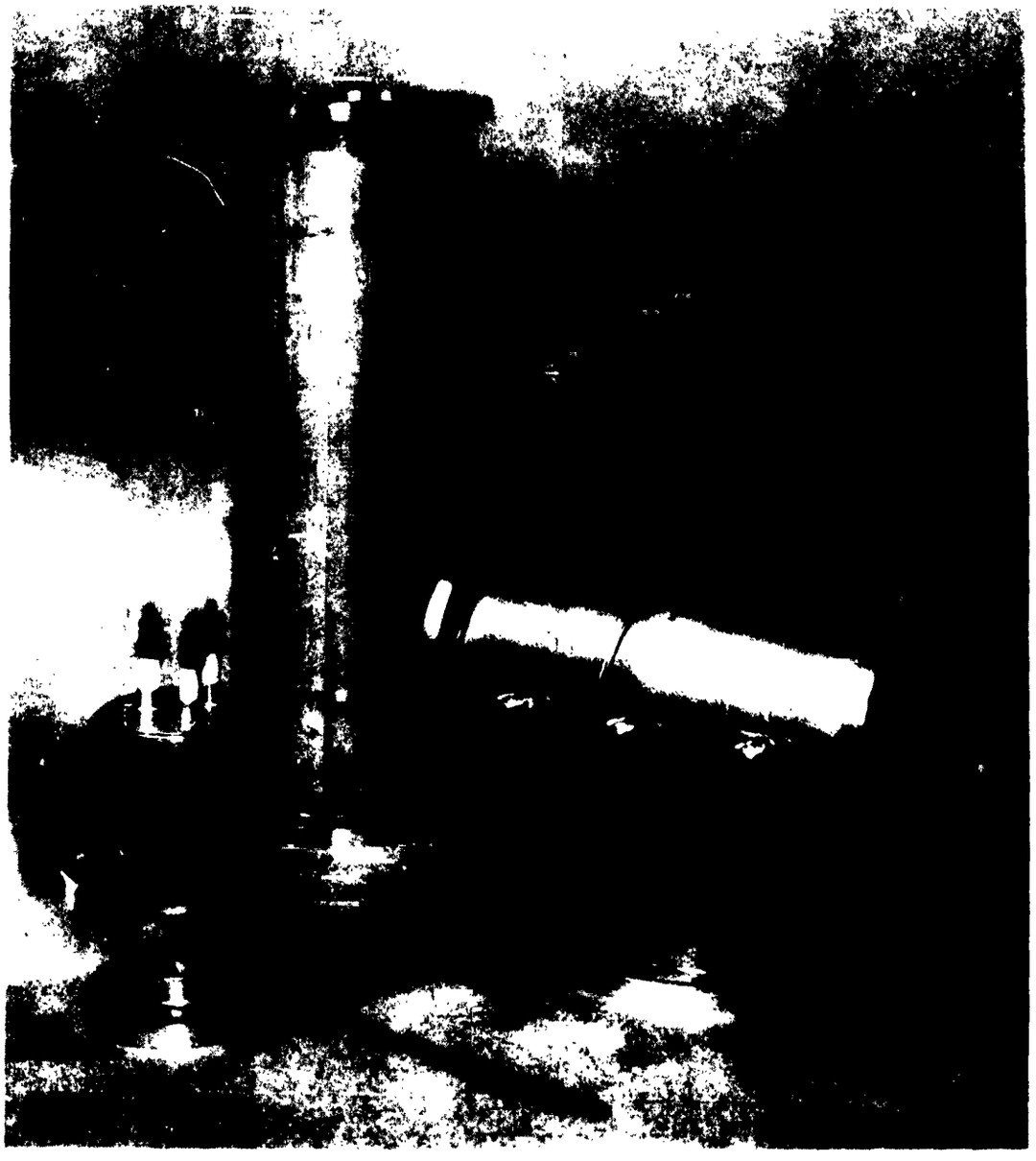

Figure 2-4. Electron Gun and Parts of Drift Tube for Beam Tester.

time it creeps, and therefore the flanges must be retightened periodically; and (2) that it melts at about 180° C, therefore high bakeout temperatures cannot be used on the beam tester. This second drawback was not serious since good ultimate pressures were easily obtained without bakeout.

When insulation was required between parts of the vacuum system, Teflon gaskets were used. In addition, of course, insulating washers were placed under the heads of the bolts that held the flanges together, and insulating sleeves were placed around the bolts. A demountable flange that provided electrical insulation is shown in Figure 2-5.

2. Flexibility and Cathode Protection

When the beam tester was being designed, it was decided that the vacuum system should be constructed so that the part of the system containing the beam-measuring apparatus could be exposed to air and changed as often as desired without damaging the cathode. This was necessary because many different measurements on the beam requiring a variety of devices inside the vacuum system were planned. In order for the measurements to have some relation to each other, they had to be carried out on the same electron beam.

Also, since an oil diffusion pump was to be used in the primary vacuum system, it was decided that the electron gun should be isolated from the primary system whenever the electron beam was not turned on to protect the cathode from oil contamination.

The best solution to these problems was to provide a high-vacuum valve between the electron gun and the part of the vacuum

system containing the beam-measuring apparatus. The only type of valve found suitable for this application was the ball valve shown in Figures 2-6 and 2-7. When in the open position, the valve permitted the electron beam to pass through the aperture in the ball. When the valve was closed, changes could be made in the measuring apparatus without affecting the cathode in any way. In addition, the cathode was protected from contamination by the oil of the diffusion pump in the primary vacuum system. The value of this precaution was brought to light after the valve had been in use for a few weeks. Each day, before taking data, a profile of the beam was taken under a standard set of conditions and this profile was compared to one taken when the cathode was initially put into operation. Normally, no variations in the profiles were noted from day to day, indicating either that the emission properties of the oxide-coated cathode were not changing, or that they had no effect on the over-all beam shape. On one occasion, however, the beam profile was found to be very different from the standard profile, even though the gun perveance had not changed. The change in the profile shape is shown in Figure 2-8. After a small amount of activation at a high filament voltage, the beam shape returned to normal. The source of the change in profile was thought to be the ball valve, which had accidentally been left open during the previous night. While the valve was open, the cathode had apparently been poisoned by oil from the diffusion pump.

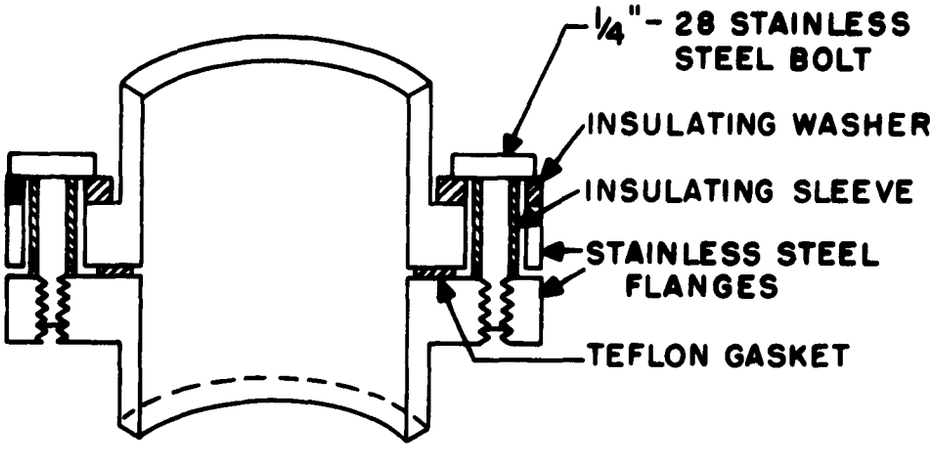

Figure 2-5. Demountable Vacuum Flange which Provides Electrical Insulation.

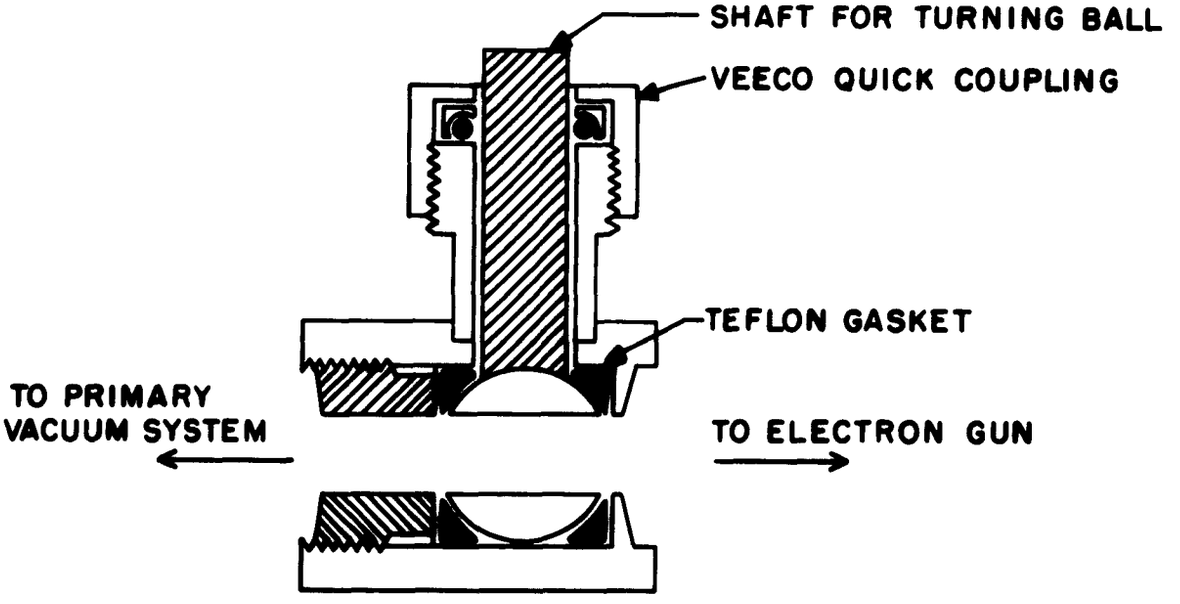

Figure 2-6. Ball Valve in Open Position.

Figure 2-7. Ball Valve and Electron Gun. (The tubing from the top of the gun goes to a vacuum pump.)

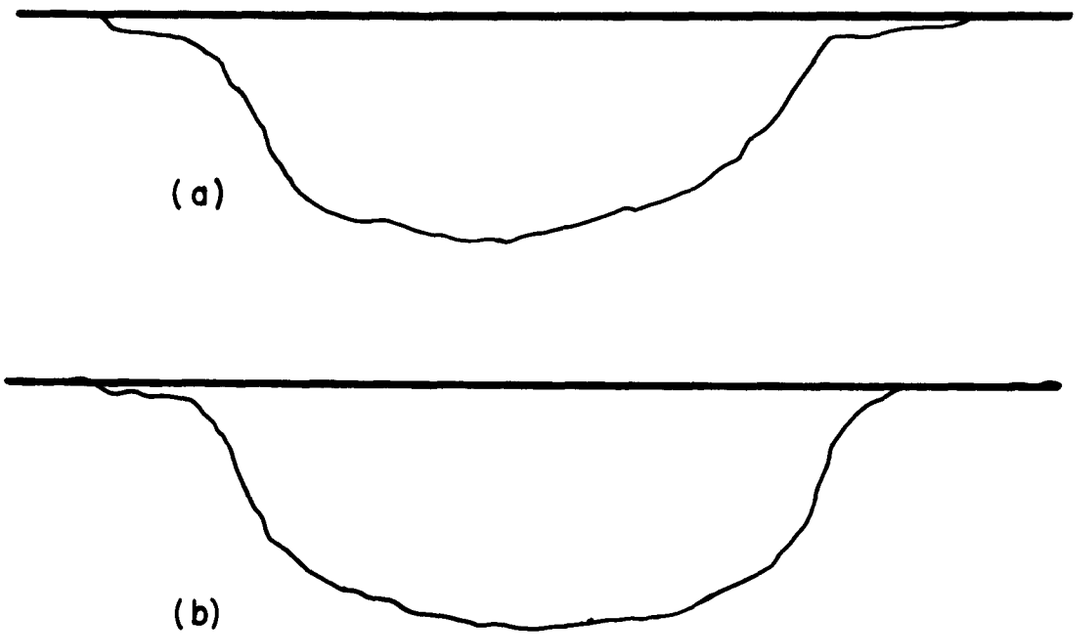

Figure 2-8. Electron Beam Profiles: (a) Cathode Poisoned by Oil from Diffusion Pump. (Ball valve accidentally left open over night.) (b) Cathode without Poisoning.

B. ELECTRON GUN AND ASSOCIATED ELECTRICAL APPARATUS

A Pierce electron gun with a perveance of 1.15×10^{-6} normally operating at 5400 volts is presently being used on the beam tester. This gun was obtained from a Sperry STL-100 traveling-wave tube.* After the gun was removed from the STL-100, it was cut open and the cathode was recoated. Flanges similar to those used on 5-liter Varian VacIon pumps were then brazed on so that the gun could be easily opened in the future. Another flange, which mated with the beam tester flanges, was brazed to the gun at the place where it was cut away from the drift-tube region.

* This was one of five donated to the School of Electrical Engineering by the Sperry Gyroscope Company

Although the electron gun from the STL-100 traveling-wave tube is capable of d-c operation at 5400 volts, it was necessary to pulse this gun on the beam tester. The duty cycle used was normally 0.001 or lower, so that less than 2.5 watts of beam power was required to be dissipated by the beam-scanning mechanism. A modulator capable of supplying up to 20 kv and 20 amperes at a duty cycle of 0.001 was obtained from the Manson Laboratories to provide the beam voltage to this gun or to other guns that might be placed on the beam tester.

The filament of the STL-100 gun is a flat noninductive wound spiral and operates at 12.6 volts from a 60-cps sinusoidal supply in the modulator. In early beam tests a great deal of 60-cps modulation from the filament magnetic field was found on the beam. Although a d-c supply would have eliminated the modulation, it would not have eliminated the disturbance of the beam by the magnetic field of the filament; therefore, the gun was pulsed at a rate of 60 cps, and the phase of the pulse was made variable so that it could be applied when the filament voltage was zero. Figures 2-9a, 2-9b, and 2-10 show the effect of the filament magnetic field on the beam. The beam cross section in Figure 2-9a was taken when the cathode was being pulsed at the instant of zero filament current, and the cross section in Figure 2-9b was taken with 7.65 amperes in the filament circuit. The horizontal and vertical axes indicate the horizontal and vertical positions in the beam, and the deflection at any point above a horizontal line is proportional to the amount of current at that point in the beam. Figure 2-10 shows the maximum beam diameters con-

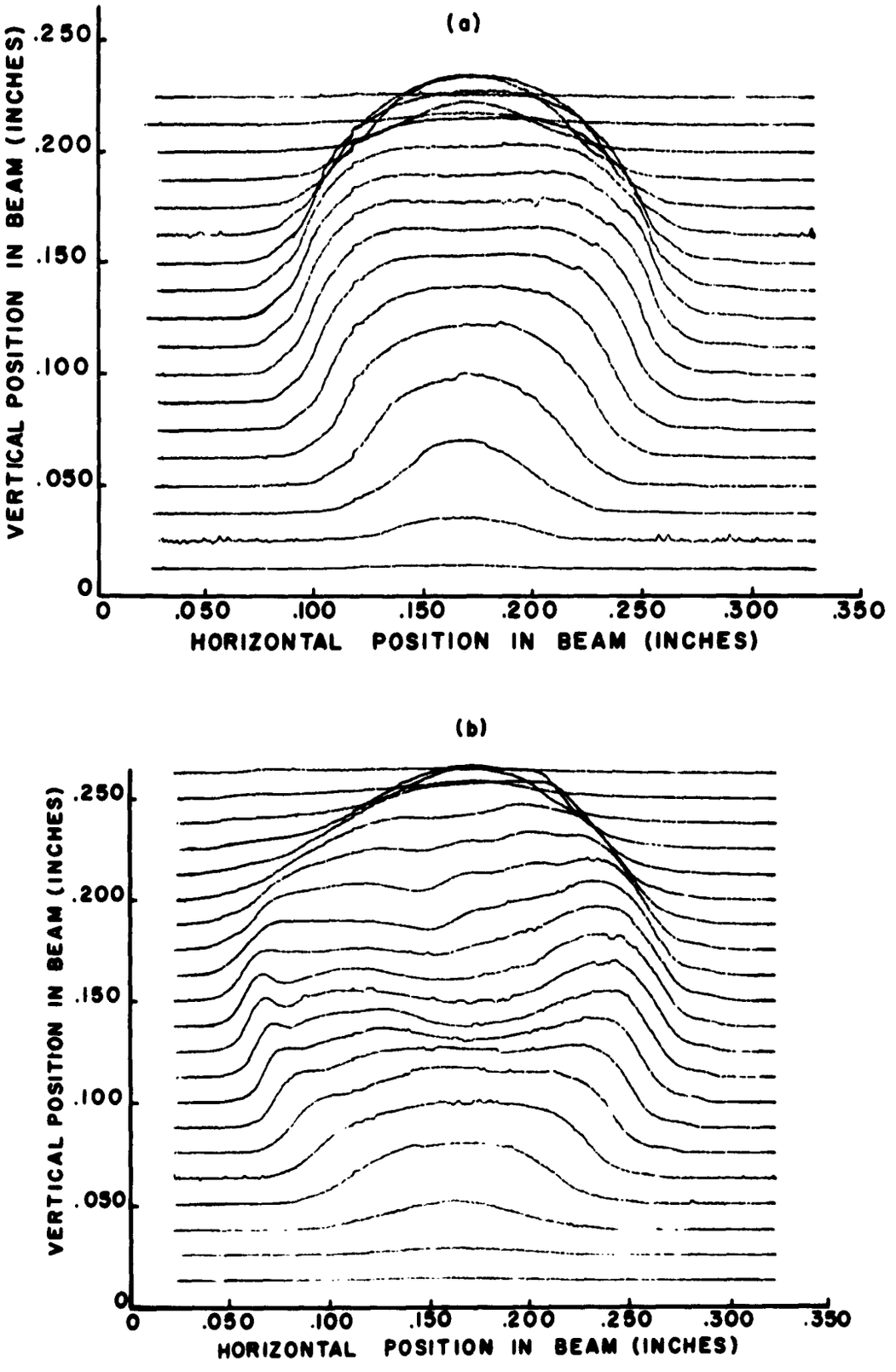

Figure 2-9. Electron Beam Cross Sections Taken under Brillouin Flow Conditions for (a) No Current through Filament (less than 2% scallop on beam), (b) 7.65 Amperes through Filament.

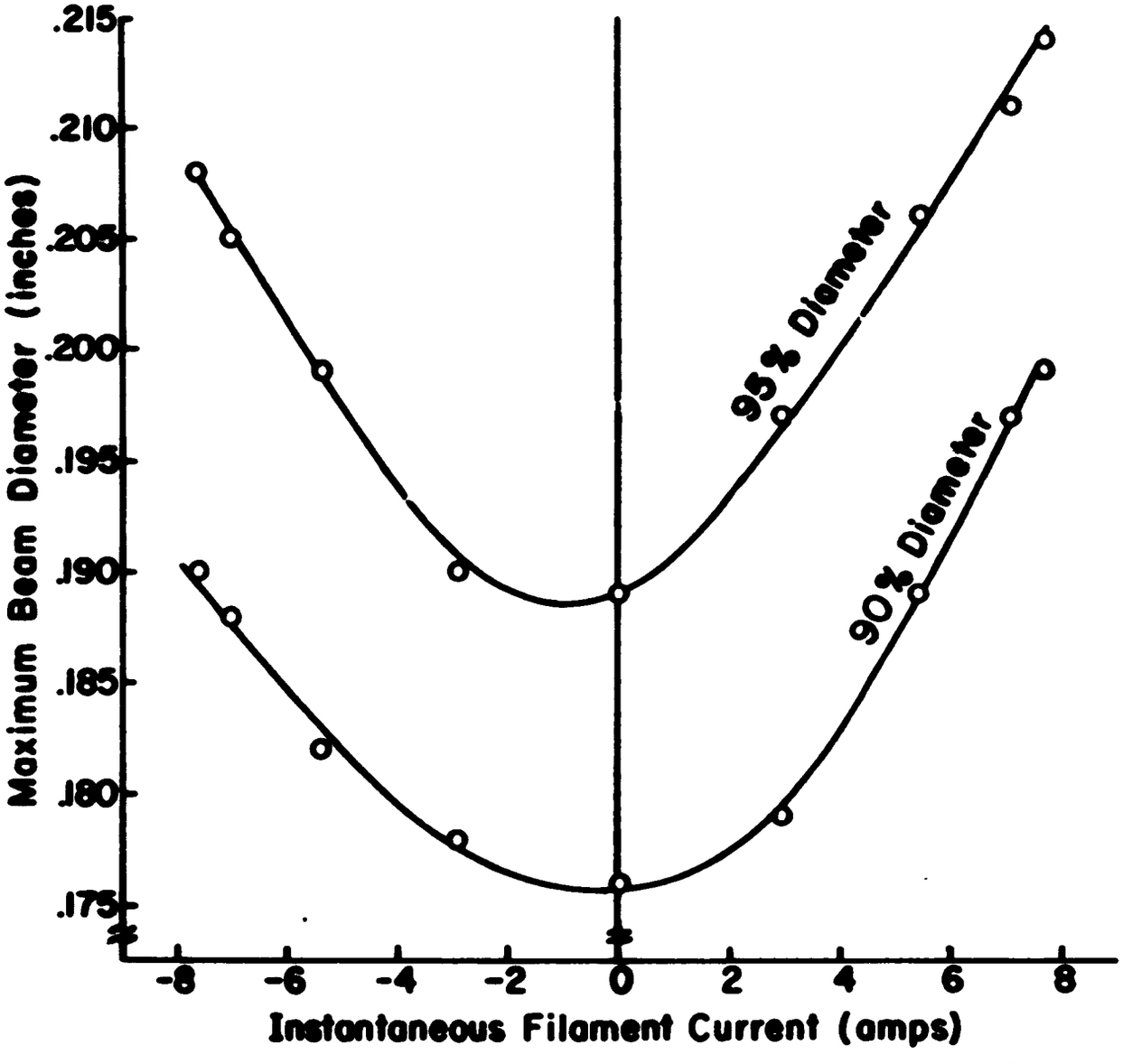

Figure 2-10. Maximum Beam Diameters Containing 90 Per Cent and 95 Per Cent Beam Current versus Instantaneous Filament Current.

taining 90 per cent and 95 per cent of the beam as a function of the instantaneous filament current. Note that the beam diameter obtained when the maximum filament current was present was over 13 per cent greater than that obtained when no filament current was present. In addition to this increase in diameter, a large amount of translaminar current was noted at all times when the cathode was pulsed while filament current was flowing.

C. MAGNETIC FOCUSING FIELD

In actual operation, the STL-100 traveling-wave tube uses a magnetic field of 420 gauss, which is about 40 per cent above the Brillouin field. The solenoid for the beam tester was constructed to provide from 0 to 1000 gauss so that a wide range of focusing conditions for the STL-100 beam could be produced and so that higher-perveance beams could be used if desired. As shown in Figure 2-11 the solenoid was built on a carriage with wheels, so that it could easily be placed in position on the tester. The magnetic field of the solenoid as a function of the axial position is shown in Figure 2-12. The STL-100 gun, the ball valve, and the drift tube are sketched above the magnetic field plot to show that the field is reasonably uniform in the region where measurements are made.

In early beam measurements it was found that stray magnetic fields, even though they were only a few per cent of the main solenoid field, had large effects on the beam. Figure 2-13 shows electron beam cross sections which were taken before and after the solenoid and the electron gun were magnetically shielded. After shielding, the magnetic

Figure 2-11. Beam Tester Solenoid with Magnetic Shielding Removed.

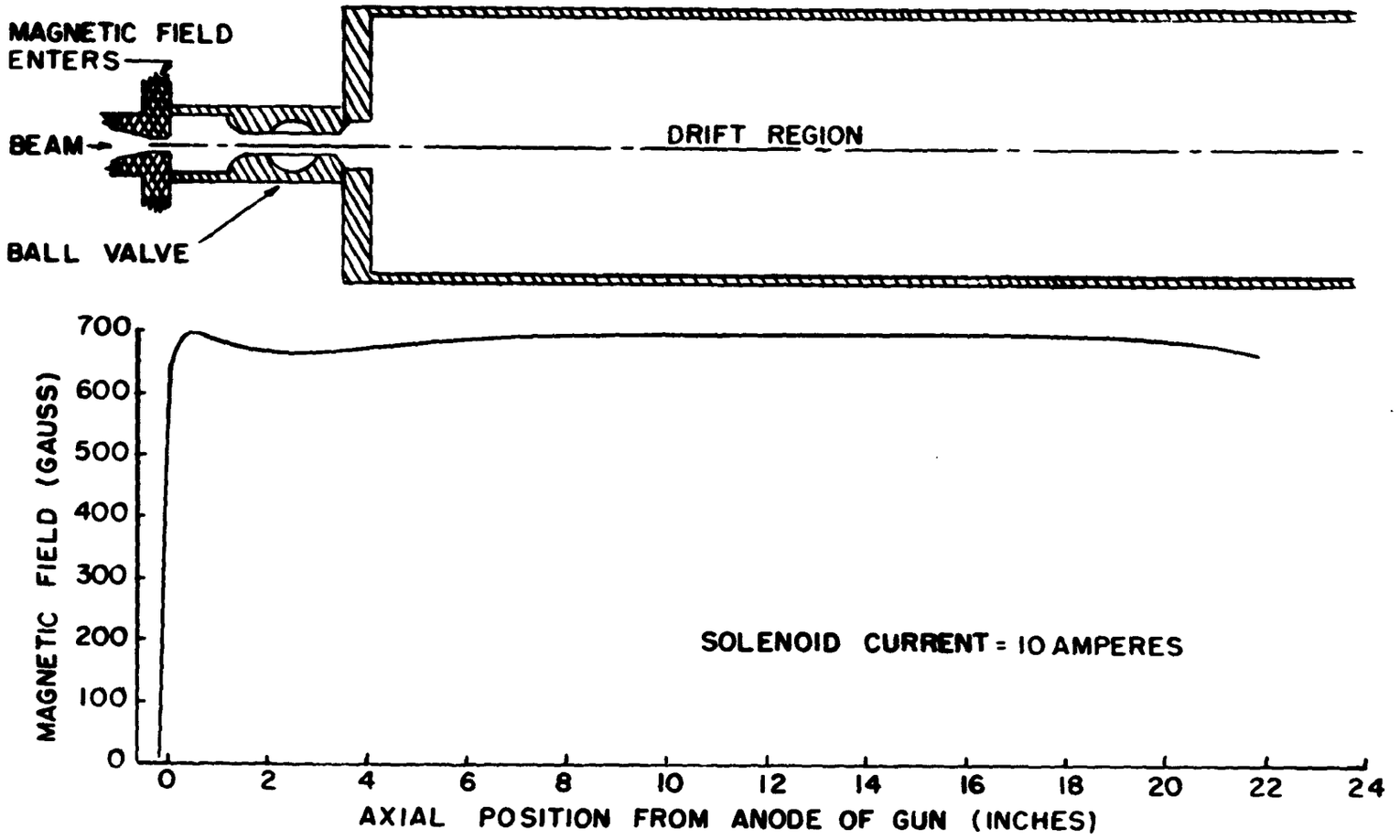

Figure 2-12. Magnetic Field on Axis of Beam Tester Solenoid for a Solenoid Current of 10 Amperes.

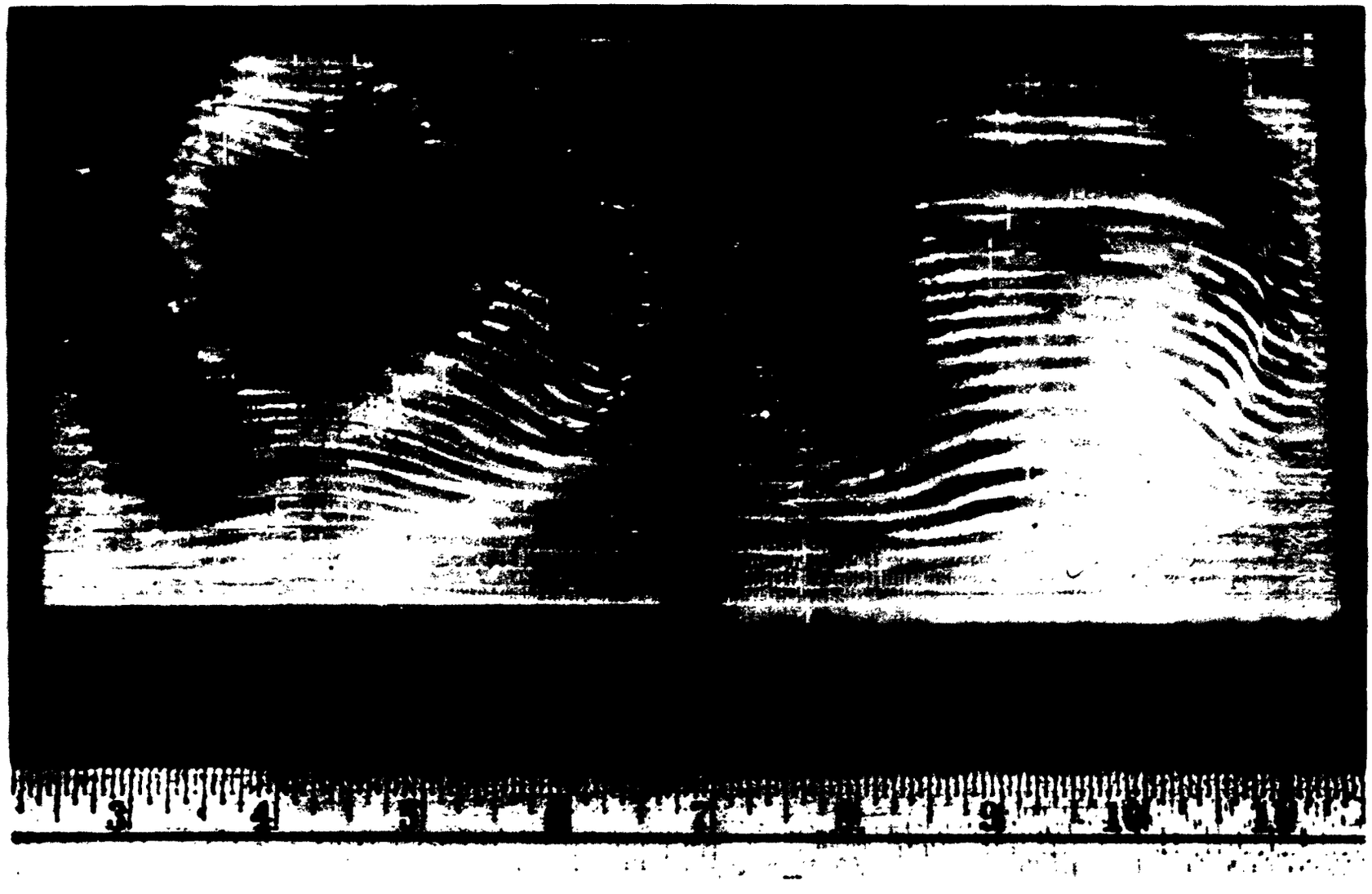

Figure 2-13. Electron Beam Cross Sections Taken Before and After Solenoid and Electron Gun were Magnetically Shielded.

field in the cathode region was found to be less than one-half per cent of the field in the drift tube and was reasonably uniform over the cathode surface. In addition to improving the beam cross section, the shielding caused the beam to travel more nearly along the axis of the drift tube.

D. BEAM SCANNING MECHANISM

1. Control of Faraday Cage Motion Inside Vacuum System

The part of the beam-scanning mechanism inside the beam tester is shown in a simplified sketch in Figure 2-14. Most of the electron beam was collected by the beam collecting plate, which was carbonized to reduce the secondary electron ratio. A small portion, however, was allowed to pass through the 0.010 in. aperture in the

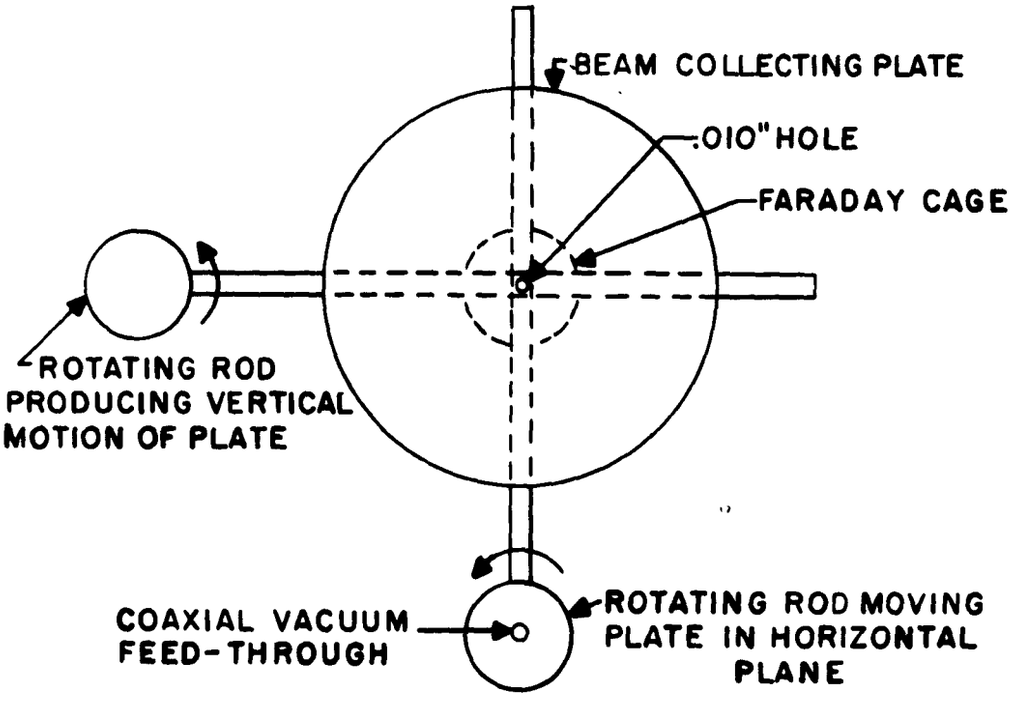

Figure 2-14. Simplified Sketch of Beam-Scanning Mechanism inside Beam Tester.

center of the plate to a Faraday cage. The electron current from the cage went out through a coaxial vacuum feed-through in the bottom control rod to an indicating device outside the tester. The collecting plate was positioned in the plane perpendicular to the axis of the solenoid by rotations of the two control rods. As is shown in the sketch, the plate could be moved horizontally by rotating the bottom rod. Vertical motion was produced in a similar manner by rotating the side rod. Teflon bearings, which were used to prevent binding between stainless steel parts, were attached to the back of the plate and slid on the lever arms attached to the side and bottom rods during horizontal and vertical motion. Although rotational motions were converted to translational motions in positioning the cage, they could be considered to be linear, since the distances moved were small compared to the length of the lever arms.

The collecting plate and positioning rods are illustrated in Figure 2-15. The disk shown behind the collecting plate and the lever arms was used to center the entire mechanism in the drift tube. As shown in Figure 2-16, this disk was guided by a Teflon bearing that rode on a rail in the drift tube and was prevented from touching the drift tube by two spring-loaded Teflon blocks. Axial motion of the cage assembly was produced by moving the control rods through the Veeco quick couplings.

2. Control-Rod Positioning Mechanism

The angular position of the control rods was adjusted by means of the micrometers shown in Figure 2-17. Each micrometer contacted a lever arm at a radius that was twice the radial position of the cage

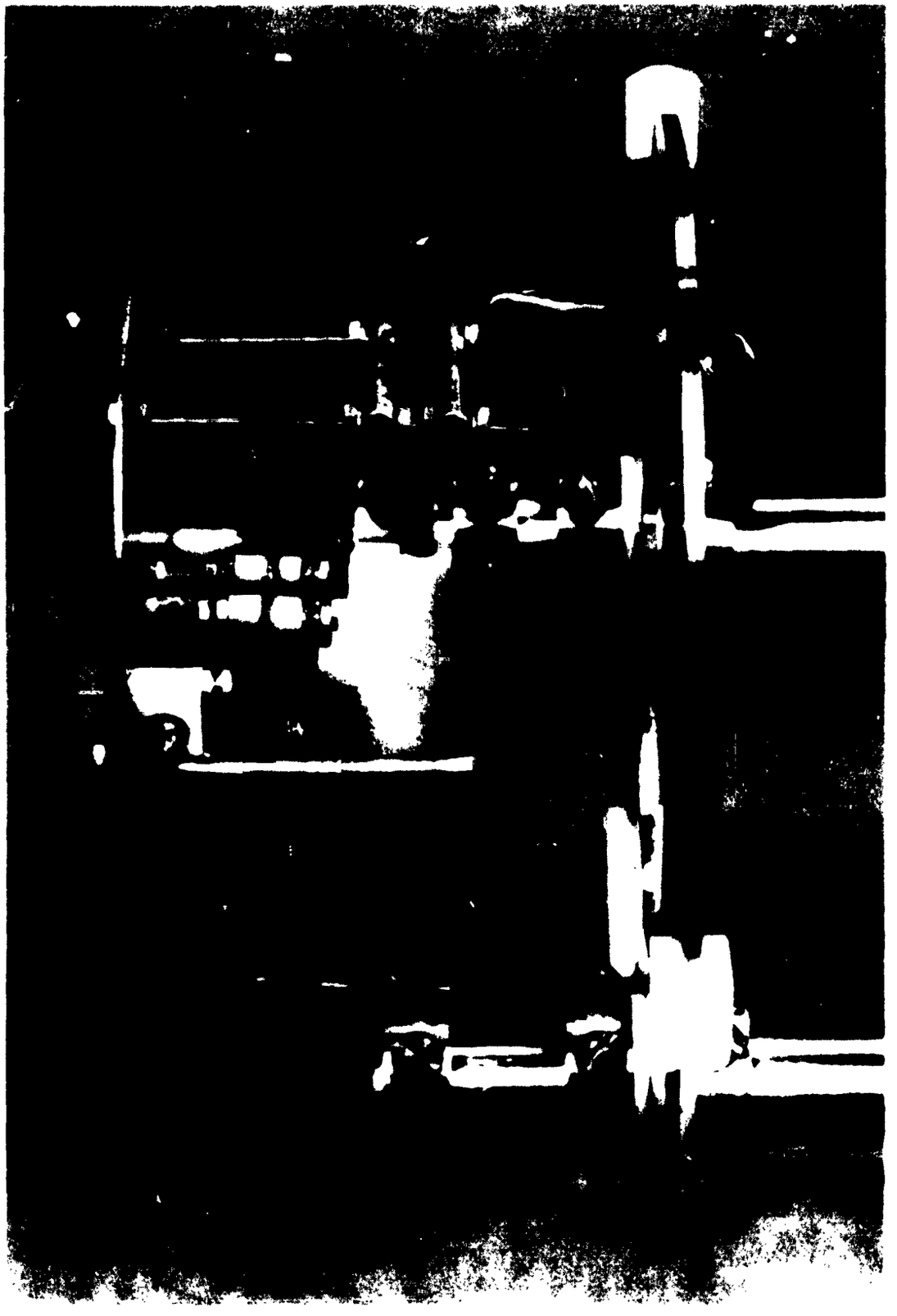

Figure 2-15. Collecting Plate and Positioning Rods.

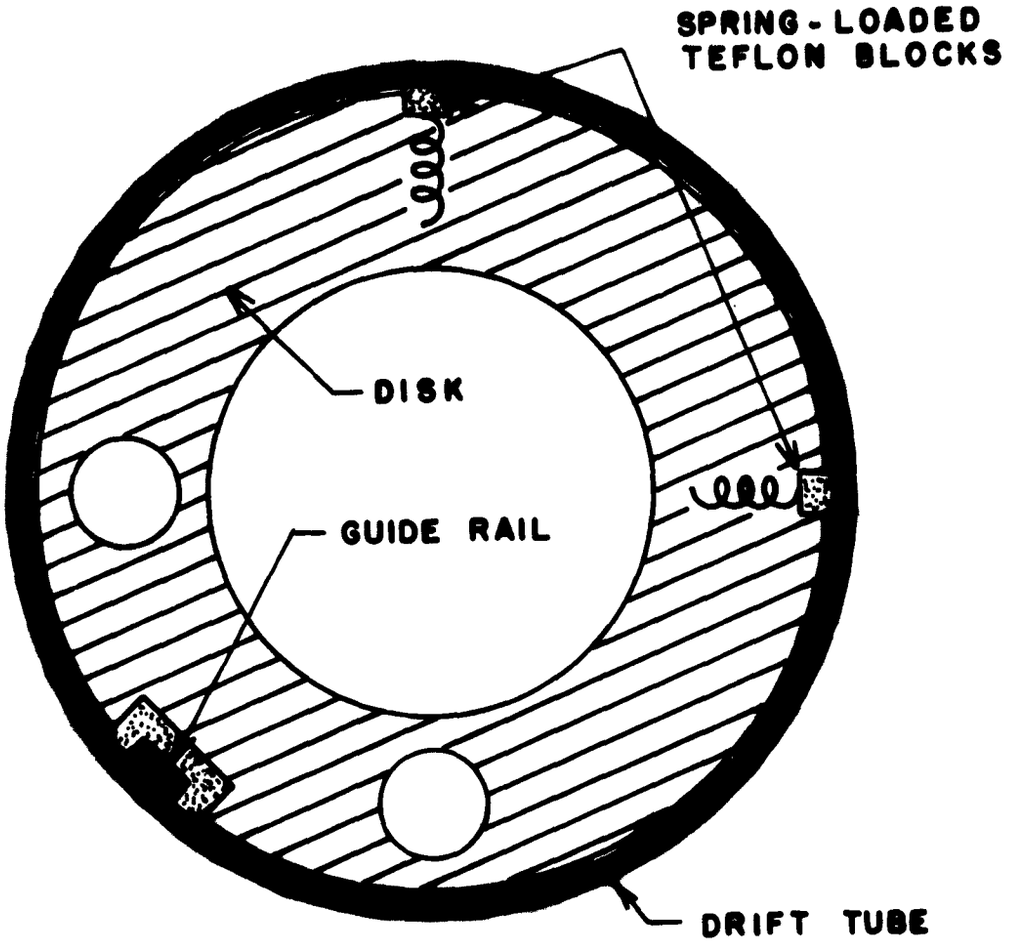

Figure 2-16. Disk Which Centers Faraday Cage Assembly.

inside the tester. Therefore incremental changes in the cage position were determined by taking one-half the incremental micrometer readings. The cage was positioned axially by using the gear and rack arrangement shown in Figure 2-12. In the first measurements taken on an electron beam, both micrometers were positioned manually. More than an hour was required to obtain a detailed cross-sectional plot of the current densities in the beam at one axial position. Since it

Figure 2-17. Control-Rod Positioning Mechanism.

was expected that hundreds of beam cross sections would be needed to determine accurately the scallop wavelength of the beam as a function of the solenoid field and as a function of the beam voltage, a motor drive was attached to the horizontal positioning micrometer. In addition, the automatic reversing switches shown in Figure 2-17 were installed to force the motor to sweep the Faraday cage back and forth automatically. A ten-turn helipot was geared to the motor to provide a voltage proportional to the horizontal position, and this voltage was applied to the x input of an x-y recorder. The current from the Faraday cage was fed to the y input of the recorder. The vertical position in the beam was indicated in the recorder by changing the y reference position. A typical beam cross-section taken in this manner is shown in Figure 2-9a.

III. CALCULATIONS AND EXPERIMENTAL RESULTS

A. CALCULATIONS

The electron beam of the d-c beam tester was magnetically focused by a solenoid, which was positioned so that the magnetic field lines were parallel to the axis of the drift tube. The Hamiltonian function is

$$H = \frac{1}{2} m (\dot{r}^2 + \dot{z}^2 + r^2 \dot{\theta}^2) - e\phi = 0 \quad , \tag{3.1}$$

where H is the sum of the kinetic energies in cylindrical co-ordinates and the potential energy. The equations of motion for the electron beam can be obtained by using the three Hamiltonian equations:

$$\frac{dP_r}{dt} = - \frac{\partial H}{\partial r} \quad , \tag{3.2}$$

$$\frac{dP_z}{dt} = - \frac{\partial H}{\partial z} \quad , \tag{3.3}$$

$$\frac{dP_\theta}{dt} = - \frac{\partial H}{\partial \theta} \quad , \tag{3.4}$$

where P_r, P_z and P_θ are the generalized momenta. The velocities are eliminated from H by using

$$P_r = m\dot{r} \quad , \tag{3.5}$$

$$P_z = m\dot{z} \quad , \tag{3.6}$$

$$P_\theta = mr^2 \dot{\theta} - erA_\theta \quad . \tag{3.7}$$

Equations (3.5) to (3.7) contain only one component of the magnetic vector potential, because as a result of the axial symmetry of the magnetic field, the field components may be written in terms of A_θ as

$$B_z = \frac{1}{r} \frac{\partial r A_\theta}{\partial r} \quad , \tag{3.8}$$

$$B_r = - \frac{\partial A_\theta}{\partial z} \quad . \tag{3.9}$$

With the substitution of Equations (3.5) to (3.7), Equation (3.1) becomes

$$H = \frac{1}{2m} \left[P_r^2 + P_z^2 + \left(\frac{P_\theta}{r} + eA_\theta \right)^2 \right] - e\phi = 0 \quad . \tag{3.10}$$

Now, by performing the operations indicated in Equations (3.2) to (3.4) and by combining the results with Equations (3.5) to (3.7), the following equations of motion for the electron beam are obtained:

$$\ddot{r} = r\dot{\theta}^2 - \eta r \dot{\theta} B_z + \eta \frac{\partial \phi}{\partial r} \quad , \tag{3.11}$$

$$\ddot{z} = \eta r \dot{\theta} B_r + \eta \frac{\partial \phi}{\partial z} \quad , \tag{3.12}$$

$$\frac{d}{dt} (r^2 \dot{\theta} - \eta r A_\theta) = 0 \quad , \tag{3.13}$$

where η is the electron-charge-to-mass ratio and where it has been assumed that the potential ϕ is axially symmetrical. Equation (3.13) may be integrated directly to yield

$$r^2\dot{\theta} = \eta\,(rA_\theta - r_cA_{\theta c}) \quad , \tag{3-14}$$

where $r_cA_{\theta c}$ is a measure of the flux at the cathode. It is necessary to keep this term, even in cases when the cathode is thought to be shielded, because a small amount of flux is always present in the cathode region (unless a bucking coil arrangement is used). It was mentioned in Section IIB that the cathode of the beam tester was pulsed at a rate of 60 cps and the pulses were phased so that the filament voltage was nearly zero during the pulse. The only magnetic field in the cathode region, therefore, was the stray field from the solenoid. Wang[4] writes Equation (3-14) in a more convenient form as

$$r^2\dot{\theta} = \eta \int_g^r rB_z dr \quad , \tag{3-15}$$

where r now applies to the outside edge of the beam, and g is a radius function, as shown in Figure 3-1, of a flux line which goes through the edge of the cathode. In the region of interest (where beam

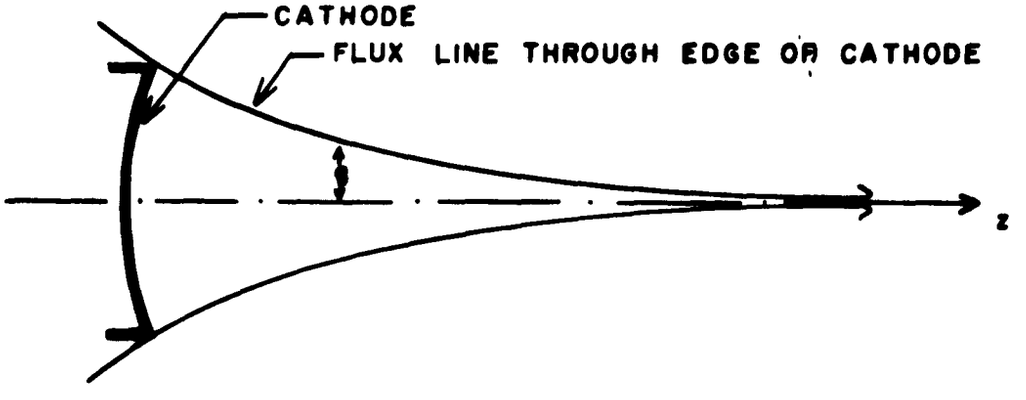

Figure 3-1. Diagram Illustrating Significance of the Radius Function g.

measurements are to be made), B_z is very nearly independent of r so that Equation (3-15) may be integrated to yield

$$\dot{\theta} = \omega_L \left(1 - \frac{g^2}{r^2}\right) \quad , \tag{3-16}$$

where $\omega_L = \frac{\eta}{2} B_z$ is the Larmor frequency. Now substituting the value of $\dot{\theta}$ from Equation (3-16) into Equation (3-11) gives the following equation for r:

$$\ddot{r} = -r\omega_L^2 \left(1 - \frac{g^4}{r^4}\right) + \eta \frac{\partial \phi}{\partial r} \quad . \tag{3-17}$$

In order to obtain any information from this equation, the term $\partial\phi/\partial r$, which is just the radial component of the electric field in the presence of the beam, must be determined. By assuming that the diameter of the beam is small compared to the scallop wavelength, and this is normally the case, the electric field E_r at the outer edge of the beam is

$$E_r = -\frac{I_o}{2\pi\epsilon_o u r} \quad , \tag{3-18}$$

where u is the axial velocity of the beam. Wang[4] has shown that u is independent of the beam radius and has the value,

$$-\sqrt{\frac{\eta}{2}(V_b + \phi_s)} \quad ,$$

where V_b is the anode potential through which the beam has been accelerated, and ϕ_s is the negative potential at the center of the beam caused by the space charge of the beam.

Now Equation (3-18) may be written as

$$\ddot{r} = -r\omega_L^2 \left(1 - \frac{g^4}{r^4}\right) + \frac{\eta I_o}{2\pi\epsilon_o u r} \quad . \tag{3-19}$$

By writing $R = r/a$ and $R_g = g/a$, where

$$a = \frac{1}{\omega_L}\sqrt{\frac{\eta I_o}{2\pi\epsilon_o u}} \quad , \tag{3-20}$$

Equation (3-19) may be simplified to

$$\ddot{R} + \omega_L^2 \left[R\left(1 - \frac{R_g^4}{R^4}\right) - \frac{1}{R}\right] = 0 \quad . \tag{3-21}$$

When the term in the square brackets is zero, the radial acceleration is zero. If the value of R that produces this condition is designated as R_e, then

$$R_e = \left[\frac{1}{2} + \frac{1}{2}\sqrt{1 + 4R_g^4}\right]^{1/2} \quad . \tag{3-22}$$

By writing R as $R_e + \delta$, where δ is the variational part of R and is considered to be small compared to R_e, we obtain the following linear differential equation for δ:

$$\ddot{\delta} + 2\omega_L^2 (1 + R_g^4)\,\delta = 0 \quad . \tag{3-23}$$

In obtaining this equation, it has also been assumed that $R_g^4 << 1$. The solution of Equation (3-23) is

$$\delta = A \sin\left[2\left(1 + R_g^4\right)\right]^{1/2} \omega_L t + B \cos\left[2\left(1 + R_g^4\right)\right]^{1/2} \omega_L t \quad . \tag{3.24}$$

The constants in Equation (3.24) may be evaluated at the axial position where the beam enters the magnetic focusing field. Figure 3-2 shows a typical beam and the manner in which it enters the focusing field. At $z = 0$, the magnitude of δ is $(r_1 - r_e)/a$ which is $R_1 - R_e$, and

$$\frac{dr}{dz} = \tan \gamma_1 = \frac{a}{u} \frac{d\delta}{dt} \quad ,$$

so $B = R_1 - R_e$ and

$$A = \frac{u_o \tan \gamma_1}{a\omega_L \left[2\left(1 + R_g^4\right)\right]^{1/2}} \quad . \tag{3.25}$$

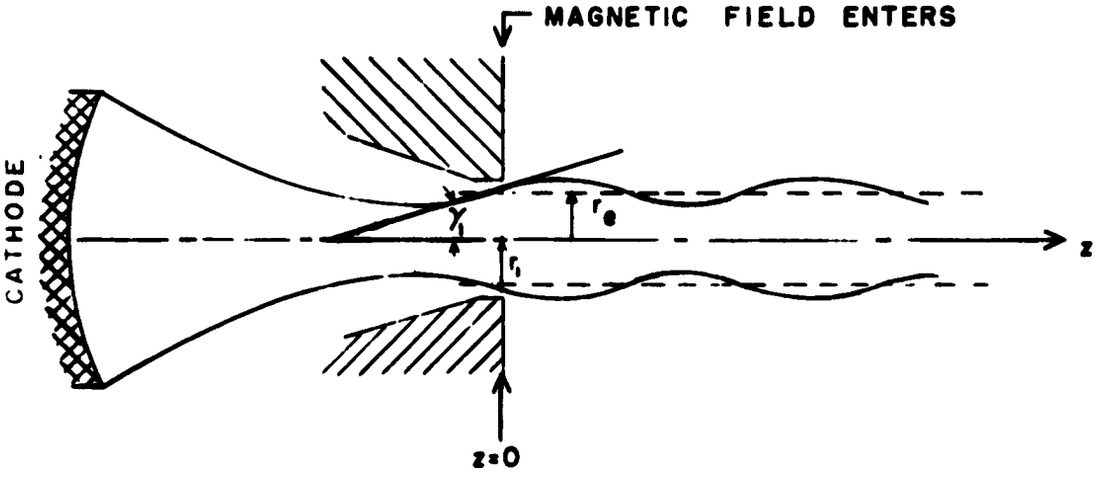

Figure 3-2. Typical Manner in which Electron Beam Enters Magnetic Focusing Field.

B. EXPERIMENTAL RESULTS

To determine how well the theory given in Section IIIA defines the behavior of a Brillouin beam of the type used in linear beam tubes, data similar to that shown in Figure 3-3 was taken on the STL-100 beam. The data was obtained by recording the current from the Faraday cage at various axial positions in the beam as the cage was moved horizontally through the beam at the beam's vertical center position. The curves in Figure 3-3b are the beam profiles for a beam voltage of 5 kv and a magnetic field level that produced very little scalloping. The curves in Figure 3-3a were also taken at 5 kv, but the magnetic field was 1.33 times the value required for no scalloping. The periodic variations in the widths of the profiles indicate the scalloping of the beam. The 5-kv beam radii containing 95 percent of the beam current as functions of the axial position in the drift tube and of the magnetic field are shown in Figure 3-4. Notice that at 285 gauss, the beam diameter varied less than 2 percent. According to the theory given in Section IIIA, the minimum diameter for a magnetic field less than 285 gauss and the maximum diameter for fields greater than 285 gauss should be the same as the 285-gauss diameter. Figure 3-4 shows that the minimum or maximum diameter decreased as the magnetic field increased. This occurred because the magnetic field increased from zero to the average value on the axis of the solenoid over a distance that was about one beam diameter. The result was that a convergent lens action occurred, which compressed the beam more and more as the magnetic field was increased.

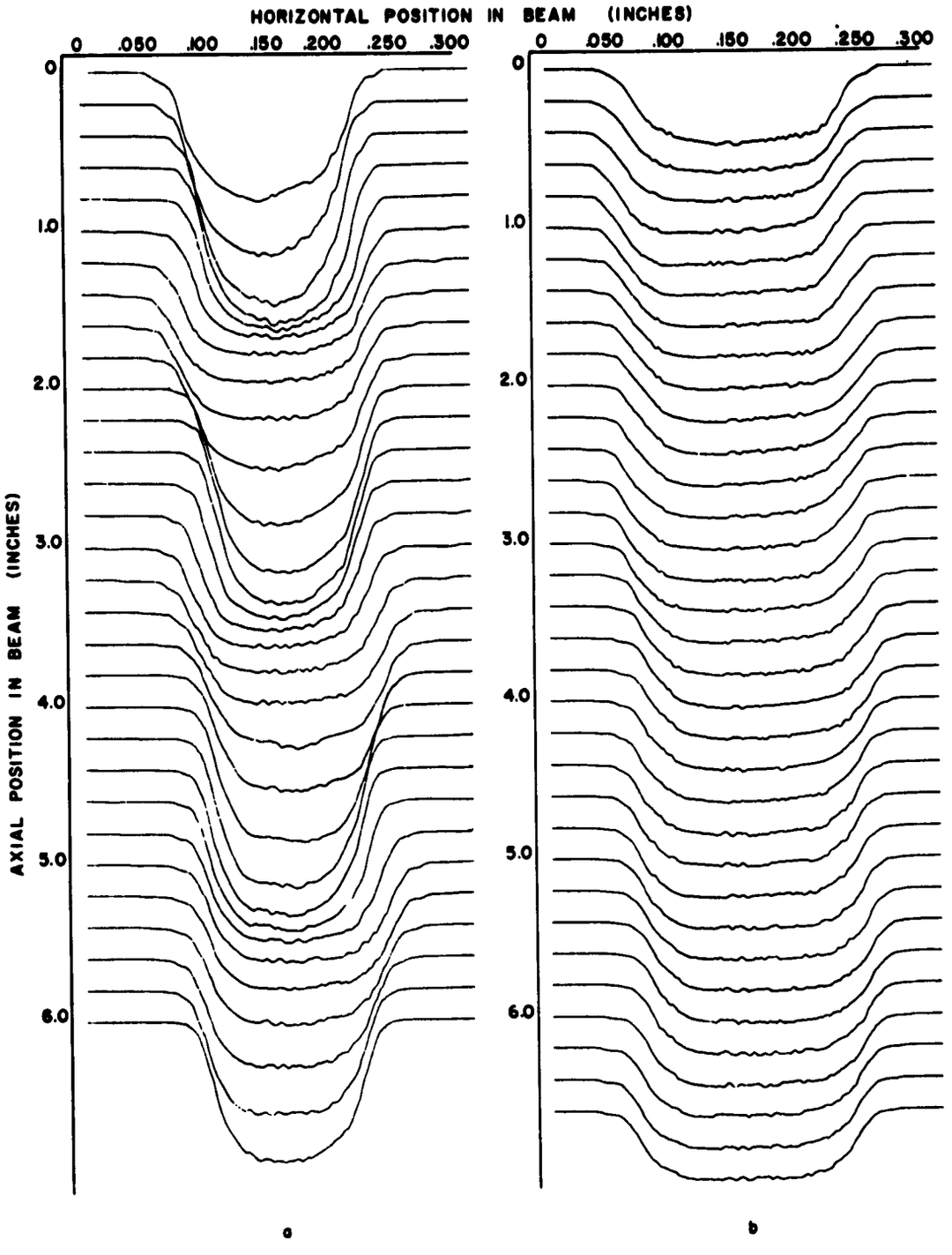

Figure 3-3. Sample Data from Which Beam Characteristics are Obtained.

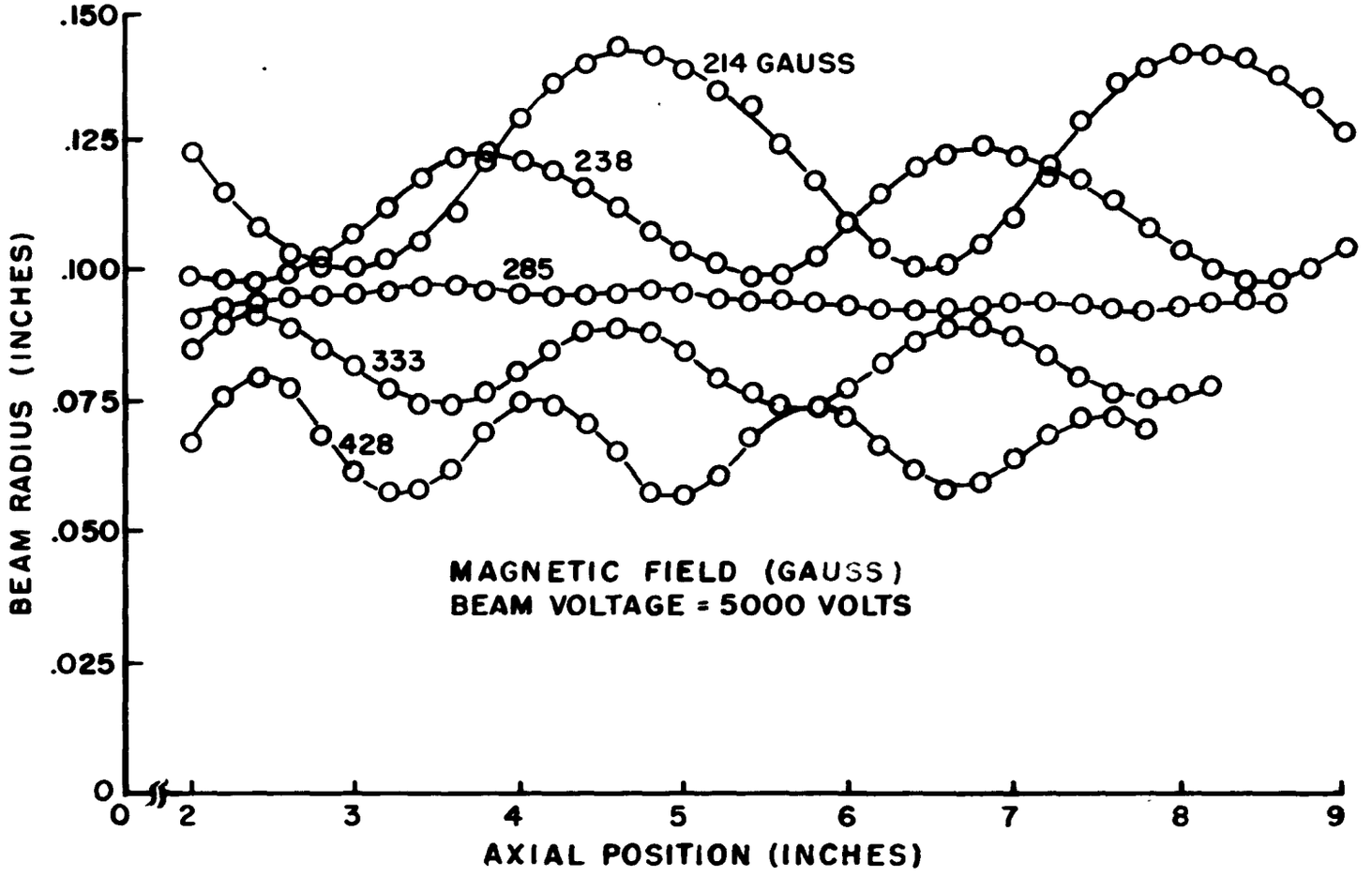

Figure 3-4. Beam Radius versus Axial Position.

In addition to the periodic variations of the widths of the profiles in Figure 3-3b there is a periodic motion of the center position of the profiles shown in Figures 3-3a and b. This motion is shown as a function of the magnetic field for a beam voltage of 5 kv in Figure 3-5. The beam-center motion could have resulted if the beam entered the magnetic field at a slight angle (as shown in Figure 3-6a) or off the axis (as shown in Figure 3-6b), or it could have resulted if the beam-collecting mechanism had a periodic motion inside the drift tube that was a function of its axial position. The second possibility was ruled out by the fact that the wavelength of the motion changed as the magnetic field was varied. Also, when complete cross sections of the beam as a function of the axial position were taken, the center position was found to move in the clockwise direction about the axis of the solenoid when the current flowed through the solenoid in one direction and in the counter-clockwise direction when the solenoid current was reversed.

In addition to showing that a periodic motion of the beam center occurred, Figure 3-5 indicates that the amplitude of the motion was a function of the magnitude of the focusing field, as is shown in Figure 3-7. Figure 3-8 shows the positions of the center of the beam with respect to the aperture in the anode for the various magnetic fields as determined by extrapolating the curves in Figure 3-5 back to the position of the anode of the electron gun. A possible explanation for the phenomenon shown in Figure 3-8 is that the beam enters the anode aperture slightly off center as shown in Figure 3-6b. Therefore, the magnetic lens at the anode forces the beam towards the center of the aperture. The position of the beam center therefore depends on the magnitude of

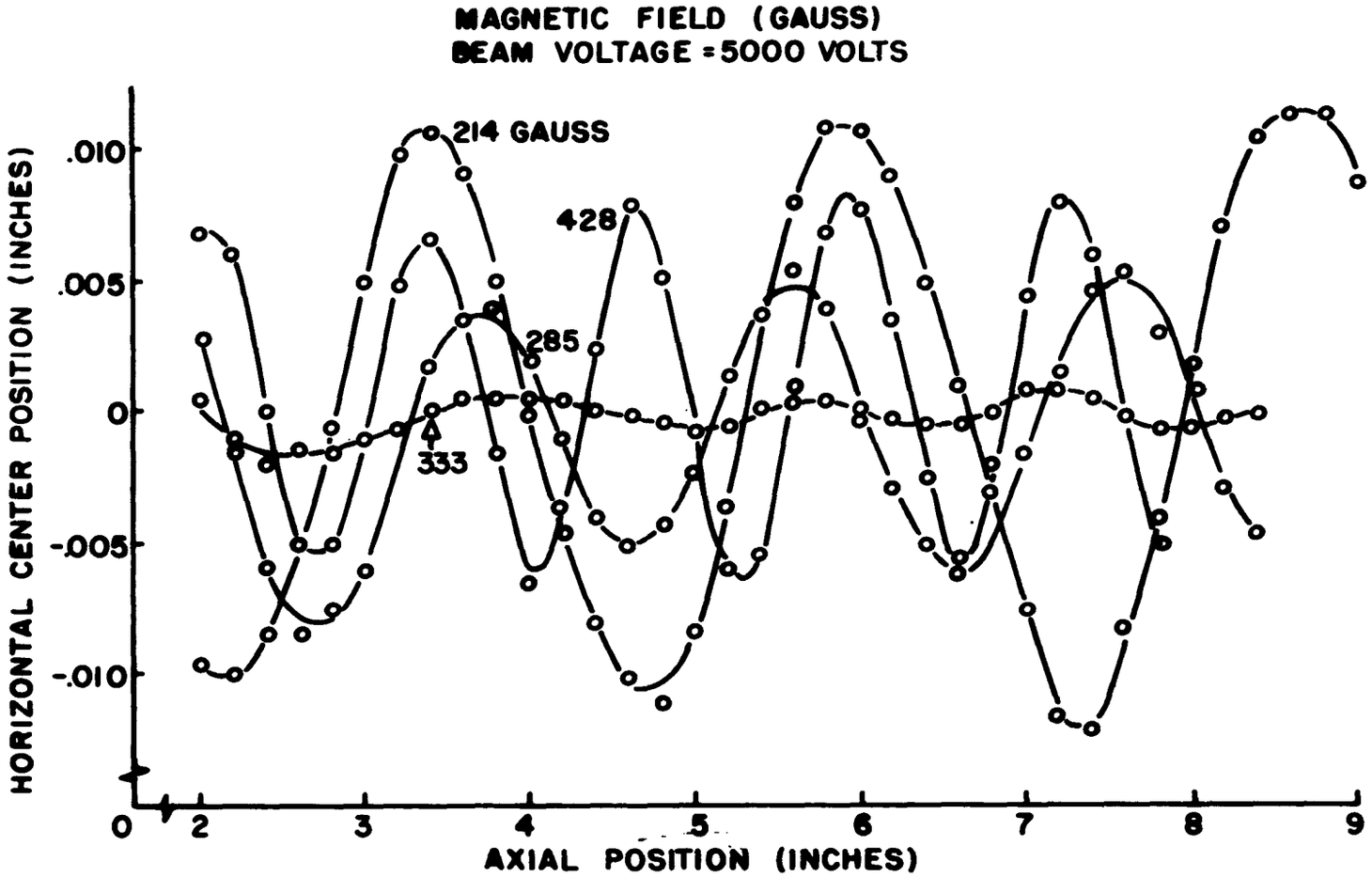

Figure 3-5. Horizontal Center Position versus Axial Position.

Figure 3-6. Electron Beam Entering Magnetic Field: a) At Slight Angle to Axis of Gun, and b) Displaced Parallel to Axis of Gun.

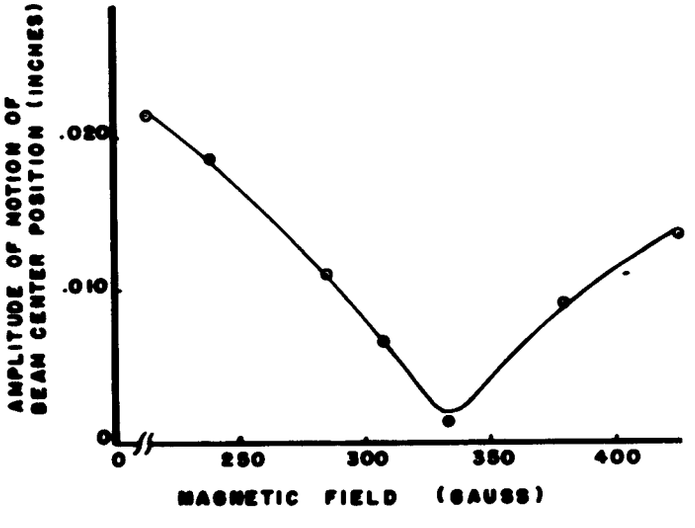

Figure 3-7. Amplitude of Motion of Beam-Center Position versus Magnetic Focusing Field for Beam Voltage of Sky.

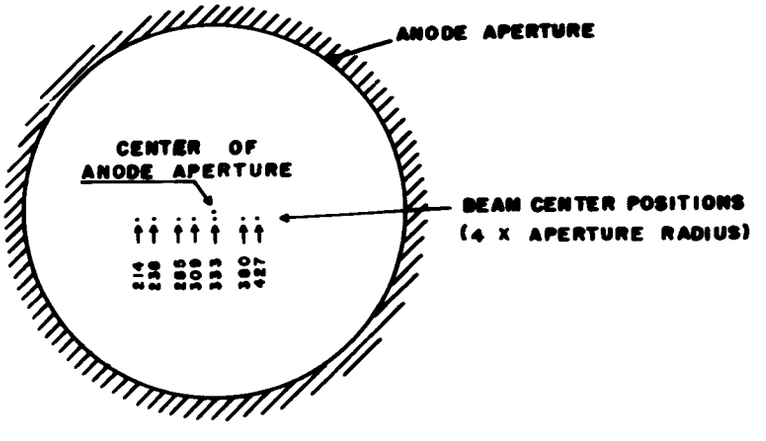

Figure 3-8. Beam Center Positions with Respect to Anode Aperture Center Position.

the focusing field. A second possible explanation is that the anode saturates nonuniformly as the magnetic field is increased, causing the lens action to be nonsymmetrical in the angular direction.

The frequency of motion of the beam center position is predicted by Equation (3-21) if the term $1/R$, which arises from space-charge forces, is neglected. When flux is present in the cathode region, Equation (3-21), without the $1/R$ term, is difficult to solve. Neglecting the R_g term, however, gives the following equation,

$$\ddot{R} + \omega_L^2 R = 0 \quad . \tag{3-26}$$

The solution to this is

$$R = A \sin (\omega_L t + \theta) \quad , \tag{3-27}$$

where A and θ depend on the initial entrance angle and axial positions of the beam as shown in Figure 3-6. As $\omega_L t$ varies from 0 to 2π radians, the radius function R varies through two complete cycles so that the beam center oscillates at the cyclotron frequency ω_c which is twice the Larmor frequency ω_L.

The wavelengths of the motion of the center of the beam (cyclotron wavelength) and the scallop wavelengths as functions of the magnetic field and the beam voltage are shown in Figure 3-9 for the beam from the STL-100 gun. The wavelength of the motion of the center of the beam is assumed to be the cyclotron wavelength, since lines having a slope of -1 fit the data points very well. According to Equation (3-24), only an appreciable amount of flux in the cathode region can prevent the wavelength of the beam center motion from being the cyclotron wave-

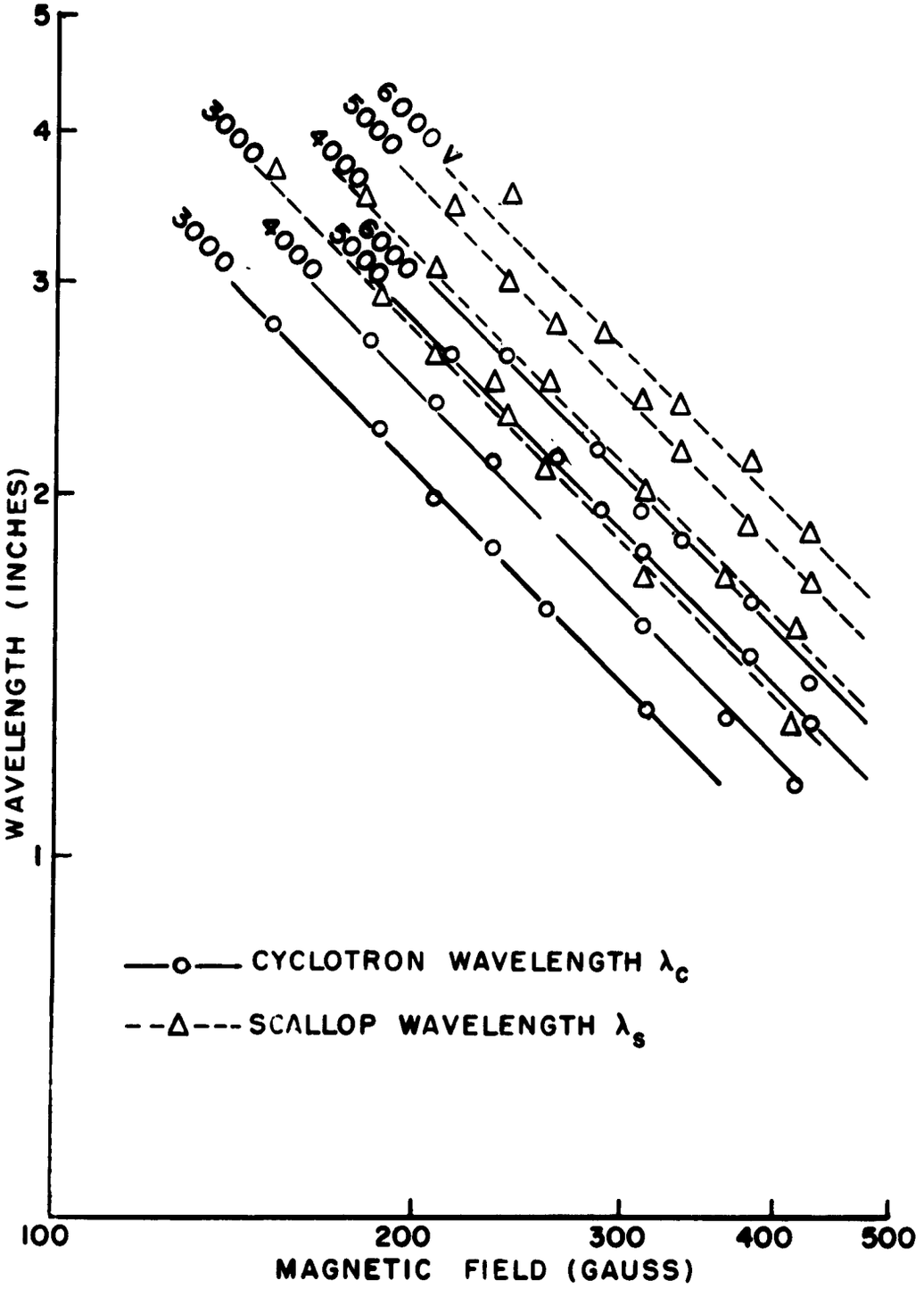

Figure 3-9. Cyclotron and Scallop Wavelengths versus Magnetic Field.

length. However, the flux in the cathode region is not important, for if it were, the scallop frequency would be

$$\omega_L \left[2(1 + R_g^4)\right]^{1/2} ,$$

and the scallop wavelength curves would bend downward from the - 1 slope lines, because R_g is directly proportional to the magnetic field; that is

$$R_g^4 = \frac{g^4}{a^4} = \frac{r_c^4}{a^4} \left(\frac{B_c}{B}\right)^2 \propto r_c^4 \left(\frac{B_c}{B}\right)^2 B^4 ,$$

where B_c is the flux density in the cathode region and the ratio B_c/B is a constant.

In Table I, the values of the cyclotron wavelength at 200 gauss as obtained from Figure 3-9 are compared with the calculated values.

Table I. Experimental and Calculated Cyclotron Wavelengths

Beam Voltage	λ_c from Figure 3-9 (in.)	Calculated λ_c (in.)
6000	3.08	3.06
5000	2.77	2.79
4000	2.45	2.50
3000	2.09	2.16

In obtaining the calculated values, the velocity change given in Appendix A, which results from the potential depression in a cylinder containing an electron beam, was taken into account.

Now, since the amount of flux in the cathode region is negligible, the scallop wavelength is

$$\lambda_s = \frac{2\pi u}{\sqrt{2}\,\omega_L} = \sqrt{2}\,\frac{2\pi u}{\omega_c} = \sqrt{2}\,\lambda_c \quad .$$

However, from Figure 3-9, the ratio λ_s/λ_c is found to be 1.31 instead of $\sqrt{2}$, which represents an error of about 7 percent. The reason for this discrepancy has not been discovered yet, but it has been verified that the positive ion concentration in the beam has little effect on the scallop wavelength at pressures of 1×10^{-6} mm Hg and below. Also, it has been found that reflected electron ratios up to about 0.25 have little effect on λ_s. Both the ion concentration and the reflected electron ratios were suspected since under certain conditions, they could introduce space-charge forces that could affect the beam dynamics.

The equilibrium radius of the beam as a function of the magnetic field is shown in Figure 3-10. The data points represent the average beam radius which contains 93 percent of the beam current. The lines are plots of Equation (3-20), which gives the theoretical value of the equilibrium beam radius. The error between the 93-percent radii and the theoretical radii is less than 3 percent. The 95-percent diameter was found to be greater than the theoretical value by about 6 percent and the 90-percent diameter was found to be less by about 69%.

After the effect of the filament magnetic field was removed from the beam, the only translaminar current that could be detected was that in the beam profile "tails" as is shown in Figure 3-11. These "tails" were found to move into and out of the beam in the manner shown in

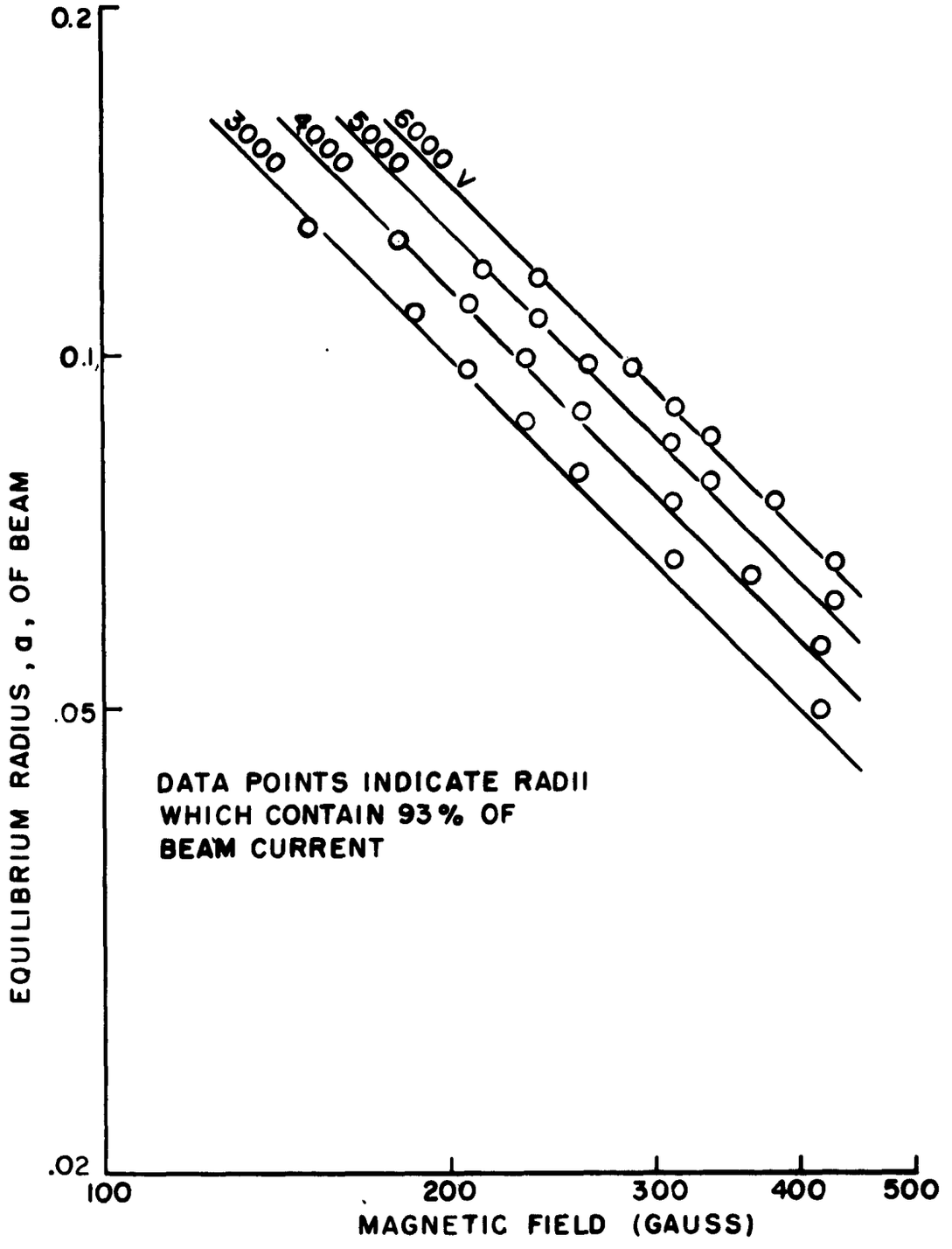

Figure 3-10. Equilibrium Radius versus Magnetic Field.

Figure 3-12, which is similar to the arrow-development in an electron beam described by Johnston.[6] By placing negative potentials on the Faraday cage, the tails were found to be made up of electrons traveling at velocities of from 95 percent to 99 $\frac{1}{2}$ per cent of the main beam velocity, which indicates that these were reflected electrons. Since the outer diameter of the tails was found to be about 0.280", which is the same as the diameter of the aperture in the electron gun anode, these reflected electrons must have emerged from the electron gun. It is known that the amount of current traveling directly from the cathode to the gun walls was less than 0.1 percent so that the reflected electrons could not have originated in the electron gun. Therefore, they must have originated at the collector, traveled along the beam into the gun, turned around near the cathode and then emerged from the gun along with the remainder of the beam.

Although the percentage of electrons reflected from the carbonized molybdenum plate was small, it was made about 60 percent smaller by replacing the plate by a graphite aperture. As a result, the "tails" on recent beam profiles are even smaller than those shown in Figure 3-11 so that few electrons with large translaminar velocities remain in the beam. There still remain, of course, the small translaminar velocities, that result from the thermal velocity distribution at the cathode.

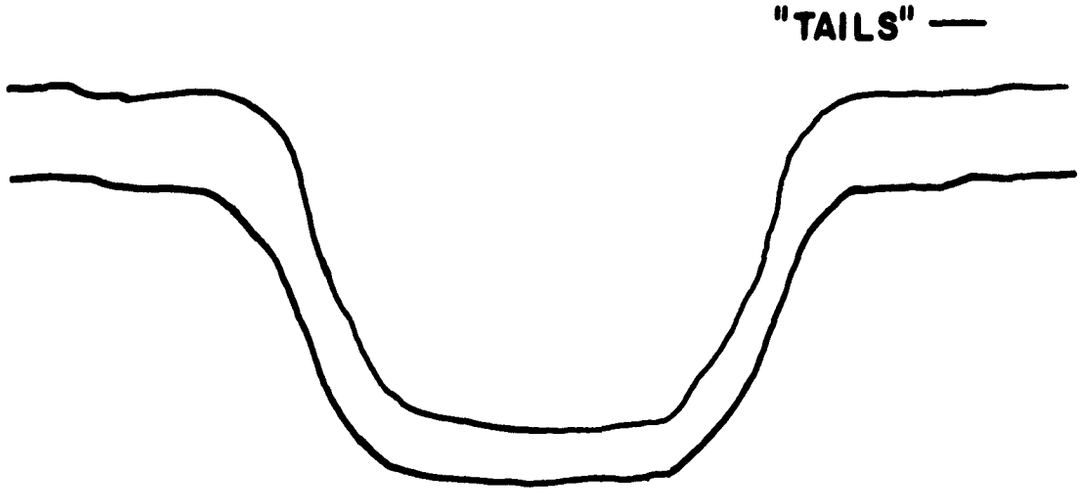

Figure 3-11. Beam Profiles Showing Low Current-Density "Tails." (These two profiles were taken at two points spaced 0.2 in. apart on the axis of the beam.)

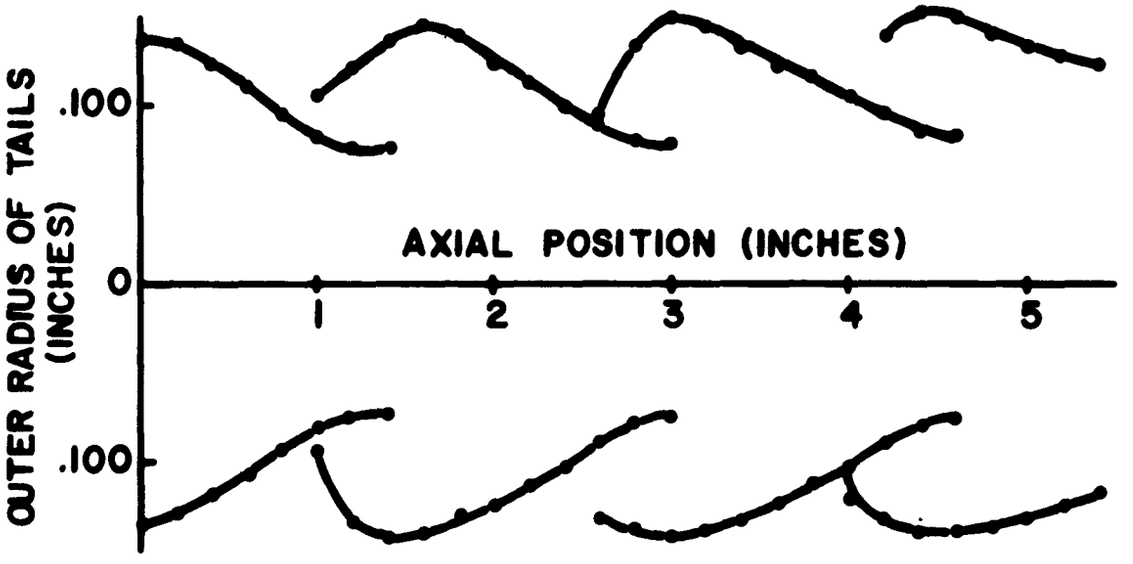

Figure 3-12. Outer Radius of Profile "Tails" versus Axial Position in Beam.

IV. CONCLUSIONS

In conclusion, it may be said that of the new developments used in the beam tester described here, the most important one is the ball valve between the electron gun and the drift tube. This valve and a VacIon pump have made it possible to protect the cathode from oil contamination and from exposure to air when changes have been made in the beam-measuring apparatus. In addition, the valve makes it possible to use the electron beam described in this report as a basis for experiments on velocity modulation. This beam, whose behavior is very close to that predicted by theory, is nearly free from scalloping and from electrons with large translaminar velocities. Therefore, it approximates closely the ideal beam normally considered to be present when theories describing velocity modulation are formulated. As a result it is expected that the experimental data obtained when the beam is velocity modulated should agree well with theoretical predictions, if the theory is valid.

APPENDIX: VELOCITY OF AN ELECTRON BEAM IN A CYLINDER OF FINITE DIMENSIONS

A. DERIVATION OF EQUATIONS FOR POTENTIAL IN CYLINDER

To determine the velocity of an electron beam moving along the axis of a circular cylinder, the distribution of the potential on the axis must be found. Shown in Figure A-1 is a sketch of a cylinder containing a beam. Region I is assumed to contain no electrons and region II is assumed to contain a beam with a charge distribution and an axial velocity that are independent of the radial position. This is the type of beam that is normally assumed to exist in a magnetic field under Brillouin flow conditions The equation to be solved, of course, is Poisson's equation, which, in cylindrical co-ordinates with no angular variations, is written in mks units as

$$\nabla^2\Phi = \frac{\partial^2\Phi}{\partial r^2} + \frac{1}{r}\frac{\partial\Phi}{\partial r} + \frac{\partial^2\Phi}{\partial z^2} = \frac{\rho}{\epsilon_o} \quad , \tag{A.1}$$

where Φ is the potential and ρ is the charge density in the beam. In region I the charge density is zero, and in region II it is

$$\rho = \frac{I}{\pi r_b^2 u} = \frac{I}{\pi r_b^2 \sqrt{2\eta(V+\Phi)}} \quad , \tag{A.2}$$

where I is the beam current and V is the potential of the cylinder relative to the cathode from which the beam originated. In order to obtain a linear differential equation, the potential Φ must be restricted

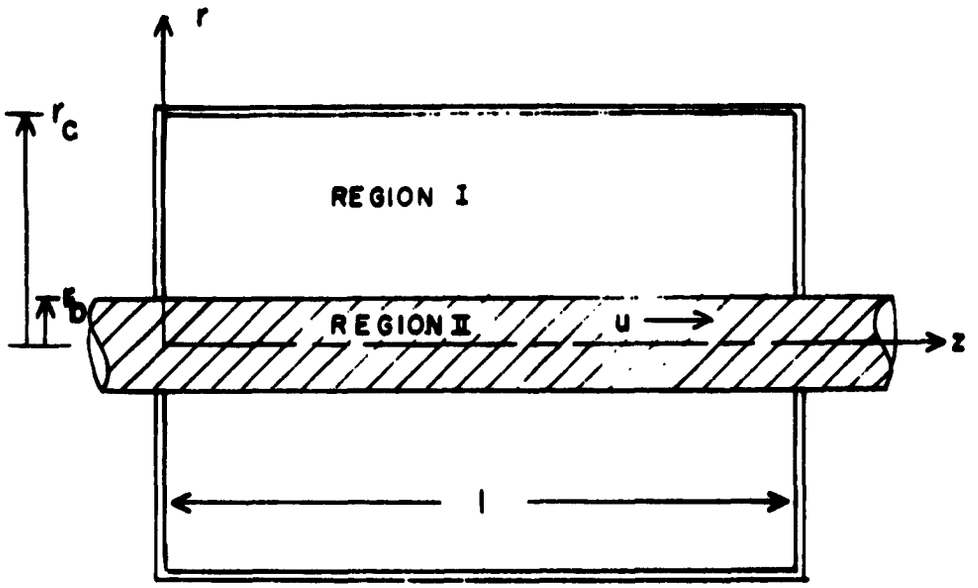

Figure A-1. Circular Cylinder of Radius r_c with Electron Beam of Radius r_b, Moving along the Axis with Velocity u.

so that it is much less than V. Under this condition Equation (A-2) may be rewritten as

$$\rho \cong \frac{I}{\pi r_b^2 \sqrt{2\eta V}} \left(1 - \frac{\phi}{2V}\right) , \qquad \text{(A-3)}$$

and so Equation (A-1) becomes

$$\frac{\partial^2 \phi}{\partial r^2} + \frac{1}{r}\frac{\partial \phi}{\partial r} + \frac{\partial^2 \phi}{\partial z^2} + \left(\frac{a}{r_b}\right)^2 \phi = \left(\frac{a}{r_b}\right)^2 2V , \qquad \text{(A-4)}$$

where

$$a^2 = \frac{I}{\pi \epsilon_o 2V \sqrt{2\eta V}} = 0.0304\, P , \qquad \text{(A-5)}$$

and P is the perveance multiplied by 10^6. The restriction that Φ be small compared to V is not serious under normal conditions, since for a beam with a perveance of 1×10^{-6}, the value of Φ/V is about 0.10 when $r_c/r_b = 20$.

The potential distribution in the cylinder can now be determined by matching the solutions of Poisson's equation in regions I and II at the edge of the electron beam. In region I, both K_o and I_o Bessel functions can exist in the radial direction. In the axial direction, only sine functions can exist, since the potential must go to zero at the ends of the cylinder. After adjusting the constants of integration so that Φ_I is zero at all walls of the cylinder, the potential in region I is found to be

$$\Phi_I = \sum_{n=1,3,5}^{\infty} A_n \left[K_o\left(n\frac{\pi}{I}r\right) - I_o\left(n\frac{\pi}{I}r\right) \frac{K_o\left(n\frac{\pi}{I}r_c\right)}{I_o\left(n\frac{\pi}{I}r_c\right)} \right] \sin n\frac{\pi}{I}z \quad , \tag{A-6}$$

where the A_n will be determined when Φ_I is matched to Φ_{II} at $r = r_b$.

In region II, only I_o Bessel functions can exist since the K_o functions diverge at the axis. In the z direction, cosine as well as sine functions may exist since the potential is not zero at the ends of the cylinder. Therefore the solution to Equation (A-4) takes the form:

$$\Phi_{II} = 2V + \sum_{n=1,3,5}^{\infty} B_n I_o \left[-a^2 + \left(n\pi\frac{r_b}{I}\right)^2 \right]^{1/2} \frac{r}{r_b} \sin n\pi\frac{z}{I}$$

$$+ \sum_{m=0,2,4}^{\infty} C_m I_o \left[-a^2 + \left(m\pi\frac{r_b}{I}\right)^2 \right]^{1/2} \frac{r}{r_b} \cos m\pi\frac{z}{I} \quad . \tag{A-7}$$

B. BOUNDARY CONDITIONS

The beam is assumed to enter and leave the cylinder through tubes with radius r_b. The potential distribution in the tubes is

$$\frac{\Phi}{2V} = 1 - \frac{J_o\left(a\,\frac{r}{r_b}\right)}{J_o(a)} \quad , \tag{A-8}$$

where J_o is a Bessel function of the first kind. When $z = 0$, Φ_{II} must be the same as the potential given by Equation (A-8), so

$$C_o = -\frac{2V}{J_o(a)} \quad ,$$

and

$$C_m = 0 \qquad \text{for } m \neq 0.$$

Now Equation (A-7) reduces to

$$\Phi_{II} = 2V\left[1 - \frac{J_o\left(a\,\frac{r}{r_b}\right)}{J_o(a)}\right] + \sum_{n=1,3,5}^{\infty} B_n I_o\left[-a^2 + \left(n\pi\frac{r_b}{l}\right)^2\right]^{1/2} \frac{r}{r_b} \sin n\pi\frac{z}{l}. \tag{A-9}$$

At the edge of the electron beam, the potential and the electric field are continuous; that is

$$\Phi_I\Big|_{r_b} = \Phi_{II}\Big|_{r_b} \quad ,$$

and

$$\frac{\partial \Phi_I}{\partial r}\Bigg|_{r_b} = \frac{\partial \Phi_{II}}{\partial r}\Bigg|_{r_b} \quad . \tag{A-10}$$

After satisfying Equations (A-10), it is found that

$$\Phi_I = -\frac{8Va}{\pi}\frac{J_1(a)}{J_o(a)}\sum_{n=1,3,5}^{\infty}\frac{I_o(\beta_n)\sqrt{\frac{r_b}{r}}\;\frac{\text{bsnh}(n\rho_c - n\pi\frac{r}{l})}{\text{bsnh}(n\rho_c - n\rho_b)}}{n\rho_b\,\text{bctnh}(n\rho_c - n\rho_b)\,I_o(\beta_n) + \beta_n I_1(\beta_n)}\;\frac{\sin n\pi\frac{z}{l}}{n} \tag{A-11}$$

and

$$\Phi_{II} = 2V\left[1 - \frac{J_o(a\frac{r}{r_b})}{J_o(a)}\right] - \frac{8Va}{\pi}\frac{J_1(a)}{J_o(a)}\sum_{n=1,3,5}^{\infty}\frac{I_o\left(\beta_n\frac{r}{r_b}\right)\frac{\sin n\pi\frac{z}{l}}{n}}{n\rho_b\,\text{bctnh}(n\rho_c - n\rho_b)\,I_o(\beta_n) + \beta_n I_1(\beta_n)} \tag{A-12}$$

where the following two Bessel hyperbolic trigonometric functions have been used:

$$\text{bsnh}(y-x) = \sqrt{xy}\left[K_o(x)\,I_o(y) - K_o(y)\,I_o(x)\right], \tag{A-13}$$

$$\text{bctnh}(y-x) = \frac{K_o(y)\,I_1(x) + K_1(x)\,I_o(y)}{K_o(x)\,I_o(y) - K_o(y)\,I_o(x)}, \tag{A-14}$$

and where

$$\beta_n = \left[-a^2 + \left(n\pi\frac{r_b}{l}\right)^2\right]^{\frac{1}{2}}, \tag{A-15}$$

$$\rho_b = \pi\frac{r_b}{l},$$

$$\rho_c = \pi\frac{r_c}{l}.$$

C. ELECTRON BEAM VELOCITY

The velocity of the beam in the cylinder is given by

$$u = \sqrt{2\eta(V + \Phi_{II})} = \sqrt{2\eta V}\left(1 + \frac{\Phi_{II}}{2V}\right) , \qquad \text{(A-16)}$$

where Φ_{II} is evaluated at the axis of the cylinder. That is,

$$\frac{u}{u_o} = 2 - \frac{1}{J_o(a)} - \frac{4a}{\pi}\frac{J_1(a)}{J_o(a)} \sum_{n=1,3,5}^{\infty} \frac{\frac{\sin n\pi \frac{z}{\ell}}{n}}{n\rho_b \, bctnh(n\rho_c - n\rho_b) I_o(\beta_n) + \beta_n I_1(\beta_n)} ,$$

(A-17)

where $u_o = \sqrt{2\eta V}$. The function $xbctnh(y-x)$ used in Equation (A-17) depends on the dimensions of the cavity and the radius of the beam, and is plotted in Figure A-2. The summation in Equation (A-17) converges very slowly for small values of x and therefore must be evaluated with the aid of a computer. Equation (A-17) is plotted in Figures A-3, A-4 and A-5 for a perveance of 1×10^{-6}. If the average velocity is all that is required, the summation may be evaluated without a computer because the terms decrease as $1/n^2$ instead of as $1/n$. When averaged over the length of the cylinder, Equation (A-17) becomes

$$\frac{\Delta\bar{u}}{u_o} = 1 - \frac{1}{J_o(a)} - \frac{8a}{\pi^2}\frac{J_1(a)}{J_o(a)} \sum_{n=1,3,5}^{\infty} \frac{\frac{1}{n^2}}{n\rho_b \, bctnh(n\rho_c - n\rho_b) I_o(\beta_n) + \beta_n I_1(\beta_n)} ,$$

(A-18)

where $\Delta\bar{u} = \bar{u} - u_o$ and $\bar{u}$ is the average velocity in the cylinder. Equation (A-18) is plotted in Figure A-6 for a perveance of 1×10^{-6}.

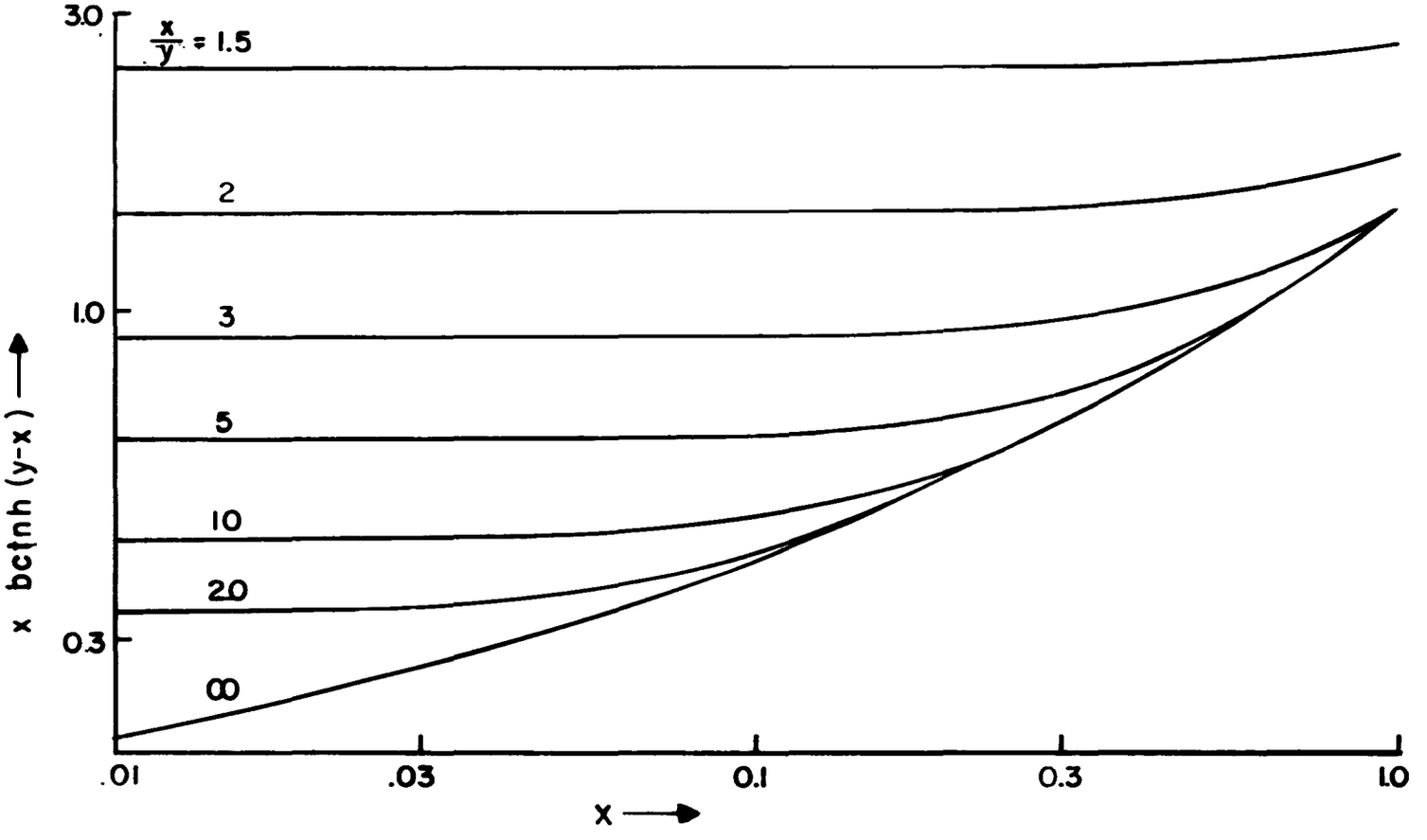

Figure A-2. Product xbctnh(y-x) as a Function of x and y/x.

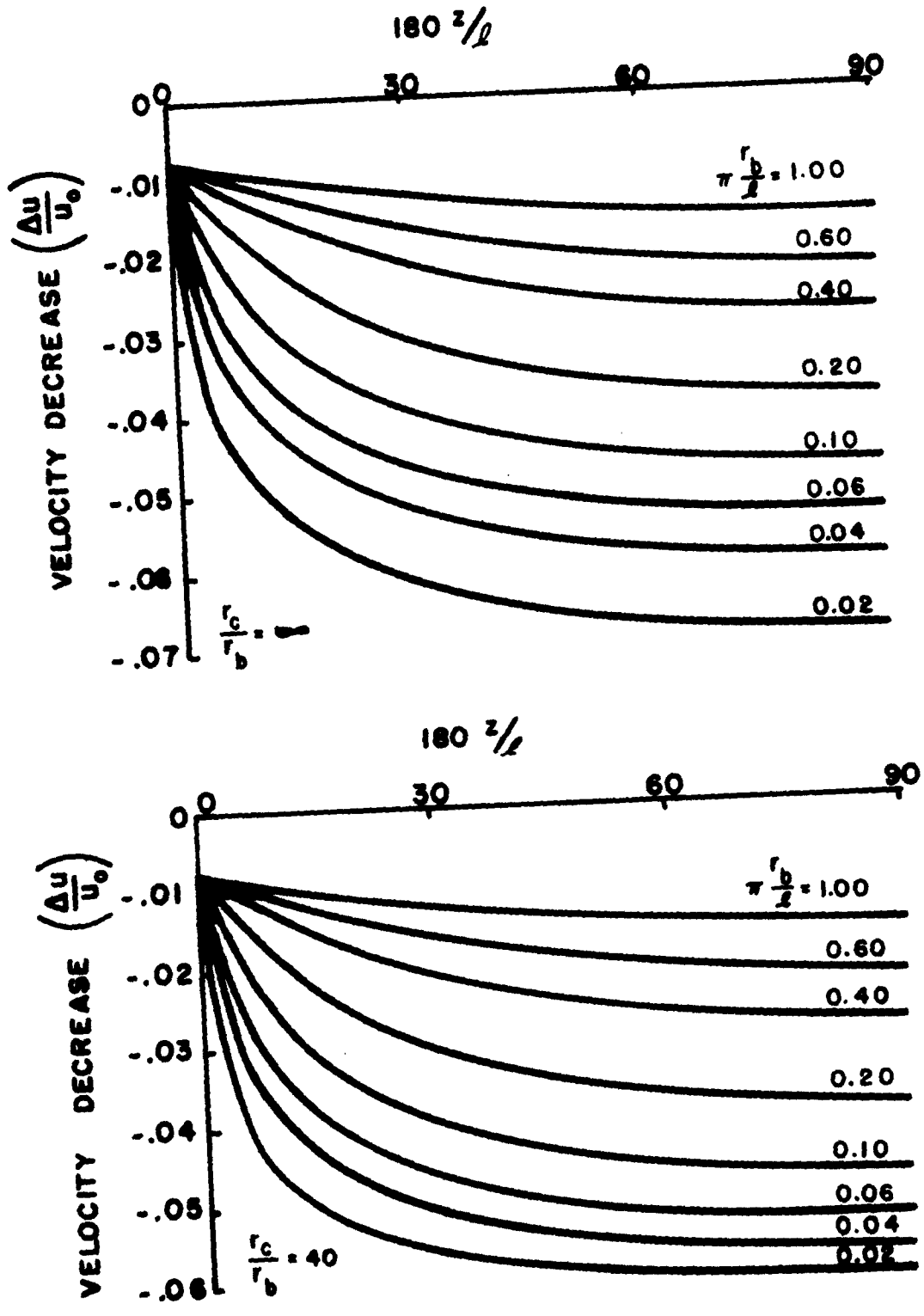

Figure A-3. Velocity Decrease as a Function of Cylinder and Beam Dimensions for a Perveance of 1×10^{-6}.

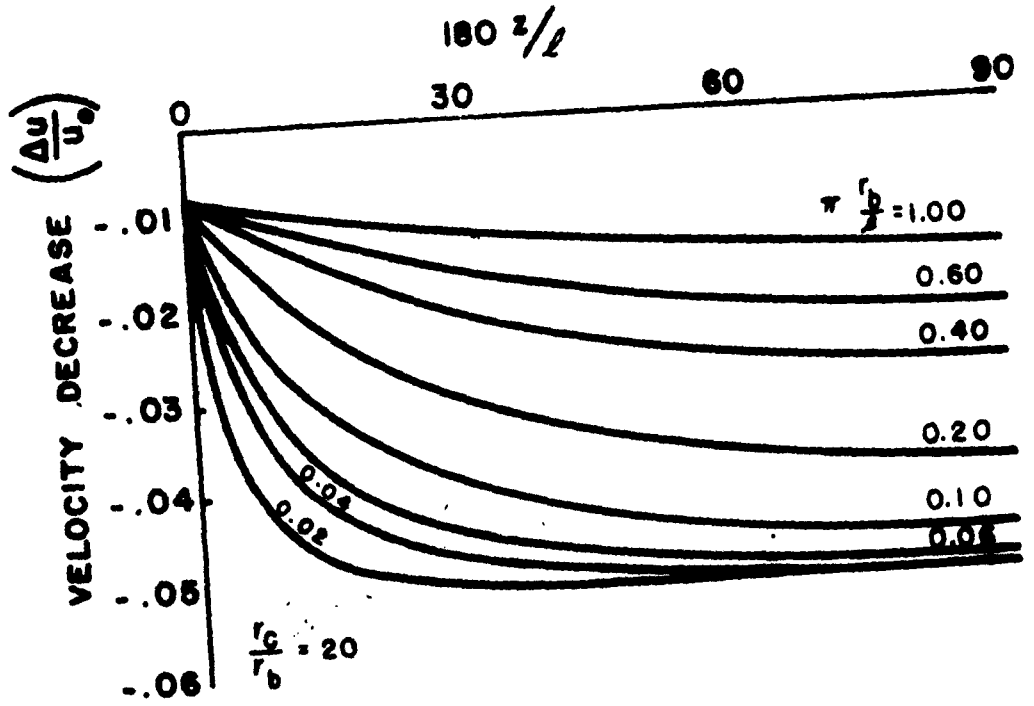

Figure A-4. Velocity Decrease as a Function of Cylinder and Beam Dimensions for a Perveance of 1×10^{-6}.

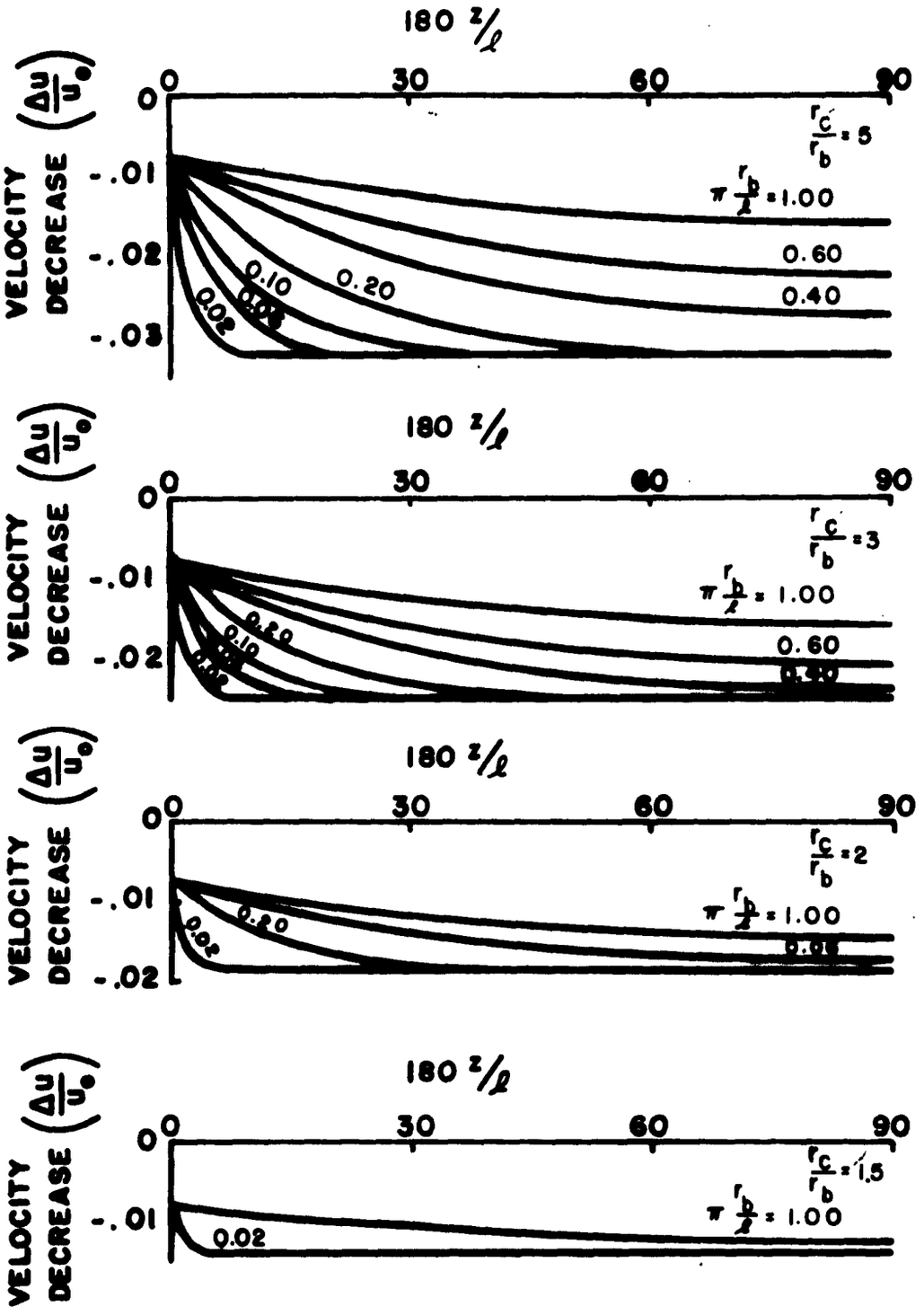

Figure A-5. Velocity Decrease as a Function of Cylinder and Beam Dimensions for a Perveance of 1×10^{-6}.

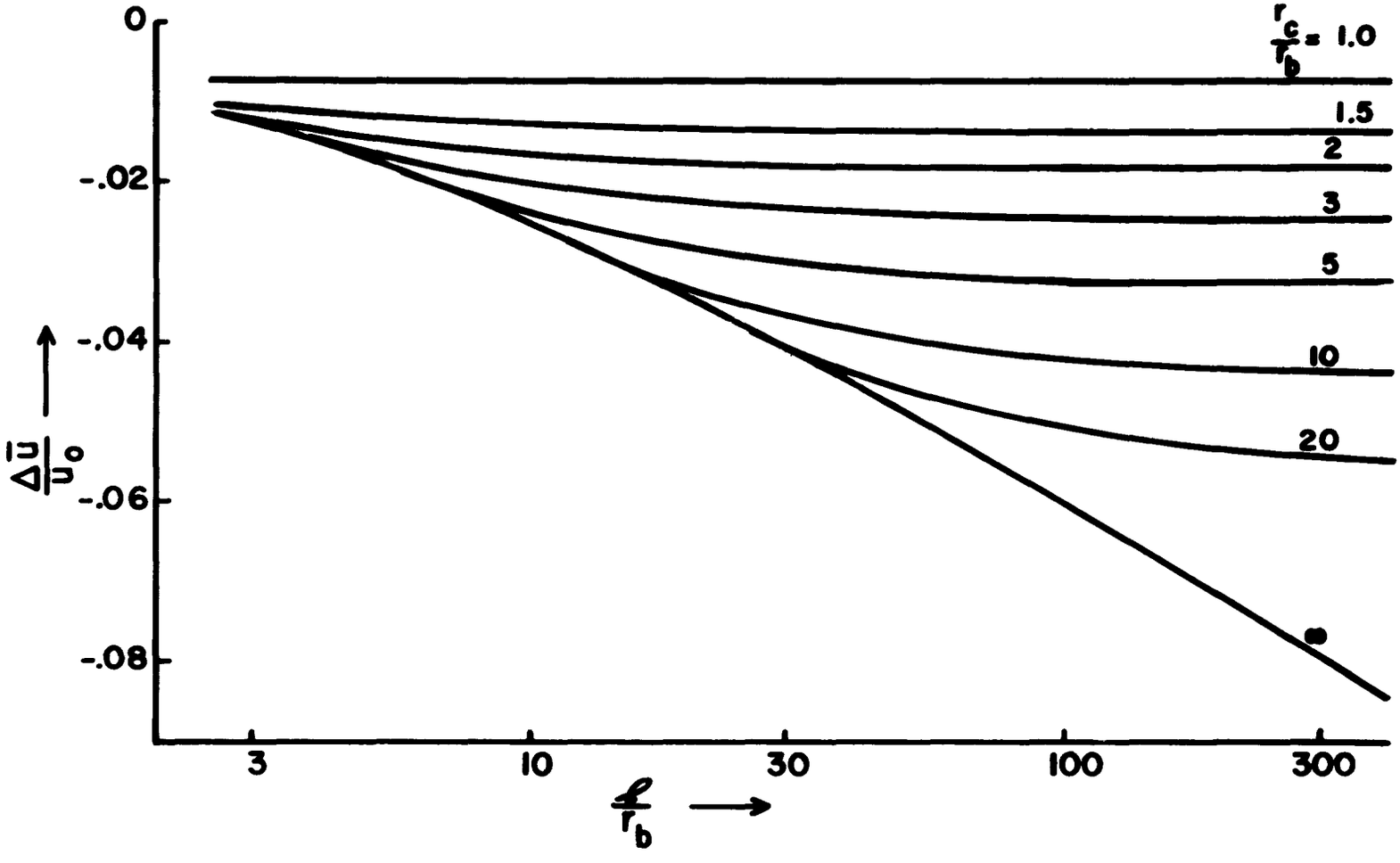

Figure A-6. Average Velocity Decrease as a Function of Cylinder and Beam Dimensions for a Perveance of 1×10^{-6}.

V. REFERENCES

1. T. G. Mihran, "The Effect of Space Charge on Bunching in a Two-Cavity Klystron," Proc. I.R.E., ED-6 (1959), pp. 54-64.

2. A. L. Cullen and I. M. Stephenson, "An Experimental Investigation of Velocity-Modulated Electron Beams," I.E.E., 105, Part B Supplement International Convention on Microwave Valves, May 1958.

3. D. K. Winslow, "The Current Distribution in Magnetically Focused Modulated Electron Beams," Rep. No. 380, Stanford University Microwave Laboratory, Stanford, Calif., April 1957.

4. C. C. Wang, "Electron Beams in Axially Symmetrical Electric and Magnetic Fields," Proc. I.R.E., 38 (1950), pp. 135-147.

5. W. J. Kleen, Electronics of Microwave Tubes, New York: Academic Press, 1958.

6. T. W. Johnston, "Nonlaminar Flow in Magnetically Focused Electron Beams from Magnetically Shielded Guns," (Letter) J. Appl. Phys., 30 (1959), pp. 1456-1457.

FINAL REPORT

PART V:

CATHODE STUDIES

SOME EFFECTS OF ION BOMBARDMENT ON THE EMITTING PROPERTIES OF OXIDE-COATED CATHODES

H. Hollister

School of Electrical Engineering
CORNELL UNIVERSITY
Ithaca, New York

RESEARCH REPORT EE 482

SOME EFFECTS OF ION BOMBARDMENT ON THE EMITTING PROPERTIES OF OXIDE-COATED CATHODES

H. Hollister

LINEAR BEAM MICROWAVE TUBES

Technical Report No. 7 30 October 1960

Published under Contract No. AF30(602)-1696
Rome Air Development Center, Griffiss Air Force Base, New York

ACKNOWLEDGMENTS

The author wishes to express sincere gratitude to Professor G. C. Dalman for suggesting and directing this study, and to Professor H. S. Sack for many helpful discussions throughout the course of this work.

He is indebted to Dr. H. D. Doolittle of Machlett Laboratories for his help in obtaining the cathodes used in this study and for the time he generously gave in discussing their preparation and operation.

He is indebted to the members of the machine shop and technical staff for their assistance in the construction of various parts of the apparatus, and to the secretarial staff for typing this thesis.

This work was made possible under the sponsorship of the U. S. Air Force under Contract No. AF 30(602)-1696.

TABLE OF CONTENTS

ILLUSTRATIONS

ABSTRACT

An apparatus was developed with which it was possible to study the effect of ion bombardment by ions of oxygen, carbon monoxide, and argon on the emitting properties of oxide-coated cathodes. A description is given of the development of an ion gun capable of delivering an ion current of up to 3 μamp/cm^2 on a target maintained at a pressure of $1(10)^{-7}$ mm Hg.

This apparatus was used in an investigation of the general effects of ion bombardment by oxygen, carbon monoxide, and argon. Since only a small amount of differential pumping was employed, the cathodes were severely poisoned during the study with oxygen, so that their emission was of the order of 50 ma/cm^2 at 830°C. Ion bombardment by oxygen further decreased the emission in all cases, oxygen arriving at the surface by ion bombardment being about one to five times as effective in poisoning the cathode as oxygen from the gas phase. The studies with carbon monoxide and argon were carried out on active cathodes, having emissions of from one to four amperes per square centimeter at 830°C, since the gases themselves had little effect on the emission. It was found that ion bombardment by carbon monoxide increased the emission of oxide cathodes under all conditions, even when the effect of carbon monoxide in the gas phase was poisoning, as well as when it was activating. The effects with argon were much smaller than those for the other gases, and were found to be of both signs. With all three gases the effect of ion bombardment on the emission was found to be completely reversible.

In order to explore the use of ionic deposition as a tool in studying the effect of chemical agents of the gas phase on the emission of oxide-

coated cathodes, a detailed study was made of the effects of ion bombardment by oxygen and carbon monoxide as functions of: voltage of the pulse used to measure the emission, ion beam density, ion energy, d-c current through the cathode, and the temperature of the cathode. In the study using oxygen it was found that: (1) the resistance of the cathodes was affected as rapidly as the emission, indicating that the effect spreads through the thickness of the coating in a very short time; (2) the recovery from ion bombardment poisoning is significantly slowed down by drawing d-c current, which is interpreted as direct evidence against the presence of mobile acceptors and indicates that mobile donors play an important part in the recovery; (3) the percentage of decrease in emission caused by a given ion current was nearly constant over the temperature range from 600°C to 900°C. In the study with carbon monoxide it was found that: (1) the effect of ion bombardment by carbon monoxide can apparently be explained on the basis of creation of donors at the surface of the cathode; (2) the activation energy of the rate-controlling process at temperatures above 800°C was about 4 ev.

I. INTRODUCTION

It is becoming increasingly clear that the oxide-coated cathode is always operating in an equilibrium between processes tending to activate it and processes tending to deactivate it. In recent years much attention has been given to the study of the details of these opposing processes in the hope that knowledge of these details will lead to both a better fundamental knowledge of the operation of the oxide cathode and improvements in the thermionic emitting properties of such cathodes. In order to study the processes determining the equilibrium in an oxide cathode, it is necessary to perturb this equilibrium in a controllable manner and observe the resulting change in the electronic properties of the cathode. Techniques of perturbing this equilibrium that have been widely used in the past are admission of gases to the cathode[1, 2, 3, 4] admission of reducing agents to the cathode from the base metal,[5] and electrolysis of the cathode coating[6, 7, 8, 9]. A technique that has been used only slightly, however, is controlled deposition of chemical agents on the cathode surface by means of ion bombardment.[10]

In the latter experiment,[10] Matheson et al. studied the process of activation of a cathode having relatively poor emission by means of mass spectrometric deposition of alkaline earth metal ions. An attempt to observe the effect of oxygen deposited in the same manner was also made, but it was found that the ion current was too weak to have a detectable effect. These experiments, however, furnished a starting point for the present investigation, the purpose of which is a study of the effect of ion bombardment, by some of the gases usually found in thermionic tubes, on cathodes initially

having high activity. Ionic deposition is felt to be a more refined technique for studying the processes in the oxide cathode than the usual technique of admitting gases, since it can be controlled much more precisely and more rapidly than can the gas pressure.

In addition to yielding fundamental information on the processes occurring in oxide cathodes, a study of the effect of ion bombardment is also of considerable interest in its own right, since the cathode in any thermionic tube is being subjected to a certain amount of ion bombardment and it is important to ascertain to what extent this affects its emission. This practical importance of ion bombardment is especially pronounced in the case of high-power beam-type tubes, since the cathodes in such tubes are subjected to considerable ion bombardment. For example, an order-of-magnitude calculation shows that the center of the cathode in a high-power klystron operating with one-ampere-average beam current (per square centimeter) at a pressure of 10^{-7} mm Hg will be bombarded with roughly one microampere per square centimeter of ion current. Since the trend is towards higher currents and longer pulse lengths, the effect of ion bombardment may be expected to become more and more important.

In order to obtain reliable data on the effect of ion bombardment on oxide cathodes, several requirements must be met. First, in order to separate the effects of ion bombardment from those of drawing current and also to study the interaction of the two effects, it is necessary to bombard the cathode from a separate ion gun rather than to use the electrons from the cathode itself to generate ions. It should also be possible to measure the emission of the cathode without introducing more ion bombardment. The second major requirement is that the ion current must be high enough

for the effects of ion bombardment to stand out from the effect of the gas from which the ions are derived. In addition, to carry out a thorough study of the effect of ion bombardment, it should be possible to vary the ion species, ion energy, total number of ions deposited, and cathode temperature independently and in a well-controlled manner. The apparatus constructed in this project was designed to meet these requirements. The gases chosen for this study are oxygen, because it is the most active poisoning agent commonly found in tubes; carbon monoxide, because it is the most abundant ambient gas found in tubes; and argon because it is chemically inert.

In order to lay the groundwork for presentation of the experimental study, this introduction is followed by a survey of the prevalent theories of the operation of the oxide-coated cathode. The experimental apparatus used for the study is then described, followed by a detailed description of the various experimental results. This report is then concluded with a discussion of the interpretation of the experimental results in terms of the theories outlined earlier, and a statement of the conclusions that have been drawn. Details of the development of an ion gun capable of meeting the necessary requirements and used in the investigation presented here are described in Appendix A.

II. THEORETICAL BACKGROUND

Before describing the experiments and results that comprise the major part of this study, a brief discussion of the present status of knowledge of the oxide-coated cathode is given, which provides both the motivation and the basis of interpretation of the experiments to be described. In providing the background for the interpretation of the observed effects of ion bombardment of an oxide cathode, this section will begin with those aspects of the physics of the oxide cathode that seem to be fairly well established. Since ion bombardment is a method of perturbing the equilibrium of an oxide cathode in a very well-controlled manner, it is felt that it provides a useful tool in studying this equilibrium. Therefore, the present theories concerning the competing processes (i.e., poisoning, activation, and pulse decay) that normally determine the equilibrium will be discussed in some detail. Since the various theories of these processes depend intimately on the specific models of the oxide cathode on which they are based, it will be necessary to describe these models in conjunction with the presentation of the theories on the processes.

A. GENERAL MODEL OF OXIDE CATHODE

According to the currently accepted model, the oxide cathode is an n-type semiconductor, having at least two donor levels and possibly one or more acceptor levels in the forbidden band. The electron affinity, χ, is believed to be 0.6 ev and the donor levels are believed to be 1.4 ev and 2.0 ev below the bottom of the conduction band. The usual procedure in drawing an energy-level diagram for the oxide cathode is to show the bulk

equilibrium energy levels and then show these levels as varying near the surface because of surface states. The point of view taken here, however, is that the equilibrium of importance in thermionic emission is the equilibrium immediately below the surface, so that this equilibrium is considered while the equilibrium that may exist in the bulk of the crystals is ignored.

It can be shown by quantum statistics[11] that the thermionic emission from any material is given by the Richardson equation:

$$J = (1 - \bar{R}) A T^2 e^{-\frac{e\phi_t}{KT}}$$

in which $\bar{R}$ is the reflection coefficient, A a universal constant (= 120 amp/cm^2 $^\circ$K), and ϕ_t the true work function of the material defined as the difference between the vacuum level and the Fermi level. The work function of the oxide cathode is the sum of two parts, the electron affinity χ (sometimes called the "outer work function") and the distance of the Fermi level below the bottom of the conduction band (sometimes called the "inner work function"). Since there is no evidence of changes in the electron affinity that are not accompanied by changes in the Fermi level, it is merely mentioned here that the electron affinity is a possible source of variation in the work function, before passing on to a discussion of variation in the Fermi level as the major source of variations in the work function.

The problem of maintaining a low work function, and hence high thermionic emission, in an oxide cathode is synonymous with maintaining a high Fermi level. Although an explicit expression cannot be derived for the Fermi level in the general case of several impurity levels, it can be

seen[12] that in general adding donors to a semiconductor raises its Fermi level while adding acceptors decreases it. In this report a donor is loosely defined as any impurity that requires less energy than the width of the forbidden band to give up an electron to the conduction band, and an acceptor as any impurity that can trap an electron in the forbidden band. In this way it is seen that the state of thermionic activity of an oxide cathode is determined by the equilibrium densities of the various impurities in the cathode.

In order to maintain as high a donor concentration as possible in the oxide cathode, various reducing agents are usually added to the base metal, so that they will diffuse into the cathode at elevated temperatures and form donors. It can be shown by thermochemical theory[13] that these impurities reduce the coating to form free barium rather than enter the coating as donors themselves. In addition to maintaining a high donor concentration in the oxide cathode, it is necessary to have a low concentration of acceptors. Although it has never been shown that acceptors exist in the oxide cathode, it is well known that oxidizing gases poison the cathode, either by entering the lattice as acceptors or by destroying donors. Indeed, as has been pointed out by Plumlee,[14] reducing the cathode tends to raise its Fermi level and oxidizing it tends to lower it, regardless of the specific donors and acceptors involved.

Besides the emission properties of the oxide cathode the conduction properties must also be considered. At present, it seems to be well established that conduction in the oxide cathode is electronic and consists of two parallel processes, both exhibiting the temperature dependence characteristic of activated phenomena but having different activation energies. As was originally pointed out by Loosjes and Vink[15] and further

substantiated by the Hall effect and magnetoresistance measurements,[16] the high-temperature conduction is by means of an electron gas in the pores of the cathode. The low-temperature conduction seems to be an n-type semiconduction process having a very low activation energy, although whether this is mainly through the bulk of the crystallites or through a thin layer at the surface of the crystallites is still in question. The general considerations with respect to activation of the thermionic emission set forth above also apply to both of these conduction mechanisms, although the applicable energy level diagrams may be quantitatively different if the low temperature conduction is actually through the bulk of the crystallites.

B. PHENOMENA AFFECTING EQUILIBRIUM

The equilibrium Fermi level, and hence cathode activity, is determined by the balance between various competing processes, both chemical and electrolytic. The chemical effects may be either favorable or unfavorable, called activation and poisoning respectively. Similarly, the electrolytic effect seems to be favorable over a prolonged period, which is called electrolytic activation, and unfavorable over a short period, which is called the pulse decay phenomenon.

With reference to the general semiconductor model of the oxide cathode, it is seen that activation in general is a matter of creating and maintaining both a high donor density and a low acceptor density in the oxide coating. Although it has long been known that reducing gases, such as methane, will activate the oxide cathode, the principal methods used in practice are the addition of reducing agents to the base metal and electrolytic activation. It has been found that very active cathodes may be produced by either means,[17] and in addition, that by introducing reducing

impurities having known diffusion characteristics in the base metal, the activation can be controlled well throughout the life of the tube. The various specific models of the oxide cathode differ with respect to activation mainly in the identity of the donor species, the relative importance of donors and acceptors, and the identity of the important transport mechanisms.

Although the poisoning process has been the subject of a great deal of research, consisting mainly of admitting an atmosphere of some oxidizing gas to the cathode and observing the amount of deactivation of the cathode under various conditions, there still does not seem to be any satisfactory theory of the details of this poisoning. It does appear, however, that the poisoning process is one aspect of the normal equilibrium operation of the cathode, rather than a separate process. It is in a study of the details of this process that ion bombardment is felt to be of great promise, since by this means poisoning agents can be deposited on the surface of a cathode in a well-controlled manner rather than the less well-controlled technique of exposing the cathode to a gas. In particular, the ion bombardment can be turned on and off at will, thus permitting a study of the rate processes.

In addition to the long-term activation by electrolysis, there is found to be a very rapid deactivation of the cathode upon drawing large currents, called the pulse decay phenomenon, which is also apparently due to electrolysis.[6, 7, 8, 9, 18] A theoretical treatment of this phenomenon[18] taking into account factors such as donor (or acceptor) mobility, space charge in the coating, and field penetration, is seen to become of sufficient complexity that few conclusions can be drawn beyond the fact that donor mobility can well account for all the phenomena observed. However, it does seem to be well established that one of the most important species in maintaining high cathode activity must be extremely mobile.

C. SPECIFIC MODELS OF OXIDE CATHODE

1. Conventional F-Center Model

The conventional model of the cathode[1] is one in which excess barium forms oxygen vacancies (F-centers), which in turn are the principal donors. Acceptors, although acknowledged to be present, are considered to be of little importance. The excess barium is believed to be in the form of F-centers both because of experimental studies[19] and because F-centers have the required high mobility.

In this model, the activation process consists of creating and maintaining a large stoichiometric excess of barium, either by reduction of the oxide or by electrolysis, and poisoning consists of destroying this excess of barium, presumably by filling the F-center with oxygen or some other oxidizing agent. Although nothing seems to be known of the transport of the poisoning agent into the cathode, it would probably be by F-centers migrating to the surface and being filled or by oxygen in some form migrating inwards and filling the F-centers. The pulse decay phenomenon is explained by the F-centers being pulled away from the surface by the electric fields and thus forming a donor depletion layer at the surface.

The principal drawback to this model is the fact that the vapor pressure of barium over the cathode would have to be many orders of magnitude greater than it actually is in order to maintain the density of F-centers required for the calculated donor density of an active cathode.[13] Rittner suggests that this difficulty can be avoided by assuming a layer of adsorbed barium on the surface of the oxide particles, although it is not explained why this layer is present on the oxide cathode and not on the barium oxide on which the vapor pressure data was originally obtained.

2. Importance of Equilibrium with Gases in Tube

It has been demonstrated experimentally[20] that an oxide cathode contains impurities that are in equilibrium with the gases in the tube, and that the equilibrium between the gases over the cathode and the impurities in the cathode depends on the current being drawn from the cathode. On the basis of (1) this experimental evidence, (2) the disparity between the calculated excess barium density and the necessary donor density, and (3) further thermochemical reasoning, Plumlee[14] proposes that these gaseous impurities are the species important in the electronic properties of the oxide cathode. In particular, he proposes that the mobile donor is an OH^- impurity, with an added electron bound to it, on an oxygen site, the OH^- being very mobile because of the ease of transferring the proton from one oxygen atom to another in the lattice.

The activation and poisoning phenomena fit quite naturally into this model as changes in the equilibria of the various chemical reactions involved toward either higher or lower donor density in the cathode. The "transport" of this equilibrium to the interior of the oxide crystals would probably be mostly by means of the OH^- impurity, but some of the other impurities might also be mobile enough to participate in this transport. The pulse decay phenomenon is explained in this model by the formation of a donor depletion layer by the action of the electric field in the cathode on the positively charge mobile donors.

3. Mobile Acceptor Model

In a recent paper, Hensley and Okumura[21] have proposed that the mobile species in the oxide cathode are barium vacancies that act as electron acceptors and that it is the density of these acceptors that determines the

activity of the cathode, the density of donors being relatively constant. This proposal is based on the experimental observation that the activation of an oxide cathode spreads to inactive parts of the cathode with a diffusion constant equal to that observed by Reddington[22] for barium vacancies in barium oxide. It seems, however, that the objection mentioned with respect to the F-center model, i.e., that the required excess barium density is much higher than that expected from thermochemical data, applies just as well to this model, since the same density of excess barium should be required for an active cathode in both cases.

According to this model the oxide cathode is created initially with high densities of both donors and acceptors, and the activation process consists of eliminating most of the acceptors while the donor density remains fixed. The poisoning phenomenon fits into this model as being due to an increase in the equilibrium density of barium vacancies in the presence of an atmosphere of oxidizing gas, and the transport would be by diffusion of these vacancies to the interior. The pulse decay phenomenon is explained in this model as being caused by electrolysis of the acceptors to the surface of the cathode, thus depressing the Fermi level by this means rather than by donor depletion. The fact that the activation energy of the process responsible for the pulse decay is given by Frost[23] as about the same as those for the spread of the activation of the cathode and for barium vacancies is quoted as further evidence in support of this model. It should be mentioned, however, that Krusemeyer and Pursley[9] found a much higher activation energy for the pulse decay in the temperature range of 800°C to 850°C.

4. Surface versus Bulk Properties

Another aspect of the oxide cathode which seems to be in question is the relative importance of the surface layers of the oxide crystallites versus the importance of their interiors. Since both the thermionic emission and the pore conductivity are determined by the state of the oxide at the surface of the crystallites, any difference between the surface and bulk properties would only appear in the low-temperature conductivity of the cathode. Therefore, the question becomes that of whether the properties of the surface layers of the crystallites differ significantly from those of their interiors, and if so, which region accounts for the low temperature conductivity of the cathode. There is a certain amount of evidence, both theoretical and experimental to indicate that such a difference does exist, and that it is the surface layers that are important for the low-temperature conductivity of the cathode as well as for the emission and pore conductivity.

On the theoretical side, Rittner,[13] after careful consideration of the alternatives, concluded that the high density of excess barium necessary for an active cathode could only be maintained by a layer of barium adsorbed on the surface of the crystallites. That such a condition at the surface can affect the properties of a thin layer under the surface can be seen from the calculations of Kane,[24] who showed that the surface states will strongly influence the position of the Fermi level for a distance of the order of the Debye length beneath the surface.

. the experimental side are the results of Kane,[24] who found that for single crystals of barium oxide, the bulk conductivity was not proportional to the emission. Thus the fact that the conductivity of oxide

cathodes is found to be proportional to the emission[3] must indicate that most of the conductivity in practical cathodes is through a layer at the surface. Further experimental evidence of such a condition is given by the results of Metson and Macartney[25] who found that the low-temperature conductivity of an oxide cathode is decreased much more rapidly by exposure to oxygen at low temperatures than should be expected if diffusion into the bulk were a factor. This is interpreted as evidence that the solid conductivity is largely a surface phenomenon.

5. Nonequilibrium Poisoning Theories

In addition to these models of the oxide cathode into which the poisoning phenomenon fits quite naturally as one aspect of the over-all equilibrium that determines the state of activity of the cathode, there are some more specialized theories of the poisoning in which it is regarded as a special phenomenon, separate from these equilibrium processes.

The first of these theories is proposed by Hermann and Wagener.[1] Here the oxygen is said to lack the activation energy to enter the lattice as O^{--} and therefore enters it as O^{-}. The fact that the O^{-} is not as firmly bound in the lattice accounts for the reversibility of the poisoning and the irreversible poisoning observed at very high temperatures is explained by these high temperatures furnishing the activation energy for the oxygen to enter the lattice as O^{--}. When this theory is interpreted in terms of the electronic structure of the oxide cathode, however, it is seen that an O^{-} ion on an O^{--} lattice site is equivalent to a hole in the valence band of the crystal. Since any holes beyond the equilibrium number are filled with electrons from the conduction band (or from donors), it is seen that the high activation energy required to maintain the number of O^{-}

sites higher than at equilibrium does not exist.

A modification of this theory was recently proposed by Surplice[26] in which the O^- ions are adsorbed on the surface of the oxide. This theory is based largely on an experiment in which it was found that by mass spectrometric analysis of the species given off from a cathode during recovery from poisoning, a considerable amount of the O^- (or S^-) given off had such high energy that it could only have arisen by sputtering from the surface by positive ion bombardment. Thus it was concluded that this sputtering was an important factor in the activation of the cathode, a subject that will be discussed further in Chapter VIII.

III. EXPERIMENTAL APPARATUS

A. VACUUM SYSTEM

The vacuum system used in this study is shown in Figure 1. The gas-handling system consisted of the gas flasks, manifold, and the valves for precise control of the amounts of gas admitted to the ion gun.

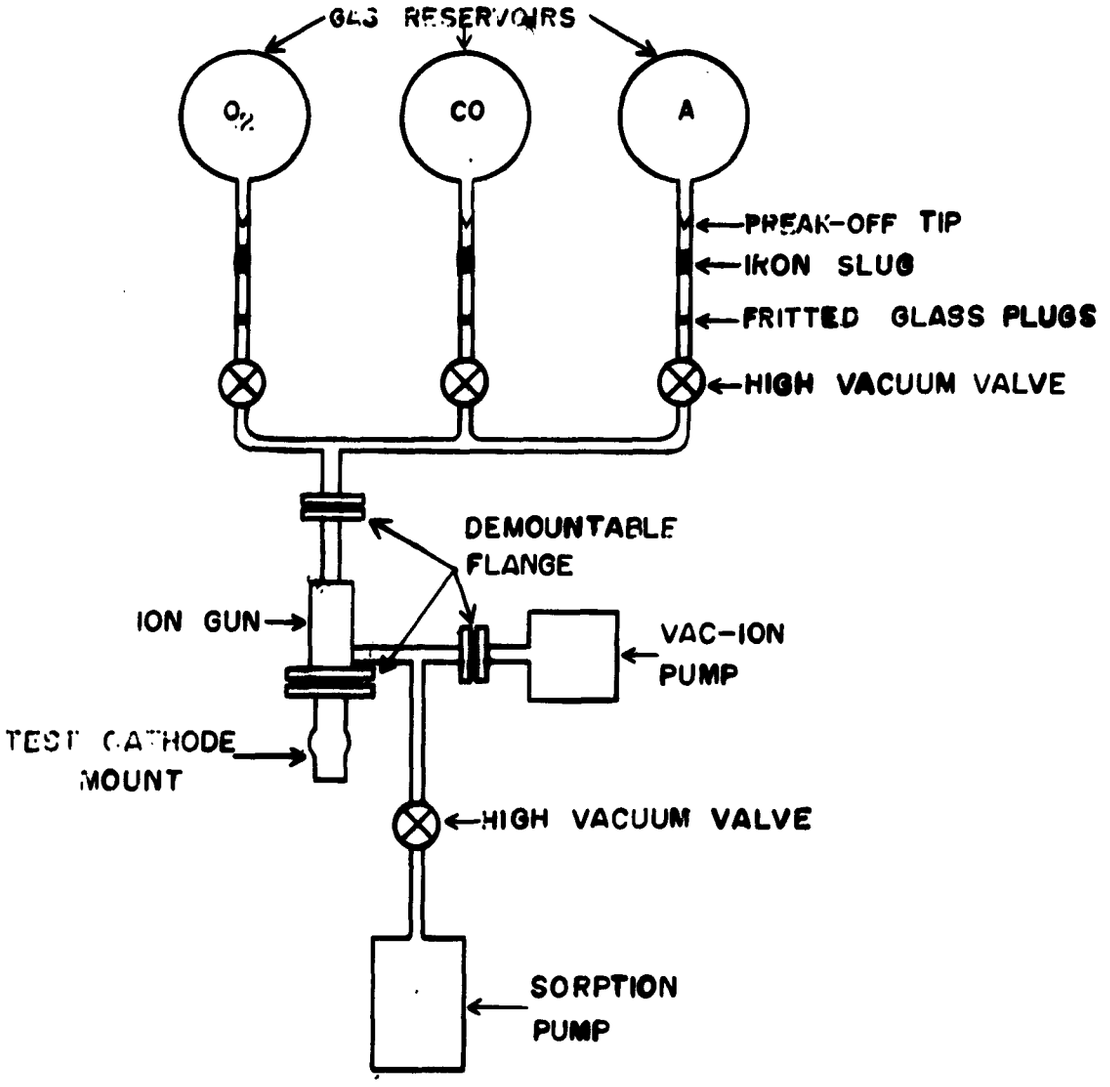

Figure 1. Diagram of Vacuum System.

The three gases used were oxygen, carbon monoxide, and argon, all of Arco reagent grade. Each flask was sealed to a Granville-Phillips Type C high-vacuum valve, and a glass-encased iron slug included for breaking off the tip. Also included were fritted glass plugs to keep glass fragments out of the valves. These three valves were connected to the ion gun by a manifold made of copper tubing, all joints being silver soldered in a hydrogen atmosphere. The gas-handling system was prepared by pumping with a VacIon pump while outgassing with a hot blower until a pressure of $1(10)^{-8}$ mm Hg was obtained. The valves were then closed and the break-off tips broken, at which time the system was ready for use.

An important feature of this vacuum system was the use of a VacIon pump which made possible the complete absence of hot filaments or oil vapors. The interaction of hot filaments with the gases in a vacuum system, such as conversion of oxygen to carbon monoxide,[27] and general outgassing have undoubtedly played an important role in many of the experiments carried out in the past on poisoning of oxide cathodes. Also, contaminants due to oil vapors cause a certain amount of uncertainty and are well avoided. The rough vacuum for this system was obtained by a sorption pump consisting of a copper tube, containing Linde Molecular Sieve 13X, which could be immersed in liquid nitrogen. Thus the introduction of oil vapors at any stage of the processing was avoided.

All demountable vacuum connections were step-joint flanges using OFHC copper gaskets, and all permanent vacuum connections were BT soldered in a hydrogen atmosphere.

The oxide cathodes were preconverted in a special tube, shown in Figure 2, constructed expressly for this purpose. This tube was constructed of stainless steel and incorporated a pyrex window to allow calibration of the surface temperature of the cathode as a function of its heater power.

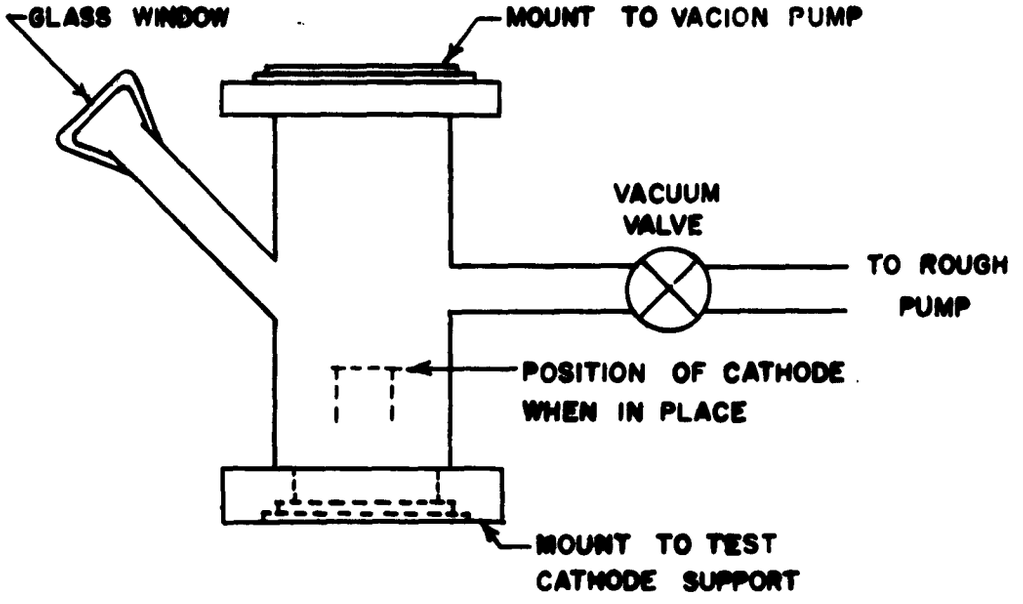

Figure 2. Tube for Preconverting Cathode.

B. ION GUN AND TEST CATHODE SUPPORT

The details of the ion gun and test cathode support are shown in Figure 3. The ion gun consisted of a cold cathode Penning discharge, through one cathode of which ions were extracted, and an ion lens to provide control of the ion beam and a certain amount of differential pumping. This design of ion gun was arrived at after preliminary

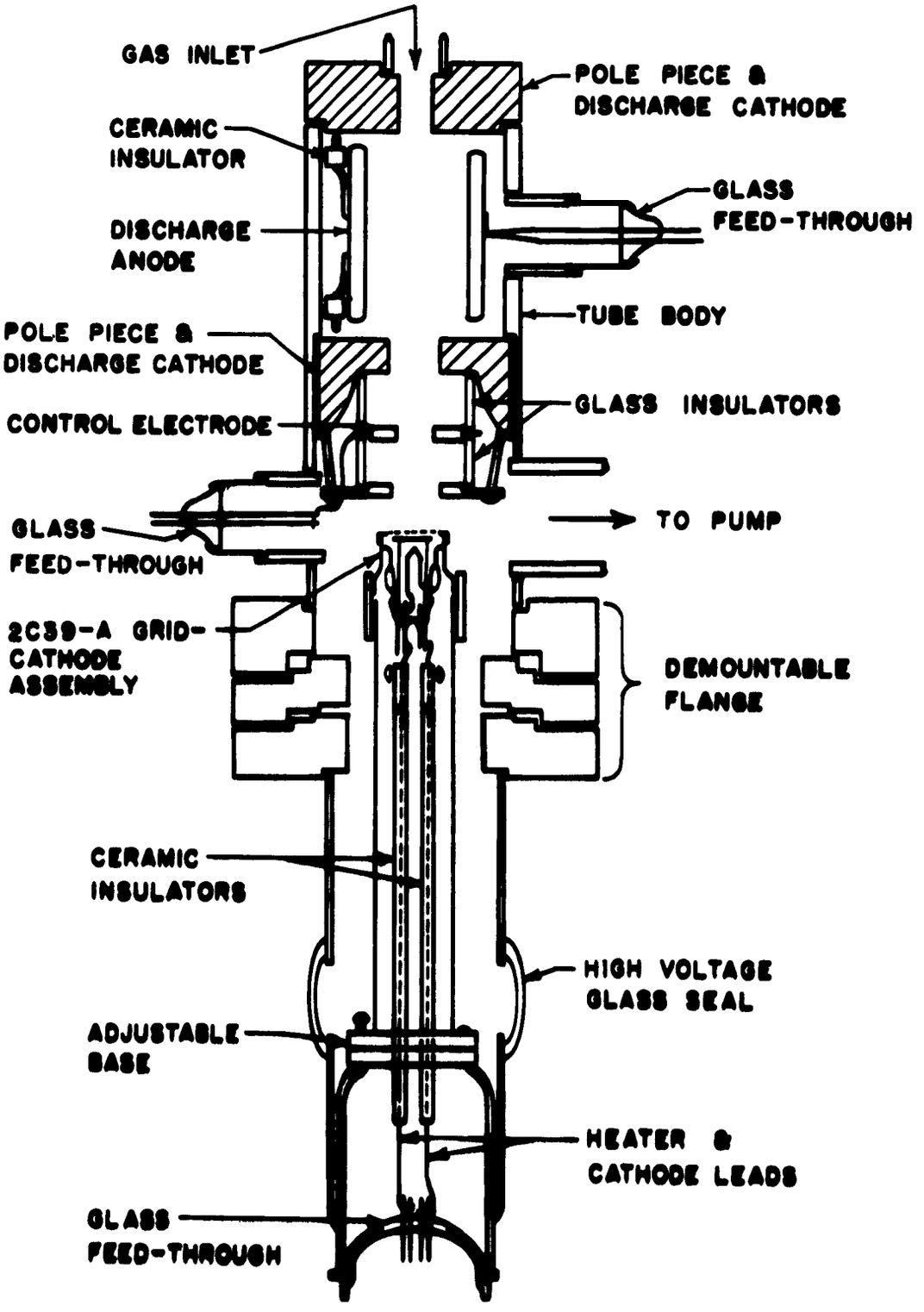

Figure 3. Ion Gun and Test Cathode Support.

experimental work (see Appendix A) had led to the conclusion that the most fruitful approach to obtaining high ion-current densities at very low pressures was through concentration of the ion beam and differential pumping. Also, for the purpose of this study, the cold discharge had the important advantage that no contaminants or side effects were introduced, as would be introduced by thermionic cathodes or incandescent filaments in the discharge. With the ion gun shown, a maximum ion beam density of about 3 $\mu amp/cm^2$ was obtained on a collector maintained at a pressure of $1(10)^{-7}$ mm Hg, which is considered very good. The main disadvantages in using such a discharge are the large energy spread in the ion beam, and the fact that there are probably large percentages of doubly charged and dissociated particles in the ion beam. Details of the energy spread of the ion beam and the focusing properties of the ion gun are given in Appendix A.

The anode of the discharge was 304 stainless steel which had been degreased and vacuum fired prior to assembly and was positioned in the tube by the ceramic beads shown. The pole pieces, which doubled as discharge cathodes, were made of Armco iron and the lens electrodes were cold rolled steel. The pole pieces and electrodes were prepared by degreasing, vacuum firing, nickel plating, and hydrogen firing. The lens electrodes were supported and positioned by short lengths of pyrex tubing, the whole assembly being held by stainless-steel screws.

The grid-cathode assembly was that of a Machlett Laboratories 2C39-A. The grid was gold-plated, .0012-in tungsten wire made into a .007-in mesh and hydrogen fired, and the effective grid-cathode spacing was .005-in. The cathode base metal was 220 nickel from which most of

the carbon had been removed by firing in wet hydrogen for several hours at 1150°C. The cathode coating itself was RCA 33-C-131C sprayed to a density of 1.2 gm/cm^3. The cathode was prepared by first mounting it in a lathe and turning the coated portion down to an area of 0.1 square centimeter. Next the cathode was mounted in the support and preconverted[28] in a separate vacuum system to minimize contamination of the grid and the rest of the experimental tube. Finally, the cathode was removed from the preconversion tube, with the heater kept at 1.5 v, the grid mounted and spot welded in place, and the whole structure mounted to the experimental tube by means of the demountable flange.

The cathode support was mounted to the base by a flat plate and screws, so that the cathode could be centered accurately by means of set screws in the mounting plate. The base was connected to the demountable flange by a high-voltage insulating seal so that the whole grid-cathode assembly could be raised to high negative potential to study the effect of ion energy. The insert in the demountable flange was included to compensate for dimensional changes made rather late in the construction of the tube.

C. METHODS OF MEASUREMENT

The purpose of this study is to explore the various phenomena associated with ion bombardment of oxide cathodes rather than to conduct a detailed study of any one of these phenomena. The measurement techniques employed were therefore aimed at versatility rather than precision. The circuit used for most of the measurements in this study is shown in Figure 4. This circuit consisted of three major parts: a d-c circuit through the cathode, a pulse circuit through the cathode,

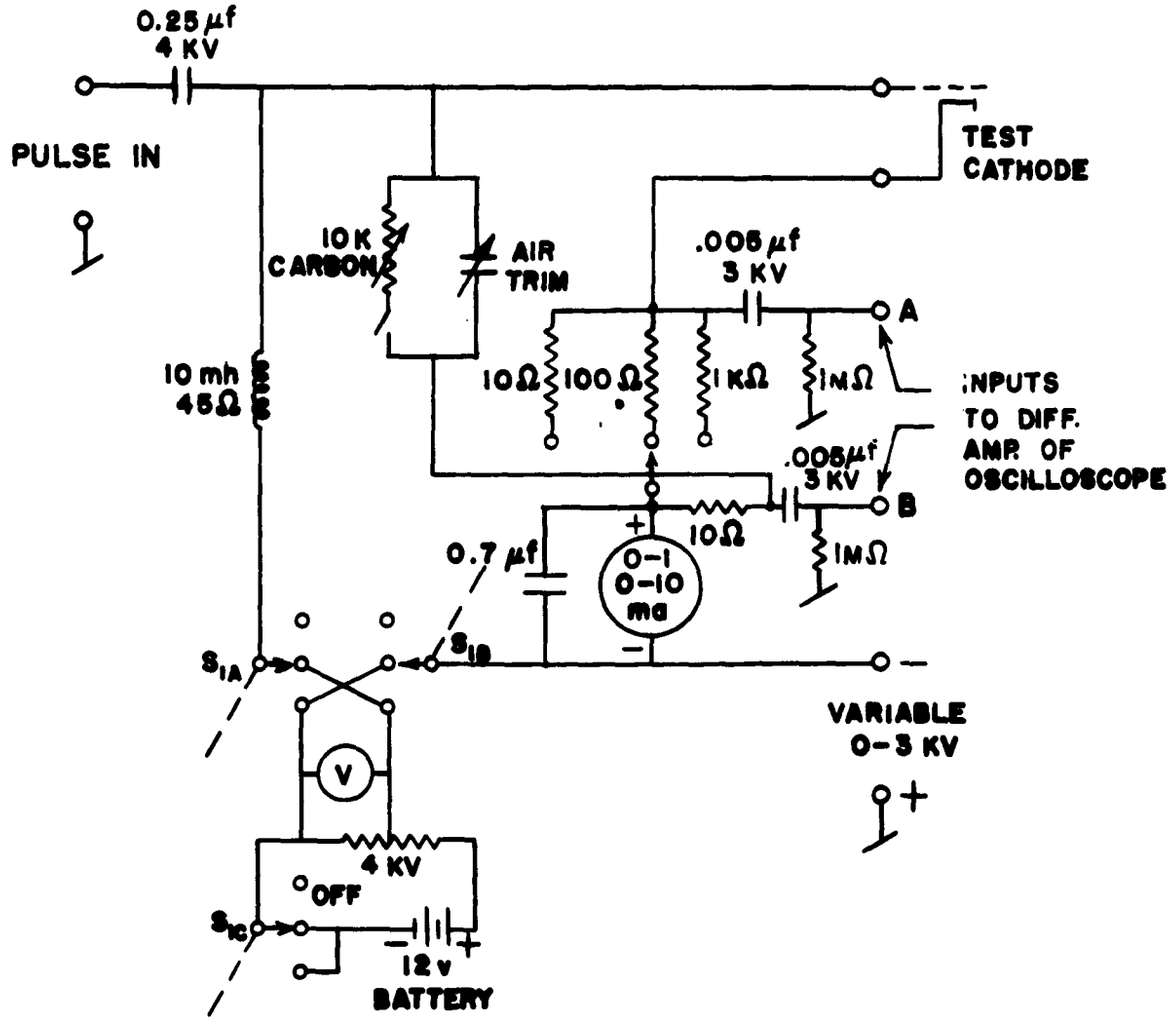

Figure 4. Circuit for Measuring Effect of Ion Bombardment on Emission of Oxide Cathodes.

and a pulse circuit bypassing the cathode. The d-c circuit contained a battery to apply voltage to the grid, which could also be reversed to back bias it, and the d-c milliammeter to monitor the d-c current. When a

pulse was applied to the grid, the 10 mh choke prevented it from being short circuited to ground and the 0.7 μf capacitor allowed it to bypass the milliammeter, the pulse current being viewed as the voltage across the variable viewing resistor. The pulse circuit bypassing the cathode contained a capacitor for compensating the grid-cathode capacitance of the experimental tube and a balancing resistor by which most of the current during the pulses could be balanced out for increased sensitivity. The whole circuit was isolated from the exterior by high voltage capacitors so that it could be raised to negative voltages as high as 3kv.

With the setup shown, the emission could be measured with a 10-μsec pulse having an amplitude of zero to 100 volts and a duty ratio of .0006 and supplied by a Hewlett Packard Model 212A pulse generator. The emission current was viewed as the voltage drop across the load resistor using the differential amplifier input to a Tektronix 545 oscilloscope. With this low duty ratio, the emission could be monitored with very little effect on the cathode itself, and the direct current from the cathode could be controlled as an independent parameter as could the energy of the ion beam. The balancing circuit was provided for increased sensitivity, since the total emission was changed only a few per cent by the ion current available. The procedure used was first to measure the total emission with the balance resistor open, then, inserting it in the circuit, to balance out most of the current pulse and raise the amplification until the desired sensitivity to change in emission was obtained. By substituting known resistances for the test diode and changing their values by known amounts, it was confirmed that the current changes observed under these conditions were actually the changes in cathode

emission. Because of the high sensitivity and low currents used, there was considerable difficulty with 60-cycle ripple or hum. This was eliminated satisfactorily by synchronizing the pulse generator very accurately to the power line by means of a three-stage amplifier clipper.

Measurements of the long-time effects of ion bombardment were made by obtaining the desired sensitivity and observing the behavior of the emission on the oscilloscope with the ion beam on or off. Measurements of the rapid transient effects were made by obtaining the desired sensitivity, setting the oscilloscope to a suitable sweep speed (usually .02 sec/cm to .2 sec/cm), and simultaneously turning the ion beam on (or off) and triggering the oscilloscope. The resulting sweep could either be observed visually or be photographed.

In summary, with the setup described it was possible to observe the effect of ion bombardment on the emission of an oxide cathode while varying the following parameters: (1) pressure, (2) ion species, (3) cathode temperature, (4) d-c emission, (5) ion energy, (6) ion beam density, (7) discharge voltage, (8) pulse voltage.

IV. GENERAL EXPERIMENTAL RESULTS

This section describes the experimental results, which comprise the major objective of this study of the effect of ion bombardment on the emission of an oxide cathode. Along with the study of the effect of ion bombardment, several incidental observations were made and are described before proceeding to the effect of ion bombardment. Then, before going into the specific results obtained with each gas, a general description is given of the effects of ion bombardment. The following three chapters are then devoted to presenting and discussing the specific effects observed by ion bombardment with the three gases: oxygen, carbon monoxide, and argon.

A. INCIDENTAL EXPERIMENTAL RESULTS

1. Preconversion of Cathode

As mentioned previously, the cathodes were prepared using the technique of preconversion.[28] This was done primarily to minimize contamination of the grid used for measuring the emission of the cathode, since any contaminants on this grid would be sputtered onto the cathode by the ion beam. Other advantages of this technique were that it also minimized contamination of the rest of the vacuum system and provided a convenient means of calibrating the surface temperature of the cathode as a function of heater power. The preconversion was carried out using the standard schedule, given in the Tube Laboratory Manual (1956) of the Massachusetts Institute of Technology, of driving off the binder, obtaining a good vacuum, and then converting the carbonate rapidly. The cathodes were then removed from the preconversion tube, the grids put in place, and the cathodes mounted in the experimental tube and pumped down as rapidly

as possible, while the heater was kept at 1.5 volts the whole time. There was no trouble in activating the cathodes after this, and an emission of 3 to 4 amp/cm^2 at 830°C was obtained shortly after outgassing had been completed. Visual examination of the grids after removing them from the experimental tube revealed that the discoloration of the grids was very much less than that of grids that had been in place during conversion of identical cathodes. Thus the preconversion was quite successful and apparently worth while for this application, since most of the visible contamination on the grids was avoided.

2. Effect of Gases on Emission

Since the threshhold for poisoning of oxide cathodes by gases is usually given in the literature[2,29] as $1(10)^{-7}$ mm Hg or above, it was hoped that by carrying out the experiments at $1(10)^{-7}$ mm Hg, it would be possible to observe the effect of ion bombardment with little or no effect of the background gas. It was found, however, that admitting oxygen at a partial pressure of a few times 10^{-8} mm Hg reduced the emission of the cathodes in the present apparatus by a factor of ten or more. Therefore, it was necessary to carry out a combined poisoning and ion bombardment study with the present apparatus, since a great deal more differential pumping would have been necessary to separate the two effects completely.

A typical poisoning curve of emission versus pressure with oxygen being admitted to an oxide cathode is given in Figure 5, along with the results of Wagener[2] for comparison. The emissions plotted in Figure 5 are the equilibrium levels obtained by allowing the oxygen to

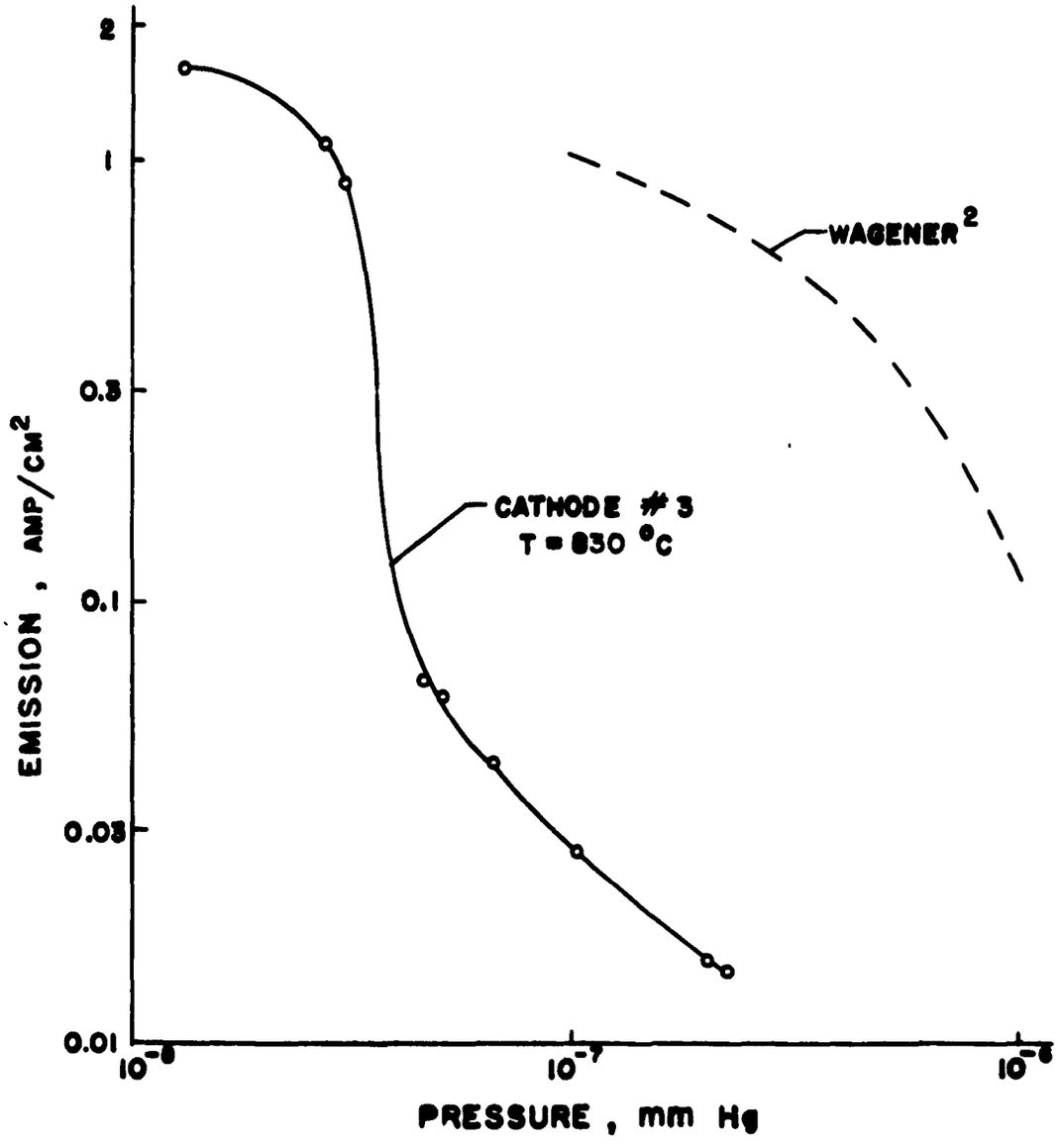

Figure 5. Poisoning of Oxide Cathode by Oxygen.

flow through the system at a constant pressure and waiting until the emission was relatively stable. At the lower pressures a very long time was required for the emission to stabilize and, in fact, the emission was still decreasing slowly even after several hours of exposure to oxygen. As can be seen from Figure 5, the amount of emission poisoning observed here at a given pressure of oxygen was much

greater than that observed by Wagener[2] and, furthermore was greater than that reported in the earlier literature[1] for oxygen pressures several orders of magnitude higher. This trend towards sensitivity to smaller amounts of oxygen seems to be correlated with advancing vacuum technology and suggests that the background gases play an important role. This is also to be expected from the work of Plumlee,[20] who found an oxide cathode to be in labile equilibrium with the surrounding atmosphere, even at very low pressures. Therefore the high sensitivity to oxygen poisoning found here may possibly be due to the greater purity of the admitted oxygen and lower vapor background of an all-metal vacuum system with the absence of any hot filament or oil vapors. The background pressure obtained with the cathode hot and the discharge operating was of the order of $1(10)^{-8}$ mm Hg. It should also be remarked that the brief increase of the emission upon admitting oxygen to an oxide cathode mentioned by Wagener[2] was not observed here.

Very small amounts of carbon monoxide had an observable effect on the emission of a cathode, but in this case the effect was small and consisted of an activation up to a pressure of $2(10)^{-7}$ mm Hg. The equilibrium emission of a moderately active cathode is shown in Figure 6 as a function of the pressure with carbon monoxide flowing through the tube. The effect of carbon monoxide is seen to be of a complicated nature, and considerably different from that observed by Wagener, who found that carbon monoxide activated an oxide cathode in the pressure range from about $3(10)^{-6}$ mm Hg to $2(10)^{-5}$ and poisoned it at both higher and lower pressures. Again, the difference seems to be explainable by a difference in background gases, since, if the effect

of carbon monoxide is due to a chemical equilibrium with the cathode, the partial pressures of all reaction products should play an important role in this equilibrium. For more active cathodes the effect of gaseous carbon monoxide was still of roughly the same form as that in Figure 6, but of even smaller magnitude.

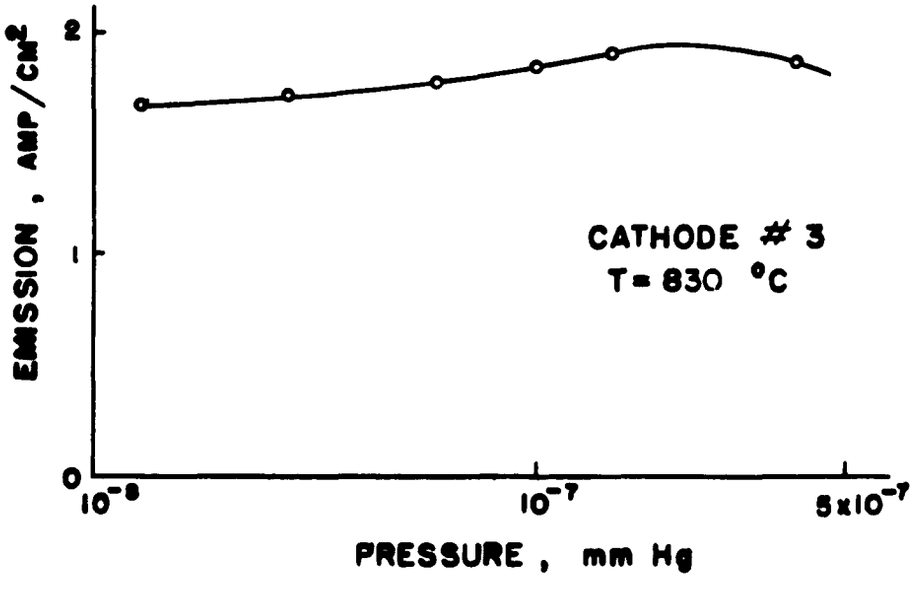

Figure 6. Effect of Carbon Monoxide on Emission of Oxide Cathode.

3. Form of I-V Curve

Because of the severe poisoning by the molecular species of oxygen, the form of the curve of emission versus voltage of the cathode was very different during the study of ion bombardment by oxygen than it was either under high vacuum or with carbon monoxide present. This can be seen from Figure 7 in which the I-V characteristic at a pressure of $5(10)^{-8}$ mm Hg of oxygen (Figure 7a) is compared with that at a pressure of 10^{-7} mm Hg of carbon monoxide (Figure 7b). In Figure 7a it is

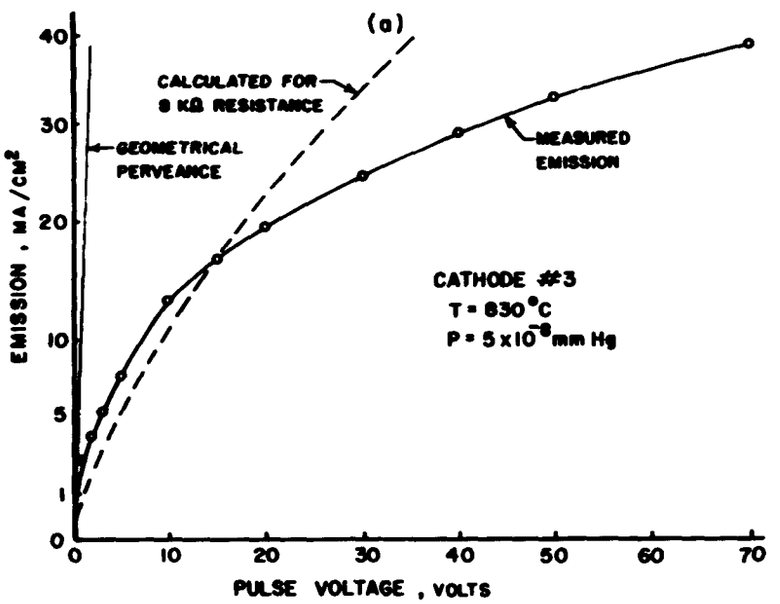

Figure 7a. I-V Characteristic in Presence of Oxygen.

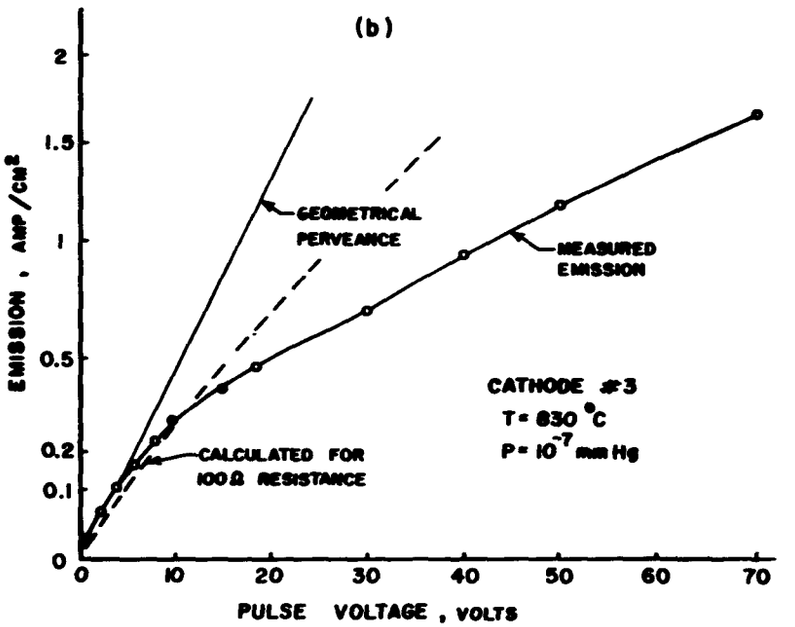

Figure 7b. I-V Characteristic in Presence of Carbon Monoxide.

seen that even at low voltages the emission is quite different from that expected from space-charge limitation for the grid-cathode spacing used (.005"). The form of the emission curve can be explained quite well by assuming a resistance of 8 KΩ in the cathode coating itself, as shown by the dashed line in Figure 7a. This corresponds to a resistance of 800 Ω for a cathode having an area of one square centimeter, which is not at all unreasonable for a somewhat poisoned cathode. The form of Figure 7a is interpreted, therefore, as the emission being space-charge limited up to about 1.5 ma with most of the voltage drop across the coating itself, and temperature limited at higher currents with an increasing proportion of the voltage drop across the vacuum space until, at a pulse voltage of 70 volts, the voltage drop is equally divided between the cathode coating and the vacuum space.

For the more active cathode of Figure 7b, on the other hand, it is seen that the emission at low voltage is very near that expected from the geometrical perveance. In this case, therefore, the coating resistance plays a minor role so that at high voltages most of the voltage drop is across the vacuum region and the emission therefore more sensitive to work function changes, and at low voltages most of the voltage drop is due to space charge, and hence insensitive to changes in the condition of the cathode.

4. Effect of D-C Emission

Rather than studying the interaction of the effect of ion bombardment with the pulse decay phenomenon[9] directly, it was decided to do this indirectly through a study of the effect of drawing a d-c current

from the cathode while simultaneously measuring the pulsed emission. In addition to being more convenient than a direct study of the pulse decay, this method had the further advantage of yielding results more amenable to analysis.[9] Typical results of the effect of drawing d-c emission are shown in Figure 8 for the cathode in three different states of activation: in high vacuum, i.e., pressure less than $1(10)^{-8}$ mm Hg; in the presence of $1(10)^{-7}$ mm Hg of carbon monoxide; and in the presence of $5(10)^{-8}$ mm Hg of oxygen. The voltage used to draw the d-c emission was always less than 10 volts and no detectable pressure rise accompanied the drawing of d-c emission.

Although it seems to be quite well established that there are electrolytic processes in cathodes of mixed oxides which lead to pulse decay, there is still a certain amount of controversy over the extent to

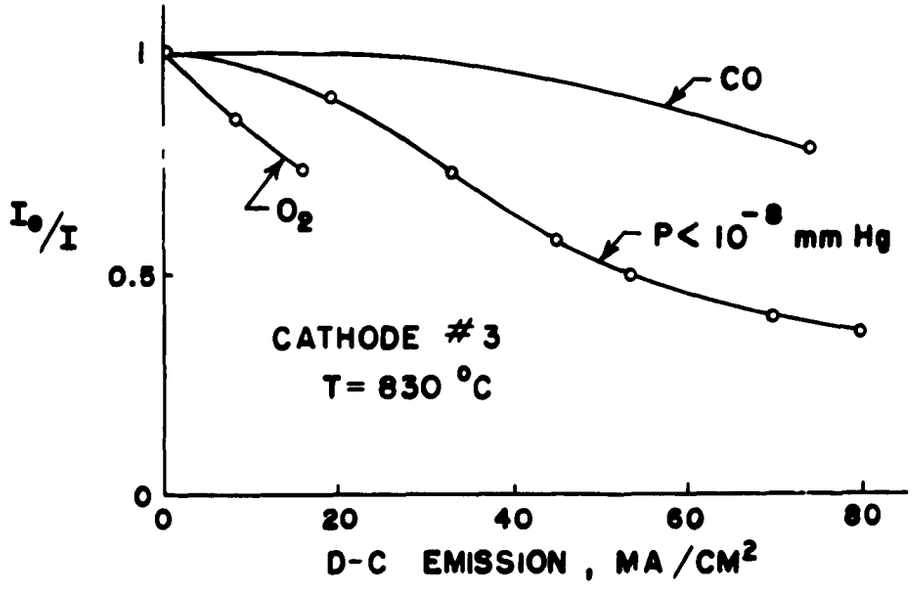

Figure 8. Effect of Drawing D-C Current on Pulsed Emission of Cathode.

which anode effects play a part in this phenomenon. That anode effects play a negligible part in the phenomenon observed here is evidenced by the fact that a similar decay was observed over a wide range of experimental conditions. In particular, any impurities given off by the anode should be negligible compared with the amount of poisoning already given the cathode by a pressure of $5(10)^{-8}$ mm Hg of oxygen.

B. GENERAL EFFECTS OF ION BOMBARDMENT

1. Precautions against Side Effects

In view of the high sensitivity of the emission of oxide cathodes to slight changes in environmental conditions, it was necessary to take certain precautions to insure that the effects observed were actually due to the incidence of ions of the gas under study upon the cathode. Preliminary experiments indicated that the change in background gas constitution accompanying either striking or quenching the discharge had a marked effect on the emission of the cathode, even though the cathode was held at a high enough potential that no ions could reach it. Therefore, it was necessary to turn the ion bombardment on and off by means of the voltage on the center electrode of the ion lens (see Figure 3) while maintaining the discharge at all times in order to maintain the most constant background gas constitution. Thus the ion bombardment was turned on by switching the voltage on the center electrode from a cut-off value to the value of optimum focusing (i.e., from 600 volts to 200 volts for a 1 kv discharge) and vice versa.

Even when the ion bombardment is controlled by the voltage on an intermediate electrode with no disturbance of the discharge, there remain two sources of uncertainty that the effects observed are actually

due to ion bombardment: (1) The current flowing to this control electrode and hence the cathode current will vary with its voltage (a "triode effect"), and (2) this varying current may cause outgassing of the control electrode and thus alter the background gas constitution. These two effects were checked by switching the voltage on the control electrode while the discharge was off and observing the change in emission of the cathode. It was found that there was a sudden jump of a fraction of one per cent in the cathode current upon switching the voltage on the control electrode, but that there were no rises or decays of the type observed during ion bombardment. Therefore, the only direct effect of the voltage on the control grid is the "triode effect" and this is easily measured under all experimental conditions and is taken into account in all the results reported here.

Although the above considerations establish that the emission changes observed throughout this study are definitely due to ion bombardment, the question of which ions are causing the effects must still be discussed. Although the gases introduced to the system are very pure, the residual pressure before introducing a gas was usually in the high 10^{-9} range and the gas was usually introduced to a pressure in the high 10^{-8} range, so that the gas could not be more than about 90 per cent pure. An additional source of impurity was the possibility that the intensification of the discharge because of the increase in pressure upon introducing a gas might cause additional outgassing of the discharge electrodes so that the partial pressure of the residual gas might rise along with that of the gas being studied. The discharge tube was believed to be sufficiently well outgassed that this effect was slight for two reasons:

(1) No increase in pressure was observed upon intensifying the discharge by raising its anode voltage; (2) With a gas flowing tnrough the system, very little pressure change was observed upon turning the discharge on or off. Therefore there is good reason to believe that the gas purity during most of the experiments to be described was about 90 per cent.

2. General Effects

The use of three different gases in this study and a comparison of the results for these different gases give evidence that the results obtained are actually characteristic of the specific gases, at least in the cases of oxygen and carbon monoxide. In the first place, the effect of ion bombardment by the residual gas in the tube was checked and was usually found to have a slight activating effect on the cathode. The gas to be studied was then admitted and, after the cathode had reached an equilibrium emission in this new atmosphere, the ion bombardment was turned on and its effect on the emission observed. When oxygen and carbon monoxide were used, the effect of the ion bombardment was always considerably greater than for the residual gas, and the effect of ion bombardment by oxygen was a poisoning of the cathode, as would be expected, while the effect of ion bombardment by carbon monoxide was an activation of the cathode in all cases. The fact that opposite effects were observed for oxygen and carbon monoxide is the most convincing evidence that the effects observed were characteristic of the gases being admitted rather than of the residual gas, since the effect of residual gas should be the same for the different gases under study. Further evidence of the reliability of the results is furnished by the study of the effect

with argon, which activated the cathode only slightly more than the residual gas present before admitting the argon.

In general, the predominant effect of ion bombardment of an oxide cathode by oxygen and carbon monoxide is a chemical one resulting from the deposition of the gas on the surface of the cathode by means of the ion beam. As mentioned this chemical effect is a poisoning of the cathode by oxygen and activation of it by carbon monoxide. In addition to this predominantly chemical effect, there seemed to be a minor mechanical effect, common to oxygen, argon, and presumably also to carbon monoxide, which was to activate the cathode somewhat. This is evidenced by the activating effect of argon and by a slight activation which was sometimes observed following the rapid poisoning by ion bombardment with oxygen. Although the chemical effects of ion bombardment predominated in the energy range studied (up to 2kv), the mechanical effects should be expected to increase with energy and so may actually predominate at the much higher voltages found in many beam-type tubes.

3. Reproducibility of Results

Because of the many experimental uncertainties usually encountered in studies on oxide cathodes, it was felt necessary to repeat the experiments on several cathodes to confirm the degree of reproducibility of the results. In all, experiments were carried out on three good cathodes and one extremely poor one. As the poor cathode was also in a poorly outgassed vacuum system, the percentage of residual gas was always very high and the results were generally valueless except to indicate further that the effect of ion bombardment by the residual

gases in a tube is usually to activate the cathode somewhat, as already mentioned. The good cathodes studied in the clean vacuum system ranged in activity from an emission, at the operating temperature of about 830°C, of 1.25 amp/cm^2 to somewhat over 4 amp/cm^2 .

The general effects of the gases, i.e., poisoning by oxygen and activation by carbon monoxide, were the same for all three good cathodes, although the extent of the effect varied considerably among the three. Even more important, it was found that the general form of the dependence of the effect of ion bombardment on the different external parameters (such as temperature or d-c emission), which makes up the central part of this study, was the same for the different cathodes.

In general, it was found that the degree of poisoning by ion bombardment with oxygen was much greater for the more active cathodes, whereas the amount of activation by ion bombardment with carbon monoxide was much less for the same cathodes. For this reason, most of this study was carried out on cathode No. 3, for which the emission in the outgassed state had leveled off at 1.25 amp/cm^2 after several sucessive days of poisoning by oxygen. On this moderately active cathode the effects of ion bombardment by both oxygen and carbon monoxide were of about the same magnitude and were sufficiently large to permit a detailed study of their dependence on external parameters.

V. EFFECT OF ION BOMBARDMENT BY OXYGEN

A. GENERAL QUANTITATIVE ASPECTS

The effect of bombarding an oxide cathode with oxygen ions was to decrease its emission under all conditions. A comparison of the poisoning effect of oxygen arriving at the cathode from the background gas with that of oxygen being deposited on the cathode by ion bombardment is shown in Figure 9. In this figure, short arrows representing the changes in emission caused by ion bombardment at several different pressures are superimposed on an ordinary curve of emission versus pressure, similar to Figure 5. To display the effect of ion bombardment in a manner convenient for comparison with the effect of the background oxygen, the amount of ion bombardment is expressed in Figure 9 in terms of an equivalent pressure increment. This equivalent pressure increment is that amount by which the pressure would have to be increased to give, according to the gas kinetic equation,

$$R = \frac{3.51\ (10)^{22}\ P}{\sqrt{M\ T}} \qquad \text{molecules/cm}^2\,\text{sec} \quad ,$$

the same increase in rate of arrival of particles at the cathode surface as that resulting from the ion bombardment, which is given by:

$$R = \frac{I_I}{1.6\ (10)^{-19}} \qquad \text{particles/cm}^2\,\text{sec} \quad ,$$

where

R = rate of arrival at cathode surface,

P = pressure in mm Hg,

M = molar weight of gas,

T = gas temperature in degrees Kelvin,

I_I = ion beam current density.

In general, when the ion gun is operated with a 1-kv discharge, the rate of incidence of ions is of the order of seven per cent that of molecules

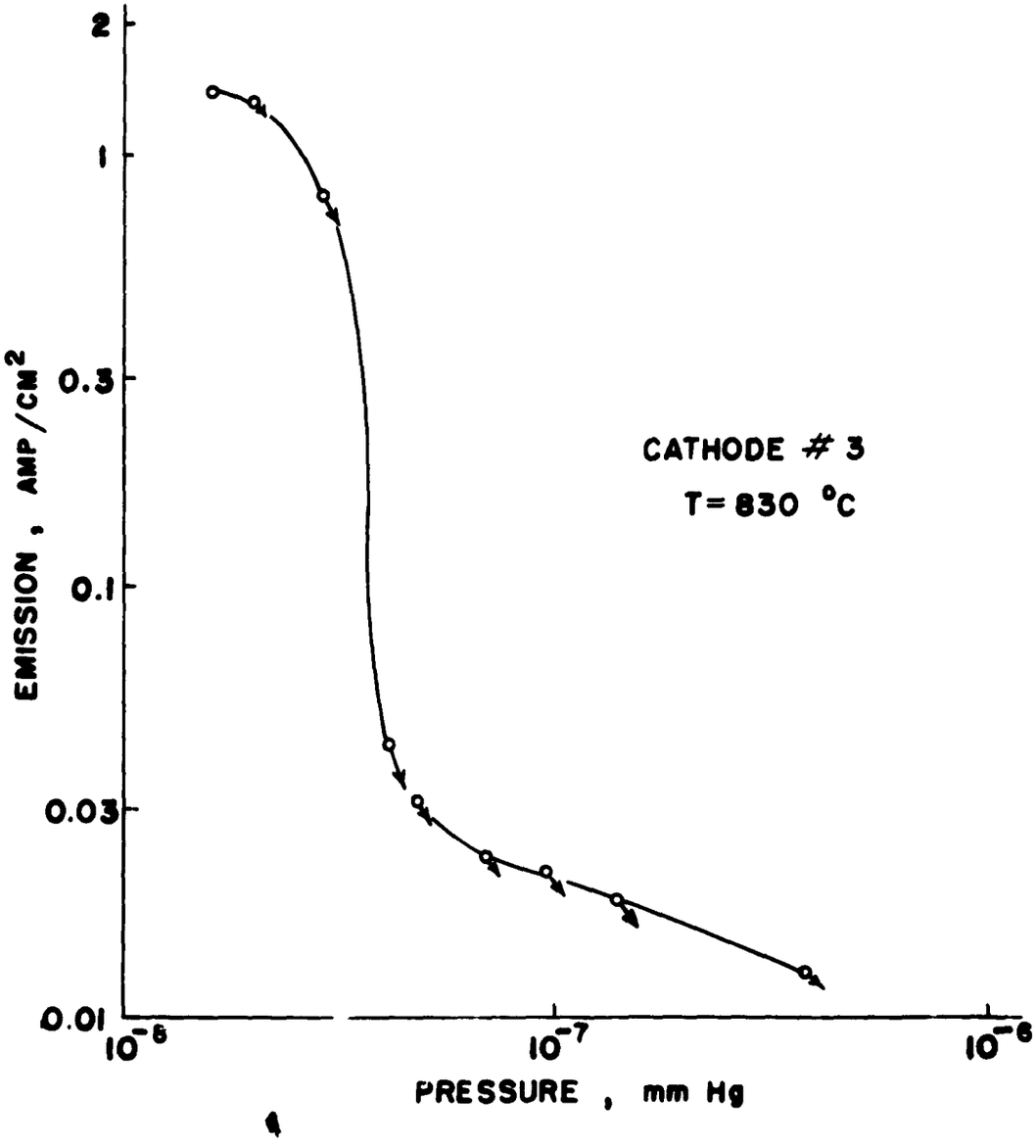

Figure 9. Comparison of Poisoning by Oxygen from Background Gas and from Ion Bombardment.

of the background gas at all pressures. Therefore, from the fact that the short arrows in Figure 9 are everywhere of steeper slope than the curve of emission versus pressure, it is obvious that oxygen particles arriving at the cathode surface by ionic deposition are somewhat more effective in poisoning the cathode than are oxygen molecules arriving from the gas phase. Perhaps the most striking feature of this result is the fact that the poisoning by ion bombardment with oxygen is only slightly greater than that by molecular oxygen.

At this point it is necessary to discuss the effect of the presence in the ion beam of O_2^{++} and O^+ ions in addition to the ordinary O_2^+ ions. First, considering the effect of the dissociated O^+ ions, it must be noted that the energy of the ions striking the cathode is mostly in the range of 200 volts to 400 volts, and since this is much greater than the dissociation energy of the oxygen molecule, most of the ions are dissociated immediately upon striking the surface. Therefore, the fact that some of the ions are already dissociated before striking the surface should have no effect on the results. As to the fact that each oxygen atom arriving in the form of O_2^{++} or O^+ is ionized, whereas only half those arriving as O_2^+ are ionized, it has been shown[30] that the state of charge of particles traveling through matter depends on their velocity and not on their initial charge before entering the material. Thus the only way in which ion bombardment by O_2^{++} or O^+ differs from ion bombardment by O_2^+ is that an oxygen atom deposited from O_2^{++} or O^+ has on the average twice as high a kinetic energy as an oxygen atom from O_2^+. Since the energy spread of the ion beam is of the order of the energy of bombardment anyway, this further spreading of the energy has only a slight effect.

The entire study of the effect of ion bombardment on oxide cathodes was carried out using a 1-kv discharge as an ion source, for which the ion current density was 0.4 μamp/cm^2 with a pressure at the cathode of $1(10)^{-7}$ mm Hg. Although this ion current could be tripled with a correspondingly by greater effect of the emission of the cathode by using higher anode voltages, the lower anode voltage offered better gas purity and less direct interaction with the emission of the cathode. Thus, since the small amount of ion current was sufficient for studying the effect on an oxide cathode, it was felt best to use this for the over-all exploratory investigation. In general, the effect of bombarding an oxide cathode with oxygen ions at these densities was to poison it 5 to 30 per cent.

B. FORM OF POISONING AND RECOVERY CURVES

Once the emission of a cathode has stabilized in the presence of a given pressure of oxygen, the poisoning by ion bombardment was found to be both completely reversible and repeatable, as shown in Figure 10. This completely reversible behavior illustrated in Figure 10 in only obtained after a cathode has been operated at a given pressure for a sufficient time for the emission to stabilize at this pressure, an apparently irreversible behavior being obtained otherwise. This irreversible behavior is illustrated in Figure 11, which shows the effect of successive periods of ion bombardment as the emission approaches a steady state at a pressure of $4(10)^{-8}$ mm Hg. Another feature of ion bombardment by oxygen on a cathode that has not reached a stable emission is that the amount of poisoning from ion bombardment is greater the farther the emission is from equilibrium, as can also be seen from Figure 11.

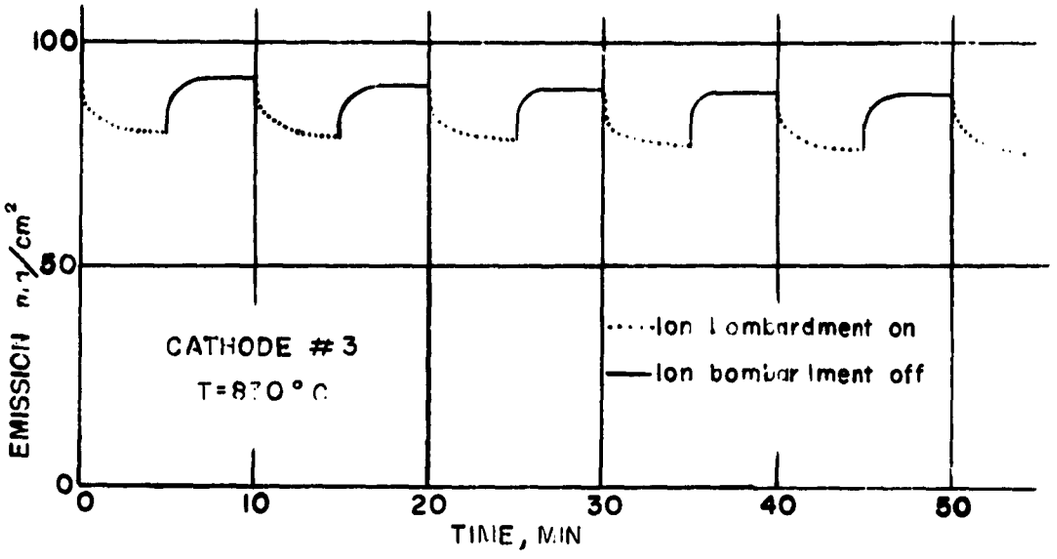

Figure 10 Reversibility and Repeatability of Effect of Ion Bombardment by Oxygen on Oxide Cathode

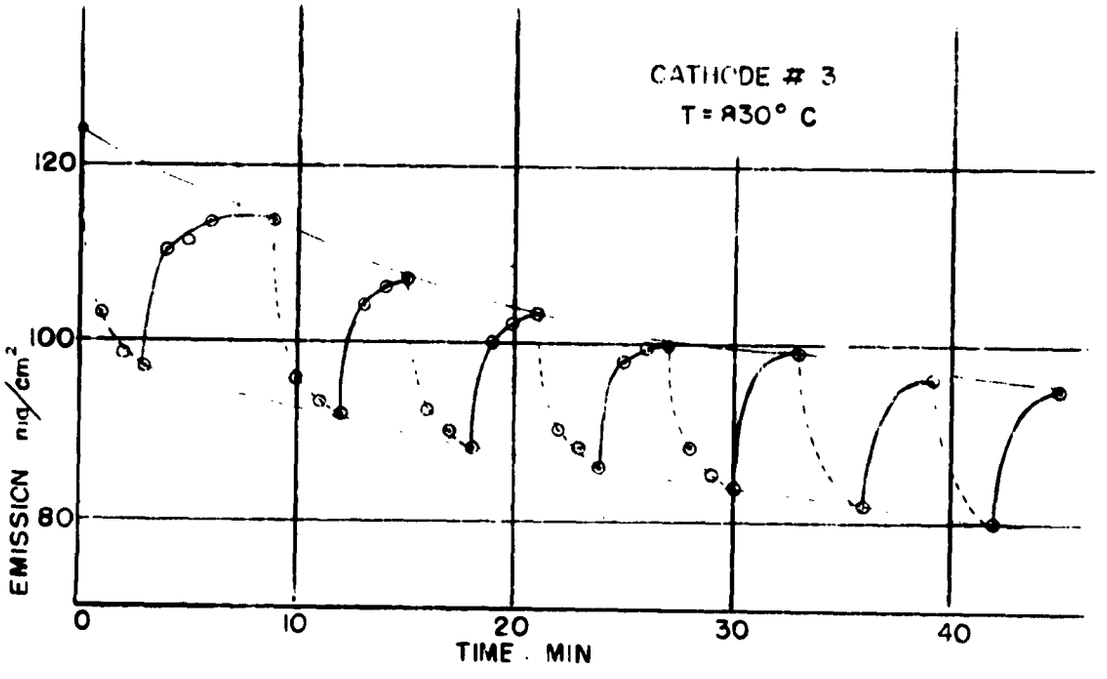

Figure 11 Behavior of Ion Bombardment Poisoning of an Oxide Cathode as Emission Approaches Equilibrium at $4(10^{-8})$ mm Hg of Oxygen

In order to obtain reproducible results, the data throughout the remainder of this study was taken only after the cathode had operated under each set of operating conditions long enough to reach a stable emission level and give results of the form shown in Figure 10.

Figures 12 and 13 are photographs of the traces on an oscilloscope of the top of the current pulse obtained as described in the section on methods of measurement. These photographs show in detail the initial portions of the curves in Figure 10, each spike representing the top of a separate 10-μsec pulse, the repetition rate being constant at 60 pulses per second and each figure containing three different sweep speeds.

In Figure 14, similar data is presented in a semilogarithmic plot, along with the curves given by Krusemeyer and Pursley[9] for the change in emission resulting from drawing d-c current. Since the curve given by Krusemeyer and Pursley is presumably the recovery of the emission after having formed a donor depletion layer by drawing d-c emission, and since it might be expected that the curve here represents the recovery after forming a donor depletion layer by deposition of oxygen, it should be expected that the curves would be of the same form. Since it is seen from Figure 14(b) that the curves are not of the same form, and in view of the considerations mentioned in the next paragraph, it is concluded that the simple picture of forming a donor depletion layer by deposition of oxygen does not adequately explain the poisoning of an oxide cathode by ion bombardment with oxygen.

From a comparison of several plots of the form shown in Figure 14, made at different times throughout the life of a cathode, it

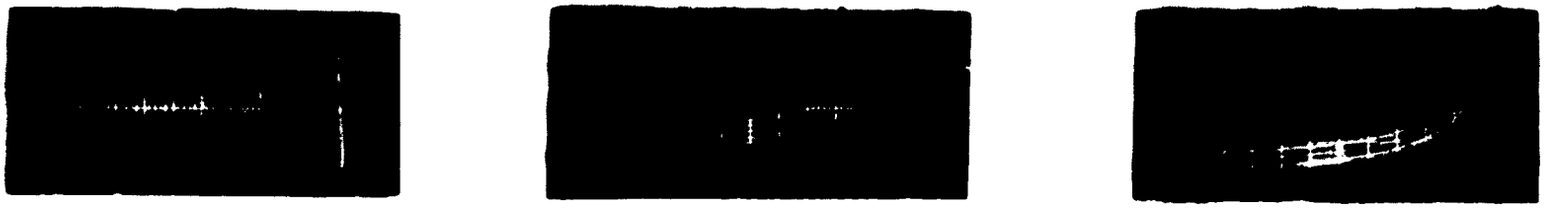

a) 0.05 sec/cm sweep b) 0.2 sec/cm sweep c) 1 sec/cm sweep

Figure 12. Decay of Oxide Cathode Emission After Ion Bombardment by Oxygen (Sweep from right to left, 0.2 ma/cm amplification).

a) 0.05 sec/cm sweep b) 0.2 sec/cm sweep c) 1 sec/cm sweep

Figure 13. Recovery of Oxide Cathode Emission After Ion Bombardment by Oxygen (Sweep from right to left, 0.2 ma/cm amplification).

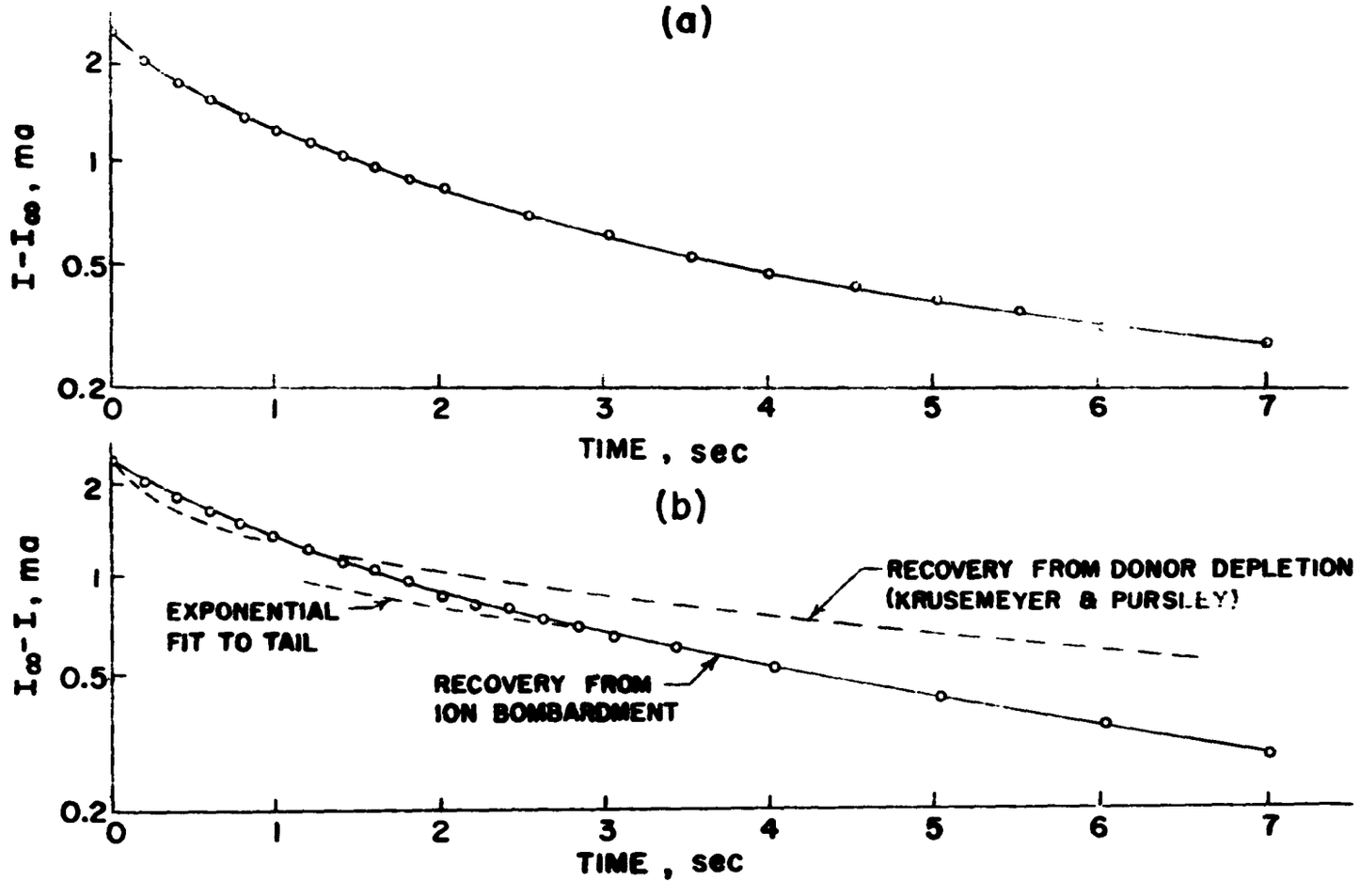

Figure 14. Semi-Logarithmic Plots of (a) Emission Decay during Ion Bombardment by Oxygen, (b) Emission Recovery after Ion Bombardment by Oxygen.

was found that the basic form of the curves varied a great deal, so that it was impossible to establish the basic form of the curve. One characteristic, however, was quite interesting and deserves some comment. As can be seen from Figure 14(b), the tail of the curve is fitted quite well by an exponential. The proportion of the curve that could be fitted well in this manner varied with the previous history of the cathodes and, indeed, in one case it was found that the whole recovery curve was almost exactly exponential in form. Thus, there is some evidence to indicate that two or more processes, one of which is exponential in form, are occurring during the recovery of the emission from poisoning by ion bombardment with oxygen. The fact that two or more processes are occurring during this recovery also explains the variation in the form of the curves as resulting from a variation in the relative importance of the different processes, which could quite easily depend on the previous history of the cathode. Rather than try to determine the various features of the form of the poisoning and recovery curves, which would probably be futile, it was felt more promising to select certain characteristics of these curves to summarize roughly the quantitative effect of ion bombardment, and to proceed to investigate their dependence on the other parameters that could be controlled.

In order to enable comparison of the effect of ion bombardment on an oxide cathode under different experimental conditions, it was necessary to decide upon certain features of the poisoning and recovery curves that characterized them quantitatively. For this purpose, the following variables were chosen as readily measurable and repeatable: the total emission change, Δ, from the cathode at equilibrium without ion

bombardment to the cathode at equilibrium with ion bombardment; the initial rate of decrease in emission, D_o, measured from the photographs during the first tenth of a second after beginning ion bombardment; and the initial rate of recovery of emission, R_o, measured in the same way. These variables are illustrated in Figure 15. To make comparison possible under different experimental conditions, and especially under different values of the initial emission current, I_p, the following five normalized variables are employed:

$$\Delta/I_p \ , \quad D_o/I_p \ , \quad R_o/I_p \ , \quad D_o/\Delta \ , \quad R_o/\Delta \ .$$

The physical significance of these normalized variables is described in Table I, and a discussion will be given in each section as to which of

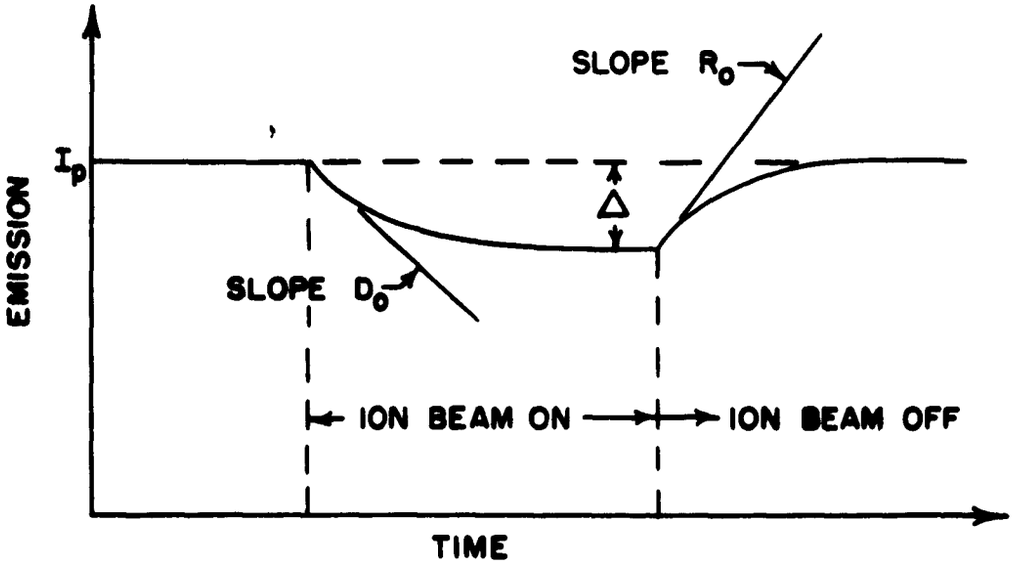

Figure 15. Basic Data Taken on Change in Emission of Oxide Cathode with Ion Bombardment by Oxygen.

these normalized variables is felt to be the most significant under variation of the particular parameter (for example temperature) being studied in that section.

Table I. Normalized Variables Representing the Effect of Ion Bombardment by Oxygen on an Oxide Cathode

Quantity	Units	Physical Significance
Δ/I_p	%	Normalized total decrement from ion bombardment
D_o/I_p	%/sec	Normalized initial poisoning rate
R_o/I_p	%/sec	Normalized initial recovery rate
D_o/Δ	sec^{-1}	Rate constant of the poisoning (proportional to reciprocal of time constant)
R_o/Δ	sec^{-1}	Rate constant of the recovery (proportional to reciprocal of the time constant)

Some discussion is in order as to the limited way in which the quantities D_o/Δ and R_o/Δ can be interpreted as the "rate constants" of the poisoning and recovery curves. If the decay (or recovery) were of the simple exponential form,

$$I = I_\infty + (I_o - I_\infty)\, e^{-\alpha t}$$

$$= I_\infty - \Delta\, e^{-\alpha t}$$

in which $\alpha(T)$ is the rate constant, then by differentiation,

$$\frac{\left.\frac{dI}{dt}\right|_o}{\Delta} \equiv \frac{D_o}{\Delta} = \alpha \quad ;$$

so that for the simple exponential form, D_o/Δ is indeed the rate constant. Now for the somewhat more general form, $I = I_\infty - \Delta f(\alpha t)$,

$$\left.\frac{dI}{dt}\right|_o = -\Delta f'(0)\,\alpha \quad ,$$

or

$$\frac{D_o}{\Delta} = (\text{const})\,\alpha \quad ;$$

so that D_o/Δ is still proportional to the rate constant in this more general form. However, this more general form is still too restricted to represent the data, since this form implies that by suitable normalization of the decrement and time scale all the curves could be made to coincide, which, as has already been mentioned, is not so. Despite these limitations on their meaning, the quantities D_o/Δ and R_o/Δ are still presented throughout the remainder of this report, since they do to a certain extent illustrate what is occurring, and since, in particular, their behavior throughout an experiment is an indication of whether the form of the decay and recovery curves remains constant.

With the cathode operating at a temperature of 830°C in an atmosphere of $5(10)^{-8}$ mm Hg of oxygen values of D_o between 5 and 10 per cent per second were obtained. This decay rate was due to an ion beam of 0.2 μamp/cm^2, or an incidence rate of $1.4\,(10)^{12}$ ions/cm^{2}sec on the cathode. The number of molecules of Ba O (or Sr O) in the cathode (in 0.1 square centimeter) is roughly $3(10),^{18}$ which, when compared with the total incident rate of $1.4(10)^{11}$ ions/sec, gives a deposition rate of oxygen atoms of roughly 10^{-7} molecular fraction per second. This figure, however, is for the cathode as a whole, so that when it is considered that the distance of penetration into the surface is less than

about ten lattice spacings, it is seen that the initial rate of build-up of oxygen at the surface must be much greater than this.

Although, as already mentioned, the poisoning by ion bombardment with oxygen was quite reproducible over short periods of time, the amount of poisoning from a given ion current was observed to vary during the life of the cathode. This dependence on previous history is found for all phenomena concerned with the oxide cathode and, indeed, is one of the major obstacles to research in the field. In this study of ion bombardment no attempt was made to determine these "previous history" effects and it was taken as sufficient to establish the results as valid when they were repeatable on a short-term basis, and when the same form of dependence on the parameters was found at widely separated times. Nevertheless, some general observations were made of the variation of the effect of ion bombardment throughout the life of the cathode. First, the effect of ion bombardment by oxygen was found to increase throughout the life of the tube. Also, it was found that operating a cathode at a high temperature decreased its sensitivity to ion bombardment by oxygen immediately after cooling to a lower operating temperature.

C. EFFECT OF PULSE VOLTAGE

Since, as shown previously, when the cathode was poisoned by the presence of oxygen most of the voltage drop at low pulse voltages was across the cathode coating itself, the effect of ion bombardment by oxygen was studied as a function of pulse voltage in order to determine whether the resistance of the coating was increased in addition to the decrease in its emission. Typical results of this study are shown in Figure 16, the normalized total decrement, Δ/I_p, being the most indicative of the

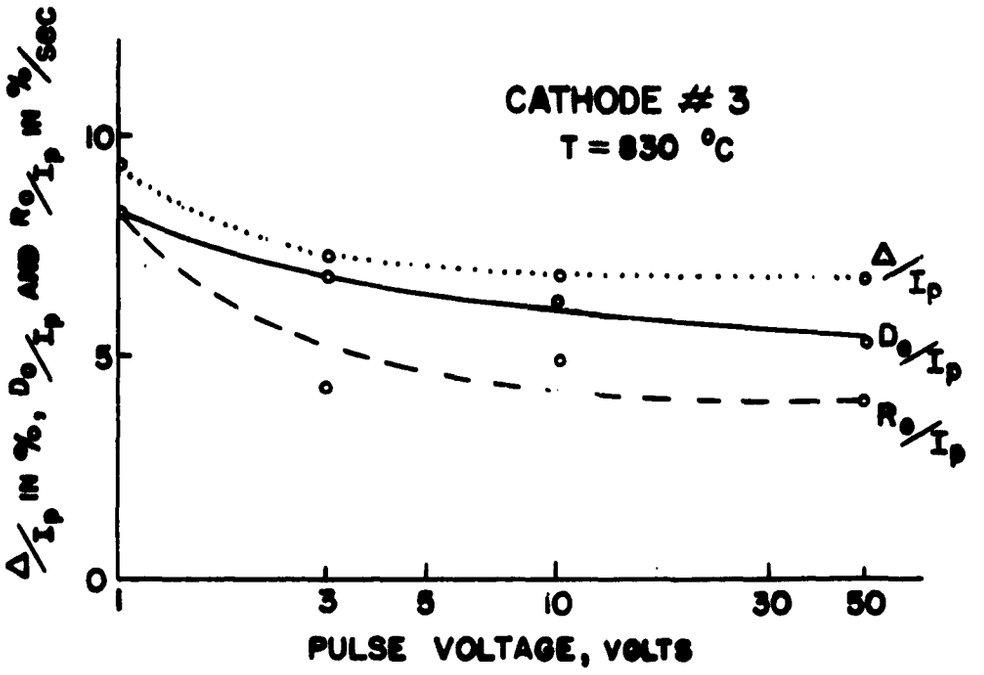

Figure 16. Dependence of Effect of Ion Bombardment by Oxygen on Pulse Voltage.

amount of poisoning, and the normalized initial rates being included as of interest also. From the fact that Δ/I_p did not fall off at low pulse voltage, it was concluded that the resistance of the cathode coating, as well as its emission was affected adversely by ion bombardment with oxygen.

Figure 16 shows two striking features: (1) the effect of ion bombardment is present at very low voltages; and (2) the initial rates of poisoning and recovery do not decrease at low voltages as would be expected if the poisoning were of the bulk resistance and required diffusion into the bulk. Furthermore, the total decrement and initial rates not only do not fall off with decreasing voltages, but actually seem to rise. Although the measurements carried out at the lowest voltage were naturally not as accurate as those at the higher voltages, the trend shown

in Figure 16 was observed in several runs and so may actually be significan..

Since the pore conductivity depends on thermionic emission from the walls of the pores, it can be seen that any change in the Fermi level should result in the same percentage change in both the saturated emission and in the pore conductivity. On the basis of a simple analysis it can be seen that this should be true of the solid conductivity also. At a given temperature, the dependences of the resistivity, ρ, and the saturated emission, J, upon the Fermi level are given by:

$$\rho = a\, e^{+ e\phi_i / KT} \quad , \qquad J = b\, e^{- e(\phi_i + \chi)/KT} \quad ,$$

where ϕ_i is the "inner work function" or the distance of the bottom of the conduction band above the Fermi level and χ is the electron affinity. Now if the effect of ion bombardment by oxygen is to lower the Fermi level by an amount $\delta \bar{\mu}$, there is an equal increase $\delta \phi_i$ in the inner work function. The corresponding changes in the resistivity and emission are:

$$\delta\rho = + \frac{e}{KT}\, a\, e^{- e\phi_i/KT}\, \delta\phi_i \quad , \qquad \delta J = \frac{e}{KT} = - \frac{e}{KT}\, b\, e^{-e(\phi_i + \chi)/KT}\, \delta\phi_i$$

so that the percentage changes are:

$$- \frac{\delta\rho}{\rho} = \frac{\delta J}{J} = \frac{e}{KT}\, \delta\phi_i = \frac{e}{KT}\, \delta\bar{\mu} \quad .$$

Although this treatment is an oversimplification in that the saturated emission is not necessarily what is measured and in that the Fermi level

and also the change in Fermi level are probably different in the bulk, it does show that the percentage changes in the resistivity and emission should be roughly the same. On the other hand, if ion bombardment by oxygen increased only the resistance of a layer near the surface of the cathode, without affecting the bulk resistance, it can easily be seen that the percentage change in the total resistance should be considerably lower; i.e., if $R = R_1 + R_2$ and only R_1 is changed, then

$$\frac{\delta R}{R} = \frac{\delta R_1}{R_1 + R_2} < \frac{\delta R_1}{R_1} .$$

Therefore, the experimental results indicate not only that ion bombardment by oxygen increases the resistance of an oxide cathode in addition to decreasing its emission, but, moreover, that all of the cathode resistance in series with its emission is affected.

In view of this conclusion, it is even more surprising that the initial rates of poisoning and recovery do not fall off with decreasing pulse voltage. Thus, if the resistance concerned is spread out through the thickness of the cathode, it must be that the diffusion times involved are small compared to the time (0.1 sec) required to measure the initial rates of poisoning and recovery, so that the effect of ion bombardment by oxygen spreads rapidly and raises the resistance of the whole coating simultaneously. On the other hand, if the effect of oxygen does not spread throughout the coating as rapidly as this, then it must be concluded that only a thin layer near the surface is affected and that most of the resistance is contained in this thin layer. In either case it must be concluded that diffusion is not the rate-limiting process in the poisoning and recovery curves.

There appear to be two plausible explanations of the apparently greater effect of ion bombardment by oxygen on the cathode resistance than on its emission, although the experimental evidence is far from conclusive. First, since the energy levels in the bulk of the crystallites are probably different from those at the surface, perhaps the Fermi level in the bulk is decreased more by the oxygen than the Fermi level at the surface. This, however, is unlikely in view of the result of Hannay, McNair, and White[3] who found the emission to be proportional to the resistance over several orders of magnitude of poisoning. Second, if the ion bombardment by oxygen were decreasing the electron affinity (i.e., by sputtering) at the same time that it was lowering the Fermi level, this would cause the emission to decrease less than the resistance increased, and thus account for the experimental results.

Another possibility is that some sort of complicated interaction of the effect of ion bombardment with the patch effect may explain the results. That is, if different patches on the cathode surface having different activities are poisoned in different amounts, the net effect would be a change not only in the work function and resistance, but also in the constant A in the emission equation. The interaction of all these changes could add up to the effect observed here.

The dependence of the rate constants of the effect of ion bombardment by oxygen on an oxide cathode on the pulse voltage is shown in Figure 17. It is seen that the rate constant for the poisoning is essentially constant, whereas the rate constant for the recovery seems to rise at the lower voltage. This is interpreted as evidence for the dual process explanation mentioned, in which the recovery of the process affecting the resistance is the more rapid one.

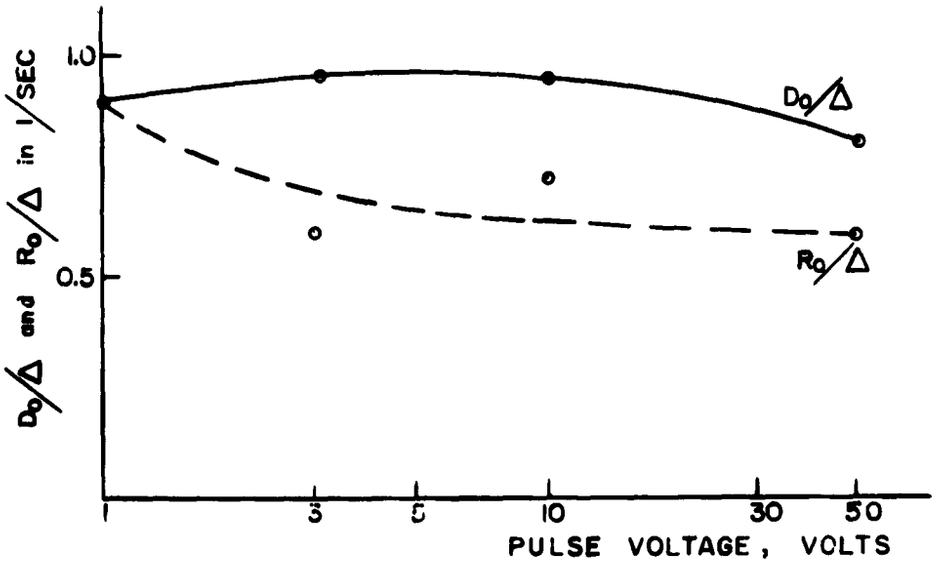

Figure 17. Dependence of Rate Constants on Pulse Voltage.

D. EFFECT OF ION BEAM DENSITY

Although the exact ion current striking the coated portion of the cathode could not be measured directly in the present experimental setup, the ion beam density could be changed more or less blindly by varying the voltage on the focusing electrode of the ion lens and the resulting changes in the different variables compared with each other.

For comparison, the observed results for the several variables are plotted in Figure 18 as a function of D_o/I_p, since this quantity is believed most likely to be proportional to the density of bombardment. Actually, even though D_o/I_p may not be proportional to the density of bombardment, the main purpose of Figure 18 is still served, since it displays the extent to which the various quantities are proportional among themselves.

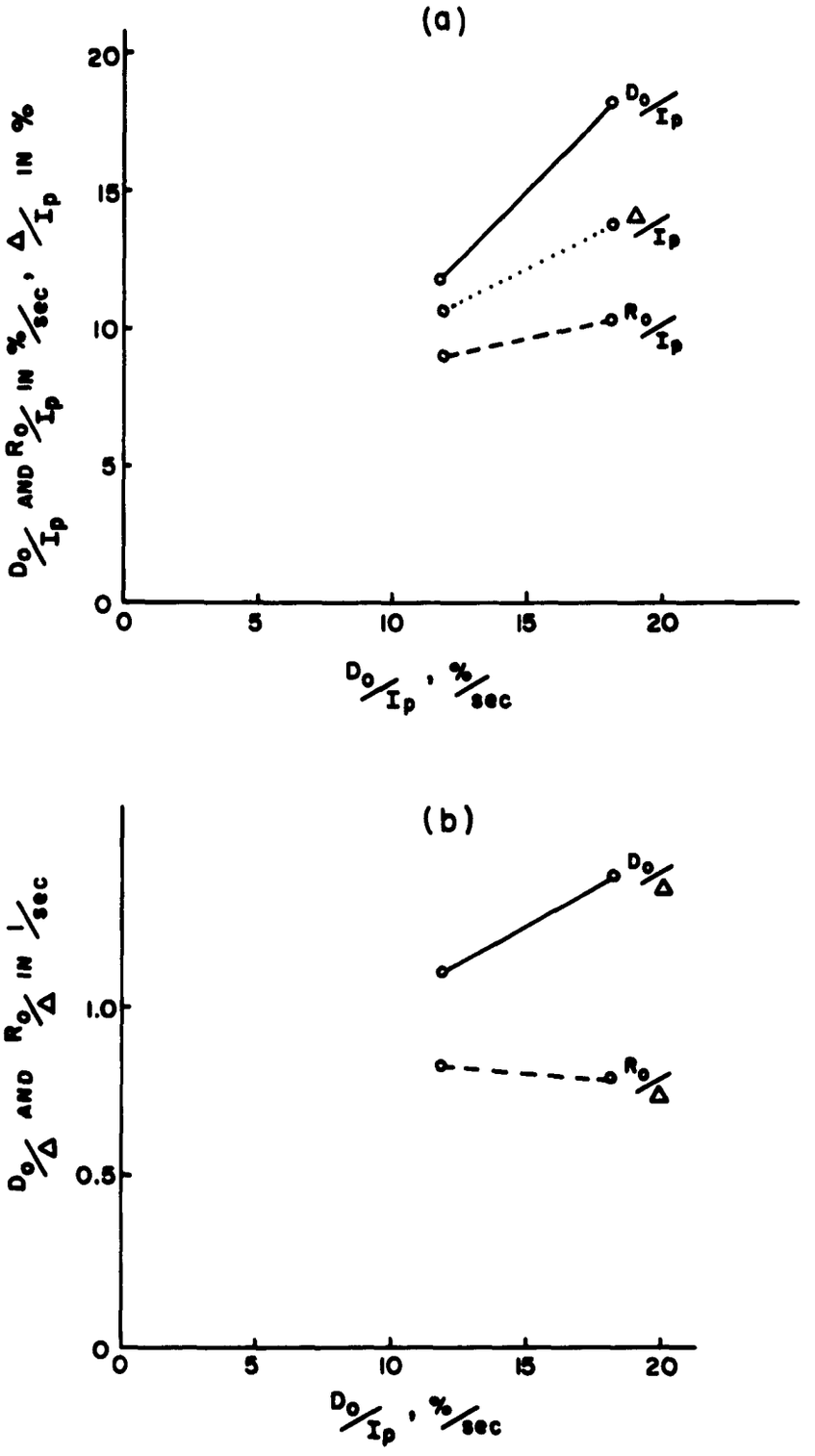

Figure 18. Dependence of Effect of Ion Bombardment by Oxygen on the Density of Bombardment: (a) Normalized Rates and Decrement; (b) Rate Constants.

It is seen in Figure 18a that the total decrement is not proportional to the ion current, and in fact is not increasing as fast as the ion current. This fact is made no less significant by the use of D_o as a measure of the ion current, since D_o should not be expected to be more than proportional to the ion current so that departure in proportionality of Δ and I_{10^+} must be as great or greater than displayed in Figure 18a. That this result cannot be explained simply by the existence of several mechanisms occurring during ion bombardment, all of which are proportional to the density of ion bombardment, can be quickly seen from the fact that the effect of all these mechanisms would still be proportional to the ion current density. Therefore this lack of proportionality between D_o and Δ must be due to the fact that Δ is large enough that a linear approximation is not adequate to express its dependence on the density of ion bombardment.

The nonproportionality of R_o and the ion beam density is to be expected from the behavio of Δ, and the fact that D_o/Δ varies is simply another statement of the effect that has just been discussed. The fact that R_o/Δ is constant indicates that the form of the return to equilibrium is the same in both cases and supports the interpretation of R_o/Δ as the rate constant of the return to equilibrium.

Perhaps the most significant aspect of this study of the dependence of the effect of ion bombardment by oxygen on the density of bombardment is the fact that the total amount of emission poisoning from the ion bombardment does increase with increasing ion current density. This confirms the fact that under ion bombardment, some sort of a readjustment of the equilibrium in the cathode occurs rather than simply an absolute

limitation on the amount of the bombarding material that can be "loaded" into the surface.

E. EFFECT OF ION ENERGY

One of the major aims of this study was to determine to what extent the energy of the incoming ions influences their effect on the emission of an oxide cathode. The apparatus used here was of limited suitability for this purpose in that the energy distribution of the ion beam was large (of the order of 200 ev - see Appendix A), thus limiting the lower extent of the energy range that could be studied. The upper limit of the energy range that can be studied is about 2000 volts, because of the establishment of some sort of a secondary discharge in the region of the cathode. The results of varying the ion energy over these limits are shown in Figure 19. Also included are lines representing the ion current density as a function of energy for comparison, since the ion current density was found to increase along with the energy of bombardment (see Appendix A).

Figure 19a shows that the initial poisoning rate is almost exactly proportional to the ion-beam density, indicating no dependence on the ion energy at all. In addition Figure 19a shows that the total decrement in emission rises less slowly than the ion-beam density with increasing ion energy. This lack of proportionality, however, is roughly of the amount to be expected from the results of the previous section (see Figure 18a), so that again there is apparently no dependence on ion energy. Again, with reference to Figure 19b, it is seen that the rate constant, R_o/Δ , of the emission recovery is essentially constant, indicating that the form of the recovery is the same, and that therefore

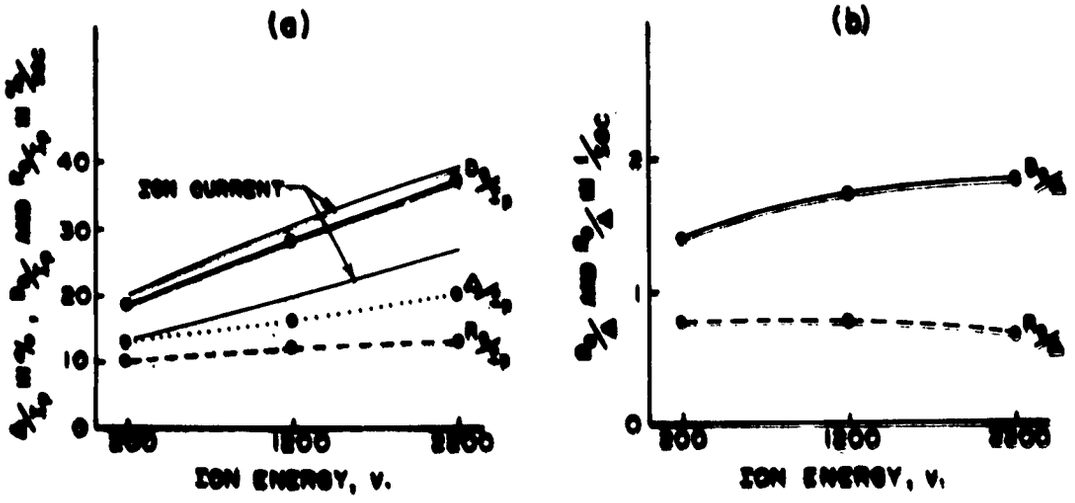

Figure 19. Effect of Energy of Bombardment on (a) Initial Rates and Total Decrement, (b) Rate Constants.

no radically different mechanisms are arising. Therefore, it is concluded that in the range of 200 ev to 2200 ev, the effect of ion bombardment by oxygen on the short-time emission properties of an oxide cathode depends little if at all on ion energy.

It can be inferred from this result that the mechanical effects of ion bombardment have little effect on the emission of an oxide cathode over short times, since these mechanical effects (e.g. sputtering and defect production) should be roughly proportional to the energy of the ions. Of course, from a long-term standpoint higher energy ions are known to be more damaging, since the cathode coating is eventually eroded away by sputtering, which increases with energy.

Since ions of oxygen have been shown to be more efficient poisoning agents than gaseous oxygen, there must be a strong dependence

of the effect of ion bombardment on the energy somewhere below 200 ev, in which a transition to the effect of particles having thermal energies occurs. This would be most difficult to study, however, since the combination of narrow energy spread and high ion-current density is difficult to realize.

F. EFFECT OF D-C EMISSION

Perhaps the most interesting aspect of the effect of ion bombardment by oxygen on oxide cathodes is its dependence on the d-c current being drawn from the cathode. In order to avoid this dependence throughout the other phases of this study, a slight negative bias was maintained on the grid at all times. In order to study the dependence on d-c emission, a positive voltage was applied to the grid and the pulse voltage decreased by this same amount in order that the voltage applied to the grid during the pulse should remain constant. Although in this case the total current being drawn during a pulse was the sum of the d-c current and the pulse current, the pulse current alone was used for the normalization in obtaining the normalized variables since it was only the change in it which was being observed as a function of ion bombardment.

The effect of d-c emission on the several variables representing the effect of ion bombardment by oxygen on an oxide cathode is shown in Figure 20, in which it is seen that all the quantities decrease with increasing d-c emission. It is possible to gain some insight into the nature of the poisoning of the emission of an oxide cathode by ion bombardment with oxygen by considering these various quantities in turn.

First, considering the fact that the initial rate of poisoning by ion bombardment with oxygen was decreased by drawing d-c current, it is

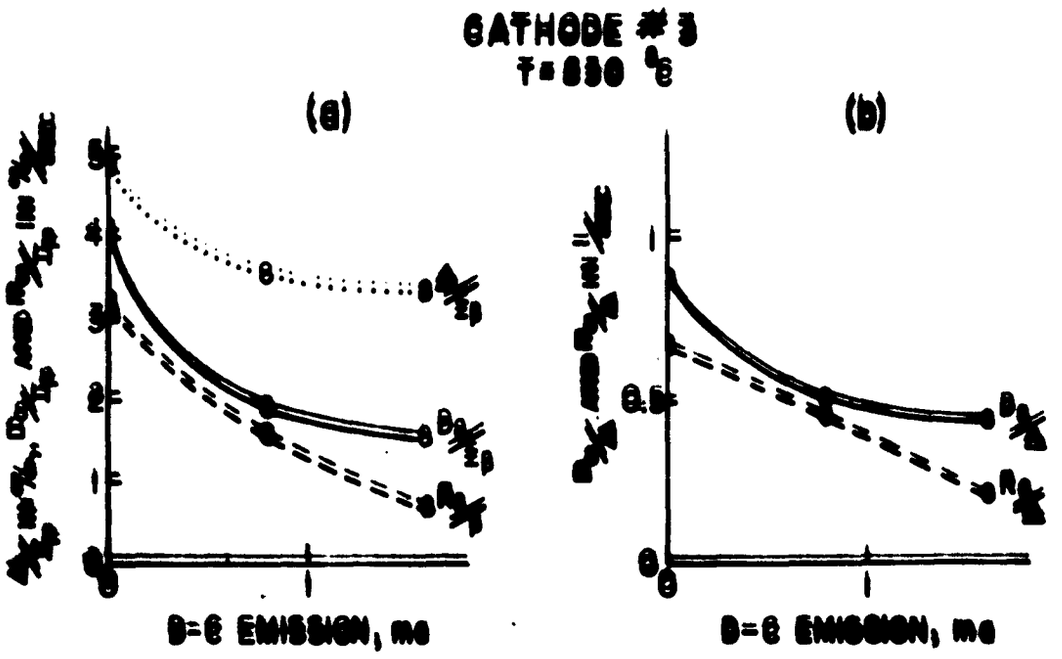

Figure 20. Dependence on D-C Emission Current of (a) Initial Rates and Total Decrement; (b) Rate Constants.

seen that, although ions of oxygen were entering the cathode at the same rate, their effectiveness was decreased sharply. If the oxygen deposited in the coating in this manner acted to poison the emission directly, say by forming acceptors, little effect on the initial rate should be observed. On the other hand, the observed result is explained qualitatively by assuming that the ion bombardment poisons the cathode by destroying donors, since for the lower donor density at the surface, with d-c current being drawn there should be less probability of an ion destroying a donor, which results in a lower poisoning rate. A similar consideration also facilitates explaining the dependence of the total decrement on d-c current, providing the additional assumption is made that each ion has a finite time after entering the cathode within which it must destroy a donor. The dependence of the total decrement on d-c current, however,

could also be explained on a model in which the ions are present in the surface of the cathode in the form of acceptors, and their equilibrium density is decreased by electrolytic elimination from the cathode.

The most distinctive result of this study is the fact that the initial rate of recovery from poisoning by ion bombardment with oxygen decreases with increasing d-c emission, and in fact, as can be seen from Figure 20a, decreases sharply. This result is distinctive, because it would be expected that, if electrolytic activation were important in the recovery from this poisoning, the recovery rate should be increased by drawing d-c emission. Since, on the contrary, the recovery is hindered by drawing d-c emission, it must be concluded that electrolytic activation plays a negligible role in this recovery, and furthermore, that the agent responsible for the recovery is hindered by the d-c field in the cathode. Therefore, the mechanism of recovery must be the replacement of removed donors, since ionized donors are the only agents that can be hindered by the applied field. A corollary of this conclusion is that a large fraction of the donors must be ionized in order to account for such a pronounced decrease in recovery rate as displayed in Figure 20a.

Furthermore, the fact that the "rate constants" of the poisoning and recovery also decrease sharply with increasing d-c current, as seen in Figure 20b, is more evidence that the basic process is changing rather than that the results are due simply to a lower sensitivity to poisoning in the condition of lower activity during d-c emission.

G. TEMPERATURE DEPENDENCE

The temperature dependence of the quantities representing the effect of ion bombardment by oxygen on an oxide cathode is shown in

Figure 21. It was originally expected that a study of the temperature dependence of the emission recovery would yield the activation energy

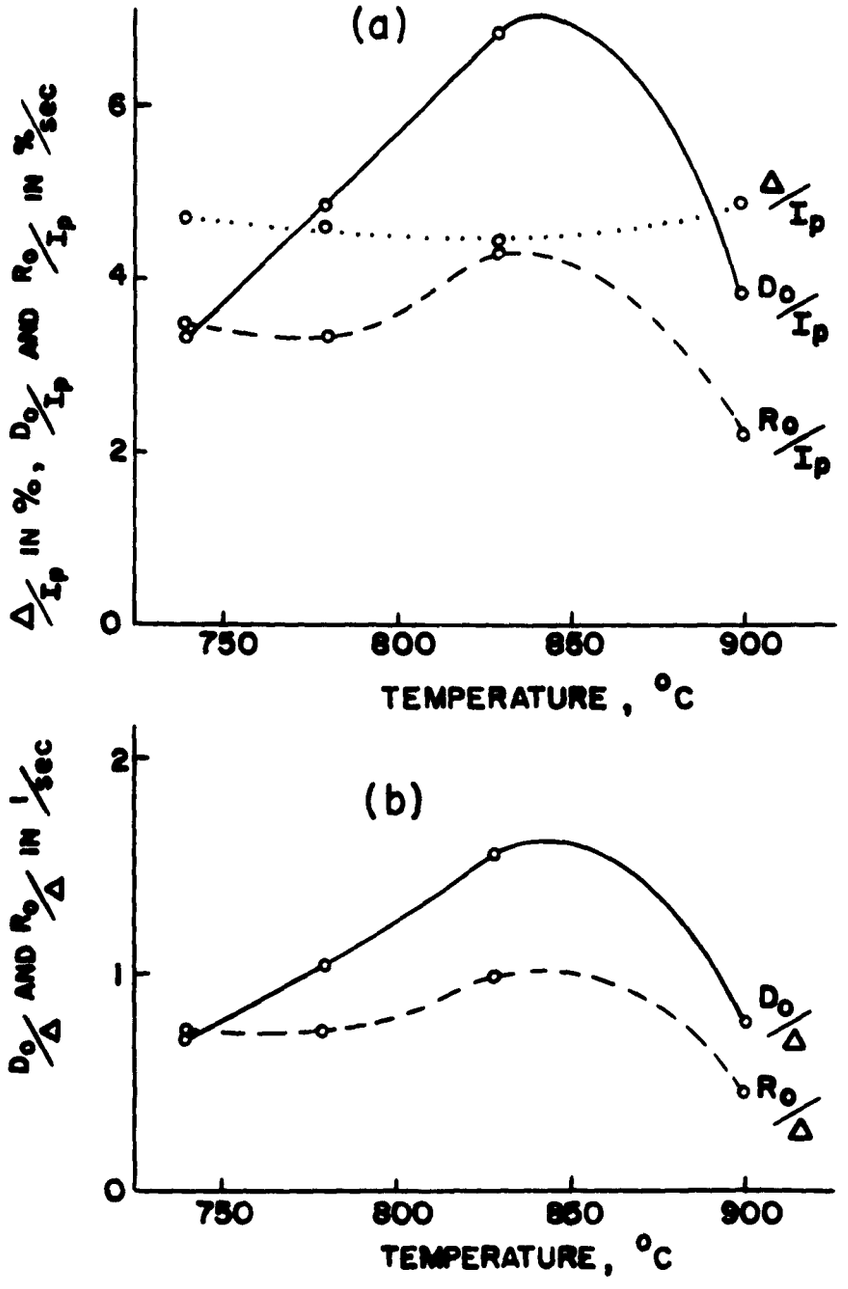

Figure 21. Temperature Dependence of (a) Initial Rates and Total Decrement, (b) Rate Constants.

of the rate limiting process, whether it were solid diffusion or a chemical reaction. However, as can be seen from Figure 21, there was no semblance of an activated type of behavior for either R_o/I_p or R_o/Δ over the temperature range studied. Although D_o did exhibit a temperature dependence over the lower half of the temperature range of the form to be expected for an activated phenomenon, it is difficult to see what significance to attach to this.

Although the emission below about 750°C was too low to apply the measurement technique used throughout this study, the emission was observed directly as a function of ion bombardment down to about 600°C. Using this method, the total decrement, Δ/I_p, could be obtained with somewhat less accuracy, and the initial rates could be only very roughly estimated. It was found that Δ/I_p fell off slightly (by about 20 per cent) at 600°C and that there was no drastic change in the initial rates.

Some consideration shows that the total decrement in the emission resulting from ion bombardment by oxygen should be just as sensitive to temperature as the initial rates would, if an activated phenomenon were involved. The reason for this is that, since the rate of arrival of ions is constant at all temperatures, and since the equilibrium is presumably reached between this arrival rate and some opposing process, then the position of this equilibrium as measured by Δ/I_p should have the inverse temperature dependence to the opposing process. Therefore, the total decrement in emission resulting from ion bombardment of an oxide cathode by oxygen being independent of temperature over the range 600°C to 900°C is further evidence that solid diffusion is not the rate-controlling factor in this phenomenon, since solid diffusion

should certainly have the strong temperature dependence characteristic of an activated process.

The fact that ion bombardment by oxygen actually poisons an oxide cathode less at low temperature brings out an apparent qualitative difference between the poisoning of a cathode by gaseous oxygen and by oxygen ion bombardment. This can be seen by reference to Figure 22, which shows qualitatively the Richardson plots of an oxide cathode in three different states: activated, poisoned by oxygen, and poisoned further by oxygen ion bombardment. Since the slope of the line of logarithm of J/T^2 versus reciprocal temperature is the Richardson work function, ϕ_R, given by

$$\phi_R = \phi_e - T \frac{\partial \phi_e}{\partial T} \quad ,$$

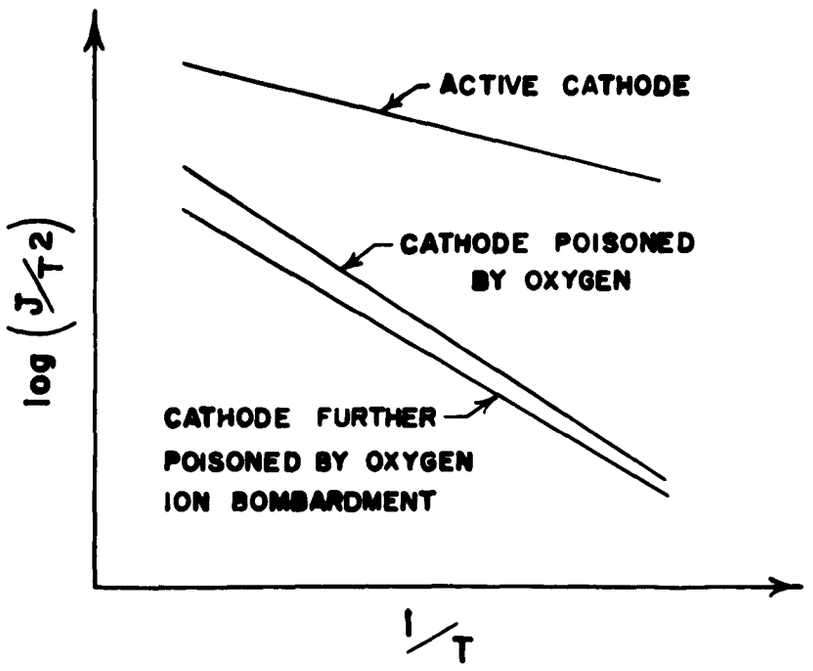

Figure 22. Qualitative Richardson Plot of Cathode in Three Different States.

where ϕ_e is the effective work function,[31] the fact that poisoning by oxygen raises the work function is seen to be equivalent to the statement that the poisoning effect of oxygen is greater at low temperature. Conversely, it also follows that the statement that oxygen ion bombardment poisons the cathode less at low temperature implies that it actually lowers the Richardson work function. However, since the emission is actually less under ion bombardment, the effective work function cannot have been lowered and it must be that $\partial\phi_e/\partial T$ was increased. An alternative explanation could be that ϕ_e was actually decreased and that the effective emitting area of the cathode was also decreased, although it is difficult to see how these two effects could occur simultaneously.

VI. EFFECT OF ION BOMBARDMENT BY CARBON MONOXIDE

A. GENERAL QUANTITATIVE ASPECTS

Bombarding an oxide cathode with carbon monoxide increased its emission under all conditions used in these experiments, which included a pressure at the cathode of $2(10)^{-8}$ mm Hg to $4(10)^{-7}$ mm Hg and a cathode temperature of 600°C to 830°C. Furthermore, the effect of ion bombardment by carbon monoxide is of a different nature from the effect of carbon monoxide molecules arriving at the cathode from the gaseous phase, as is illustrated by Figure 23.

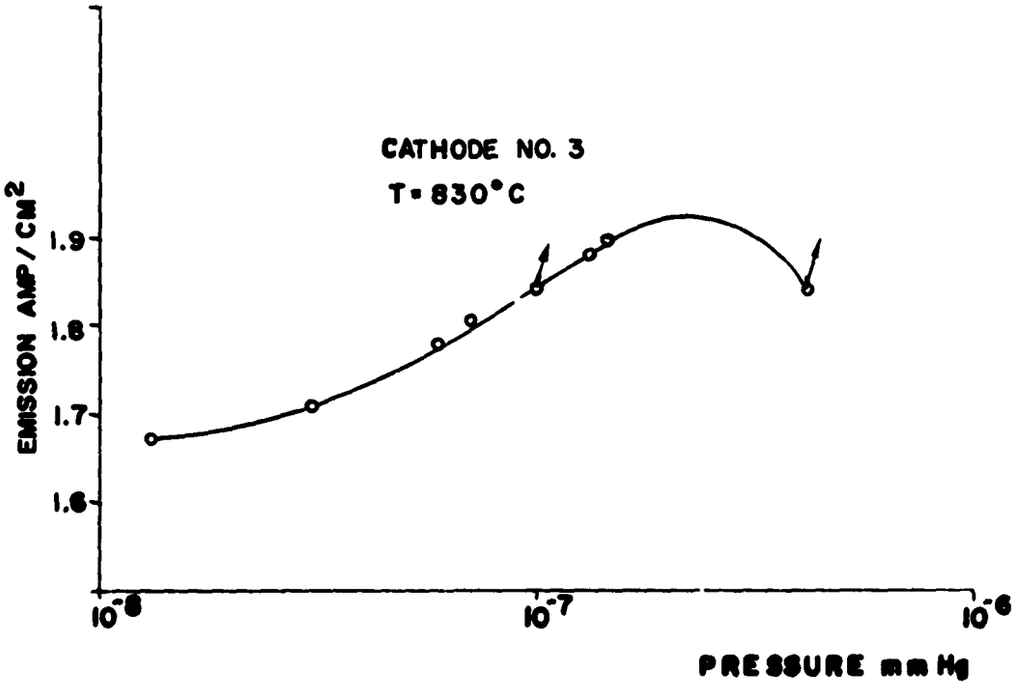

Figure 23. Comparison of Effect of Carbon Monoxide from Gas Phase with that from Ion Bombardment at Operating Temperature.

In this figure, the emission of an oxide cathode is plotted as a function of the pressure of carbon monoxide over the cathode, and also as a function of the rate of arrival of ions expressed as an equivalent pressure increment. This equivalent pressure increment is defined as the amount by which the pressure would have to be raised to increase the rate of arrival of carbon monoxide molecules at the surface by the same amount as they are arriving in the ion beam and is calculated in a manner similar to that for oxygen. As seen from the figure, the effect of increasing the arrival rate of particles by ion bombardment is much greater than that of increasing it by an increase in the pressure of carbon monoxide. Even more significant is the fact that the effect of ion bombardment is to activate the cathode even in a region where increasing the carbon monoxide pressure poisons it. Thus, the effect of ion bombardment by carbon monoxide cannot be explained simply by the change in the equilibrium of the cathode by a slight increase in the arrival rate of carbon monoxide molecules at its surface.

Another example of the difference in the effect of carbon monoxide arriving at the surface of the cathode by ion bombardment as compared to its effect arriving from the gas phase is the temperature dependence. Although the activation by gaseous carbon monoxide was slight in all cases and showed little temperature dependence, the effect of carbon monoxide deposited by ion bombardment increased strongly with decreasing temperature until, at about 600°C, it was possible to increase the emission by 60 per cent by ion bombardment. This pronounced behavior at the lower temperature is illustrated in Figure 24, the dashed line extending the

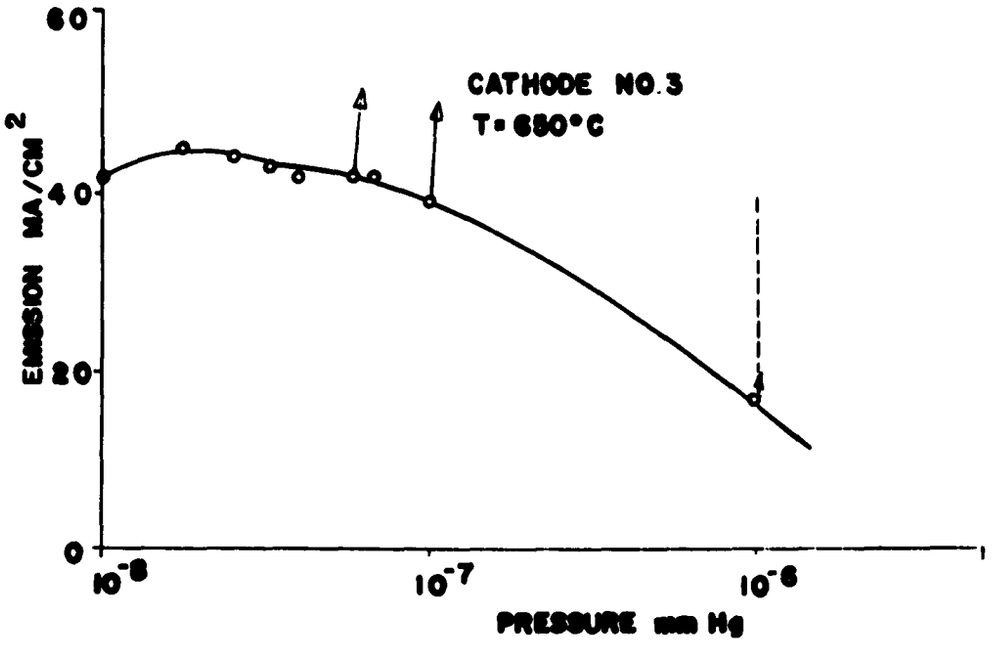

Figure 24. Comparison of Effect of Carbon Monoxide from Gas Phase with that from Ion Bombardment at Low Temperature.

arrow representing ion bombardment at the highest pressure is a rough estimate of the equilibrium emission that would have been reached, had the ion bombardment been allowed to continue long enough. The temperature dependence of the effect of ion bombardment by carbon monoxide will be discussed more thoroughly later in this chapter.

One obvious source for the difference in the nature of carbon monoxide arriving at the surface from the ion beam as compared to its arriving from the gas phase is the presence of several different species in the ion beam from an intense discharge such as that used here. Specifically, in addition to CO^+, the ion beam probably contains large percentages of CO^{++}, C^+, and O^+. Since most of the molecules entering a solid with energies of several hundred electron volts dissociate immediately,

and since the charge of a particle traveling through a crystal lattice is determined by its velocity rather than by its initial charge, the only difference between the effects of CO^+ and CO^{++} is a further increase in the effective energy spread. These considerations also apply directly to those amounts of C^+ and O^+ that are present in the ion beam in the same amounts. Thus, the only effect of the high degree of multiple ionization and dissociation in the ion source is that resulting from a stoichiometric excess of either C^+ or O^+ in the ion beam. Since C^+ and O^+ are usually present in approximately the same amounts,[32] such a stoichiometric excess is expected to amount to a small fraction of the total ion beam, but it could, nevertheless, have a strong activating effect if the excess is C^+. This must certainly be investigated in looking more closely into the fundamentals of the effects of ion bombardment by carbon monoxide on an oxide cathode, but for the present exploratory investigation, the presence of the several species is satisfactory and even desirable, since it corresponds closely to the case of the cathode in an electronic tube being bombarded by carbon monoxide ions from the residual gas in the tube.

B. FORM OF ACTIVATION AND DECAY CURVES

As with oxygen, the effect of ion bombardment by carbon monoxide was found to be both repeatable and reversible once a cathode had reached an equilibrium at a given pressure, as shown in Figure 25. In contrast to the results obtained for ion bombardment by oxygen, the form of the curves for the change in emission during ion bombardment by carbon monoxide was found to change with temperature. This is illustrated in Figure 26 in which it is seen that at a low temperature the activation during ion bombardment by carbon monoxide begins with a rapid rise and then proceeds for a

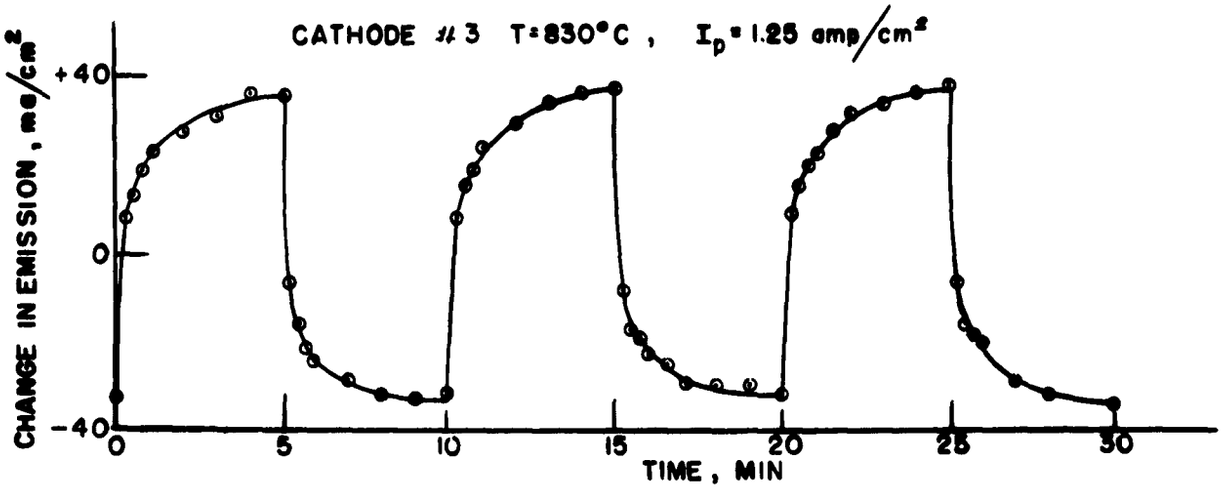

Figure 25. Reversibility and Repeatability of Activation of Oxide Cathode by Ion Bombardment with Carbon Monoxide.

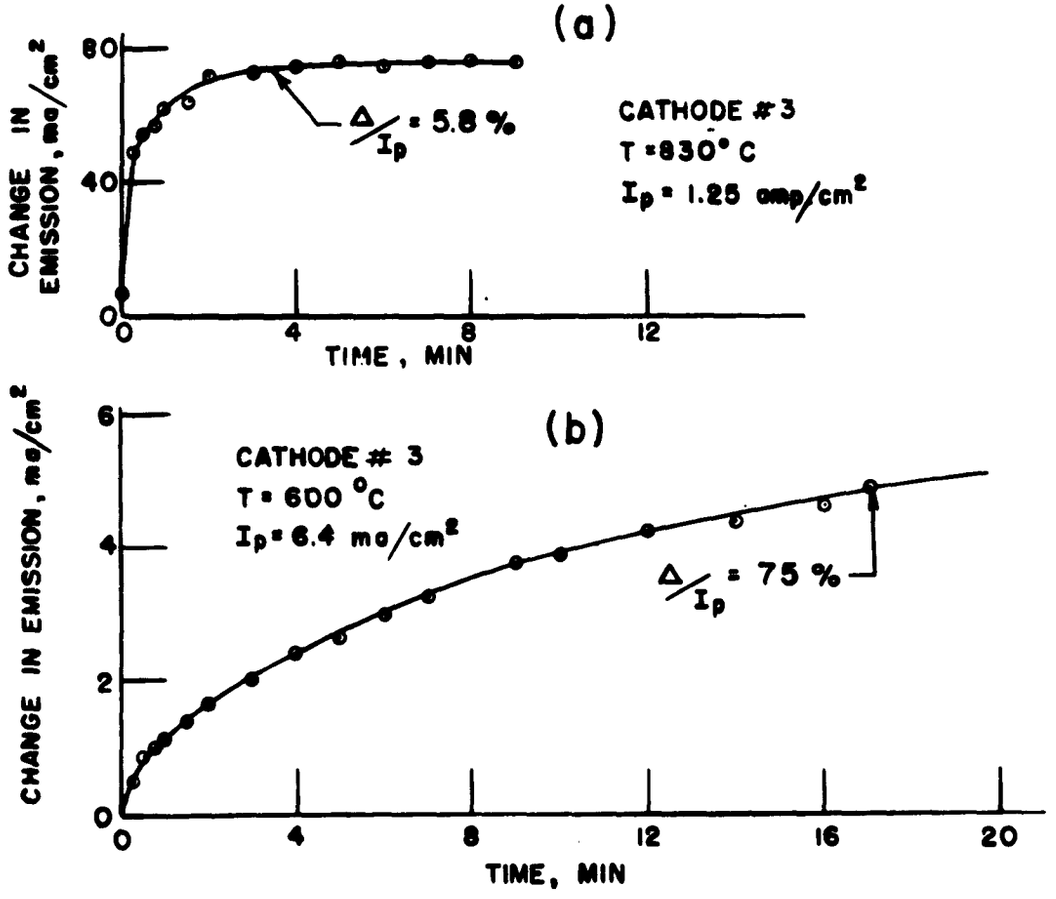

Figure 26. Effect of Cathode Temperature on Form of Activation Curve During Ion Bombardment by Carbon Monoxide: a) High Temperature, b) Low Temperature.

long time with a much slower rise, this long slow rise being absent at the higher temperature. The activation by bombardment with carbon monoxide at lower temperatures was also reversible, the decay curve having approximately the same form as the activation curve. This temperature dependence of the activation by ion bombardment with carbon monoxide is discussed further at the end of this chapter.

Details of the form of the activation curves resulting from ion bombardment by a $0.4\ \mu a/cm^2$ beam of carbon monoxide ions are shown in the photographs in Figure 27, the form of the decay curves in Figure 28, and semilogarithmic plots of these curves are given in Figure 29. Also included for comparison in Figure 29 are points of the curve published by Krusemeyer and Pursley[9] of the recovery of emission after having drawn d-c emission. Although there is no obvious reason why the activation by formation of donors by ion bombardment should follow the same curve as the activation after forming a donor depletion layer by drawing d-c emission, the agreement of the two curves is so good that it seems to be worth noting.

In order to characterize the effect of the ion bombardment by carbon monoxide in a study of the effect of varying different parameters, the initial rates of emission change and the total decrement were chosen in the same manner as for ion bombardment by oxygen. For clarity these rates are illustrated in Figure 30 and the normalized variables obtained from them are similar to those in Table I except that A_o is used instead of D_o.

A typical initial activation rate by an ion beam of $.4\ \mu a/cm^2$ on a cathode having an initial emission of $1.25\ amp/cm^2$ was 5 ma/sec, or about 4 %/sec. As in the case of oxygen, this rate of emission change is produced by a rate of deposition of carbon monoxide molecules in the cathode

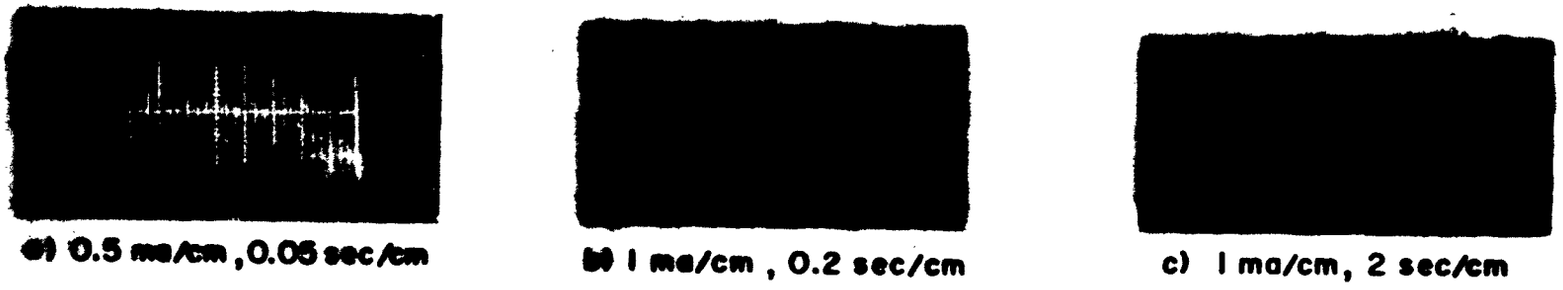

Figure 27. Activation of Oxide Cathode by Ion Bombardment by Carbon Monoxide.

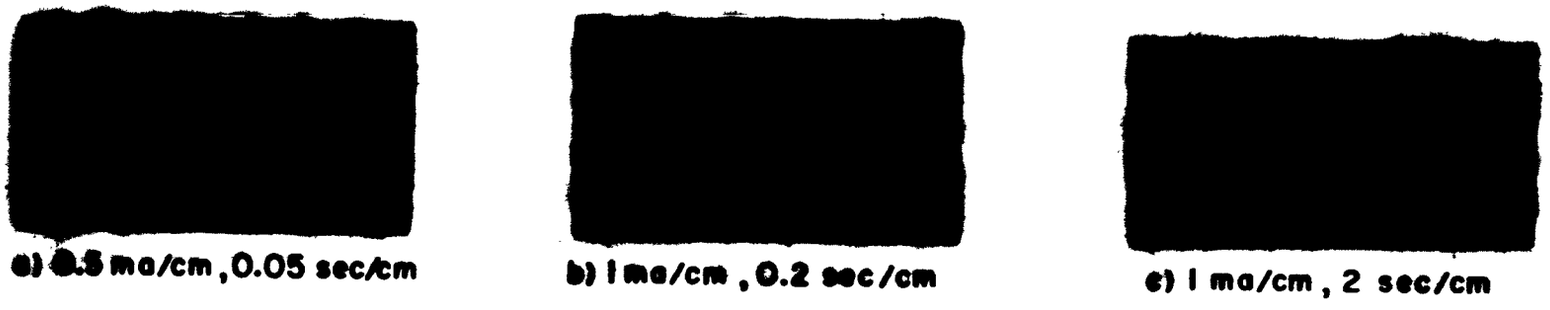

Figure 28. Decay After Cessation of Ion Bombardment by Carbon Monoxide.

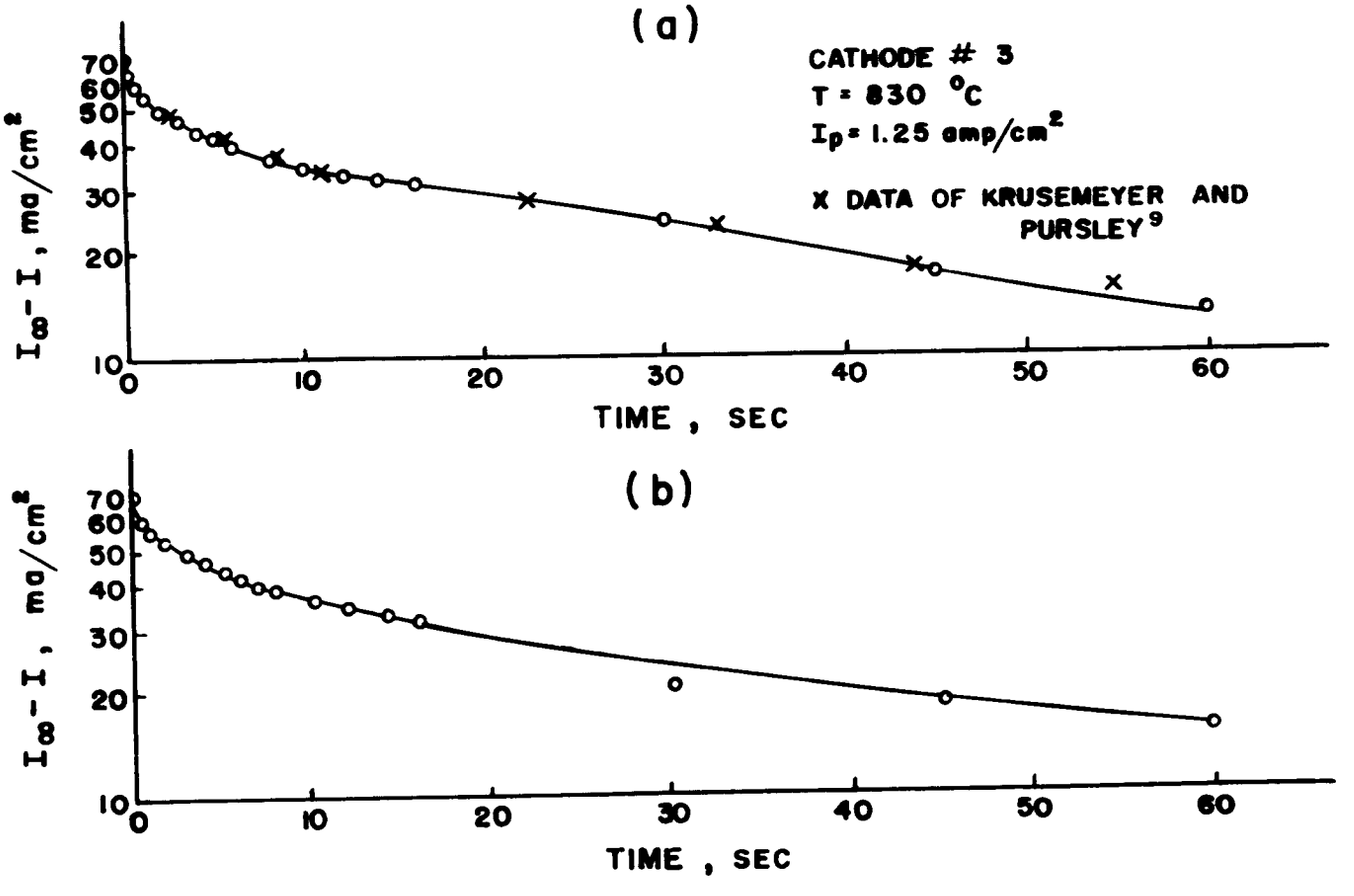

Figure 29. Semilogarithmic Plot of: (a) Activation by Ion Bombardment, (b) Decay after Ion Bombardment by Carbon Monoxide.

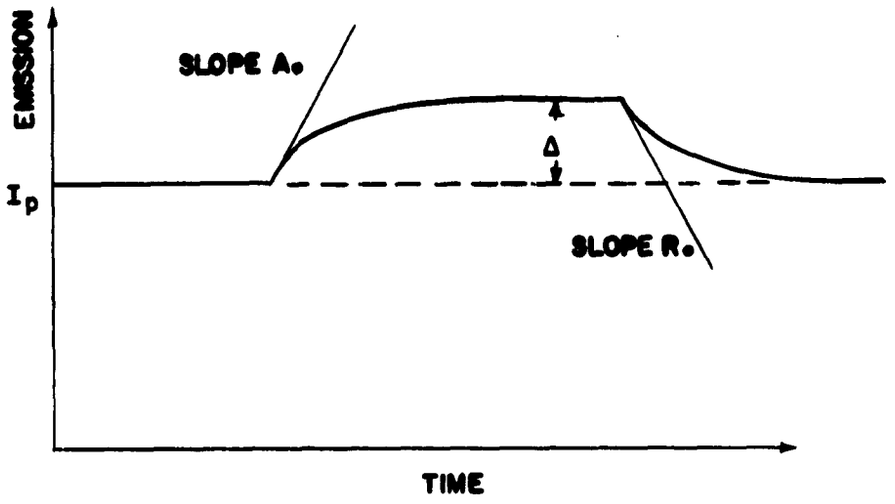

Figure 30. Variables Chosen to Summarize Effect of Ion Bombardment by Carbon Monoxide on Oxide Cathode.

amounting to 10^{-7} molecular fraction of the BaO molecules in the cathode per second. Again, unless this carbon monoxide is distributed throughout the cathode in much less than a second, the initial rate of building up of carbon monoxide at the surface must be much greater than this. Both the total increments and initial activation rates were much lower than this for cathodes having emissions of 3 amp/cms^2 to 4 amp/cm^2, but the effect was still activating in all cases.

As would be expected, the effect of ion bombardment by carbon monoxide varied throughout the life of a cathode, but the same variation as a function of the external parameters was observed independently of the previous history of the cathode as well as for different cathodes.

C. EFFECT OF PULSE VOLTAGE

The dependence of the quantities representing the effect of carbon

monoxide ion bombardment on the voltage of the pulse used to measure the emission is shown in Figure 31. It is seen that the effect of ion bombardment by carbon monoxide is very small for low pulse voltages. This is entirely in agreement with the previous conclusion that the cathode in its active condition has a low enough resistance that the voltage drop across the diode for low voltages is due to the space charge, with very little voltage drop across the coating itself. Thus changes in the resistance of the coating should have very little effect on the current flowing so that ion bombardment should be expected to have very little effect at low pulse voltages, which is what was found experimentally.

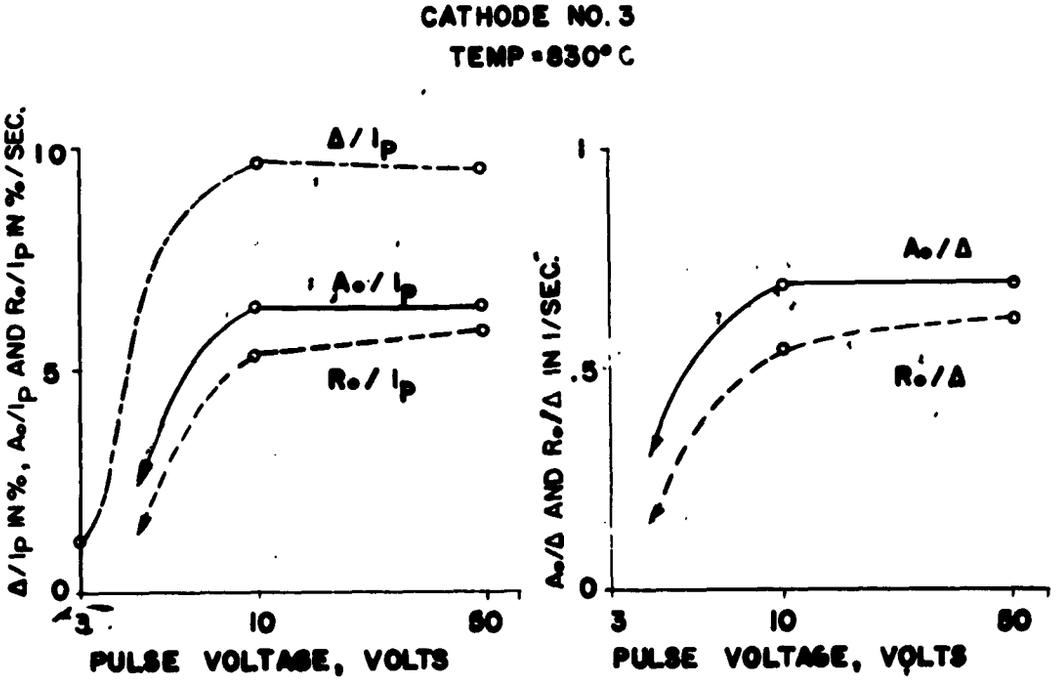

Figure 31. Dependence on Pulse Voltage of (a) Total Increment and Initial Rates, (b) Rate Constants. (The rates A_o and R_o in the low-voltage region were too low for accurate measurements.)

D. EFFECT OF DENSITY OF ION BOMBARDMENT

To display the effect of the density of ion bombardment without a method of measuring this density accurately, the various quantities observed are plotted in Figure 32 as a function of the initial rate of change of emission during ion bombardment in the same way as for oxygen. Assuming that the initial activation rate is proportional to the ion beam density, it is seen that the total increment in emission is more than proportional to the ion beam density. Since there is no reason to expect any sort of co-operative phenomenon, this effect, if real, must again be due to this amount of ion current having a great enough effect on the emission of an oxide cathode that a linear approximation is not valid.

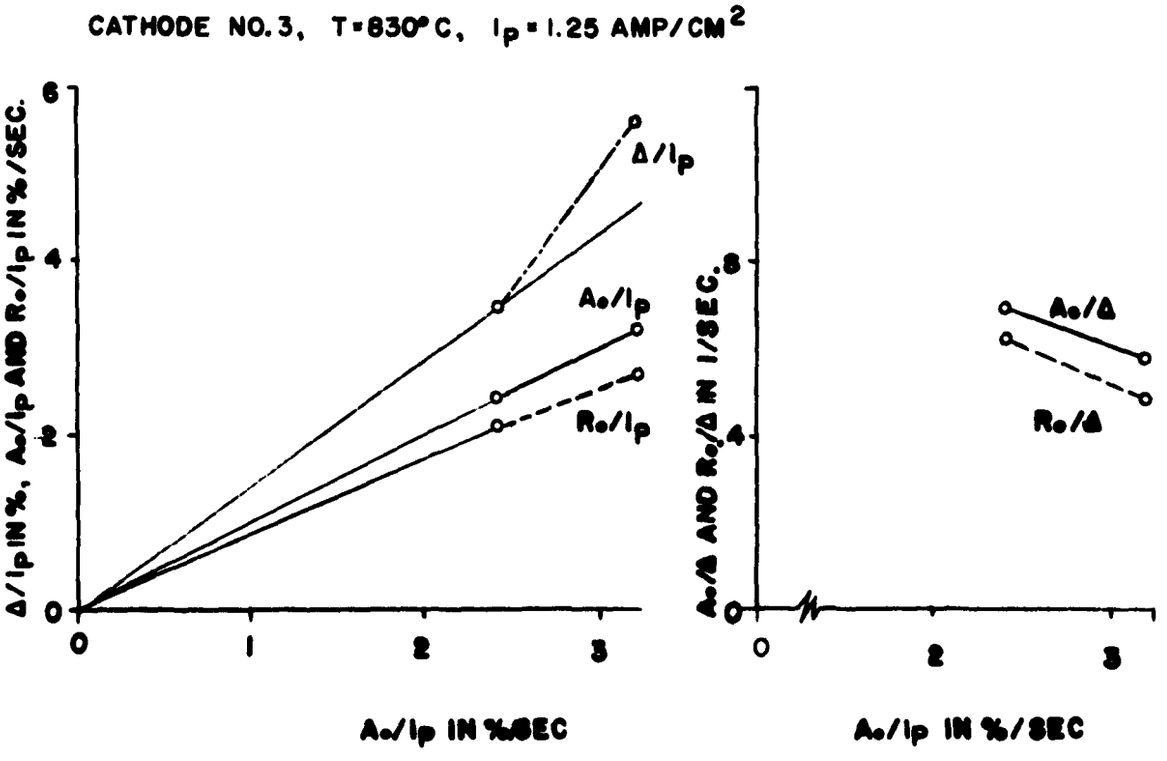

Figure 32. Dependence on Ion Beam Density of: a) Total Increment and Initial Rates, b) Rate Constants

Although the data concerning this phase of the study is not accurate enough to warrant any definite conclusions, the results do seem consistent enough with the corresponding results for ion bombardment by oxygen to allow a certain amount of speculation. Taking the results for both carbon monoxide and oxygen as valid, and making the assumptions that ion bombardment by oxygen causes a decrease in the donor density at the surface proportional to the ion current density, and that the activation by ion bombardment by carbon monoxide is due to an increase in the donor density at the surface that is proportional to the ion current density, it is seen that the results for both gases are in agreement; that is, the emission of the cathode is more than proportional to the donor density. This would indicate, for example, that the cathode is operating under conditions where the Fowler approximation does not apply, since this approximation predicts that the emission should be proportional to the square root of the donor density, which is the opposite of the result obtained here. In summary, it indicates that with the ion-current densities obtained, the effect on an oxide cathode is not simply proportional to the ion bombardment density, so that a careful study of the dependence of this effect on the density of bombardment should yield fundamental information on the operating conditions of the cathode.

As was mentioned in the case of ion bombardment by oxygen, the mere fact that the total increment was found to increase with increasing density of bombardment is of major importance, since this indicates that there is actually an adjustment of the operating equilibrium of the oxide cathode under ion bombardment by carbon monoxide rather than a simple limit to the amount of carbon monoxide that can be loaded onto the cathode surface by ionic deposition.

E. EFFECT OF ION ENERGY

The dependence of the quantities characterizing the effect of ion bombardment by carbon monoxide on the energy of the ions is shown in Figure 33, along with lines representing the ion-current density for reference. The energy dependence was only studied up to 1 kv with carbon monoxide since there was a noticeable outgassing at higher voltages

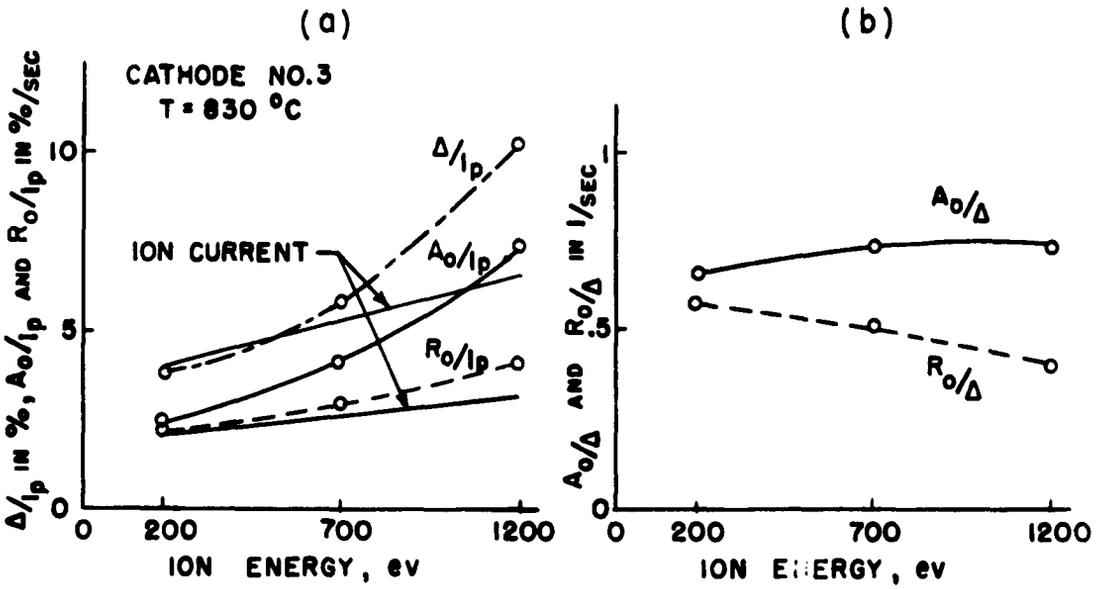

Figure 33. Dependence on Ion Energy of: a) Total Increment and Initial Rates, b) Rate Constants.

which rendered the results questionable. The reason the study could be carried to higher voltages with oxygen was that there was much less outgassing by the lower emission current of the poisoned cathode. Figure 33 shows that both the initial rate of activation and the total increment in emission increase with increasing ion energy more rapidly than does the ion current density. Thus, the activating effect of ion bombardment by carbon monoxide seems to be enhanced by increasing the energy of the bombarding ions.

Since the situation is complicated by the fact that the total increment in emission, Δ/I_p, increases more rapidly than in proportion to the ion current density, it is necessary to interpret the results of Figure 33 in the light of this nonproportionality as exemplified in Figure 32a. In order to facilitate this interpretation, the total increment is plotted in Figure 34 as a function of the ion beam density, varied both by increasing the ion bombardment energy and by defocusing the ion beam. Comparison of the effect of increasing the ion bombardment density in the two ways indicates that the increase in total increment with increasing energy of bombardment may be accounted for by the increase in ion beam density that accompanies increasing the energy of bombardment.

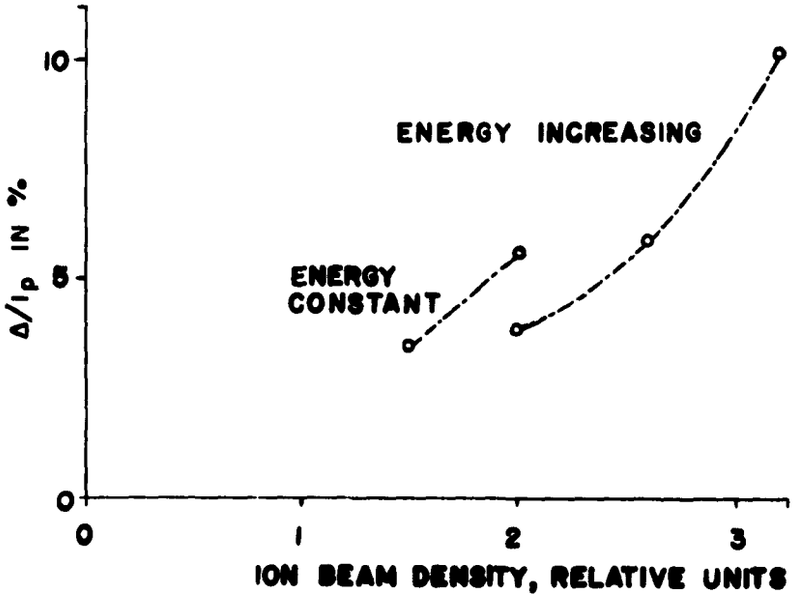

Figure 34. Dependence of Total Increment on Ion Beam Density with and without Increasing the Energy of Bombardment.

Therefore, the result of increasing the energy of ion bombardment by carbon monoxide seems to be to increase the initial rate of activation by the ion bombardment with little or no effect on the total amount of activation. The situation is sufficiently complicated, however, by the nonlinear dependence of the effect of ion bombardment on the ion bombardment density, that in order to draw any conclusions about the dependence on ion energy, it will be necessary to repeat these experiments with an apparatus in which the cathode is better isolated from the discharge than in the present set up so that the energy of bombardment can be increased without increasing the ion bombardment density.

F. EFFECT OF D-C EMISSION

The effect of d-c emission on the variables characterizing the effect of ion bombardment by carbon monoxide on an oxide cathode is shown in Figure 35. This shows that both the amount and initial rate of activation by ion bombardment with carbon monoxide increase with increasing d-c emission, and that the initial rate of return to equilibrium does likewise. The increase in the activating effect of ion bombardment by carbon monoxide in the presence of d-c emission is compatible with a donor depletion hypothesis in that replenishing a donor depletion layer should be expected to have more effect than adding donors to a cathode already at equilibrium. The fact that the initial rate of return to equilibrium is faster in the presence of d-c emission indicates that in this case migration of the donors into the bulk of the cathode must play an important part.

It is necessary, in interpreting the results of the effect of d-c emission for ion bombardment by carbon monoxide, to realize that the

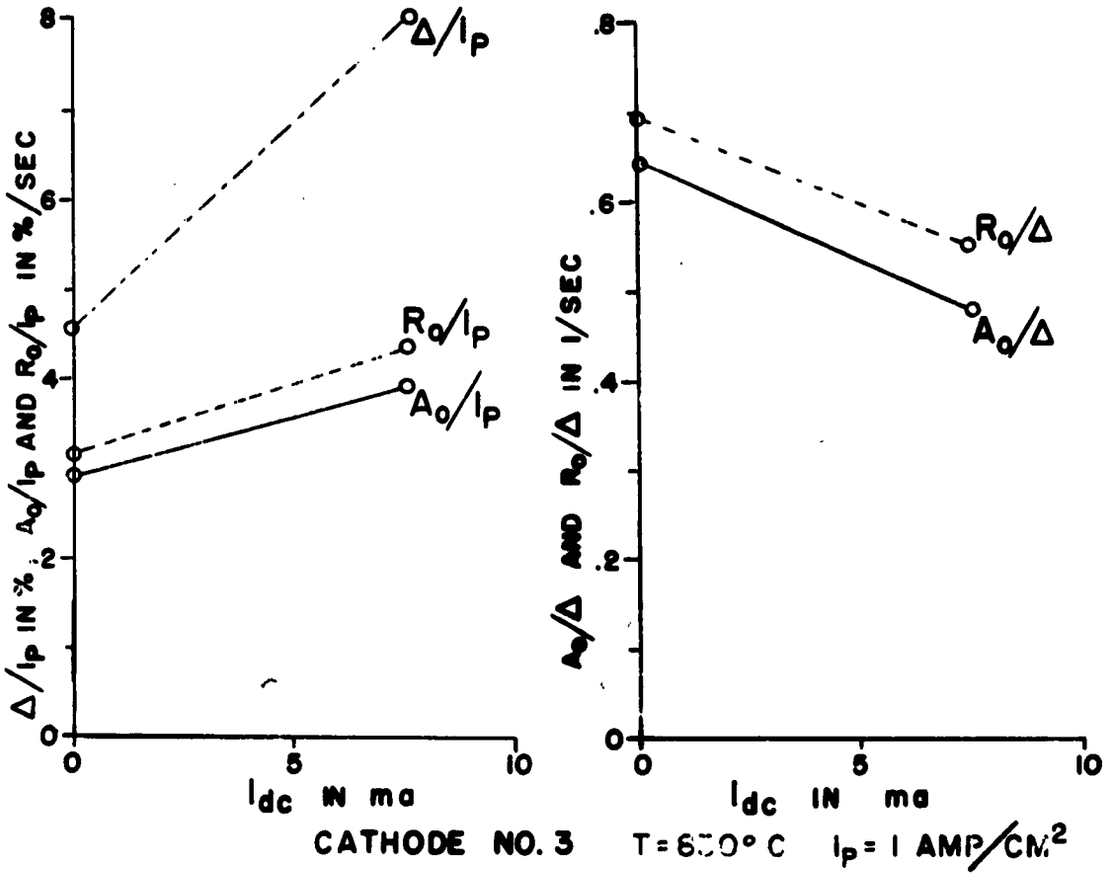

Figure 35. Effect of D-C Emission On: (a) Initial Rates and Total Increment, (b) Rate Constants.

true voltage during the pulse is the sum of the pulse voltage and the d-c voltage, and that the true emission current is the sum of the pulse current and the d-c current The variation observed during ion bombardment, however, is only the variation in the pulse current, as shown in Figure 36. As can be seen, normalizing to I_p will give values of the normalized variables that are somewhat too large, so that, neglecting the slight effect of ion bombardment on the space-charge limited current, the proper value to use for normalizations is $I_p + I_{dc}$. This has the effect of lowering the values of the variables in Figure 35 for the case of d-c emission by about

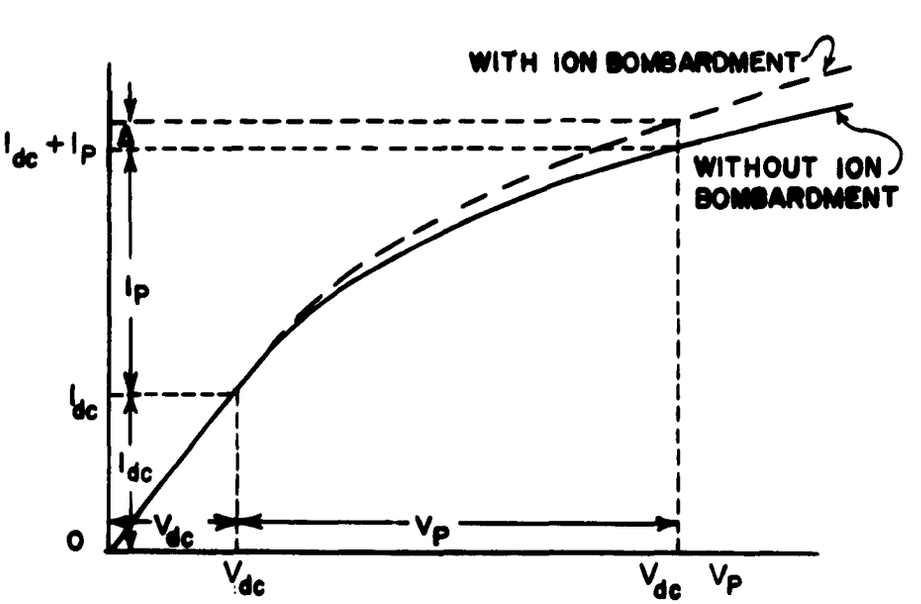

Figure 36. Voltages and Currents During Pulsing of Cathode in the Presence of D-C Emission.

7 per cent, which has no effect on the qualitative aspects. This correction was not necessary in the case of ion bombardment by oxygen since in that case both the space-charge limited and emission-limited currents were affected by the ion bombardment to approximately the same degree.

G. TEMPERATURE DEPENDENCE

Unlike the results for oxygen, the effect of ion bombardment of an oxide cathode by carbon monoxide showed a strong temperature dependence. An example of this has already been shown in Figure 27 and the effect will be presented here in more detail. The temperature dependence of the quantities characterizing the effect of ion bombardment is shown in Figure 37.

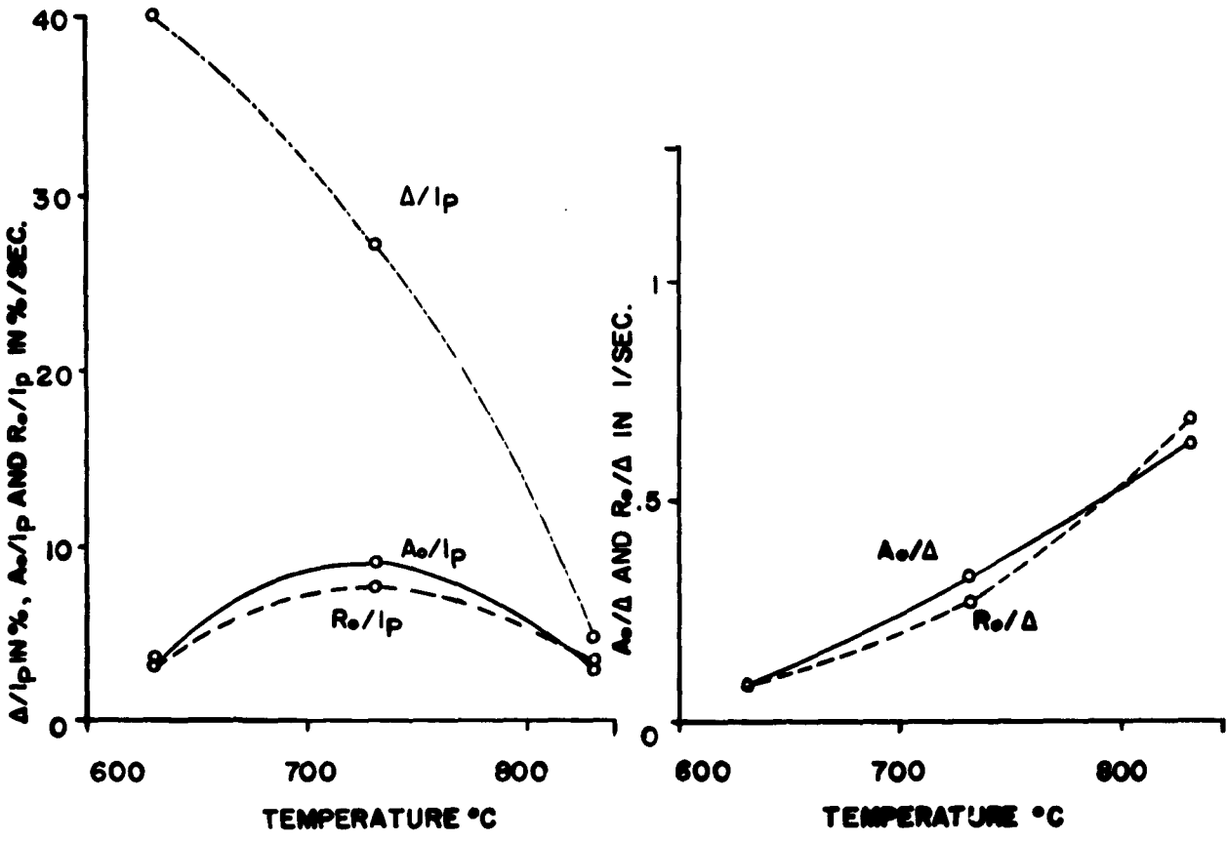

Figure 37. Temperature Dependence of: (a) Total Increment and Initial Rates, (b) Rate Constants.

In order to obtain information about the processes occurring in the oxide cathode from this temperature dependence, it is first necessary to determine the significance of the observed variables under varying temperature. If the quantities that are called the "rate constants" throughout this report were truly the rate constants of the processes involved, then their temperature dependence should yield the activation energy of the rate-governing process. Unfortunately, however, it is seen from Figure 26 that the forms of the curves are very different at high and at low temperatures,

so that the similar forms required for A_o/Δ to be actually a rate constant do not exist. The same problem, although not illustrated here, was encountered with the return to equilibrium after cessation of ion bombardment so that neither of the loosely termed "rate constants" seem to have a definite physical significance with variation in temperature.

When the adjustment of the emission of the cathode from equilibrium without ion bombardment to a new equilibrium in the presence of ion bombardment is considered generally, it can be seen that the new equilibrium must be reached between a constant rate of arrival of ions at the surface and a temperature-dependent opposing process (i.e., evaporation of donors, migration to interior of cathode, destruction by poisoning agents, etc.). Since the rate of arrival of ions at the surface is the same at all temperatures and it is only the rate of the opposing process that varies with temperature, the total emission change in adjusting to the new equilibrium, as measured by Δ/I_p, should be roughly proportional to the opposing rate process. That the emission change is not truly proportional to the donor density and hence to the opposing rate processes can be seen from the previously discussed nonlinear dependence of the emission on the ion-current density. Nevertheless, the total increment in emission seems to be the best measure available, from the present data, of the rate process opposing the activation of an oxide cathode by ion bombardment with carbon monoxide, and its logarithm is therefore plotted as a function of $1/T$ in Figure 38. As may be seen from Figure 38, there is no semblance of the straight line which should be expected for an activated phenomenon, except possibly at the higher temperatures.

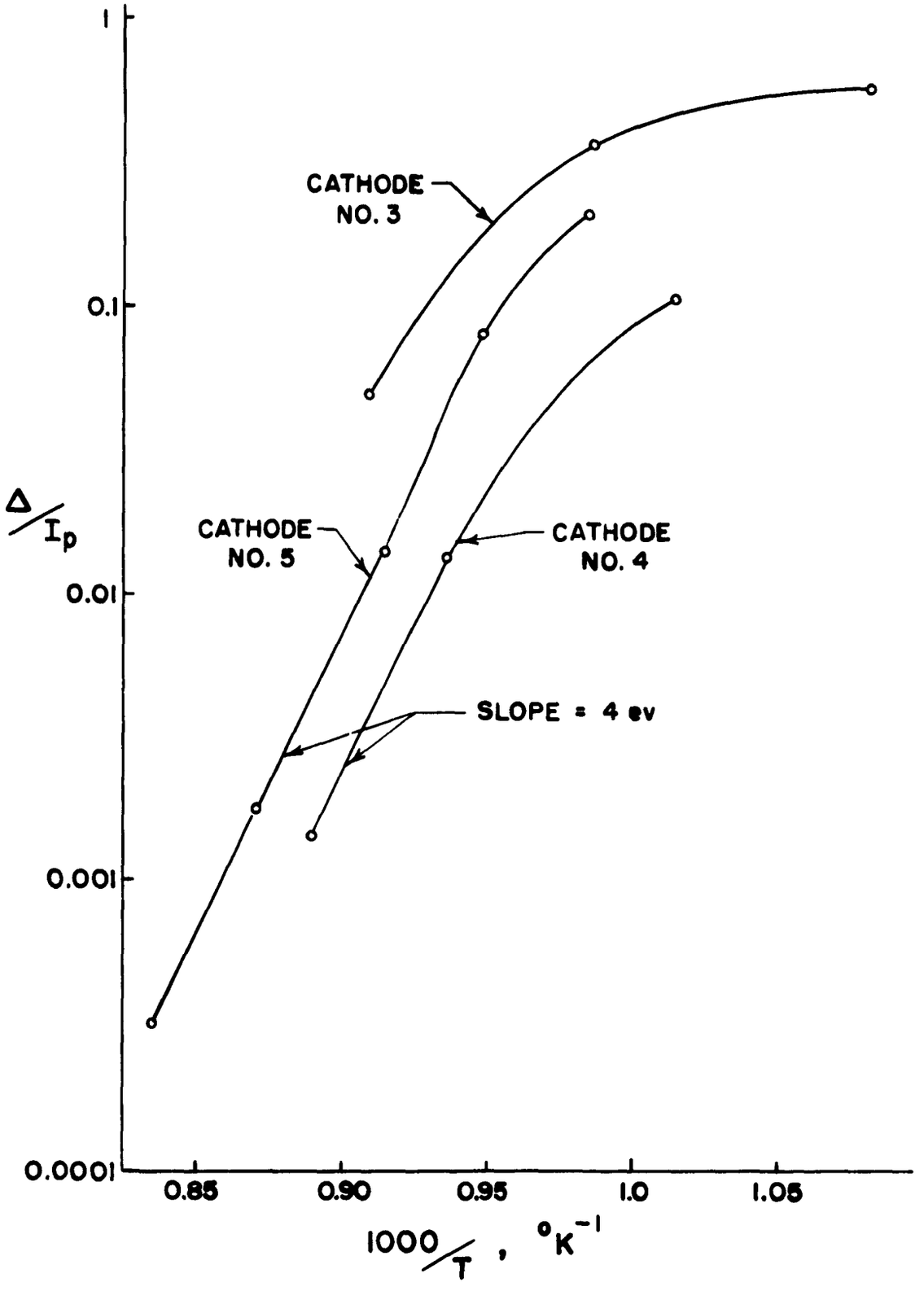

Figure 38. Activation Energy Plot of Total Increment in Emission by Ion Bombardment with Carbon Monoxide.

Because of the complications of the emission being a nonlinear function of the donor density, and the apparent existence of more than one rate-controlling process, it is not surprising that a straight line is not obtained for the logarithm of the increment versus $1/T$. However, since the increment is small at the higher temperature, thus allowing less non-linearity, and on the chance that a single process predominates at higher temperature, the activation energy is obtained for the high temperature portion of the curves in Figure 38. The activation energy thus obtained is 4 ev, which is to be regarded as a rough estimate for the reasons mentioned. It is interesting to note, however, that this value of 4 ev compares moderately well with the activation energy of 3.3 ev found in the same temperature range by Krusemeyer and Pursley[9] for the recovery from drawing d-c current.

VII. ION BOMBARDMENT BY ARGON

A. EFFECT OF ION BOMBARDMENT BY RESIDUAL GAS

Since it was expected that the effect of argon would be considerably less than that of the chemically active gases, oxygen and carbon monoxide, and hence more sensitive to impurities in the ion beam, the tube was again baked out and a brief study made of the effect of ion bombardment by the residual gases remaining in the tube. After bakeout, the residual pressure was $7(10)^{-9}$ mm Hg with the cathode at a temperature of 780°C and the discharge operating at 1 kv. Under these conditions, the emission of the cathode was 340 ma/cm^2 and the behavior under ion bombardment as shown in Figure 39.

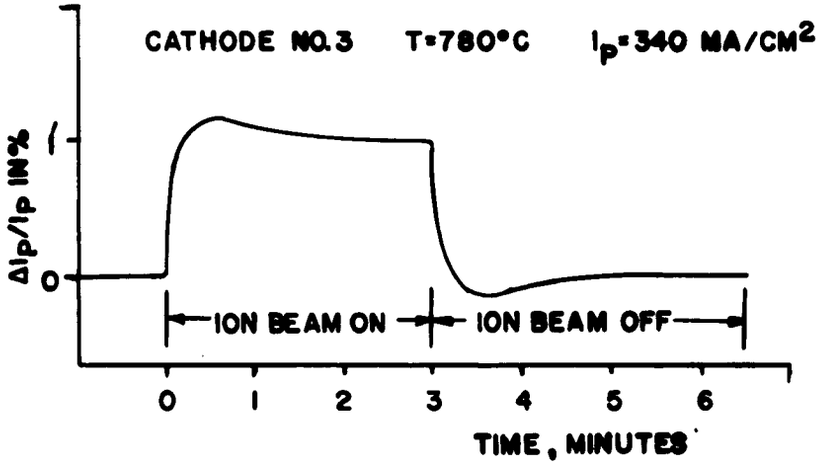

Figure 39. Effect of Ion Bombardment by Residual Gas at a Pressure of $7(10)^{-9}$ mm Hg.

As may be seen, the behavior under ion bombardment by the residual gases is somewhat more complicated than for either oxygen or carbon monoxide. Whereas with oxygen and carbon monoxide the emission either

rose or fell to an equilibrium value, it was found that when the cathode was bombarded with ions of the residual gas, the emission first rose through a maximum, then decreased slowly to an equilibrium value. Similarly, with the cessation of ion bombardment, the emission first dropped to a minimum, then rose slowly to an equilibrium value. This complex behavior is very likely due to the fact that there are several different residual gases present in the tube, which have opposing effects on the emission of the cathode. It is to be noted that the maximum emission change under ion bombardment by the residual gases in the tube is of the order of one per cent of the total emission, which is small compared to the effects observed for oxygen and carbon monoxide at higher pressures.

B. EFFECT OF ION BOMBARDMENT BY ARGON

The behavior during and after ion bombardment by argon is even more complex than that observed for the residual gas, as can be seen from Figure 40. The behavior up to point A in Figure 40a is quite similar, both in magnitude and in rate, to that for the residual gases. From point A on, however, instead of leveling off as for the residual gases, the emission rises slowly but steadily. This slow rise in emission reaches an equilibrium about 3 per cent above the initial emission of the cathode. If the ion bombardment is interrupted at point A, the emission behaves as after ion bombardment by the residual gas, but if the ion bombardment by argon is allowed to continue until the final equilibrium emission is reached, the emission returns monotonically to its initial value. In the latter case the emission had apparently been increased sufficiently by the long slow activation that the return to equilibrium completely masked the slightly rising emission

observed in Figure 40b. Thus, the behavior during ion bombardment with argon in the ion gun seems to be a very slow activation superimposed on the behavior observed with the residual gases.

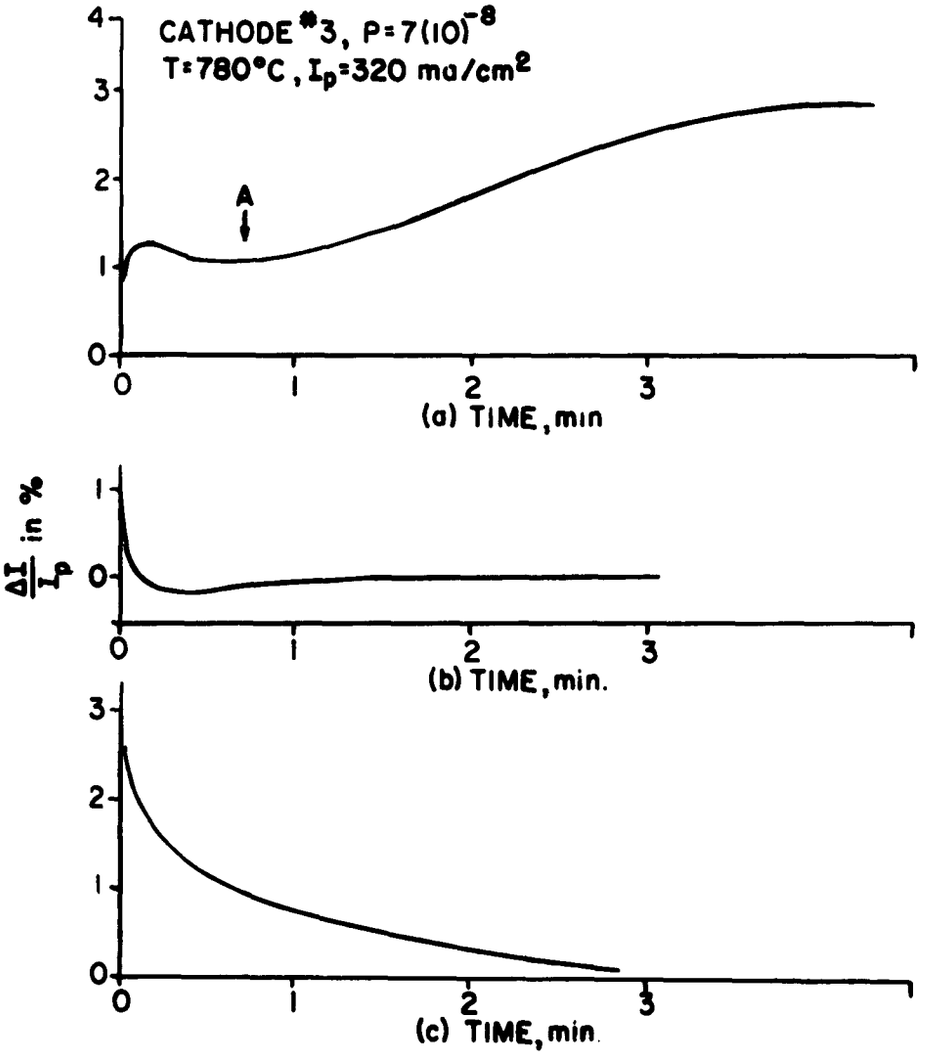

Figure 40. Effect of Ion Bombardment by Argon: (a) Ion Beam On, (b) Ion Beam Off at A, (c) Ion Beam Off After Equilibrium Reached.

C. SIGNIFICANCE OF RESULTS

Although an effect was definitely observed with argon, which was absent with the residual gases, some doubt still remains as to its source. This is first because argon is an inert gas and any effect caused by it could easily be overshadowed by more active gases, and secondly because the effect that was observed was not much greater than the effect previously observed with the residual gases. If the slow activation observed were actually due to ion bombardment by argon, this would be of special interest because these effects must be purely mechanical in nature, i.e., sputtering or defect production, and must therefore be occurring also for the more chemically active gases in addition to their chemical effects. Thus a study of the effect of argon can clarify to what extent the phenomena observed for the other gases are due to mechanical effects, and therefore render the chemical effects more amenable to analysis.

There are two major sources of gas in the tube: the cathode heater structure and the discharge which serves as the source of ions. Those gases arising from the cathode heater structure are determined only by the cathode temperature and are not affected by admitting a gas to the system. Thus these gases are completely accounted for by studying the effect of ion bombardment by the residual gases. On the other hand, those gases arising from outgassing of the discharge itself are determined by the intensity of the discharge and hence depend on the total pressure. Thus, for example, when argon is admitted to the system, those residual gases originating from outgassing of the discharge tube should increase along with the argon pressure. Although there is still some doubt, this was probably not occurring, since the discharge tube was sufficiently well out-

gassed at this stage that increasing its anode voltage had no effect on the pressure.

Therefore, the only conclusion that can be drawn from this part of the study as to the effect of ion bombardment by argon itself is that apparently it causes a slow activation of the oxide cathode, but there was sufficient doubt as to the real source of this effect that the study was not pursued further with the present experimental setup. However, there is enough evidence of such an effect to indicate that a more careful study should be made with a beam of A^+ ions resolved by a mass spectrometer.

The chief significance of this study of the effect of ion bombardment by argon is that it put an upper limit on the extent to which residual gases in the tube could have been influencing the experiments with oxygen and carbon monoxide. The effect of the residual gases was checked occasionally before admitting the gas to be studied and was always found to be very small and even of varying sign depending on the gases that had previously been admitted. The residual gases that may have increased along with the introduction of the gas to be studied would have been about the same as for argon, and thus could have had an effect no greater than that observed here, which is still much smaller than the effects actually observed for oxygen and carbon monoxide.

Also, since the mechanical effects accompanying ion bombardment by oxygen and carbon monoxide should be similar to those from argon, the results with argon put an approximate upper limit on the extent to which these effects could have been influencing the results with oxygen and carbon monoxide; therefore, the interpretation of the results with these gases as being mainly due to their chemical properties is justified.

D. ADDITIONAL STUDIES WITH ARGON

The brief study mentioned above of the effect of ion bombardment of an oxide cathode by argon is the only one in which the care was taken to bake the system out immediately before admitting argon. In addition to this, the effect of ion bombardment by argon was observed on another cathode without taking this precaution and hence starting with a residual pressure of about $1.5(10)^{-8}$ mm Hg. In this case it was found that the ion bombardment by argon decreased the emission of the cathode about two per cent.

To learn more about how the effect of ion bombardment by argon is related to the state of the cathode, a composite experiment was carried out in which oxygen was first admitted to a pressure of $5(10)^{-8}$ mm Hg, the effect of ion bombardment studied, and then argon admitted to a total pressure of $1.2(10)^{-7}$ mm Hg [i.e., $7(10)^{-8}$ mm Hg of argon], and the effect of ion bombardment again studied. The result was that in both cases, the poisoning characteristic during ion bombardment was almost identical, both in amplitude and rate. Surprisingly enough, however, there was a marked difference in the form of the curves of the recovery in emission, which is shown in Figure 41. This figure shows that the recovery from the poisoning was much slower when argon was present in the ion beam than when absent. The reason for this is not apparent.

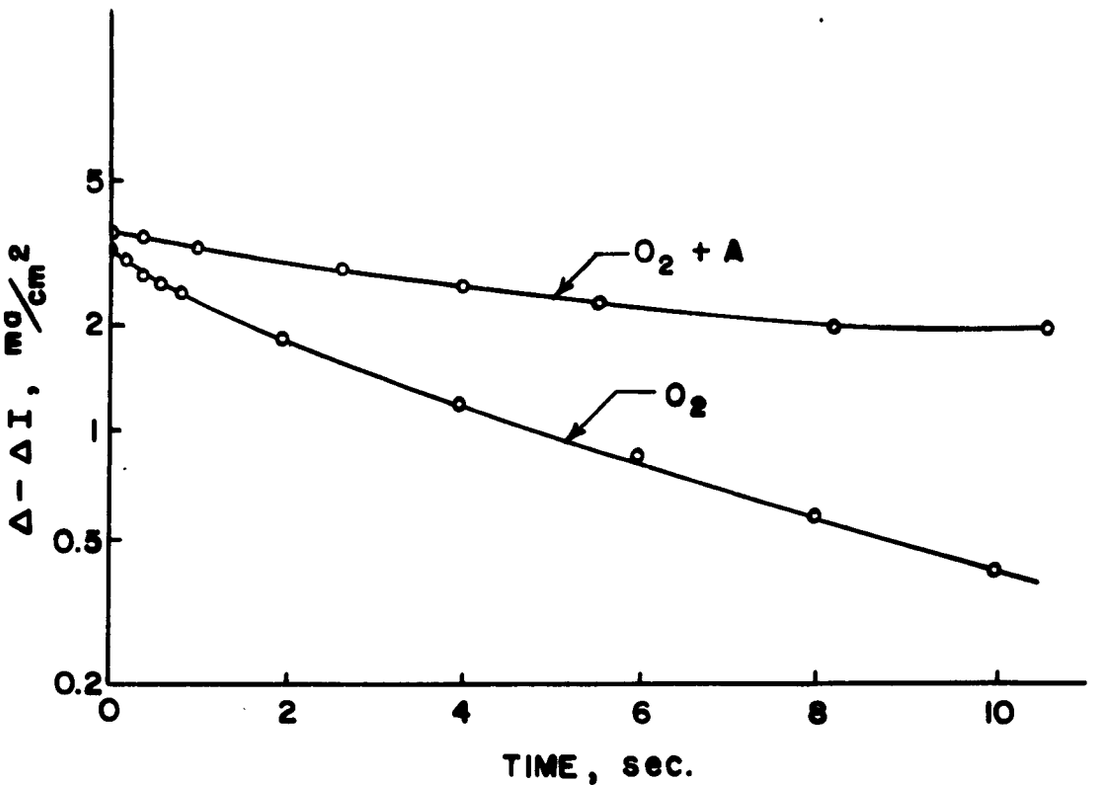

Figure 41. Comparison of Form of Curves of Recovery from Ion Bombardment by Oxygen and by Oxygen plus Argon.

VIII. INTERPRETATION

In this section, the results of the study of ion bombardment on oxide cathodes will be interpreted in terms of present theories of the operation of the oxide cathode and a discussion will be given of the extent to which the results can be considered as evidence for any of the specific models of the oxide-coated cathode given in Chapter II. The nature of the effect of ion bombardment on an oxide cathode will be discussed first, for its own interest and also to establish to what extent evidence obtained by ion bombardment is pertinent to the usual equilibrium processes in an oxide cathode. Then, in the light of this, a discussion will follow as to which of the various phenomena believed to be of importance in establishing the equilibrium are supported by the evidence brought out in this study.

A. NATURE OF EFFECT OF ION BOMBARDMENT

The effects of ion bombardment on an oxide cathode can be divided into three groups: effects caused by the charge of the ions, effects caused by the chemical properties of the gas from which the ions originate, and those effects caused solely by the kinetic energy of the incoming ions. These three aspects will be discussed in this section and an estimate given of the relative importance of each in accounting for the experimental observations.

1. Charge Effects

There seem to be three possible ways in which the charge of an incoming ion may influence an oxide cathode: charge localization, the increased chemical activity of an ion, and the increased current through the

cathode to neutralize the ions. The possibility of charge localization, i.e., the ion entering the cathode as such, is ruled out by the fact that the ionization energies of all the ions used are larger than the electron affinity of the cathode so that they would be neutralized shortly before arriving at the surface of the cathode. Furthermore, the conductivity of the cathode at the temperatures used in this study was high enough that electrical neutrality could be reached in a very short time. The second possibility, that of the increased chemical activity of an ion is also ruled out by the fact that the ions would be neutralized before reaching the surface of the cathode.

With regard to the third possibility, that the neutralization of the positive ion current to the surface of the cathode requires an increased electron current through the cathode, and thus may rearrange the potential distribution within the cathode, it is to be noted that the ion currents employed were always several orders of magnitude less than the electron emission currents, so that any effect resulting from this slight added current would be negligible. It was found by Matheson et al.,[10] in a study of the effect of alkaline-earth metal ions on the emission of an oxide cathode, that using ion currents twice as large as the emission currents or larger gave results that were apparently caused by the ion current affecting the potential distribution in the cathode. However, they found that smaller ion currents (or larger emission currents) never gave this effect, and the emission in this study was always greater than the ion current; therefore it is concluded that any effects from the charge of the incoming ions were negligible.

2. Chemical Effects

There are two aspects to the chemical effects of impurities deposited on an oxide cathode by ion bombardment: first, the chemical behavior to be expected of the impurity itself, and second, the extent to which this behavior is modified by the fact that these impurities are arriving with high kinetic energies.

First, the possible history of an oxygen molecule after arriving on the surface of an oxide cathode from the gas phase will be considered. In order to be adsorbed at the elevated temperature, this molecule must enter into chemical combination with the oxide, which probably means that it must be ionized, since the binding in the oxide is ionic. In addition, it must probably be dissociated. At this point there are two possibilities: it may remain on the surface as a negative ion (singly charged according to Surplice[26]); or it may enter into the bulk of the cathode, probably as additional oxygen.[20] At some step in this process an activation energy is probably required, so that there is some probability that the activation would not occur and that not all the oxygen molecules arriving at the surface would be adsorbed. The equilibrium is finally reached when the rate of oxygen molecules thus adsorbed is balanced by the rate being re-evaporated or destroyed by reducing agents migrating outward from the cathode base.

Consider, on the other hand, the history of an O_2^+ ion arriving at the surface with an energy of a few hundred electron volts. This ion will be neutralized shortly before arriving at the surface, but will still arrive with its full kinetic energy. Then, upon its first collision with a particle of the oxide it will be dissociated, and then travel on for a few collisions as two oxygen atoms (or ions). Thus, any activation energy required for

dissociation is automatically provided. Furthermore, since the incoming particle must undergo several collisions before it can lose its energy, it will have a much greater probability of coming to rest somewhere within the crystal than on the surface, so that if the surface absorption of O^- ions is an important part of the effect of molecular oxygen, as proposed by Surplice,[26] the effect of oxygen arriving in an ion beam should be qualitatively different. The only other possibility of a qualitatively different behavior by ion bombardment with oxygen is the existence of a state having such a high activation energy that it could only be reached by a particle arriving with greater than thermal energy. Such a state would produce an irreversible behavior, however, which was not observed. Now, with respect to the equilibrium, it is seen that in the case of ion bombardment, the new equilibrium is achieved between the rate of all the ions arriving (rather than some fraction as in the case of molecular oxygen), and the same opposing processes as before, so that the shift in equilibrium from a certain arrival rate of ions at the surface should be greater than for the same arrival rate of oxygen molecules. That this is actually observed may be seen from Figure 9. Therefore, the chemical effects to be expected from ion bombardment by oxygen are essentially those to be expected from the gas except for an added efficiency resulting from such activation energy as is supplied by the kinetic energy of the incoming ion.

In the case of carbon monoxide all the above considerations apply, with the added complication that the carbon monoxide is composed of two elements, which have the possibility of behaving differently after becoming dissociated on the surface of the cathode. Thus, it may well be that either the carbon or the oxygen has a greater probability of entering the lattice

(This would be equivalent to admitting the possibility of reactions of the form $BaO + CO \rightarrow BaO_2 + C$.) In this case the behavior under ion bombardment would be qualitatively different since both constituents are being forced into the oxide in equal amounts. Thus, the observed qualitative difference between the effect of carbon monoxide arriving at the surface from an ion beam and from background gas can be accounted for without resorting to the presence of a stoichiometric excess of either C^+ or O^+ in the ion bombardment. Because of the possibility of the presence of such an excess, however, more refined experiments will be necessary to decide between the two explanations.

3. Mechanical Effects

The mechanical effects associated with ion bombardment (i.e., solely from the kinetic energy of the incoming ions) are sputtering, defect production, and heating of the cathode. Although all of these processes are capable of producing an effect on the emission of an oxide cathode, the following experimental observations indicate that these effects played a secondary role in the study presented here: (a) Argon, for which the mechanical effects mentioned above should be roughly the same as for the other gases, had a much smaller effect than the other gases. (b) This slight effect of argon even varied in sign indicating that other gases may have played an important part in the effect. (c) The effects of carbon monoxide and oxygen being of opposite sign indicates that their chemical properties predominated.

B. CONCLUSIONS FROM EXPERIMENTAL RESULTS

Since the effect of bombardment of an oxide-coated cathode by ions

of oxygen and carbon monoxide appears to be associated mainly with the deposition of the chemical agents in a thin layer at the surface of the cathode, the experimental results can be interpreted to yield evidence bearing on certain of the models discussed in Chapter II of this report. Ion bombardment is a more powerful tool than the usual gaseous poisoning experiments for the following reasons: (1) The deposition by ion bombardment can be turned on and off instantaneously, thus allowing a better study of the transient effects. (2) The chemical agents are deposited at the front face of the cathode, and in those parts of the pores visible from the front, by ion bombardment, rather than throughout the pore system as by gaseous poisoning.

Contrary to what was expected, the evidence indicates that diffusion is not a limiting factor in either the spreading of or the recovery from poisoning by ion bombardment with oxygen. The evidence for this conclusion is contained in the results of the studies of the dependence of the effect of ion bombardment on temperature and on pulse voltage.

In the study of the temperature dependence it was found that the poisoning by oxygen ion bombardment was nearly independent of temperature over the range from 600°C to 900°C. Since diffusion through the bulk requires an activation energy, and hence shows a strong temperature dependence, it is concluded that such diffusion, if present, cannot be a controlling factor in determining the equilibrium activity of the cathode under oxygen ion bombardment.

More direct evidence of this same fact is offered by the results of the study of the dependence on pulse voltage, from which it was concluded that the resistance of the cathode coating is affected just as rapidly as is

the emission of the cathode. In order to interpret this evidence it is necessary to bear in mind the physical nature of the cathode coating. This coating is known[1] to be a very porous agglomeration of crystallites, the mean pore size being approximately five microns. Since the ions only penetrate into the crystallites a distance of a few lattice spacings, which is negligible compared to the size of the crystallites, it is seen that the ions are deposited directly on only those regions of the coating that are optically visible from the front. Since the surface of the coating is rough, this region includes the insides of those pores bordering the vacuum boundary, so that the thickness of this region is approximately equal to the mean pore diameter of five microns. Since the thickness of the coating is about 70 microns, it is seen that the ions are deposited directly in a region comprising less than the outer ten per cent of the cathode coating. Therefore, it must be concluded that the effect of the ion bombardment spread throughout the pore system, either by Knudsen flow or surface diffusion, in a time very short compared to the time constants observed for ion bombardment poisoning and recovery, so that this diffusion was not a limiting factor.

The above conclusion applies only to the spreading of the effect through the thickness of the coating on the surfaces of the pores, and not to the penetration of the effect into the crystallites. This is because, at the temperature used in this experiment, the conduction through the coating is primarily by the electron gas in the pores,[15] so that both the emission and conductivity of the cathode are determined by the conditions at the surface of the crystallites. However, if the apparatus were refined, so that these same experiments could be performed at lower temperatures, where solid conduction predominates, and if a probe wire were included in the

coating to permit direct resistance measurements, an analysis of the results similar to that given here should yield further and more conclusive data on the problem of the importance of surface versus bulk properties of the oxide-coated cathode.

The study of the effect of oxygen ion bombardment as a function of the d-c current flowing through the cathode yields further information on the mechanism of spread of the poisoning through the cathode, as well as evidence against one of the models of the cathode mentioned in Chapter II. The evidence referred to is that the rate of recovery from poisoning by oxygen bombardment was decreased drastically by the presence of d-c emission. Since, if the oxygen had been present in the coating in the form of acceptors, the d-c field would have speeded up their removal, it is concluded that it was not present in this form. Therefore, this result is interpreted as evidence against the theory that the mobile species responsible for variations in cathode activity is an acceptor. Furthermore, the fact that the recovery was hindered so strongly by the d-c field seems to indicate that replacement of donors was necessary for recovery, rather than elimination of the poisoning agent from the coating.

Evidence against the "nonequilibrium" poisoning theories is afforded by the fact that the poisoning by ion bombardment with oxygen was completely reversible. This is because a key point in these nonequilibrium theories is that the reversibility of the poisoning by gaseous oxygen is made possible by the oxygen not having entered into chemical combination with the cathode. Specifically, it is claimed that the activation energy required to form O^{--} is too large so that oxygen is present as O^{-}, either in the cathode or on its surface. On the other hand, it would be expected that the energy of an

incoming ion would supply any such activating energy that might be necessary, this expectation being supported by the fact that oxygen arriving from the ion beam was observed to be a more effective poisoning agent than oxygen arriving from the gas phase.

The fact that both the rate of poisoning and the total decrement by oxygen bombardment were as high when argon was also present in the ion beam as when argon was absent indicates that sputtering of oxygen from the surface by ion bombardment is not an important factor in the recovery of an oxide cathode from poisoning by oxygen. The fact that the cathode was already poisoned to a considerable extent by the background atmosphere of oxygen throughout this experiment adds to the significance of the above statement. The fact that the recovery from the poisoning by ion bombardment with oxygen was much slower when argon was also present in the ion beam, however, is still without explanation.

Quite unexpectedly, the effect of ion bombardment by carbon monoxide on an oxide cathode seems to be explainable by the hypothesis that this ion bombardment introduces donors into the coating. The evidence for this is as follows: (a) The effect of ion bombardment by carbon monoxide was an activation of the cathode in all cases. (b) There is a remarkable agreement of the curve of activation by ion bombardment versus time at normal operating temperatures with a curve published by Krusemeyer and Pursley[9] of the recovery from forming a donor depletion layer by drawing d-c current. (c) The rate-controlling process in ion bombardment by carbon monoxide has an estimated activation energy (4 ev) comparable to that obtained by Krusemeyer and Pursley for the migration of donors (3.3 ev).

IX. CONCLUSIONS AND RECOMMENDATIONS

A. CONCLUSIONS AND SUMMARY

1. With the apparatus that has been developed the effect of ion bombardment by oxygen, carbon monoxide, and argon on the emitting properties of oxide-coated cathodes can be studied with reasonable certainity that it is actually the effect of the ion bombardment which is being studied.

2. The effect of oxygen ion bombardment is a poisoning of the cathode under all conditions; oxygen arriving at the surface by ionic deposition being anywhere from one to about five times as effective a poisoning agent as the same amount of oxygen arriving at the surface from the gas phase.

3. Ion bombardment by carbon monoxide activates the cathode in all cases. This includes conditions under which the gaseous phase of carbon monoxide poisons the cathode as well as conditions under which the gaseous phase activates the cathode.

4. Since (a) there is usually very little oxygen present in vacuum tubes, (b) the principal gas is usually carbon monoxide, and (c) the other gases would be nearer to carbon monoxide in effect than to oxygen, it is concluded that ion bombardment by ions from the gases in the tube is not a very serious problem in maintaining high cathode emission in vacuum tubes. Of course, ion bombardment is still a serious problem in high-voltage beam-type tubes from the long-range point of view, since the cathode coating will eventually be eroded away by sputtering. On the other hand, since decomposition of contaminants on the anode is known to release oxygen, and even to release O^+ ions directly;[33] then from the results obtained here a small number of such ions would seriously deactivate an oxide-coated cathode.

5. The amount of poisoning by a given current density of oxygen ion bombardment is nearly independent of temperature over the range 600°C to 900°C.

6. The recovery from oxygen ion bombardment poisoning is slowed up significantly by drawing d-c emission, indicating that donors rather than acceptors are the mobile species.

7. The activation by carbon monoxide ion bombardment was very slight for active cathodes at high temperatures and increased with decreasing cathode activity and decreasing temperature.

8. An activation energy of 4 ev was estimated for the rate controlling process in carbon monoxide ion bombardment at temperatures above 800°C.

9. The effect of ion bombardment by argon was much less than that of either oxygen or carbon monoxide, and was found to be of both signs.

B. RECOMMENDATIONS FOR FURTHER STUDY

It is felt that the results of this study indicate that ion bombardment can be a powerful tool in the study of the oxide cathode and should be exploited further. Some specific studies that are indicated by the results obtained here are as follows:

1. By repeating the experiments with oxygen ion bombardment at low enough temperatures that solid conduction predominates, and by incorporating a probe wire for direct measurement of the conductivity variations, it should be possible to resolve the question of the relative importance of the surface versus bulk properties of the cathode. This will necessitate the development of a more refined apparatus in which the effect of ion bom-

bardment can be studied with less influence from the background gas. Some suggestions of how this may be done are given in Appendix A.

2. It is also important for practical purposes to carry out a study of the effect of ion bombardment by oxygen on an unpoisoned cathode, since this corresponds more nearly to the situation in a tube with a contaminated anode, and since the effect of ion bombardment by oxygen is expected to be much greater under these circumstances.

3. The results obtained here for ion bombardment by argon indicate that a beam of A^+ ions resolved by a mass spectrometer may be necessary for a conclusive study of this gas. A study similar to the present one, but with a mass spectrometer included in the vacuum system might be a good first approach, however.

4. A mass-spectrometrical analysis of an ion beam will also be necessary to resolve the question of whether the activation by ion bombardment with carbon monoxide is due to a stoichiometric excess of C^+ in the ion beam or is a fundamental property of ion bombardment by CO^+ itself.

APPENDIX A. ION GUN STUDY

The major part of the work of this project was spent in developing an ion gun capable of delivering sufficient ion current at a very low pressure. In the course of this work considerable light was shed on the details of operation of a Penning discharge in high vacuum. Since this is of interest in a number of applications, it is presented here in some detail.

I. FIRST ION GUN

The form of ion gun chosen for the study of the effect of ion bombardment on oxide cathodes is that of a Penning discharge with the ion beam extracted through one cathode. The basic form of such a discharge is shown in Figure A-1. The operation of this discharge is based on the

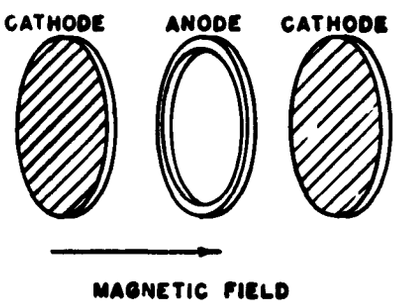

Figure A-1. Basic Form of Penning Discharge.

fact that electrons emitted from the cathodes are confined to spiral paths by the magnetic field and therefore oscillate back and forth between the cathodes; the electrons therefore have very long effective path lengths and are able to form many ions. Such a discharge operates in two quite

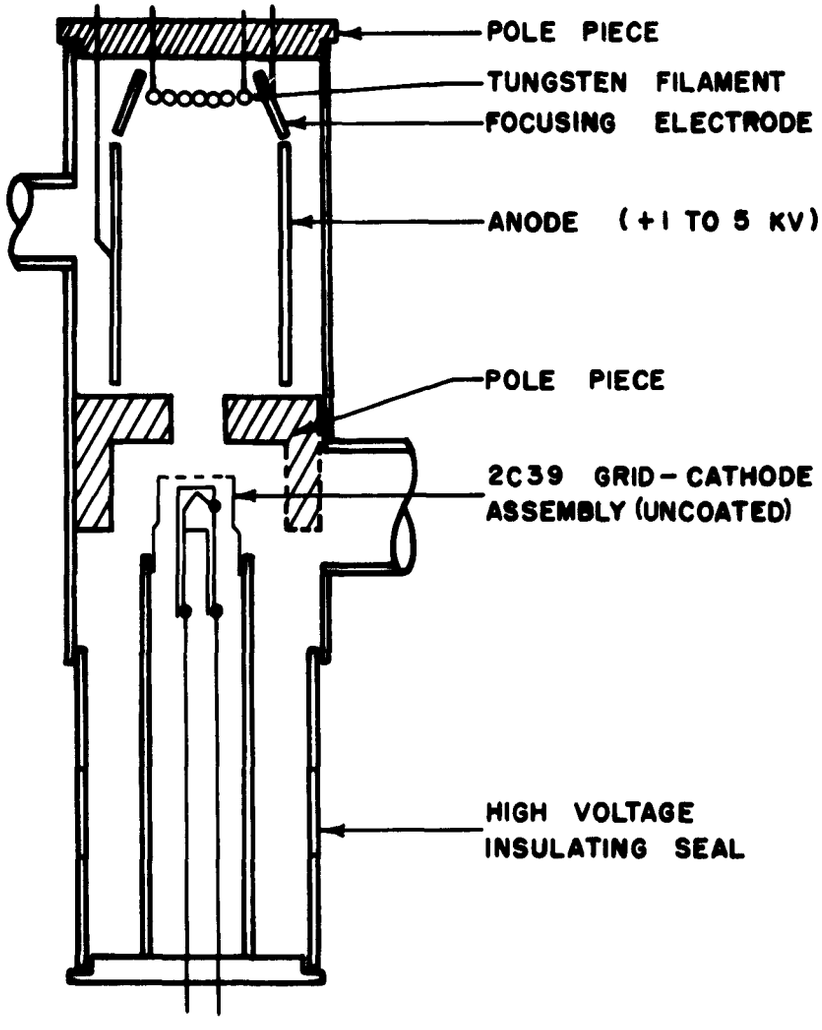

Figure A-2. Ion Gun and Collector Assembly.

distinct modes: a high-pressure mode at pressures of about one micron and above, and a low-pressure mode at pressures below one micron. Very high ion currents may be obtained from this type of discharge operating in the high-pressure mode, and accordingly most previous investigations have been restricted to this mode.[34] For the purpose of studying the effect of ion bombardment on oxide cathodes, however, it is necessary to operate with the pressure at the cathode of the order of 10^{-7} mm Hg. Therefore, it appeared that the best course was to investigate the low-pressure mode of this discharge in the hope of obtaining sufficient ion current from it.

A. Experimental Results

The form of ion gun used was that of Figure A-2 which can be seen to be basically the same as Figure A-1 except that there was a tungsten filament included to give a large source of primary electrons and a hole in one cathode for extracting ions. The long cylindrical anode was used rather than simply a ring, both because Penning[35] reported that a cylindrical anode gave a slightly stronger discharge, and also in the hope of obtaining a certain amount of "cathodic focusing" as discussed by Sommeria[36] in connection with various types of ion sources. In order to study the characteristics of this ion gun, the system was assembled with an uncoated cathode as collector, and a vacuum obtained. In this condition, the cathode made an excellent collector for studying characteristics of the ion beam, since the grid could be used for suppression of secondary electrons.

The first result obtained using this apparatus was that an electron emission current from the filament caused no increase in the ion current from the gun and, in fact, actually seemed to decrease the ion current as shown in Figure A-3. This result was quite unexpected and seemed to

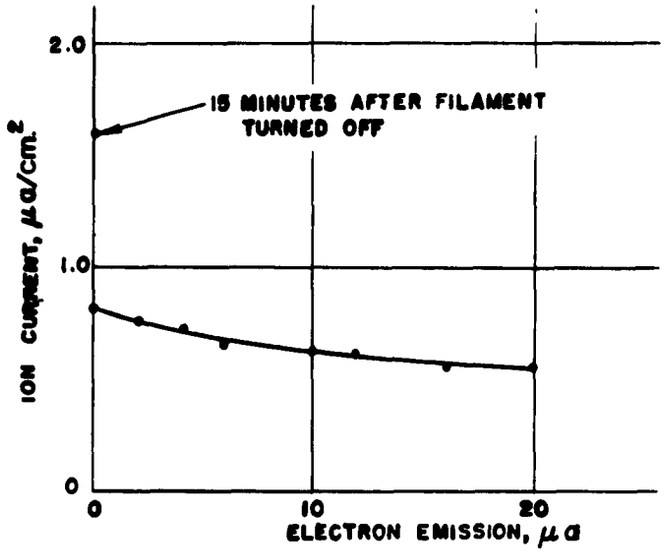

Figure A-3. Effect of Hot Filament on Ion Current from Ion Gun.

indicate that the operation of the discharge was limited by the negative space charge in the region of the discharge. In fact, if the decreasing ion current as a function of electron current was significant, it must be that the emitted electrons rearranged the space-charge distribution in such a manner as to yield fewer ions. There is some question as to the significance of the decreasing ion current, however, since the ion current and intensity of the discharge are strongly affected by the type of gases present and the condition of the surfaces as defined by previous operation. This is well illustrated by the upper point in Figure A-3 which was taken fifteen minutes after the filament was cooled off, the pressure being maintained constant at $2(10)^{-7}$ mm Hg by increasing the flow of oxygen.

The dependence of both the extracted ion current and the anode current on the magnetic field is shown in Figure A-4 for a representative anode voltage of 1 kv. The fact that the extracted ion current reached a

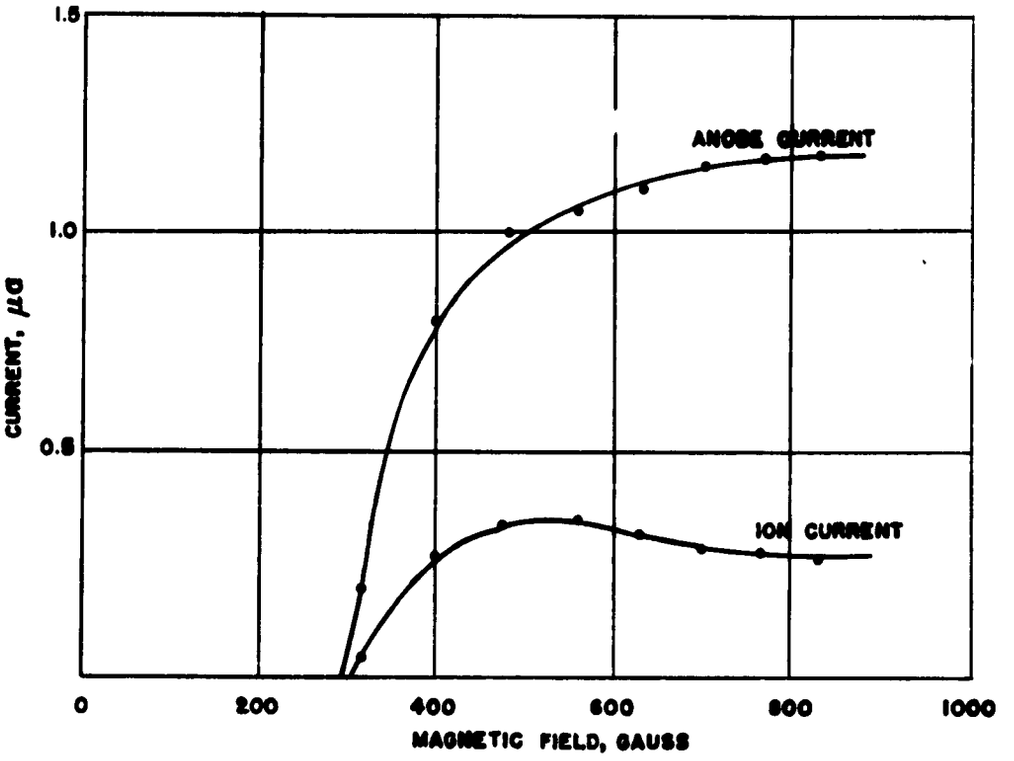

Figure A-4. Dependence of Extracted Ion Density and Anode Current of Cold Cathode Discharge on Magnetic Field.

peak and then fell off as the magnetic field was increased further is interpreted as evidence that focusing was actually obtained, and that the stronger magnetic field interfered with this focusing. However, recent results by Lichtman,[37] using a transparent mesh anode to study the Penning discharge, indicate that the discharge in the low-pressure mode is limited to a narrow line down the center. This being the case, focusing would not be expected to be necessary so that the observed falling off of extracted ion current with increasing magnetic field may be due to some more subtle effect. The intensity of the discharge, as measured by the current to the anode, is seen to rise rapidly at first, and then reach a

sort of plateau where it rises very slowly as the magnetic field is increased.

The energy distribution of the extracted ions has been studied in order to obtain more information on the manner in which the operation of the low-pressure mode of the Penning discharge is limited by the negative space charge, and also for its direct importance in interpreting the results of the ion bombardment study. All of these experiments were carried out using a cold cathode discharge in oxygen at a pressure of $1(10^{-7})$ mm Hg, the energy distribution of the ions being obtained by differentiating the curve of ion current to the collector as a function of the collector potential. The grid was held negative at all times in order to turn the electrons back from the discharge and also to suppress secondary electrons from the collector. The energy distribution obtained for three different anode voltages is shown in Figure A-5.

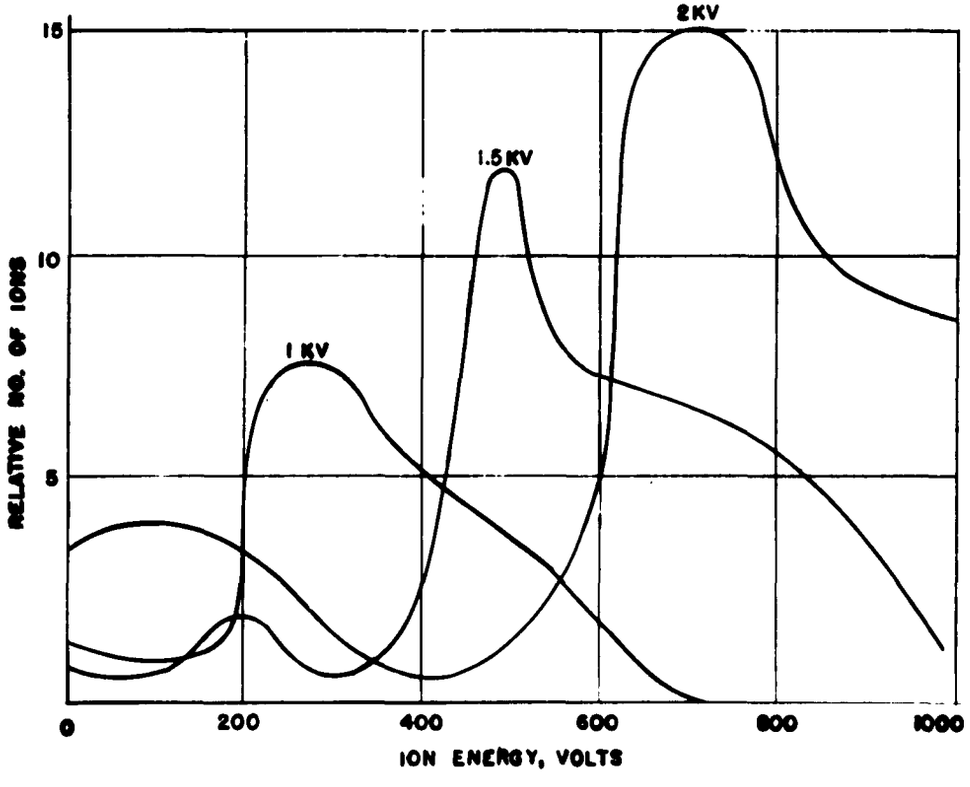

Figure A-5. Energy Distribution of Ions Extracted from Cold Discharge.

The outstanding features of these energy distributions are that (1) there are very few low-energy ions present, (2) the low-energy edge of the bulk of the distribution rises very sharply, and (3) the high-energy edge of the distribution is well defined and is several hundred volts below the anode potential.

The energy distribution of the extracted ion beam may be considered as a crude probe of the space-charge distribution inside the discharge, since the rate of ion formation at a given point is roughly proportional to the electron space-charge density at that point times the average electron velocity at the same place, and since each ion will have an energy very nearly equal to the potential at the point where it was formed. Interpreting Figure A-5 from this point of view leads, first of all, to the quite surprising conclusion that the most negative region in which an appreciable number of ions are formed is at least 200 volts above cathode potential in the case of the 1-kv discharge and much more for the higher voltage discharges. That the low-energy ions are actually absent and not merely being lost in the extraction process is seen from Figure A-6, in which the energy distribution of a 1-kv discharge is shown for different values of the voltage on the grid in front of the collector. It would be expected that large negative voltages on the grid should increase the extraction efficiency for low-energy ions and thus that such a plot should show their presence. As may be seen from the figure, this increased extraction efficiency does exist for ions in the range of 200 to 400 volts, and shows rather conclusively that there are very few ions of lower energy. In fact, the result casts doubt on the presence of the lower energy ions shown in the curve for -50 volts, their apparent presence being possibly due to incomplete

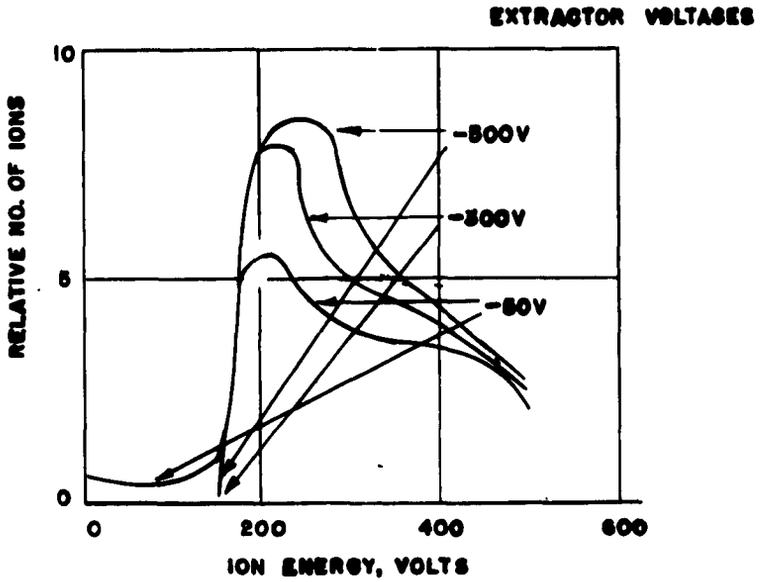

Figure A-6. Effect of Extractor Voltage on Energy Spread of Ions.

suppression of secondary electrons at the lower collector voltages.

The conclusion, therefore, is that the region of high electron space-charge density in the discharge extends down only to a region of +200 volts potential or perhaps +150 volts, since the lower velocity electrons would produce very few ions. This conclusion indicates that electrons given off by the cathodes play a minor part in the operation of the discharge since they extend up to a region of zero volts potential, and that the bulk of the ionization is carried out by secondary electrons formed within the discharge in the process of ionization. This explanation is in agreement with the fact that, as was pointed earlier in this section, additional emission of electrons from the cathode causes no improvement in ion current. Lastly, it should be pointed out that the high-energy limit of the energy distribution is compatible with the theory that the potential in the center of the discharge is depressed to this value by space charge.

Further information on the mechanism of the discharge can be obtained from the effect of the magnetic field on the energy distribution of the ions, as shown in Figure A-7. An examination of this figure shows

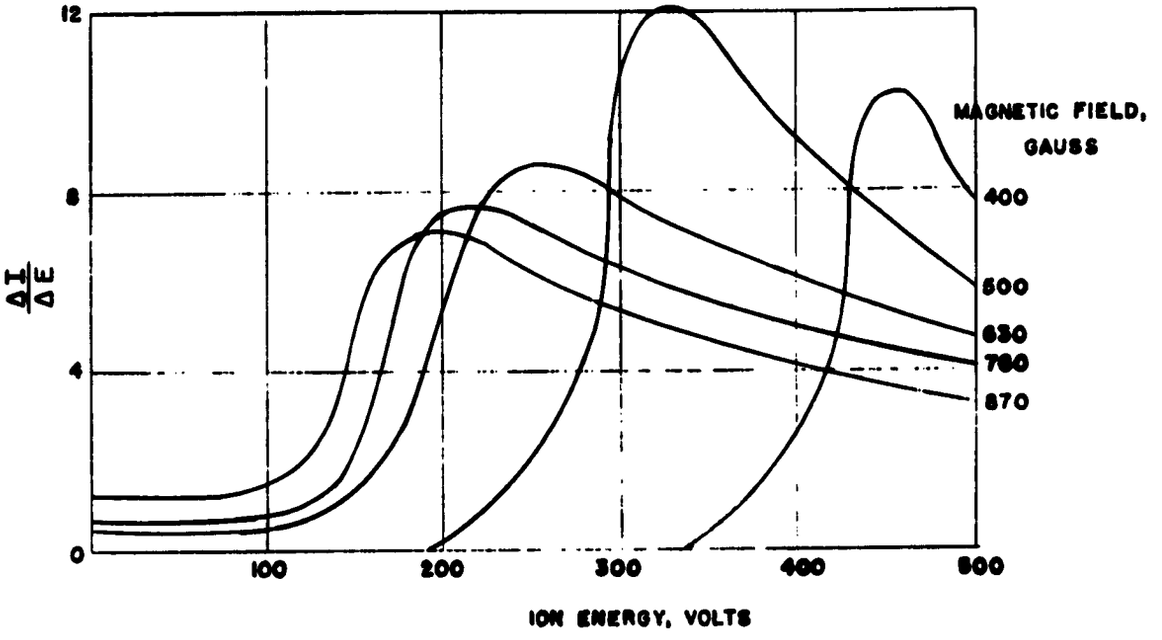

Figure A-7. Effect of Magnetic Field on Energy Distribution of Ions.

that the effect of increasing the magnetic field is to allow the space charge to be maintained in regions of more negative potential and also probably to maintain a higher space charge in regions where it already exists.

B. Interpretation

The preceding experimental results can be interpreted consistently on a model in which the operation of the discharge is space-charge limited. As already mentioned, this model is indicated by the fact that electron emission causes no increase in ion current, since if the operation were

limited by some other mechanism, such as the rate at which electrons can diffuse across the magnetic field through collisions with gas molecules, electron emission should give an increase in ion current. As it is, electron emission just causes electrons to escape to the anode at a higher rate or perhaps even readjusts the space-charge configuration so that a lower total number of electrons are trapped in the discharge.

Brillouin[38] developed conservation conditions from which it follows that, for the case of a cylindrical electron beam in a longitudinal magnetic field, the space-charge density is completely determined by the magnetic field and is proportional to its square. Although the situation in the Penning discharge is more complicated than that considered by Brillouin, it still has radial symmetry in a longitudinal magnetic field so that the same general considerations should apply. The equilibrium condition considered by Brillouin is that in which the outward forces resulting from space charge and centrifugal force are exactly balanced by the inward force due to the magnetic field, i.e.,

$$F_{\text{space charge}} + F_{\text{centrifugal}} = F_{\text{magnetic}} \,.$$

In the case of the Penning discharge, there must be added to this an additional outward force from the radial component of the electric field due to the anode voltage:

$$F_{\text{space charge}} + F_{\text{centrifugal}} + F_{\text{anode}} = F_{\text{magnetic}} \,,$$

so that the resulting space-charge density will be somewhat less than in the Brillouin case. Since the electrons are all produced within the magnetic field, the appropriate conservation condition in this case leads to the

relationship for the angular velocity $\dot{\theta}$ of an electron at a radius r from the axis of the discharge

$$\dot{\theta} = \omega_H \left[1 - \frac{a^2}{r^2}\right] \quad ,$$

where ω_H is the cyclotron frequency and a the radius at which the electron was created. Since this relationship between $\dot{\theta}$ and r must hold at all times, it is shown by Brillouin that a static equilibrium ($\dot{r} = 0$) can only be realised for a charge distribution given by

$$\rho = 2\epsilon_o \frac{m}{\ell} \omega_H^2 \left[1 + \frac{a^4}{r^4}\right] \quad .$$

Since this becomes infinite at $r = 0$, it is seen that this static equilibrium can only be obtained in devices in which the electrons are prevented from reaching the axis. Therefore, it follows that in a Penning discharge the equilibrium obtained must be of a dynamic nature, and therefore the forces in the above equilibrium expressions must be interpreted as averaged over an appropriate period of time. The observed dependence of the energy distribution of the ion beam on the magnetic field can now be explained by observing that the radial field due to the anode voltage is stronger towards the ends of the discharge, so that a magnetic field strong enough to maintain appreciable space charge at the center may still be too weak to do so near the ends. As the magnetic field is increased, this space charge can be supported nearer the ends, and hence in regions of lower potential, which accounts for the observed results.

II. EFFECT OF ELECTRON EMISSION

In order to study the effect of electron emission further, the ion

gun was modified as shown in Figure A-8. This form of the ion gun has the

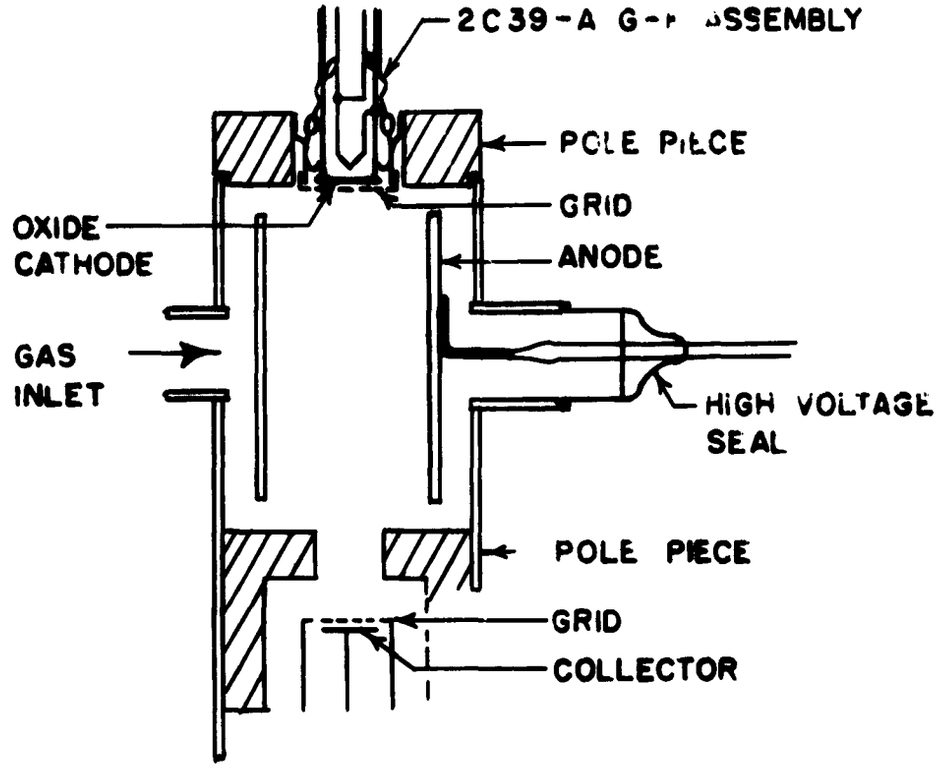

Figure A-8. Modified Ion Gun for Studying the Effect of Electron Emission.

advantage that the electron emission can be controlled simply by varying the potential of the cathode with respect to the grid without changing the temperature of the cathode. Thus the effect of large emission currents can be studied with a minimum effect on other parameters of the discharge such as gas constitution, pressure, and the condition of the surfaces bounding the discharge. On the other hand, it has the disadvantage that electrons from the cathode will not be trapped in the discharge unless they undergo a collision on the first traversal of the discharge, since

the emission cathode is at a lower potential than the cathodes of the discharge. However, if anything, this should act to decrease the effect of adding electrons.

The characteristics of this ion gun were studied using the same technique as for the first ion gun, except that atmospheric air was used instead of oxygen. The effect of drawing an electron current is shown in Figure A-9, in which the ion current from the discharge is plotted as

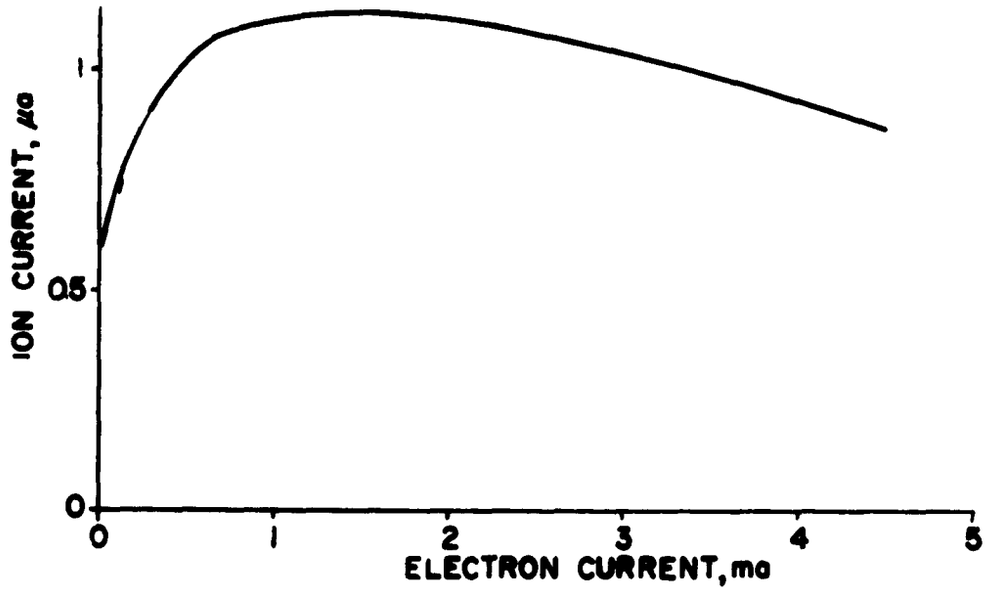

Figure A-9. Effect of Electron Emission on Ion Current from Penning Discharge.

a function of the electron current from the cathode. Here the ion current is seen to drop abruptly from its zero emission level to a much lower level as a small amount of electron current was drawn. As the electron current was increased further the ion current passed through a maximum, at which it was very nearly the same as from a cold discharge, and then

decreased as the emission was still further increased. Thus, apparently a very small electron current was sufficient to force the discharge into a new mode of operation in which several milliamperes of emission were necessary to yield the maximum ion current. The significant fact is that the maximum ion current from the discharge is roughly the same in both modes of operation. This again is quite compatible with the operation of the discharge being limited by space charge, since the maximum space charge that can be maintained in the region should be roughly the same for any mode.

That the two modes are distinctly different is illustrated by a comparison of the energy distribution of ions from a cold discharge with the energy distribution of ions from a discharge operating with approximately 1 ma of electron emission, as shown in Figure A-10. As can be seen from

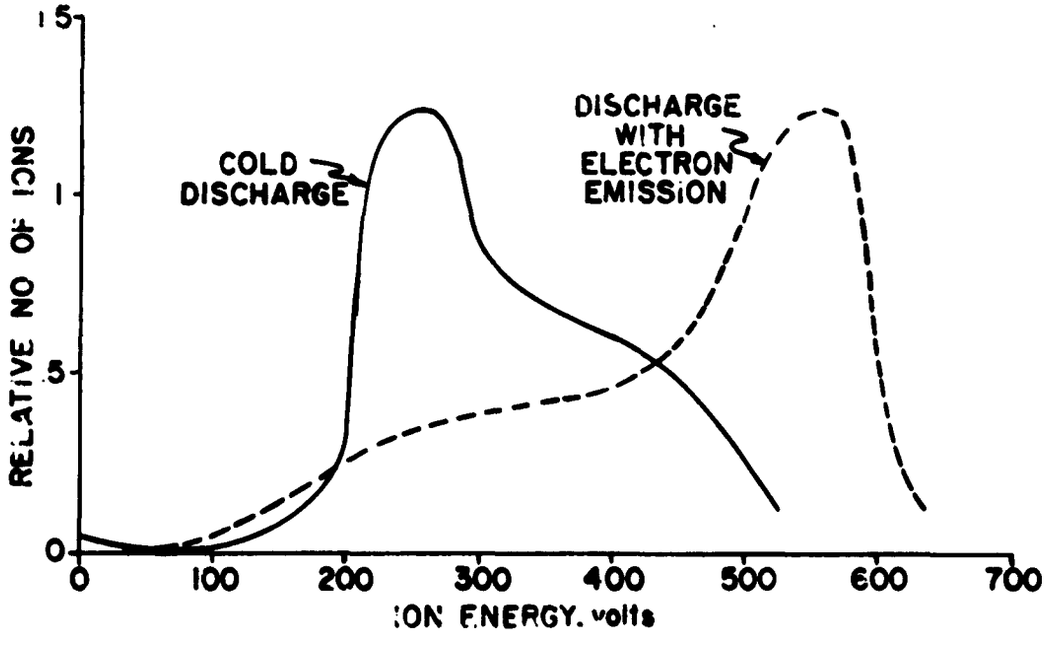

Figure A-10. Comparison of Energy Distributions of Ions from Discharge with and without Electron Emission.

this figure, the energy distributions are quite different, indicating two distinct modes of operation, and yet the maximum ion current is about the same from both modes.

In view of these results, it is felt that any significant improvement in the ratio of ion current density to ambient pressure for an ion beam extracted from the low-pressure Penning discharge must come about through concentration of the ion beam or differential pumping, or both.

III. FINAL ION GUN

The final form in which the ion gun was constructed is shown in Figure A-11, along with the special collector constructed to evaluate its

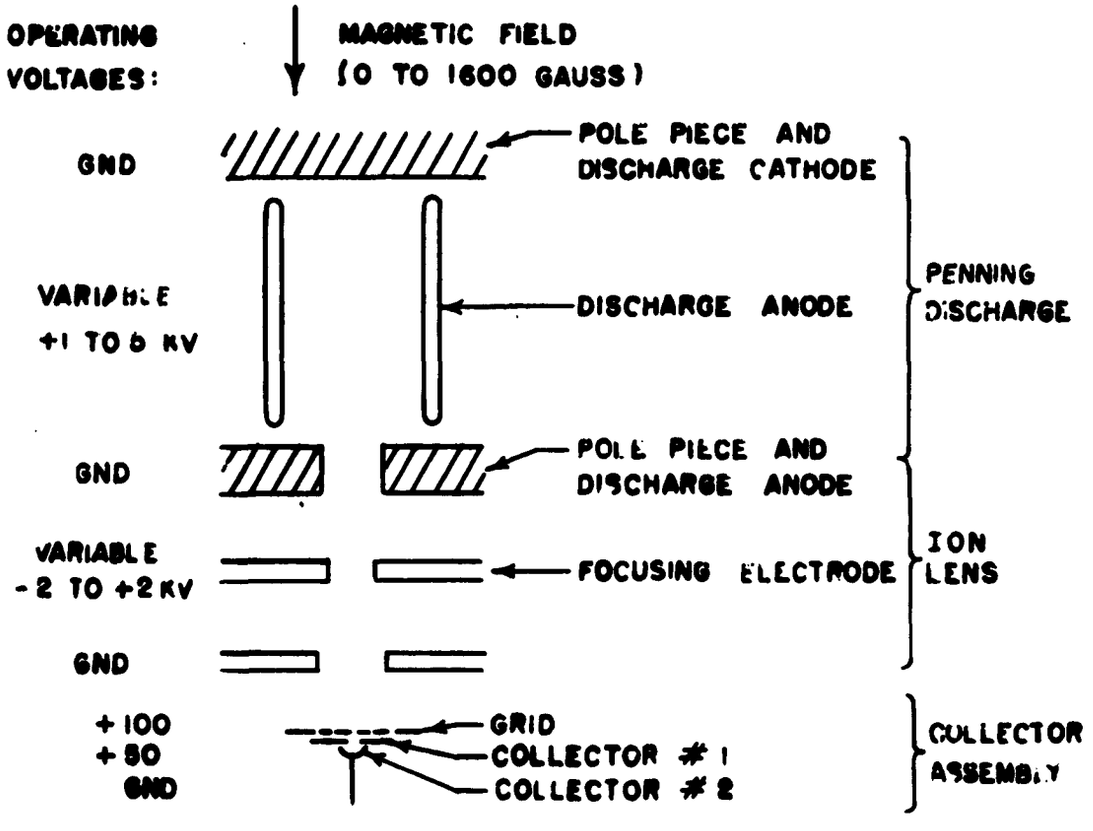

Figure A-11. Final Form of Ion Gun: Penning Discharge, Ion Lens, and Collector.

operation. An Einzel lens was provided at the extraction aperture of the Penning discharge for the threefold purpose of obtaining differential pumping, concentrating the ion beam, and turning the ion beam on and off without disturbing the discharge. As can be seen from the figure, the ion source was simply a cold cathode Penning dishcarge with a 3/8" aperture in one cathode. This aperture along with the next two electrodes, which were simply plates with 1/4" and 3/8" apertures in them, formed an ion lens quite similar to the Einzel lens used in electron optics.[39] Since the focusing properties of an electrostatic lens are independant of e/m , (charge to mass ratio of the particles) results for electron lenses carry over to ion lenses. The focusing properties of Einzel lenses do not apply directly to the situation here, however, for two reasons: the potential in the discharge was higher than that at the collector side of the lens, whereas for a true Einzel lens the potentials are the same on both sides, and the energy spread in the ion beam was of the o·der of a few hundred volts; whereas for an electron beam it is usually negligible. Despite these difficulties, the lens was designed to operate with a negative potential on the center electrode and, since in this case the particle path was near the axis of the lens in the vicinity of the center electrode,[39] the aperture in this electrode was made smaller in the hope of obtaining more differential pumping without intercepting much of the beam. Assuming a pumping speed from the collector region of 3 litres/sec, a straight-forward calculation[40] shows that the pressure in the discharge would be about three times that at the collector. In order to study the focusing properties of the system, a special collector was constructed consisting of a second collector behind a first collector having

a hole in its center with an area of .05 cm^2.

The focusing characteristic of this ion gun are shown in Figure A-12

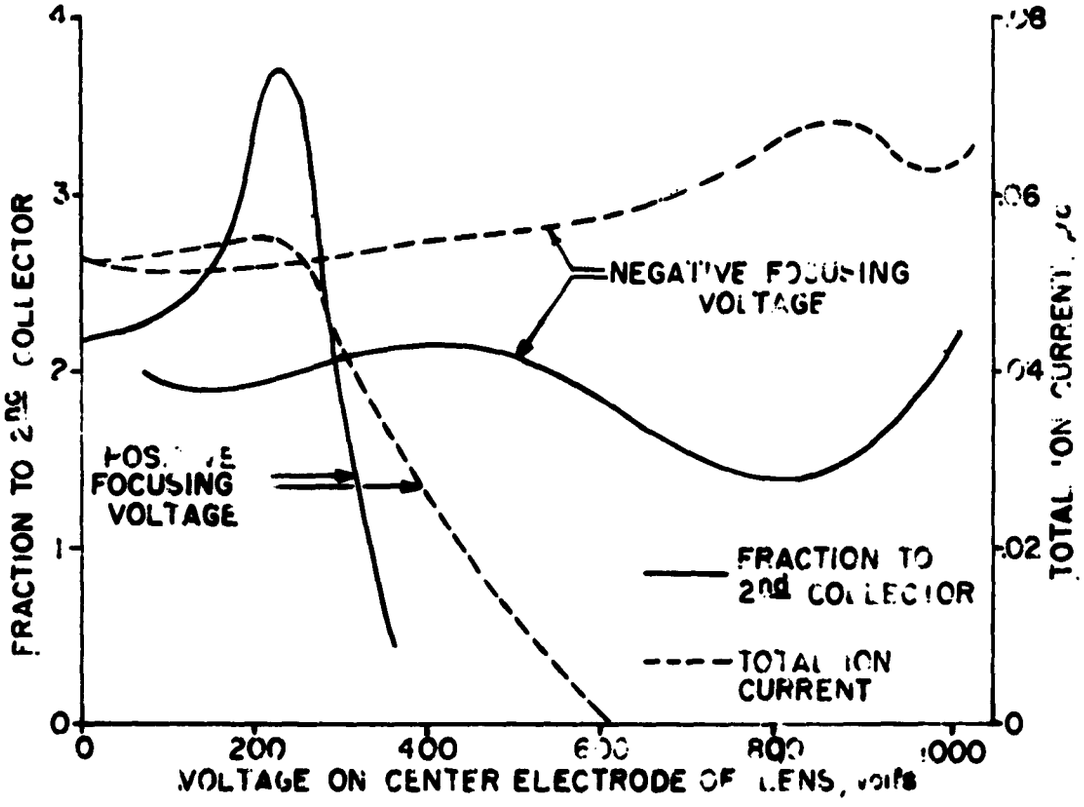

Figure A-12. Focusing Characteristic of Ion Gun Operating with 1-kv Discharge.

for a 1-kv discharge. This characteristic had two somewhat unexpected features: the focusing was much sharper for positive voltage on the center electrode of the lens, and the total ion current through the lens was only slightly greater for negative voltage. Because of these characteristics, it was decided to operate with a positive voltage on the center electrode, and the rest of this study was carried out using these

positive voltages. This also had the practical advantage that turning the ion beam on and off is simply a matter of switching the voltage of the center electrode between 200 and 500 volts.

A comparison of the total ion current from the second ion gun with that from the first, both with a pressure of $1(10)^{-7}$ mm Hg at the collector, is shown in Figure A-13. Bearing in mind that the discharge of the second

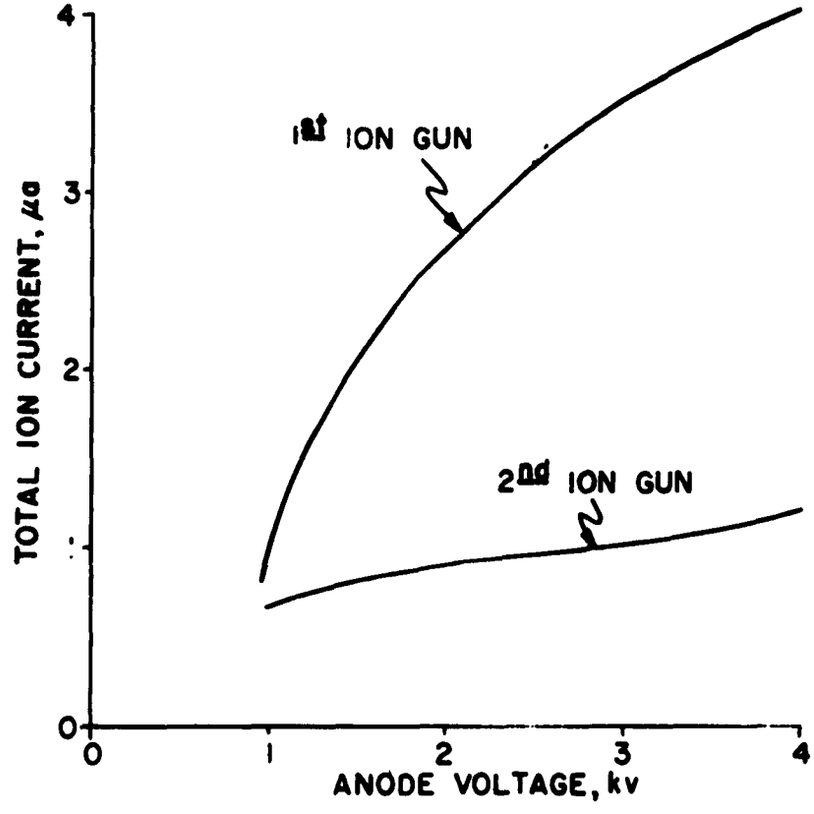

Figure A-13. Comparison of Total Ion Current from 1st and 2nd Ion Guns..

ion gun is actually at about twice as high a pressure as that of the first ion gun, one can see that from 50 per cent to 90 per cent of the ion beam was being intercepted by the lens. Despite this, the ion current density from the second ion gun was still greater than that from the first because

of the focusing action of the lens. Redesigning the lens to account for the ion path with positive voltage on the center electrode should increase the ion current by a factor of 3 or 4 .

In order to determine the proper operating values of the magnetic field and the focusing voltage, their interaction was studied for several values of the discharge anode voltage. A representative result, for a 1-kv discharge, is shown in Figure A-14. From these curves, the optimum

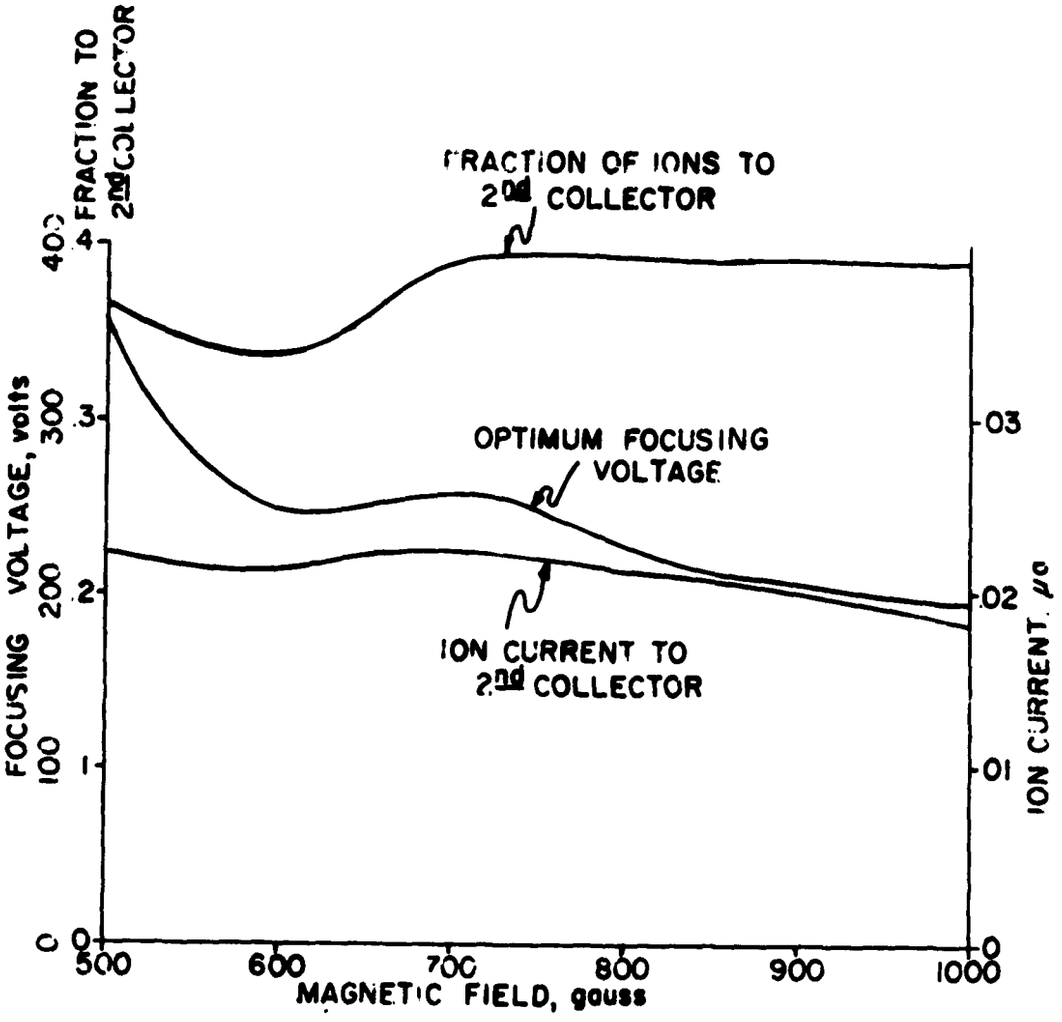

Figure A-14. Effect of Magnetic Field on Ion Optics for 1-kv Discharge.

magnetic field was chosen as that field for which a large current to the second collector was obtained and for which the value of focusing voltage was the least sensitive to changes in the magnetic field. This was repeated for several values of the anode voltage, and the results are summarized in Figure A-15, which was used for determining the correct values of magnetic

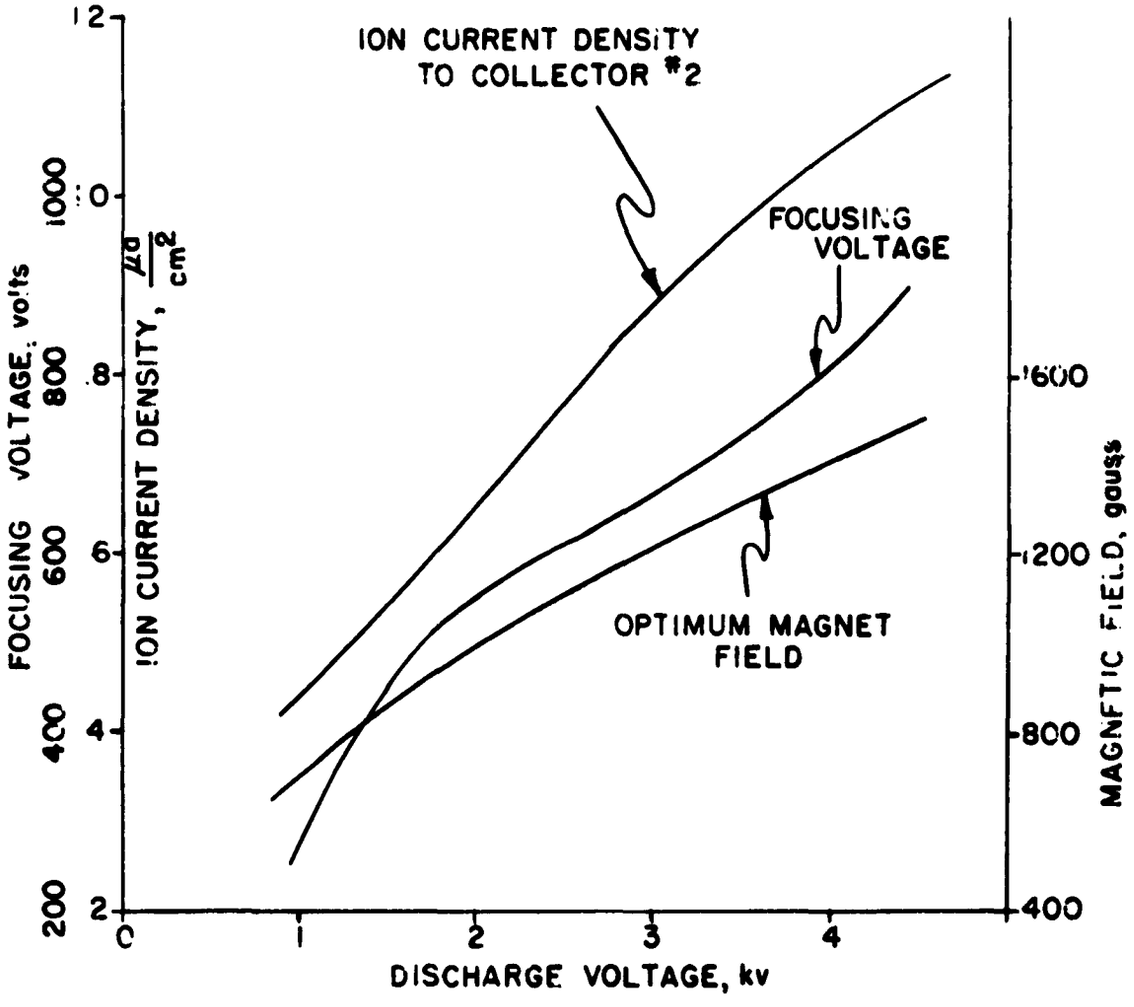

Figure A-15. Summary of Optimum Operating Conditions for Ion Gun No. 2 Using Positive Focusing Voltage at a Pressure of 10^{-7} mm Hg.

field and focusing voltage throughout the study of the effect of ion bombardment on oxide cathodes.

Since the energy of the bombarding ions is controlled by raising the potential of the whole grid-cathode assembly, it was necessary to determine the effect of this on the ion optics also. The results of this are presented in Figure A-16. Here it is seen that this negative potential not

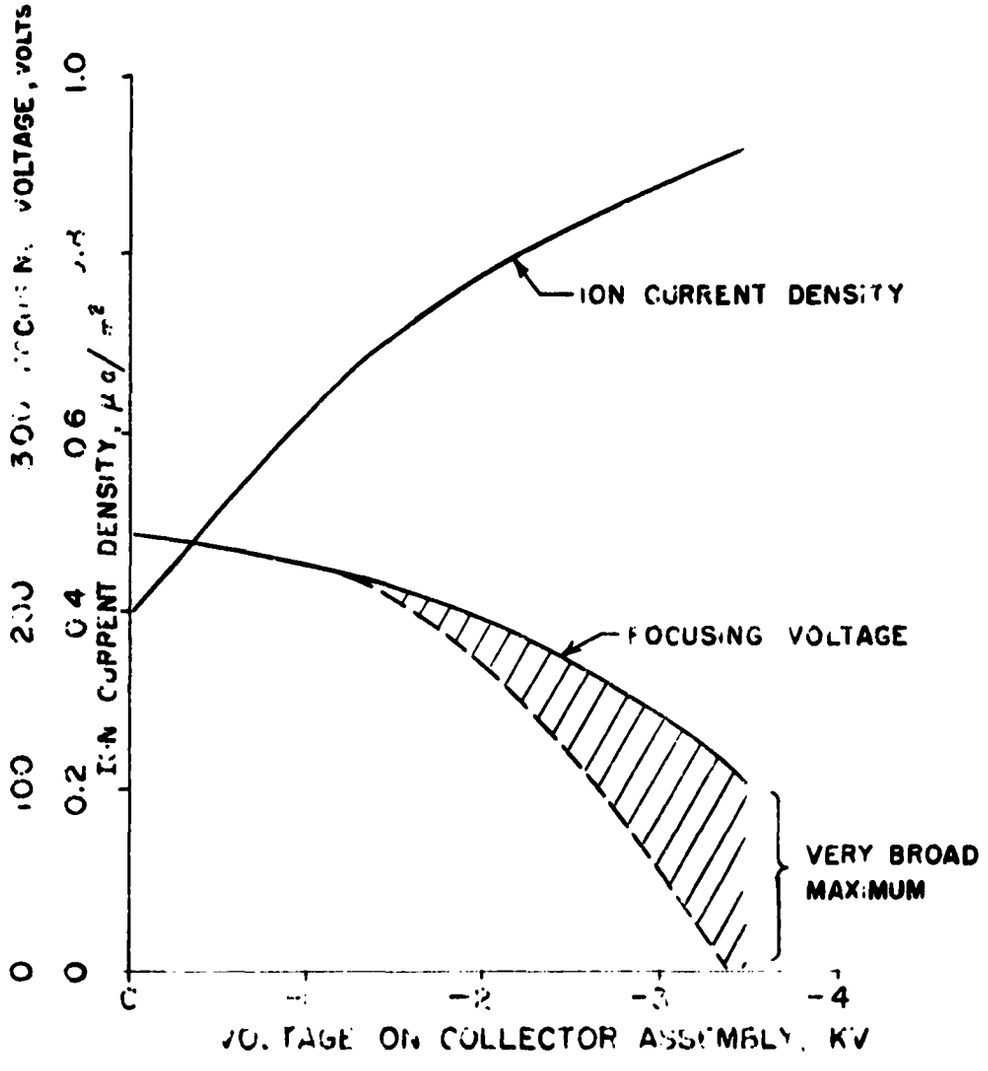

Figure A-16. Effect of Large Negative Potential on the Collector Assembly on Ion Optics

only increased the ion current to the second collector, but also decreased the optimum voltage on the focusing electrode. Voltages greater than 3.5 kv could not be used because a secondary discharge was formed in the region between the collector and the ion lens.

IV. RECOMMENDATIONS

On the basis of the experience gained in this study, several recommendations can be made towards obtaining high-ion current density on a target maintained in a very good vacuum:

1) Because of the space-charge limitations of the discharge, very little improvement is to be expected in the intensity of the discharge itself, other than from the "brute-force" approach of going to higher magnetic fields and anode voltages.

2) Intensifying of the discharge by differential pumping and concentration of the ion beam by focusing appear to be the most fruitful directions for improvement.

3) In view of the results of Lichtman[39] the extraction apertures used in the ion guns in this study are very probably too large and an aperture of 1/8 in. diameter might do as well and would considerably increase the pressure differential.

4) It has been found that despite the large energy spread in the ion beam, very sharp focusing can be obtained using an Einzel lens with positive voltage on the center electrode. Designing the lens for operation with positive voltage on the center electrode by making the aperture of this electrode 2 or 3 times as large as the aperture in the discharge cathode should increase the total ion current by a factor of at least 3 or 4.

5) If still larger ion currents are needed, the Einzel lens can be used to focus the ion beam on a small aperture and another pump can be placed beyond this aperture. In this way the pressure differential can be increased by another order of magnitude.

REFERENCES

1. G. Hermann and S. Wagener, The Oxide-Coated Cathode, Vol. II, London: Chapman and Hall, 1951.

2. S. Wagener, "Reactions Between Oxide Cathodes and Gases at Very Low Pressures," Proc. Phys. Soc., 67B (1954), p. 369.

3. N. B. Hannay, D. MacNair, and A. H. White, "Semi-Conducting Properties in Oxide Cathodes," Jour. App. Phys., 20 (1949), p. 669.

4. G. H. Metson and E. Macartney, "The Conductivity of Oxide Cathodes," Proc. I. E. E., 107 (1960), p. 91.

5. R. W. Peterson, D. E. Anderson, and W. G. Shepherd, "Influence of the Cathode Base on Chemical Activation of Oxide Cathodes," Jour. App. Phys., 28 (1957), p. 22.

6. J. A. Becker, "Phenomena in Oxide Coated Filaments," Phys. Rev., 34 (1929), p. 1323.

7. R. L. Sproull, "An Investigation of the Short-Time Thermionic Emission from Oxide-Coated Cathodes," Phys. Rev., 67 (1945), p. 166.

8. L. S. Nergaard, "Studies of the Oxide Cathode," RCA Rev., 13 (1952), p. 464.

9. H. J. Krusemeyer and M. V. Pursley, "Donor Concentration Changes in Oxide-Coated Cathodes Resulting from Changes in Electric Field," Jour. App. Phys., 27 (1956). p. 1537.

10. R. M. Matheson, L. S. Nergaard, and R. H. Plumlee, "Activation of an Oxide Cathode by Deposition of Alkaline Earth Metal Ions via a Mass Spectrometer," RCA Rev., 18 (1957), p. 385.

11. C. Herring and M. H. Nichols, "Thermionic Emission," Rev. Mod. Phys., 21 (1949), p. 185.

12. N. B. Hannay (ed.), Semiconductors, New York: Reinhold, 1959.

13. E. S. Rittner, "A Theoretical Study of the Chemistry of the Oxide Cathode," Philips Res. Repts., 8 (1953), p. 184.

14. R. H. Plumlee, "The Electron Donor Centers in the Oxide Cathode," RCA Rev., 17 (1956), p. 231.

15. R. Loosjes and H. J. Vink, "The Conduction Mechanism in Oxide-Coated Cathodes," Philips Res. Repts., 4 (1949), p. 449.

16. R. Forman, "Measurement and Theoretical Study of Electrical Conductivity and Hall Effect in Oxide Cathodes," Phys. Rev., 96 (1954), p. 1479.

17. W. S. Shepherd, "Dynamic Equilibrium Processes in Oxide-Coated Cathodes," Proc. Fourth Nat. Conf. Tube Techniques, New York: New York Univ. Press, 1959.

18. G. A. Haas, "Analysis of the D-C and Pulsed Thermionic Emission from BaO," Jour. App. Phys., 28 (1957), p. 1486.

19. R. L. Sproull, R. S. Bever, and G. Libowitz, "Oxygen Vacancies in Barium Oxide," Phys. Rev., 92 (1953), p. 77.

20. R. H. Plumlee, "Electrolytic Transport Phenomena in the Oxide Cathode," RCA Rev., 17 (1956), p. 190.

21. E. B. Hensley and K. Okumura, "Mobile Acceptor Model for Oxide-Coated Cathodes," Bull. Am. Phys. Soc., Series II, 5 (1960), p. 69.

22. R. W. Reddington, "Diffusion of Barium in Barium Oxide," Phys. Rev., 87 (1952), p. 1060.

23. H. B. Frost, "Transient Changes in Oxide Cathodes," Thesis, Mass. Inst. Tech., Cambridge, Mass., 1954.

24. E. O. Kane, "Thermionic Emission and Semi-Conduction in Single Crystals of Barium Oxide," Ph. D. Thesis, Cornell University, 1954.

25. G. H. Metson and E. Macartney, "The Conductivity of Oxide Cathodes," Proc. I. E. E., 107 (1960), p. 91.

26. N. A. Surplice, "Reversible Poisoning by Sulphur, Oxygen, and Other Gases of Oxide-Coated Cathodes at High Temperatures," Brit. J. A. P., 10 (1959), p. 359.

27. R. E. Schlier, "Mass- Spectrometer Measurement of Oxygen Adsorption and Desorption on Tungsten," Bull. Am. Phys. Soc., Series II, 3 (1958), p. 46.

28. G. A. Haas and J. T. Jensen, Jr., "Preconversion of Oxide Cathodes," Naval Res. Lab. Problem R08-05, Project N. R. 410-00, Task N. R. 410-003, Washington, D. C., 1959.

29. A. A. Shepherd, "The Effects of Oxygen on the Electrical Properties of Oxide Cathodes," Brit. Jour. App. Phys., 4 (1953), p. 70.

30. N. Bohr, "The Penetration of Atomic Particles through Matter," Kgl. Danske Vid. Selsk. Matfys. Medd., 18, No. 8 (1948).

31. E. B. Hensley, "Thermionic Emission Constants and Their Interpretation," Tech. Rept. No. 25, Univ. Missouri, 1960.

32. H. S. W. Massey and E. H. S. Burhop, Electronic and Ionic Impact Phenomena, Oxford: Clarendon Press, 1952.

33. J. R. Young, "Evolution of Gases and Ions from Different Anodes under Electron Bombardment," Jour. App. Phys., 31 (1960), p. 921.

34. J. Backus, "Studies of Cold Cathode Discharges in Magnetic Fields," Jour. App. Phys., 30 (1959), p. 1866.

35. F. M. Penning and K. Nienhuis, "Construction and Applications of a New Design of the Phillips Vacuum Gauge," Philips Tech. Rev., 11 (1949), p. 116.

36. J. Sommeria, "Un Nouveau Principe Général d'Extraction dans les Sources d'Ions," Jour. de Phys. et Rad., 13 (1952), p. 645.

37. D. Lichtman, Sperry Gyroscope Co., Private communication.

38. L. Brillouin, "A Theorem of Larmor and its Importance for Electrons in Magnetic Fields," Phys. Rev., 67 (1945), p. 260.

39. A. H. W. Beck, Thermionic Valves, Cambridge: University Press, 1953.

40. S. Dushman, Scientific Foundations of Vacuum Technique, New York: Wiley, 1949.

STUDIES OF CONTINUOUSLY OPERATED CATHODES

N. Erdibil

School of Electrical Engineering
CORNELL UNIVERSITY
Ithaca, New York

RESEARCH REPORT EE 469

STUDIES OF CONTINUOUSLY OPERATED CATHODES

N. Erdibil

LINEAR BEAM MICROWAVE TUBES

Technical Report No. 6 15 August 1960

Published under Contract No. AF30(602)-1696
Rome Air Development Center, Griffiss Air Force Base, New York

ACKNOWLEDGMENTS

During the course of this investigation, the author had the co-operation and assistance of many people. He wishes to thank R. G. Talpey, Manager Microwave System and Application Engineer, Radio Corporation of America, for supplying the L cathode and also J. P. Sackinger, Westinghouse Electric-Corporation, Electronic Tube Division, Elmira, New York, for supplying the SM-17 thorium-tungsten cermet cathode.

The author gratefully acknowledges the assistance of W. R. Brown, who constructed the test diodes and to D. P. Reynolds for his constructive criticism of the original manuscript. Also, he thanks the U. S. Air Force who supported this work under Contract No. AF 30(602)-1696.

Finally, the author wishes to express his indebtedness and gratitude to Professor G. C. Dalman, without whose constant guidance and assistance this thesis would not have been possible.

CONTENTS

ILLUSTRATIONS

ABSTRACT

Gas evolution in a thorium-tungsten cathode of an L-cathode during processing and operating periods have been investigated.

Temperature-independent components of the work function for the above cathodes have been found from the emission. Emission levels have been obtained by the application of shot-noise reduction factor measurement technique.

Effects of carbon monoxide, carbon dioxide, hydrogen, and oxygen on the emission activity of the cathodes have been studied. Also, an attempt was made to explain the physical nature of oxygen poisoning.

I. INTRODUCTION

In vacuum tubes some of the contaminations introduced at various stages of the manufacturing process will always be present as residual gases. These residual gases can affect the atomic balance of the cathode surface and consequently affect its emission activity.

Before studying the effects of residual gas components on the emission properties of the cathode, however, it is necessary to investigate the composition of gases introduced at each stage of the manufacturing process. One of the most reliable methods for determining the composition of gases is using a mass spectrometer. This method has been used by Pikus[1, 2] in the study of gas evolution from oxide cathodes for long periods of operation of all-glass sealed-off analyzer tubes under normal operating conditions. The work of Ptushinskii and Chuikov[3] for

the determination of residual gases in vacuum tubes with porous-metal cathodes is also of interest. This method could be applied equally well to the evolution of gases by thorium-type cathodes[4] and L-cathodes.[5]

One of the purposes of this study, therefore, was the determination of the gases evolved from a thorium-type cathode and from an L-cathode during baking, activation, and operation as well as the determination of the residual gas components. The objective was a qualitative clarification of the general mechanism of gas evolution rather than a quantitative study of the mass spectrum.

The ultimate purpose of this work was to study the effects of various gases on the emission properties of these two cathodes. One of the best methods of determining the emission level of diodes is by the shot-noise reduction-factor measurement technique.[6,7] This technique was used in this study.

II. EXPERIMENTAL APPARATUS

The layout of the vacuum system is shown in Figure 1. The mass spectrometer was connected to the system by knife-edge flanges with OFHC copper blocks between them. The system employed a three-stage glass oil pump with a charcoal trap that prevented back-streaming of oil.

A. RADIO FREQUENCY MASS SPECTROMETER

A linear-beam radio-frequency spectrometer developed and tested

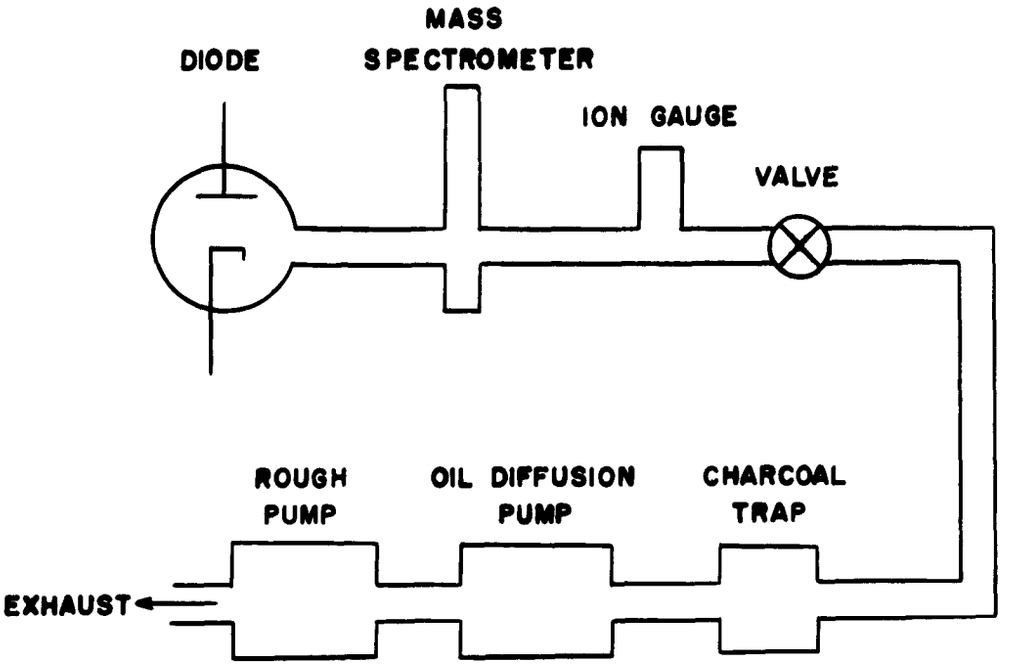

Figure 1. Layout of Vacuum System

by Gilmour,[8] was used to investigate the composition of gases. The electrical circuit of this mass spectrometer is shown in Figure 2.

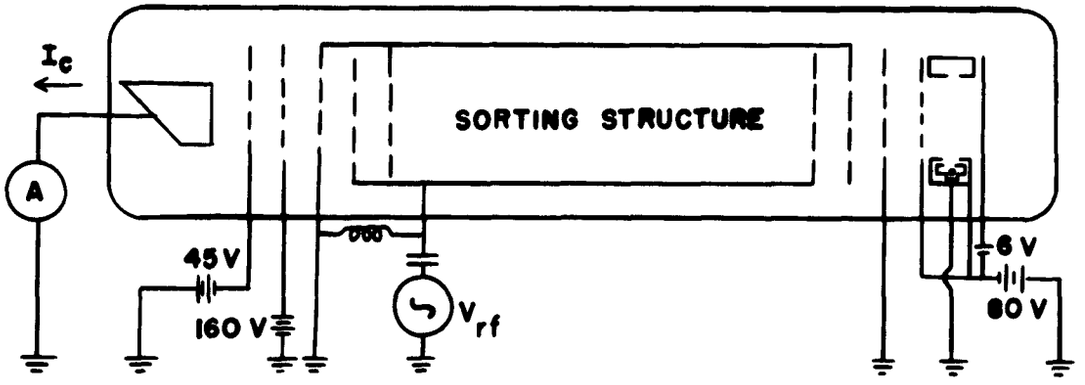

Figure 2. Electrical Circuit of Mass Spectrometer

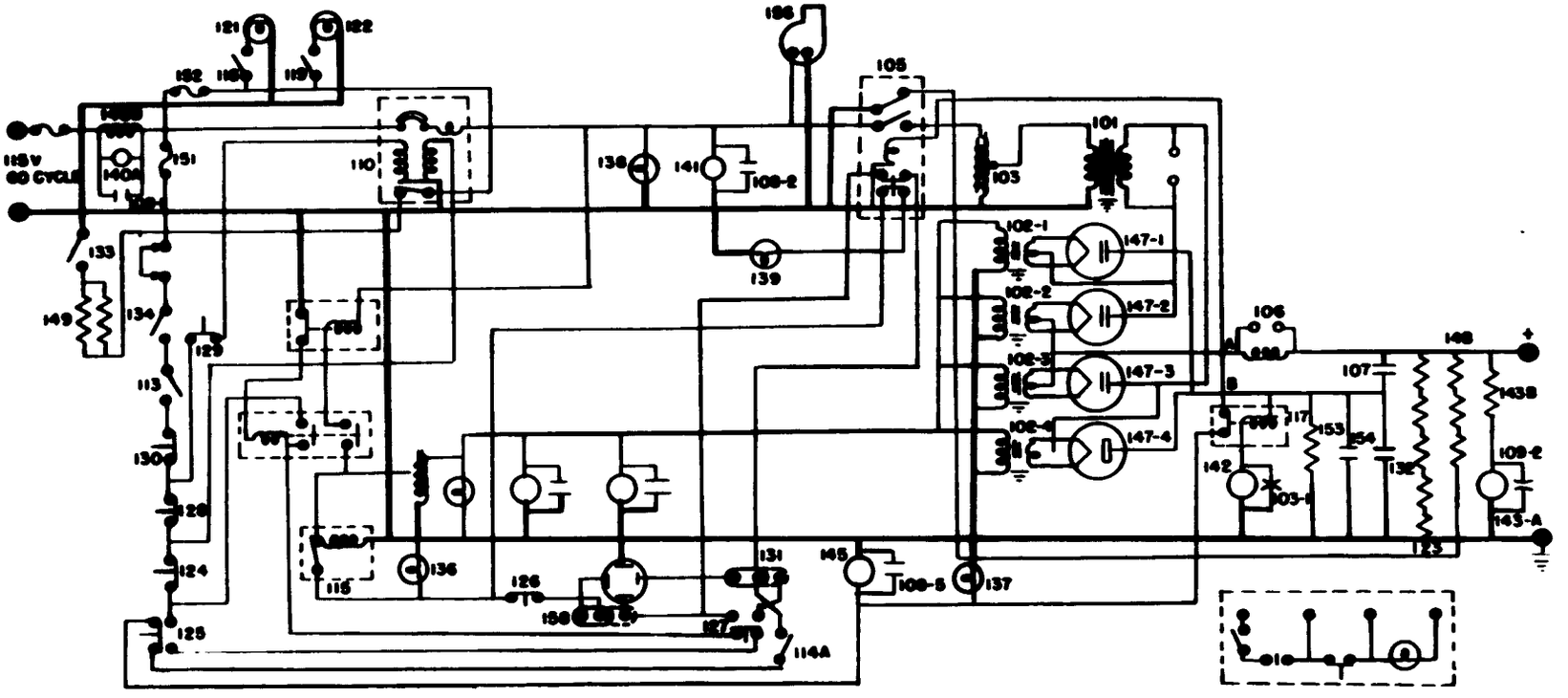

Figure 3. Circuit Diagram of RA-38 D-C Power Supply.

The gas is ionized by 80-volt electrons and then accelerated into the sorting structure through a potential of 80 volts. At a given frequency of the r-f voltage applied to the alternate grids, only those ions having the proper velocity will gain enough energy to get past the 160-volt repeller grid and arrive at the collector. Thus by sweeping the r-f voltage frequency, the mass spectrum of any gas could be obtained.

B. DIRECT-CURRENT POWER SUPPLY

A direct-current power supply (15 kv, - 0.5 amp) of RA-38 type was used. The electrical circuit of the device is shown in Figure 3. The polarity of the output voltage was reversed at points A and B so that the positive terminal was grounded. Also, the connections to the direct-current ammeter (142) and to the direct-current voltmeter (143 amp) were interchanged to get upscale readings.

C. SHOT-NOISE REDUCTION FACTOR MEASUREMENT CIRCUIT

A block diagram of the measuring circuit is shown in Figure 4.

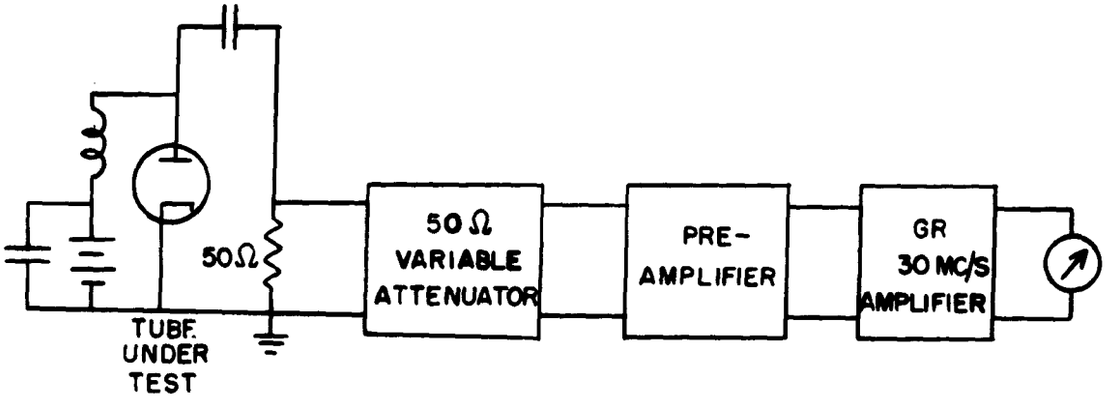

Figure 4. Block Diagram of Experimental Circuit for Shot-Noise Reduction Factor Measurements.

The instrumentation and the method of measurement were patterned after the work of I. Turkekul.[6] The noise reference used was the tube under test operated in the temperature-limited region. The output noise power under these conditions was attenuated to equal the output noise power under test conditions. Then the shot-noise reduction factor was found simply by dividing the anode current under temperature-limited conditions by the product of the anode current under test conditions and the amount of attenuation, that is,

$$\Gamma^2 = I_a'/I_a \cdot A \quad , \tag{1}$$

where

Γ^2 is the shot-noise reduction factor,

I_a' is the anode current in the temperature-limited region,

I_a is the anode current under test conditions,

A is the amount of attenuation.

A low-noise preamplifier with a noise figure of about 2-3 db and a General Radio Type 1216-A, 30 Mc/s IF amplifier were used for the amplification of the output noise power. Direct-current balancing of the output meter to suppress the zero scale was accomplished by the circuit shown in Figure 5.

III. THORIUM-TUNGSTEN CATHODE

A Westinghouse SM-17, thorium-tungsten cathode with 89 $\frac{1}{2}$ per cent tungsten, 10 per cent ditungsten carbide, and $\frac{1}{2}$ per cent thorium

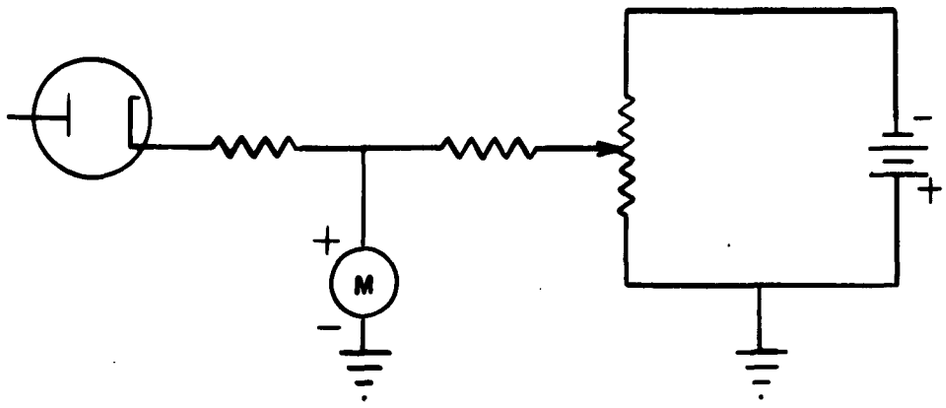

Figure 5. D-C Balancing Circuit with Output Meter of GR 30 Mc/s IF Amplifier.

hydride was used as the test cathode.

A. GAS EVOLUTION OF THORIUM-TUNGSTEN CATHODE

1. Baking

The tube shown in Figure 6 was baked for eight hours. The baking temperature was increased in steps of 100°C up to 400°C. A general picture of the gas evolution during this period is shown in Figure 7. The spectrum consists of five peaks corresponding to masses 1, 2, 16, 28, and 44. There is no doubt that peak 2 belongs to molecular hydrogen, since the tube was hydrogen fired during the construction period. The peak corresponding to mass 1 could be either atomic hydrogen or doubly charged hydrogen ions. Mass 16 belongs to a mixture of CH_4 and atomic oxygen. Atomic oxygen probably appears as a result of dissociation of CO_2, since O_2 (m = 32) is absent from the spectrum. Mass 28 consists of a mixture of CO^+ and N_2^+, and mass 44 is CO_2^+.

From Figure 7 it is seen that the amounts of H_2^+ and H^+ or H_2^{++}

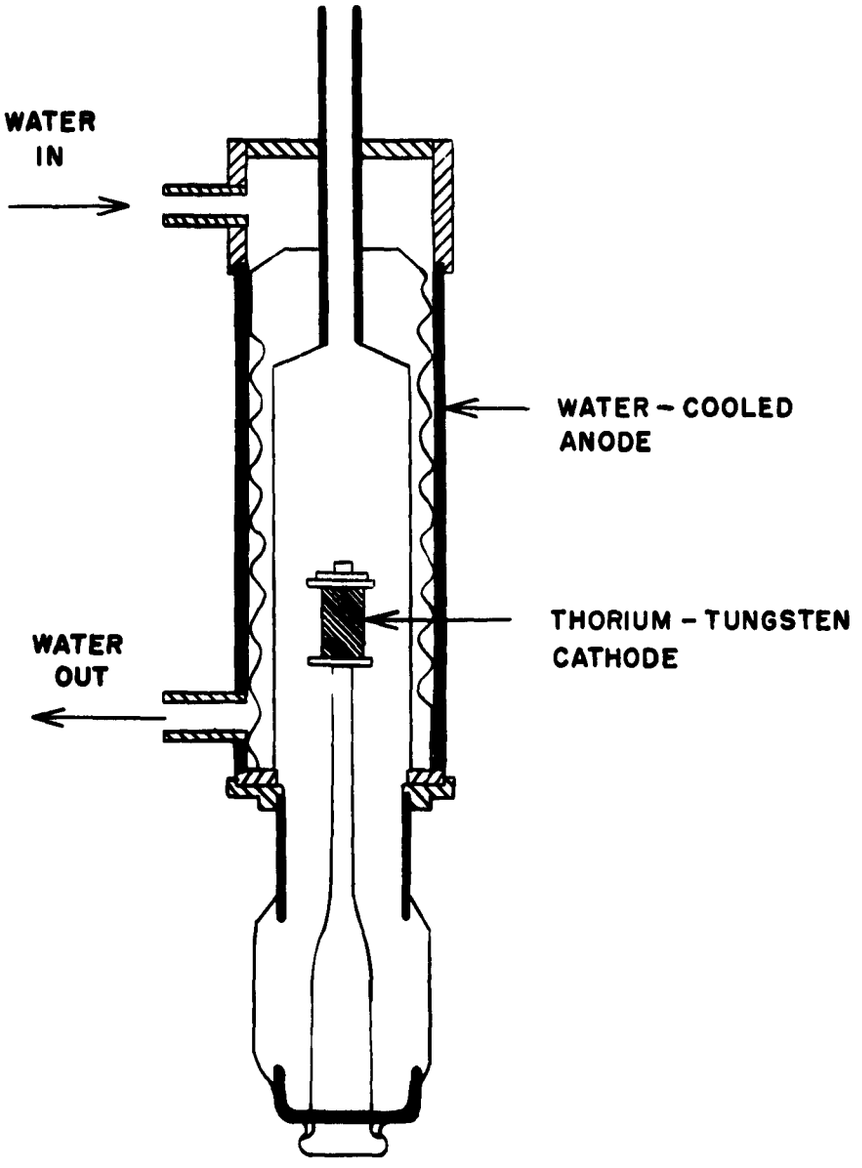

Figure 6. Experimental Diode

are very small compared to the amounts of masses 44, 28, and 16. As the baking temperature is increased above 200°C a sudden decrease in the amount of mass m = 44 occurs with a corresponding increase in

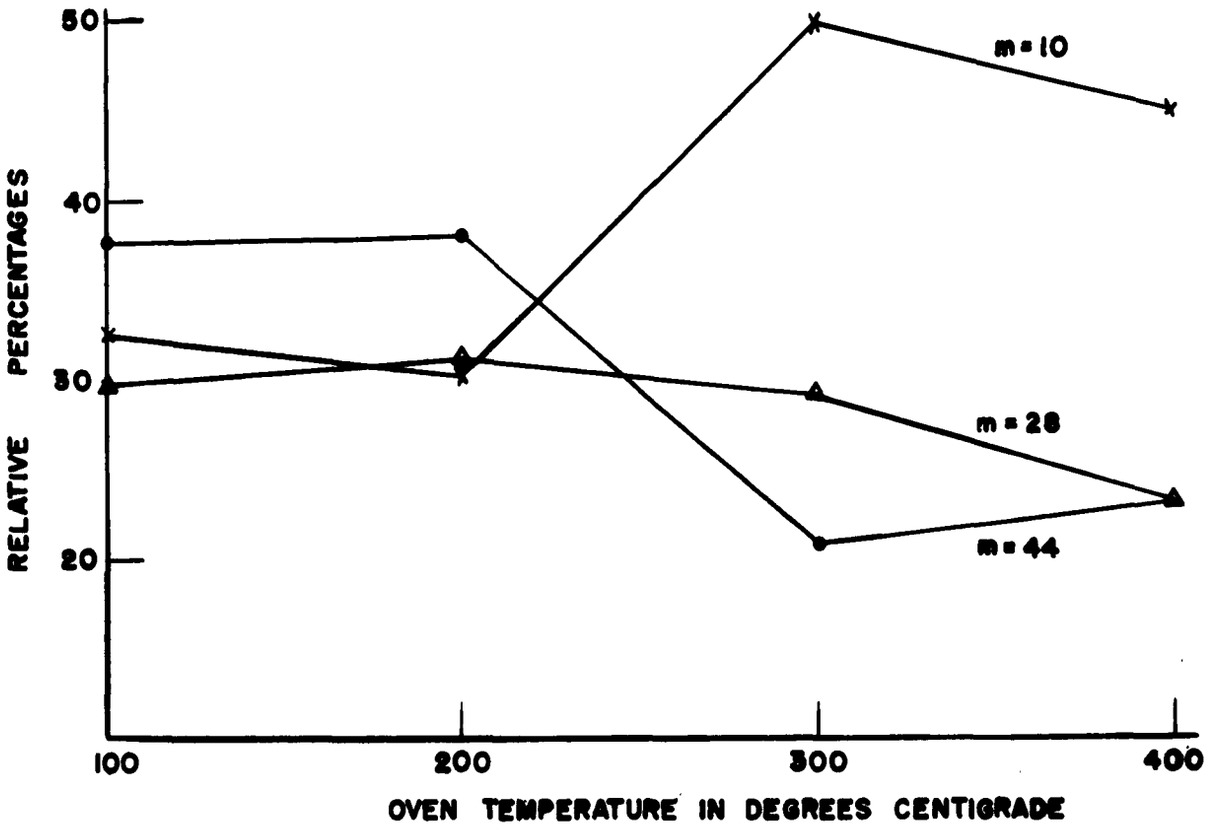

Figure 7. Spectrum of Gas Evolution during Baking

mass 16.

The oven temperature was kept fixed at 400°C for four hours and fifteen minutes and the relative percentages of gases evolved during this period are shown in Figure 8. The main gases consist of masses of 16, 28, and 44. Spectrometer current with respect to time is shown in Figure 9. As the pumping time increased there was a corresponding decrease in all gas components.

2. Activation

Heater voltage was increased in small steps; each increase in the voltage being followed by a gas burst. Relative percentages of the

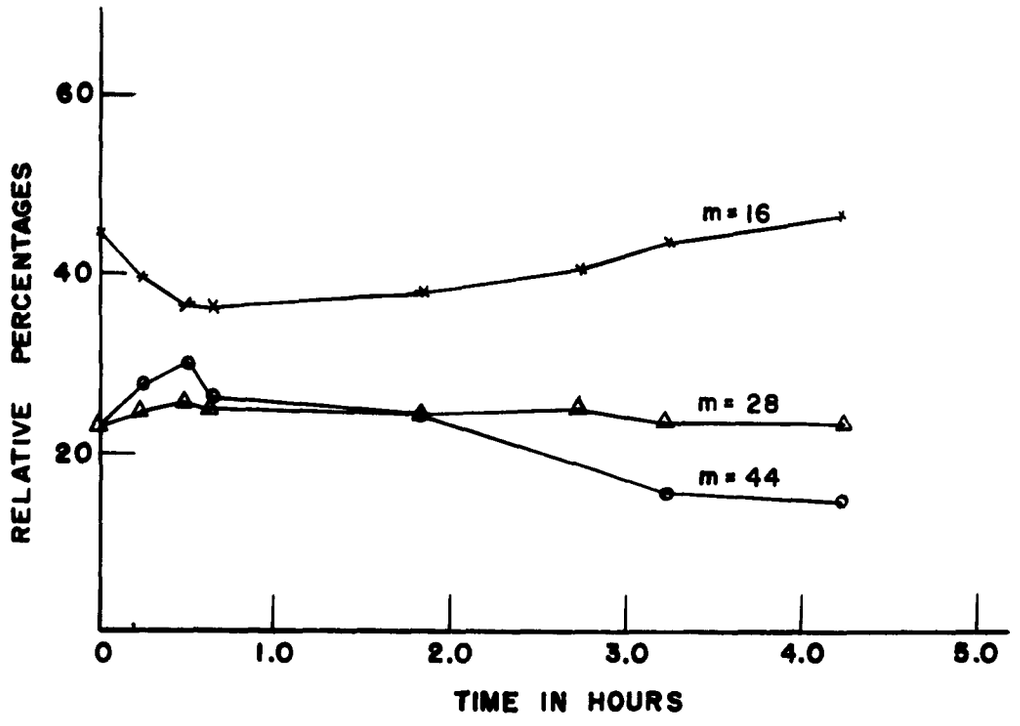

Figure 8. Spectrum of Gas Evolution at 400°C Oven Temperature

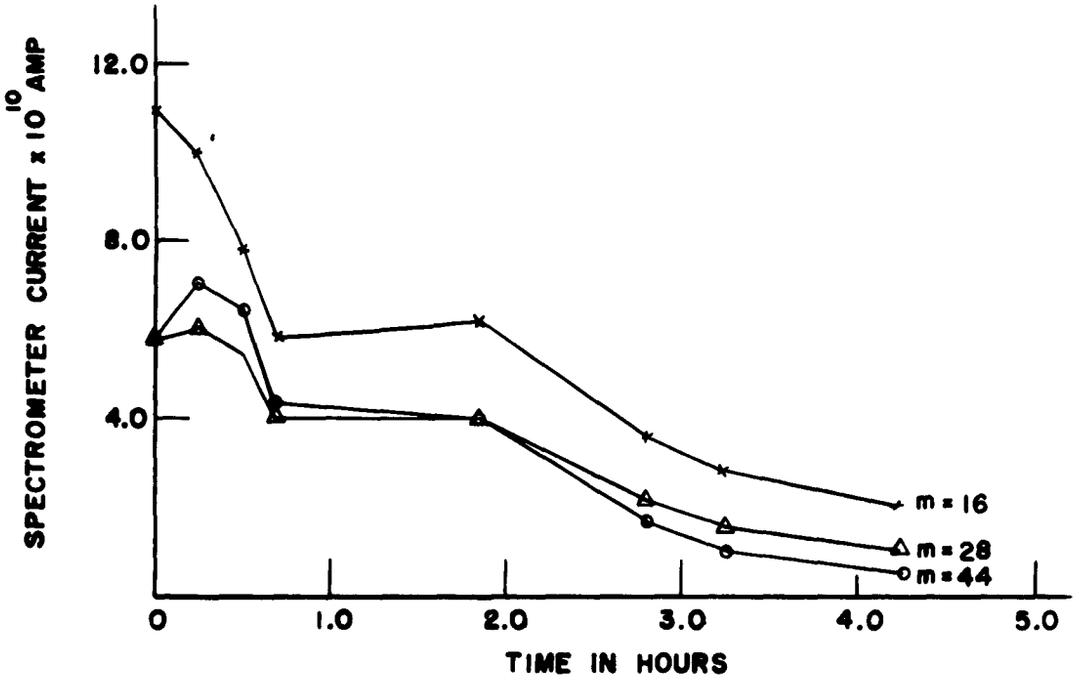

Figure 9. Spectrometer Current versus Time at 400°C Oven Temperature

different components of the gases evolved during this period are shown in Figure 10. It is seen that the main gas evolved during this period is carbon monoxide. This can be explained as follows:

As the sintering temperature of the cathode is increased, the thorium hydride loses its hydrogen and starts to alloy with the tungsten. At the same time thorium carbide is formed from the carbon available in tungsten carbide:

$$ThH_2 \longrightarrow Th + H_2 \qquad (2)$$

$$Th + W_2C \longrightarrow ThC + 2W \qquad (3)$$

In the presence of wet air, thorium carbide is unstable and will form C_2H_2 and ThO_2 according to the formula

$$ThC + H_2O \rightleftarrows ThO_2 + C_2H_2 + \text{Other Hydrocarbons} \qquad (4)$$

In the tube, then, the tungsten carbide will react with the thorium oxide and form carbon monoxide according to the reaction

$$ThO_2 + 2W_2C \rightleftarrows 4W + Th + CO \qquad (5)$$

An excess of carbon monoxide might cause a gassy tube, but heating the tube to a high enough temperature and for a long enough period while pumping it minimizes this possibility.

The other gases evolved during this period are of masses 16 and 12. Mass 12, which corresponds to carbon appears as a result of the dissociation of carbon monoxide above seven volts of heater voltage.

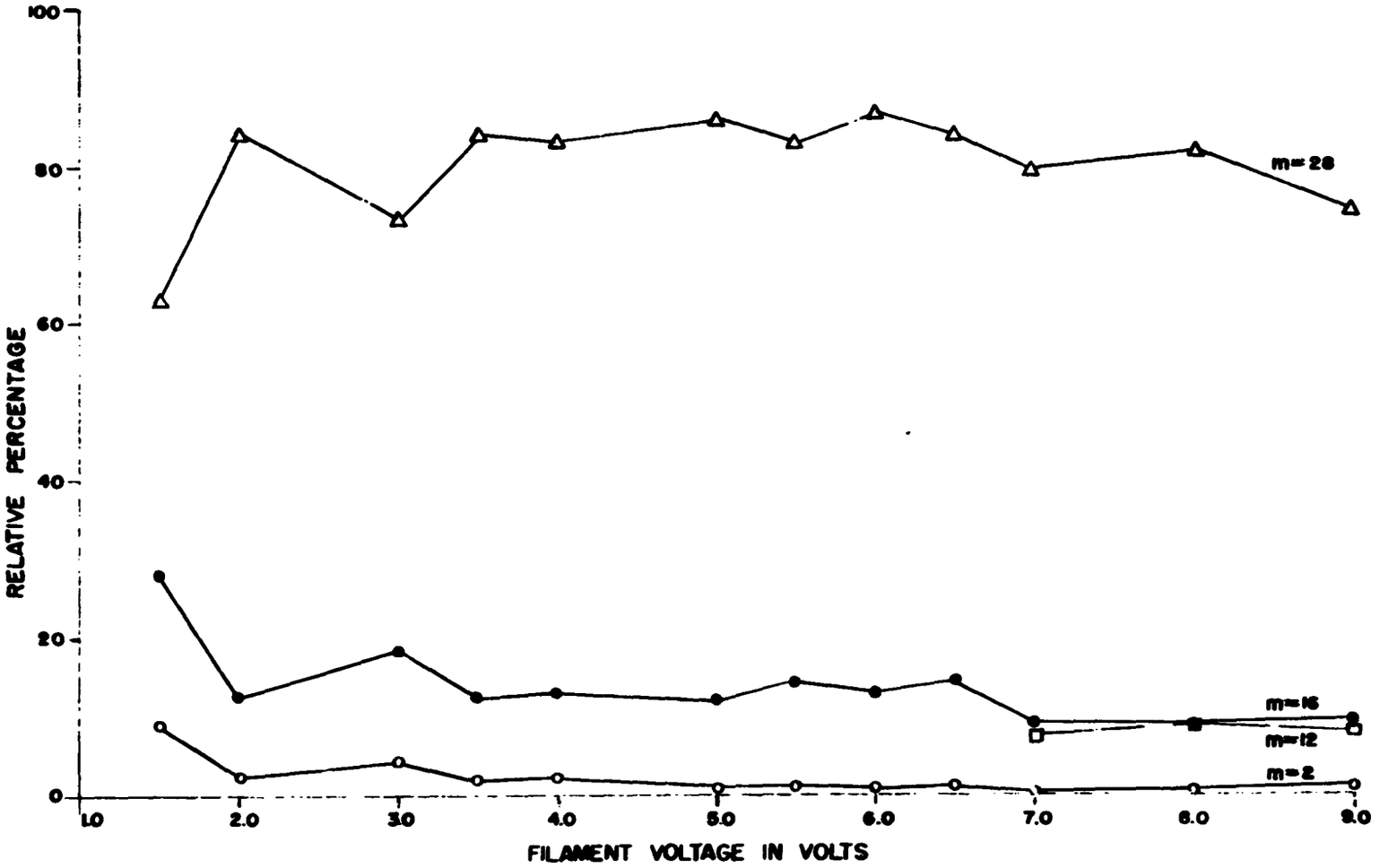

Figure 10. Gas Spectrum of Thorium-Tungsten Cathode During Activation Period.

3. Residual Gases

After activation the pressure in the tube was maintained at 3×10^{-7} mm Hg, a vacuum which approaches that of commercial electronic devices. Gas composition was then determined under three conditions:

1. cathode cold,
2. cathode heated to 1410°C for ten minutes,
3. cathode heated to 1410°C and emitting 280 ma.

The results are shown in Table I, where it can be seen that heating the cathode and drawing current causes a progressive increase in the percentage of carbon monixide and a decrease in the percentages of all other residual gas components.

Table I. Relative Percentages of Residual Gases of Diode with Thorium-Tungsten Cathode.

Gases	Cathode Cold	T_c = 1410°C	T_c = 1410°C I_a = 280 m.a
CO_2^+ (%)	14.0	8.1	7.9
CO^+ (%)	38.0	61.8	71.6
O^+ (%)	38.0	23.0	17.3
H_2^+ (%)	5.5	3.9	1.45
H^+, H_2^{++} (%)	4.5	3.2	1.75

B. DETERMINATION OF EMISSION LEVEL

Emission levels for different filament voltages were determined

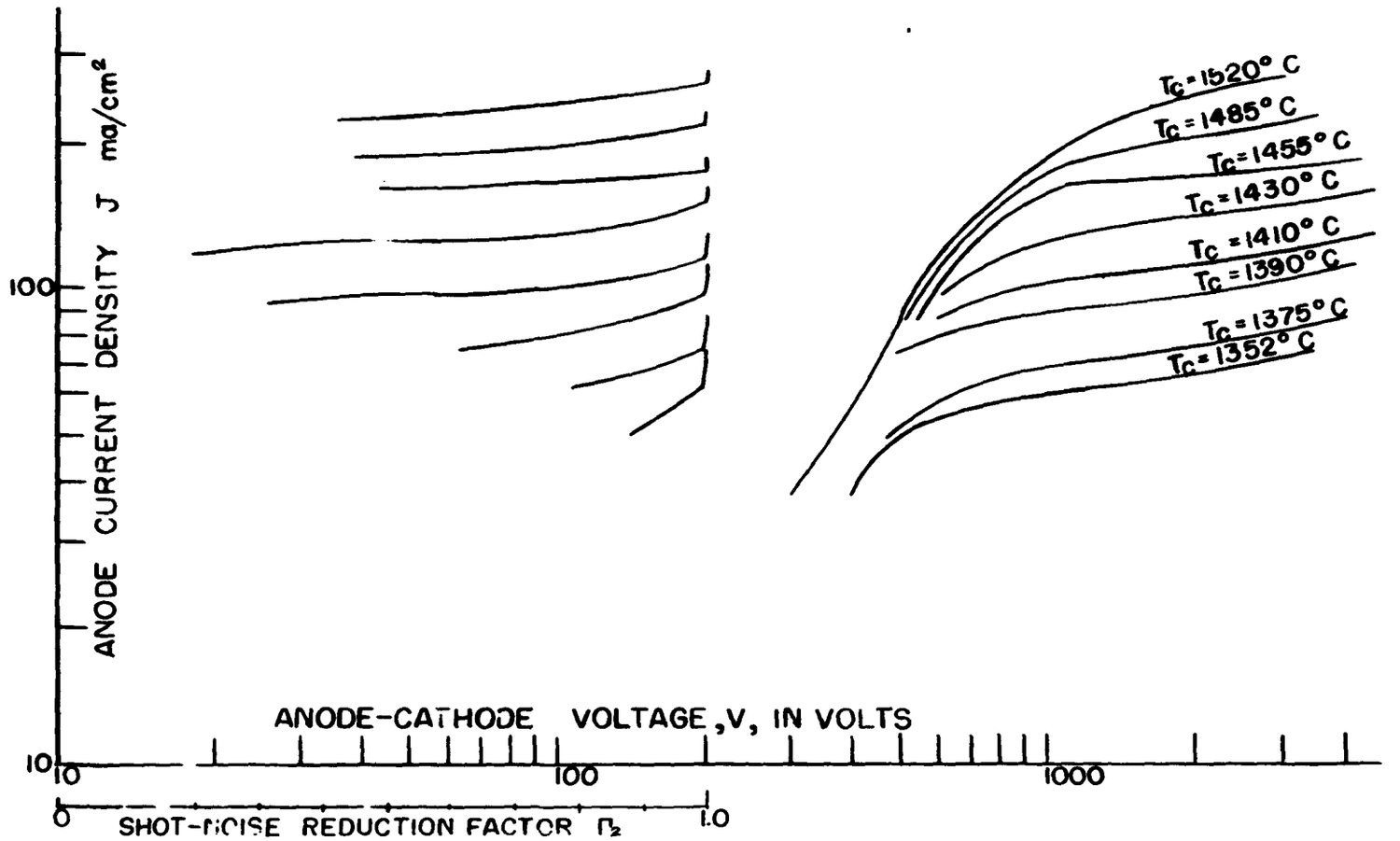

Figure 11. Anode Current Density versus Anode-Cathode Voltage, Anode Current Density versus Shot-Noise Reduction Factor at Various Cathode Temperatures.

by the application of shot-noise reduction factor measurements. The voltage-current characteristics of the tube and graphs of anode current versus shot-noise reduction factor are given in Figure 11. From these curves the emission levels were read at points where the shot-noise reduction factor became unity.

The temperature-independent component of the work function was obtained from a plot of the Richardson equation

$$J = A_o T^2 e^{-Q/kT}$$

This resulted in a work function ϕ of 2.39 ev. Details of the calculation are shown in Table II and Figure 12.

Table II. Calculation for Richardson's Plot

P (watts)	T_B (°C)	T_T (°C)	T (°K)	I_s (ma)	$10^3/T$	I_s/T^2	J_s/T^2
81.3	1310	1352	1625	100	0.615	33.5×10^{-9}	20.1×10^{-9}
85.0	1330	1375	1648	120	0.608	44.1×10^{-9}	26.5×10^{-9}
88.6	1345	1390	1663	160	0.600	57.7×10^{-9}	34.6×10^{-9}
92.3	1365	1410	1683	190	0.594	66.7×10^{-9}	40.0×10^{-9}
96.4	1378	1430	1703	240	0.587	82.4×10^{-9}	49.5×10^{-9}
101.2	1405	1455	1728	280	0.579	93.4×10^{-9}	56.0×10^{-9}
108.2	1435	1485	1758	350	0.570	112.8×10^{-9}	67.4×10^{-9}
116.5	1470	1520	1793	430	0.557	135.8×10^{-9}	81.5×10^{-9}

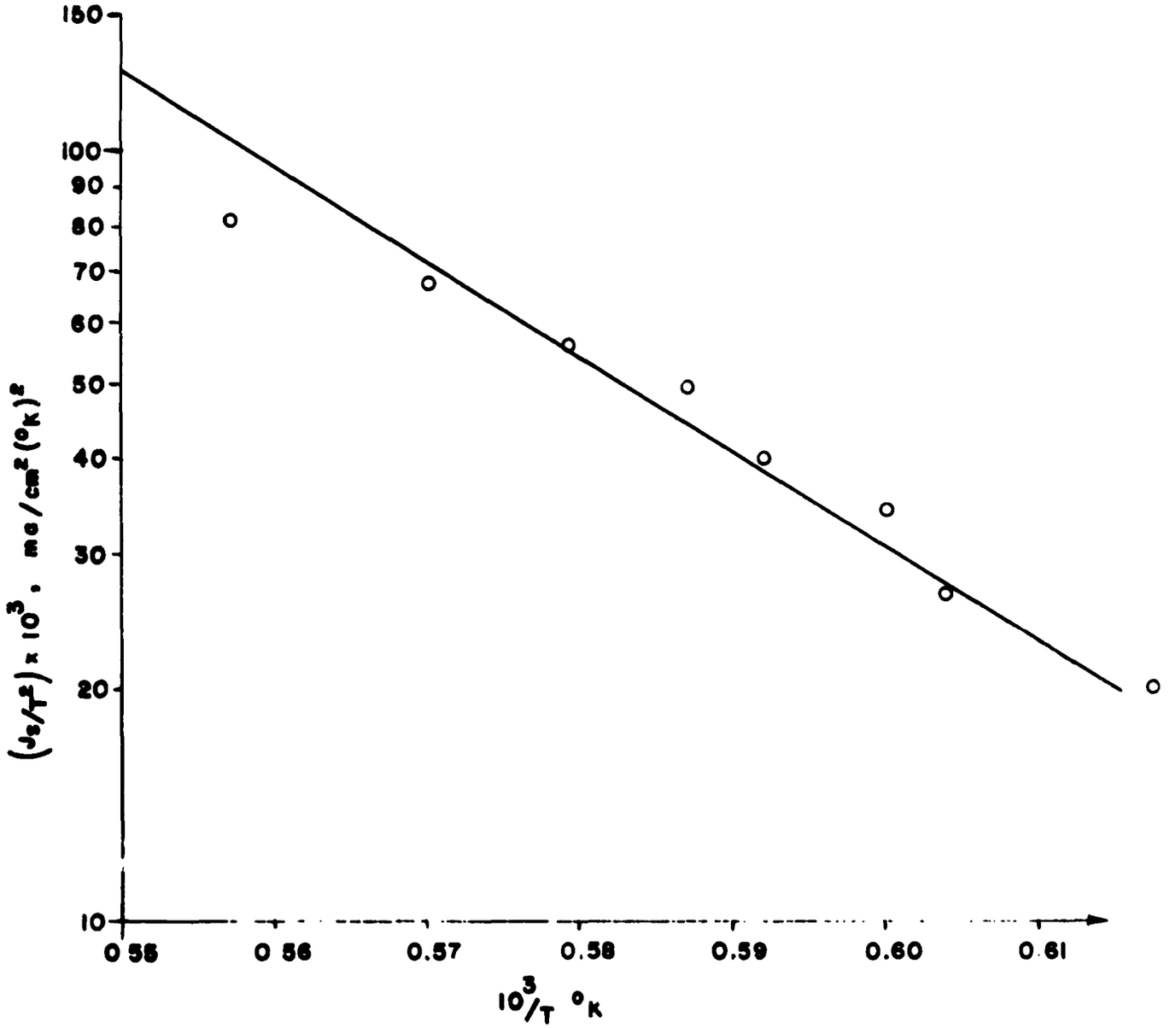

Figure 12. Richardson Plot (ϕ_o = 2.39 ev).

C. EFFECTS OF VARIOUS GASES ON THE THERMIONIC EMISSION OF A THORIUM-TUNGSTEN CATHODE

The residual gases found in the tube were composed of carbon monoxide, carbon dioxide, and atomic oxygen. In the study of the effect of each gas on the emission activity of the cathode, the gas was admitted into the system through a high-vacuum valve and a constant pressure p

was maintained throughout the measurements.

1. Effect of Carbon Monoxide and Carbon Dioxide on Emission

When system pressure was 4.0×10^{-7} mm Hg, carbon monoxide was admitted into the system by opening a high-vacuum valve. The valve was closed within one minute, when system pressure had risen to 2.5×10^{-6} mm Hg. Thereafter, pressure was controlled manually at 2.5×10^{-6} mm Hg by admitting more carbon monoxide as pressure dropped. The variation of emission with time at different cathode temperatures under these conditions is shown in Figure 13.

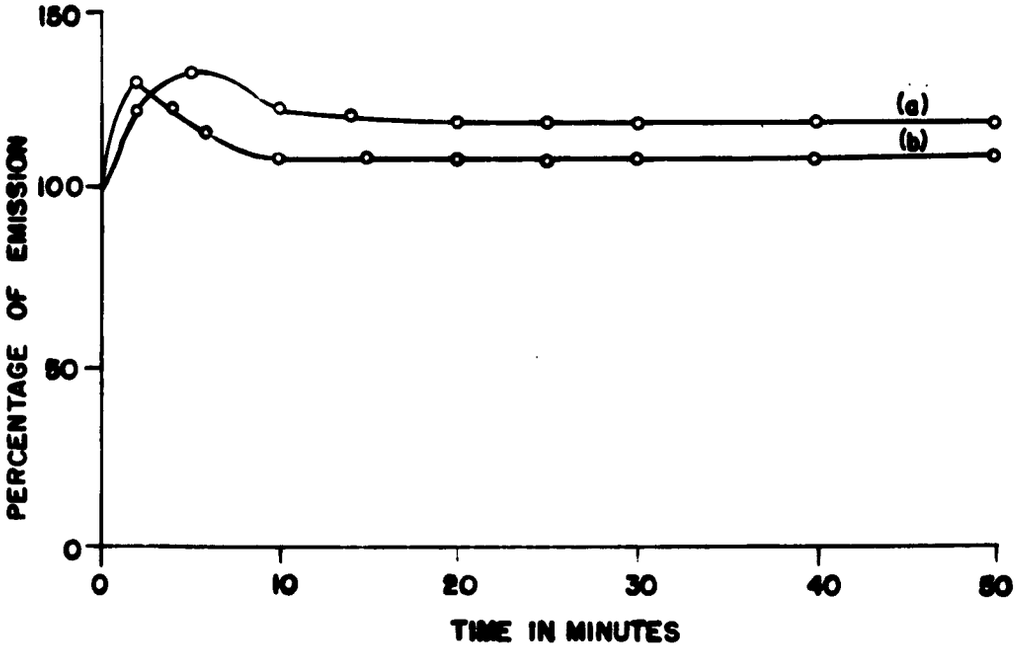

Figure 13. Effect of Carbon Monoxide on Emission Level of Thorium-Tungsten Cathode; $p = 2.5 \times 10^{-6}$ mm Hg, (a) $T_c = 1520^{\circ}C$, (b) $T_c = 1390^{\circ}C$.

The initial slope of the curve is dependent upon the rate of opening of the valve and the distribution of the gas in the system. After an initial increase, the emission gradually falls and reaches a constant value, which

is higher than the original value. Also, from Figure 13 it can be seen that the lower the cathode temperature, the less time it takes for emission to assume a constant value.

When the valve was closed and the pressure allowed to fall to the original value (4.0×10^{-7} mm Hg) the variation of emission with time is shown in Figure 14. It can be seen that in this case faster recovery was obtained at the higher cathode temperature.

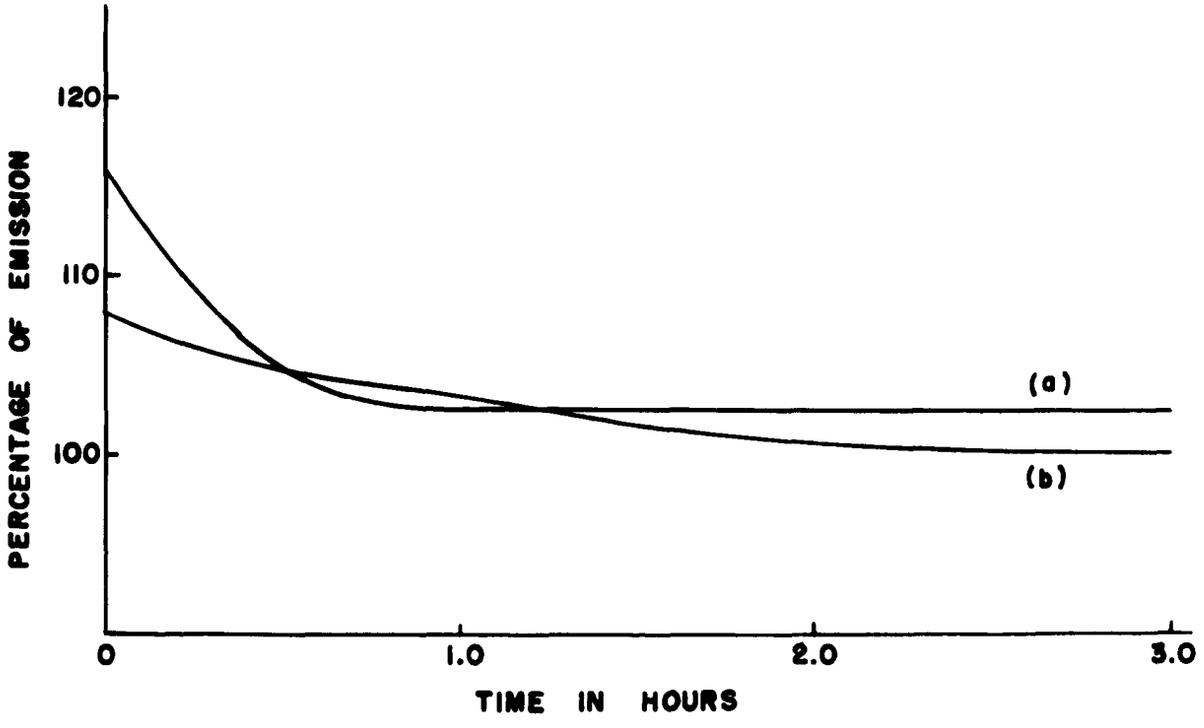

Figure 14. Recovery of Emission from Carbon Monoxide.
(a) $T_c = 1520^{\circ}C$, (b) $T_c = 1390^{\circ}C$.

The effect of carbon dioxide was determined in the same way as the effect of carbon monoxide, and similar results were obtained. The only difference was that the effect of carbon dioxide was much smaller than the effect of carbon monoxide. This could be explained by the two

effects of carbon dioxide--the major effect which is activating,and the minor effect, which is an oxidizing effect and tends to reduce the emission.

2. Effect of Oxygen on Emission

At the very start of the work with oxygen it became clear that because of the strong poisoning effect of oxygen,the emission diminished within less than a minute; therefore it was not possible to obtain the necessary data for the variation of emission with time.

IV. L CATHODE

A type "A" L cathode filled with B_aCO_3 was used as the test cathode. A sketch of the cathode is shown in Figure 15.

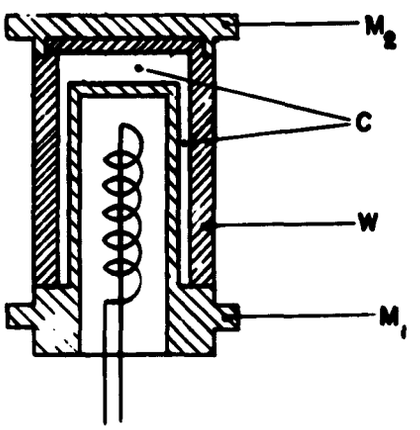

Figure 15. Cylindrical L-Cathode

(M_1, M_2 molybdenum holder, W porous tungsten body, C chamber with barium compound).

This cathode consists of a body, W, of porous tungsten (porosity in the range of 17 - 27 per cent) welded to molybdenum holders M_1 and M_2.

A tablet consisting of a mixture of barium carbonate and strontium carbonate is placed in the cavity C. The strontium is added to prolong cathode life.

After dissociation of the carbonates, barium oxide is reduced to barium by tungsten. Then barium is transported through the pores of the tungsten to the emitting surface. The presence of barium on the tungsten surface, possibly in conjunction with oxygen, results in a dipole layer which lowers the work function of the metal. During the operation, barium lost from the emitting surface is continuously replenished by the chemical reduction process.

A. GAS EVOLUTION FROM L CATHODE

1. Baking

The thorium-tungsten cathode of the diode shown in Figure 8 was replaced with an L cathode and the tube was baked for seven hours. A general picture of the gas evolution during this period is shown in Figure 16 and 17. The spectrum consists of three peaks corresponding to masses 44, 28, and 16. As previously indicated in part III, these numbers correspond to carbon dioxide, carbon monoxide, and atomic oxygen respectively.

From Figure 16, it can be seen that, as the baking temperature was increased from 200°C to 300°C, the percentage of atomic oxygen decreased with a corresponding increase in the percentage of carbon dioxide. This relation could also be observed (Figure 17) when the oven temperature was kept fixed at 400°C. During the baking period the percentage of carbon monoxide was relatively low and approximately constant.

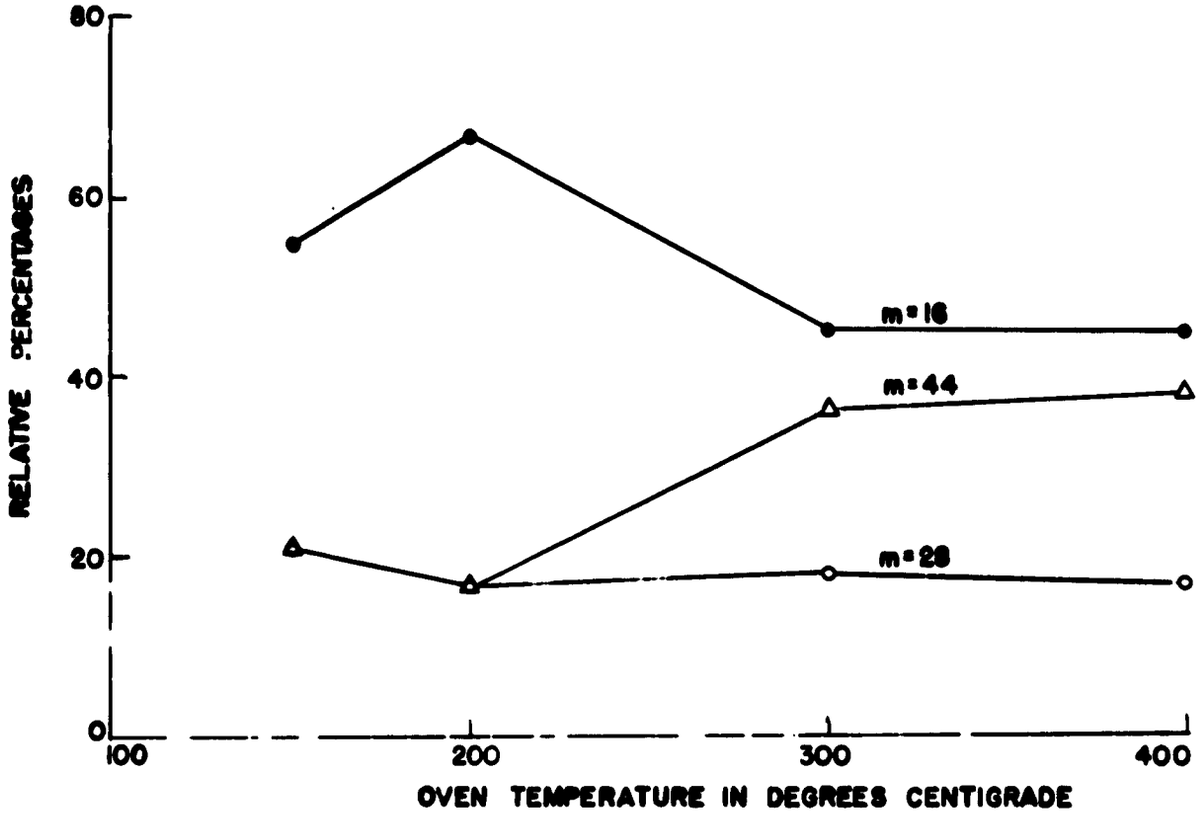

Figure 16. Relative Percentages of Gases versus Oven Temperature for L-Cathode.

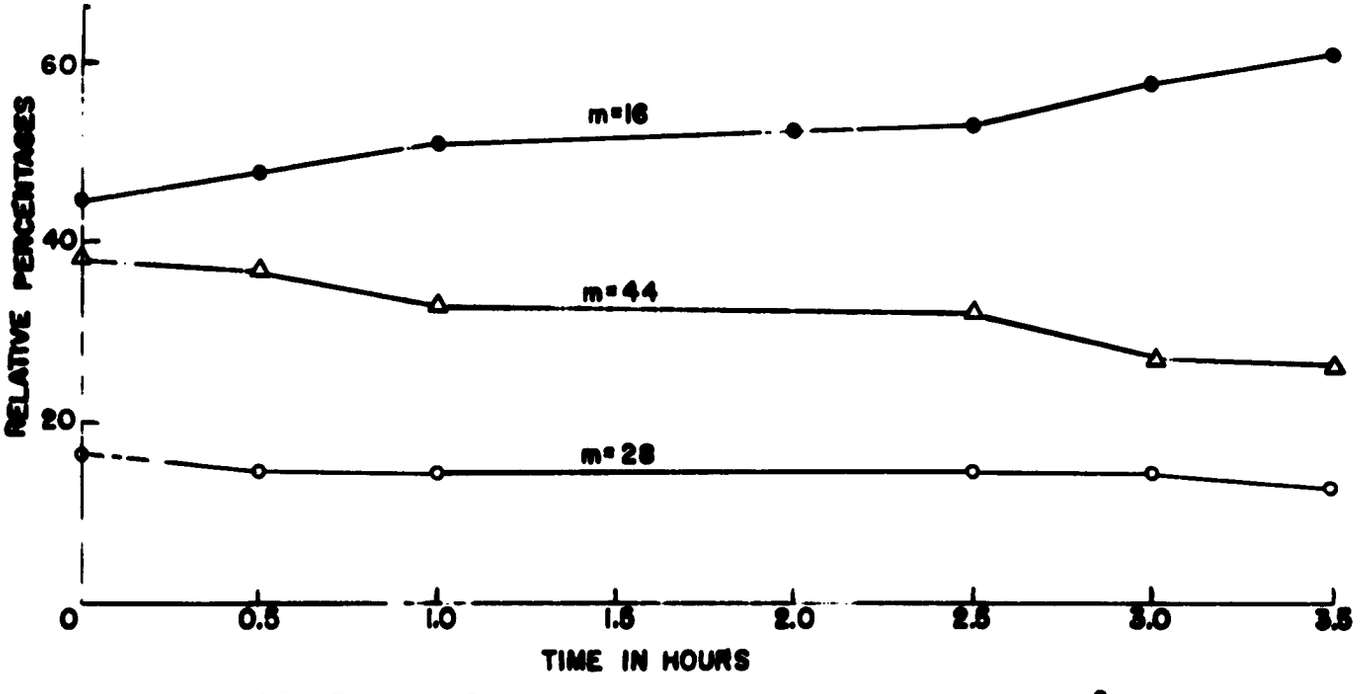

Figure 17. Relative Percentages of Gases versus Time at 400°C Oven Temperature for L-Cathode.

2. Breakdown and Activation.

The mass spectrum of gases evolved during the breakdown and activation process is shown in Figure 18.

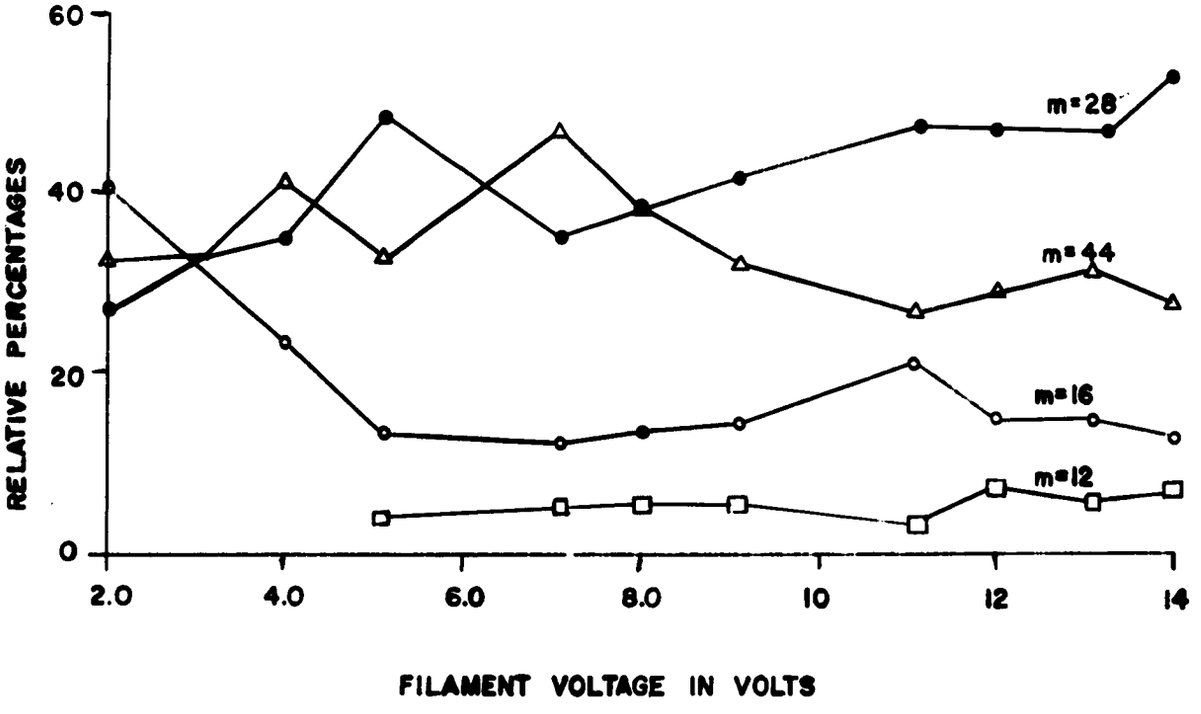

Figure 18. Gas Spectrum of L-Cathode during Breakdown Process

As the filament voltage is increased from two volts to five volts there is a sudden decrease in the percentage of atomic oxygen. From two volts to eight volts the percentages of carbon dioxide and carbon monoxide vary. Above eight volts the percentage of carbon dioxide decreases. As the cathode is heated the carbonates decompose, forming mixed crystals of barium and strontium oxides. The carbon dioxide liberated by the

decomposition leaves the cathode through the porous tungsten body and is pumped off.

The activation process was continued up to a temperature of about 1250°C. The electron emission from the porous tungsten surface was initially slight and then showed a roughly uniform increase. After this, the rate of increase became relatively slow. At this stage, the current-voltage curves and current versus shot-noise reduction factor curves were obtained and are shown in Figure 19.

The gas evolution from the L cathode during the breakdown process is quite similar to that of the oxide cathode.[6] This is not unexpected because in both cathodes decomposition of the carbonates occurs during this period.

3. Residual Gases.

After the activation process the tube was evacuated to a pressure of 4.0×10^{-7} mm Hg and constant emission was obtained, indicating the completion of activation. Gas composition was then determined under four conditions:

1. cathode cold,
2. cathode heated to 1100°C for ten minutes,
3. cathode heated to 1100°C and emitting 100 ma,
4. cathode heated to 1100°C and emitting 200 ma.

The results are shown in Table III. It can be seen that heating the cathode does not cause any change in the percentages of the residual gases. Drawing current, however, causes some increase in the

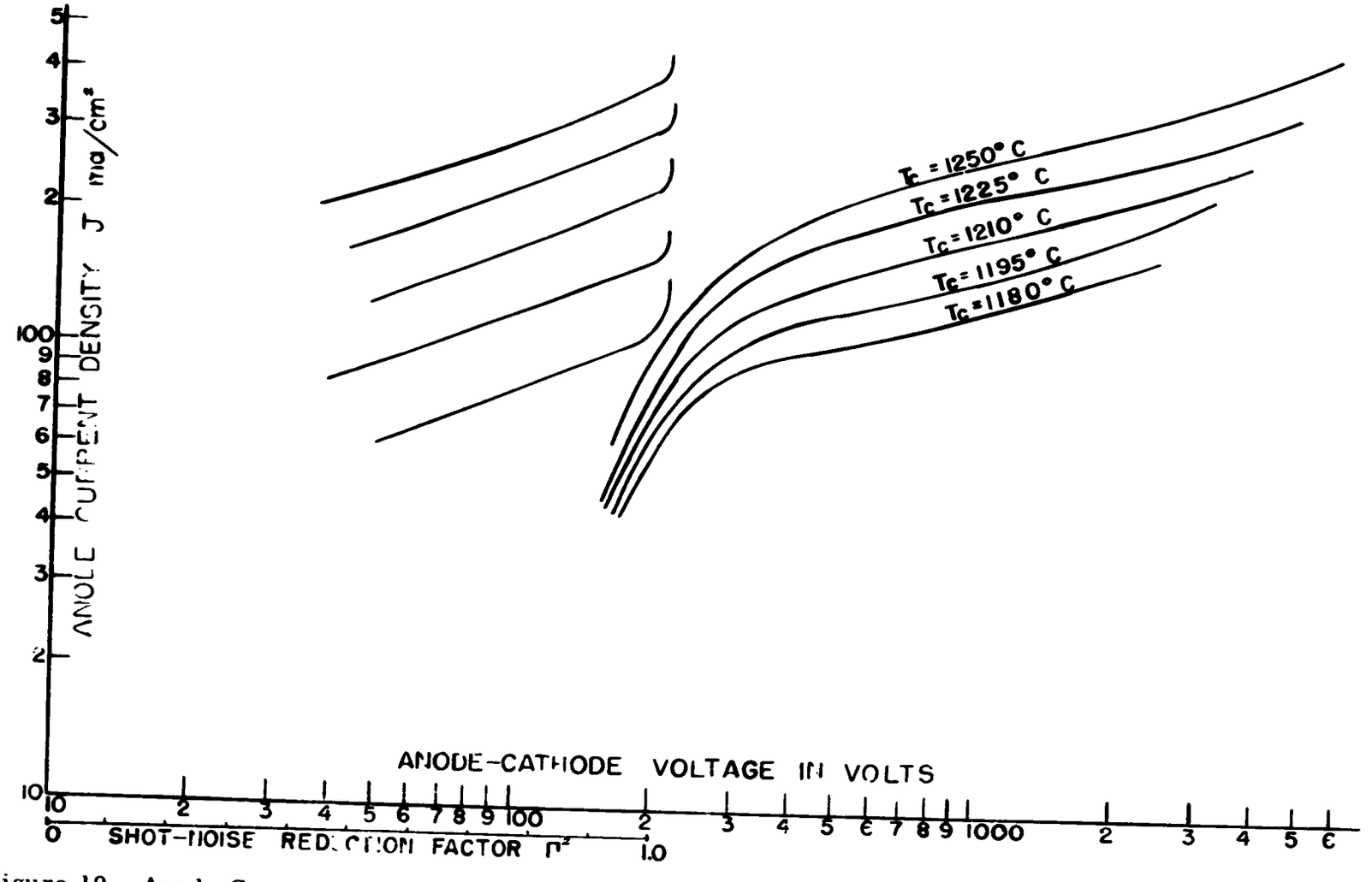

Figure 19 Anode Current versus Anode Voltage and Anode Current versus Shot-Noise Reduction Factor for L-Cathode before Aging

percentage of carbon monoxide with a corresponding decrease in all other gas components.

Table III. Relative percentages of Residual Gases in Diode with L-Cathode

Gases	Cathode Cold	$T_c = 1100^oC$	$T_c = 1180^oC$ $I_a = 100$ ma	$T_c = 1180^oC$ $I_a = 200$ ma
CO_2^+ (%)	25.9	24.7	16.7	10.7
CO^+ (%)	37.7	40.0	52.9	62.8
O^+ (%)	31.7	30.6	24.5	18.9
C^+ (%)	4.7	4.7	5.9	7.6

B. DETERMINATION OF EMISSION LEVEL

After a vigorous electron bombardment of the anode a constant emission was obtained. Under these conditions the emission levels for different cathode temperatures were determined by the application of shot-noise reduction factor measurements. The voltage-current characteristics of the tube and curves of anode current versus the shot-noise reduction factor are shown in Figure 20. The emission levels were read at the points where the shot-noise reduction factor Γ^2 became unity.

The component of work function ϕ_o, which is independent of temperature, was obtained from a plot of the Richardson equation,

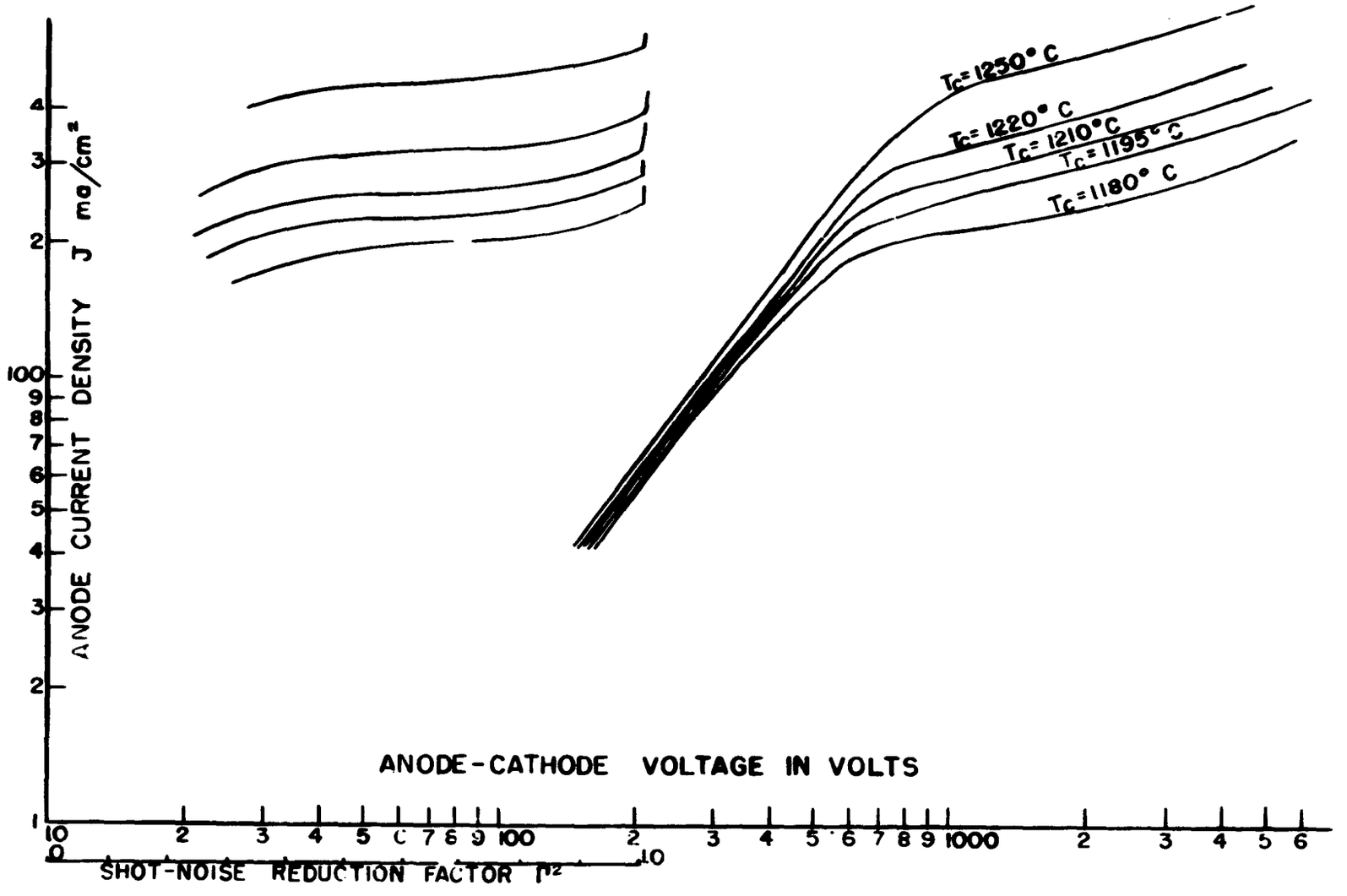

Figure 20 Anode-Current Density versus Anode-Cathode Voltage and Anode Current Density versus Shot-Noise Reduction Factor at Various Cathode Temperatures.

$$J = A_o T^2 e^{-\phi/kT}$$

From Figure 21, ϕ_o was found to be 1.67 ev. Details of the calculation are shown in Table IV.

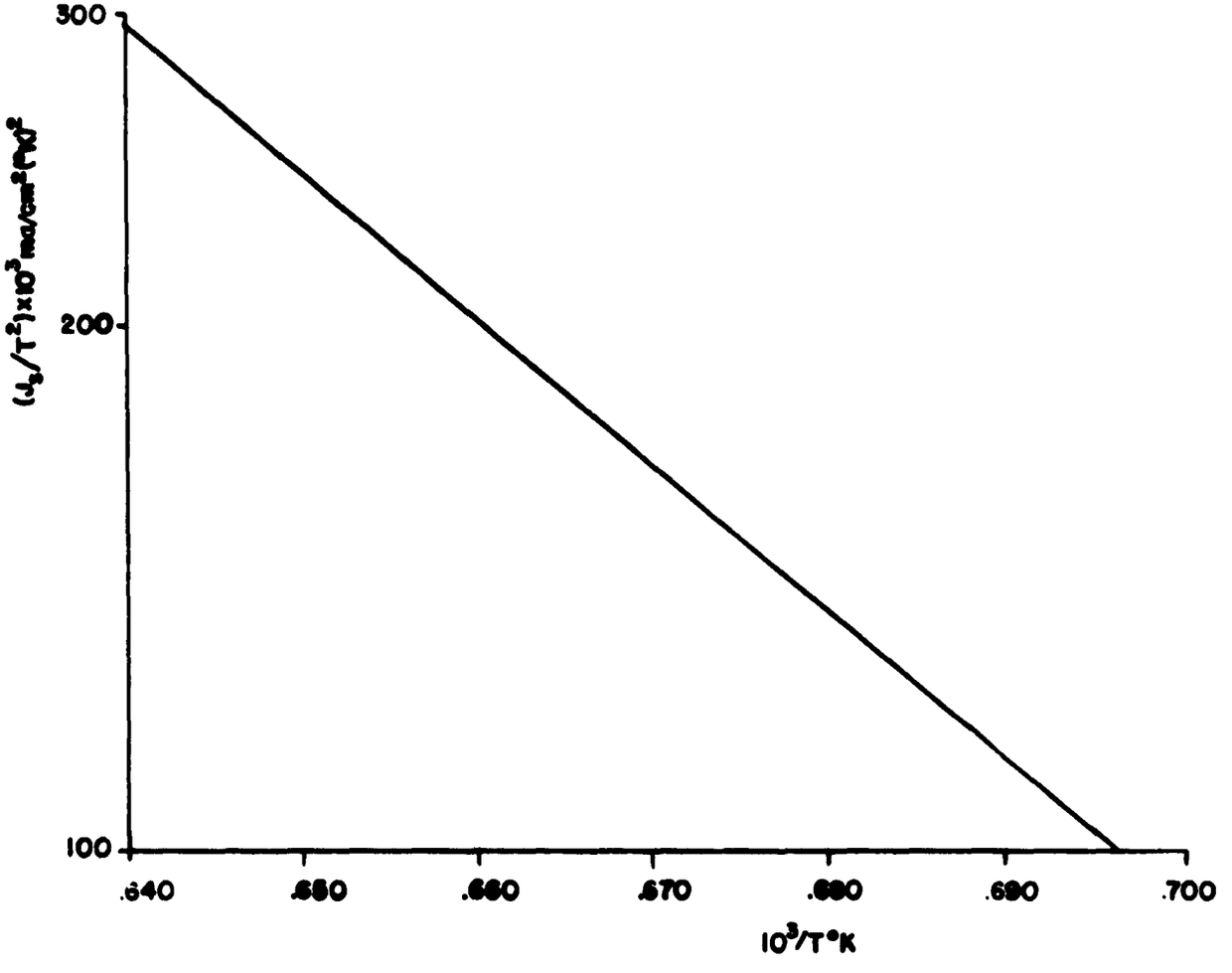

Figure 21. Richardson Plot (ϕ_o = 1.67 ev).

Table IV. Calculations for Richardson Plot

T (°C)	T (°K)	$10^3/T$	J_s (ma/cm^2)	J_s/T^2
1180	1453	0.687	250	117
1195	1468	0.682	290	135
1210	1483	0.674	330	150
1220	1493	0.664	392	175
1250	1523	0.656	528	227

C. EFFECT OF VARIOUS GASES ON ELECTRONIC EMISSION OF L CATHODE

The residual gases found in the tube were composed of carbon dioxide, carbon monoxide, atomic oxygen, and a trace of carbon. These gases may affect the atomic balance of the cathode surface and as a result affect its emission activity, therefore the chemical effects on cathode emission of carbon monoxide, carbon dioxide, hydrogen, and oxygen were studied.

The gas under study was admitted to the system through a high-vacuum valve and a constant pressure p was maintained by manual adjustment of the valve.

1. Effects of Carbon Monoxide and Carbon Dioxide

At the very start of the work with carbon monoxide and carbon dioxide, their strong activating effects on the emission activity of the cathode were observed. Therefore, in order to avoid operating the tube in the space-charge-limited region, the anode-cathode voltage was

increased about forty per cent above the voltage at which the tube becomes temperature limited for a particular cathode temperature. Under these conditions carbon monoxide was admitted to the system through a high-vacuum valve and the system pressure was increased from 3.0×10^{-7} mm Hg to 2.0×10^{-6} mm Hg. Variation of emission with time at two different cathode temperatures is shown in Figure 22. After an initial increase, the emission gradually fell down and assumed a constant value, which was higher than the original value. The amount of increase in emission is 70 per cent at a cathode temperature of 1250°C and 25 per cent at a cathode temperature of 1210°C. The initial amount of increase of the emission at both temperatures, however, is almost the same. Also, from Figure 22 it can be seen that the higher the cathode temperature the longer the time it takes for emission to assume a constant value.

When the valve was closed and the pressure was allowed to fall to the original value (3.0×10^{-7} mm Hg) there was a variation in emission with time, which is shown in Figure 23. It can be seen that in this case it took longer for emission to assume a constant value at the lower temperature. Although the system pressure was the same as the original pressure (3.0×10^{-7} mm Hg), the emission of the cathode was increased 16 per cent at a cathode temperature of 1250°C and 6 per cent at 1210°C.

The effect of carbon dioxide on the emissive activity of the L-cathode was determined in the same way as the effect of carbon monoxide. The variation of emission with time for two cathode temperatures is shown in Figure 24. After the transient activating effect on emission the increase in emission remains constant. After having the cathode in the carbon dioxide atmosphere for thirty minutes, the emission increases to

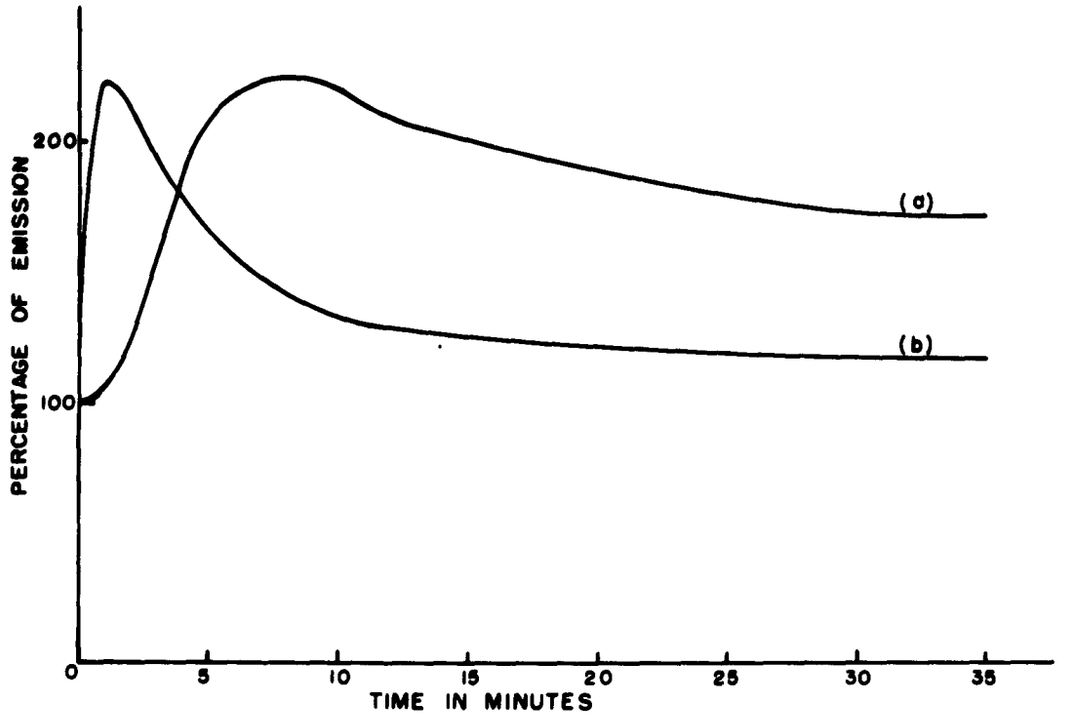

Figure 22. Effect of Carbon Monoxide on Emission Level of L-Cathode (a) T_c = 1250°C, E_f = 18.0 v; (b) T_c = 1210°C, E_f = 17 v.

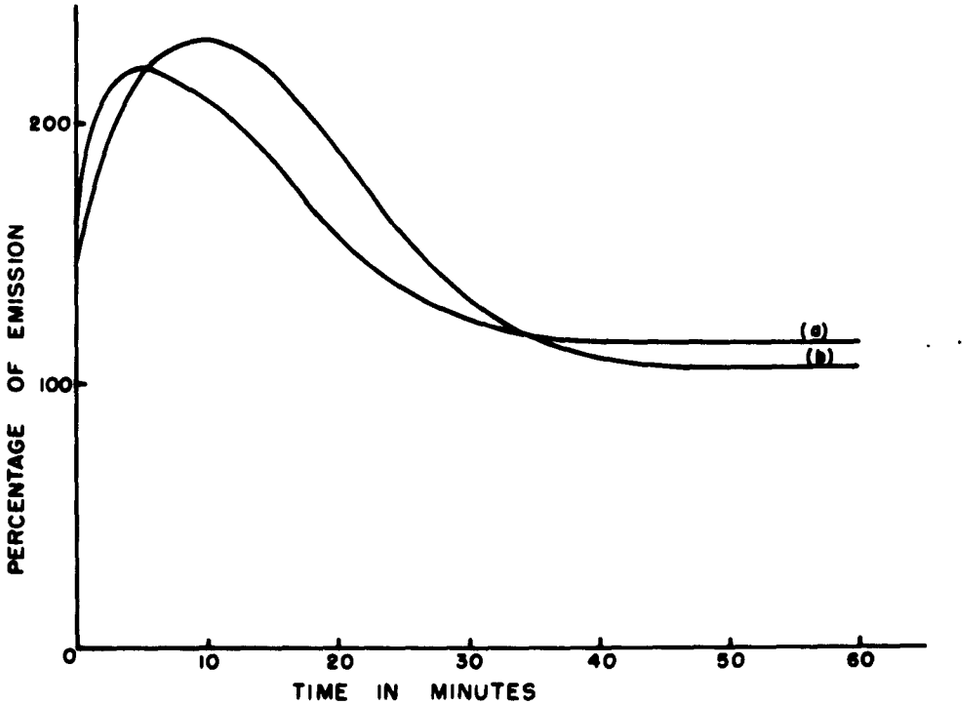

Figure 23. Recovery from Carbon Monoxide in L-Cathode (a) T_c = 1250°C, (b) T_c = 1210°C.

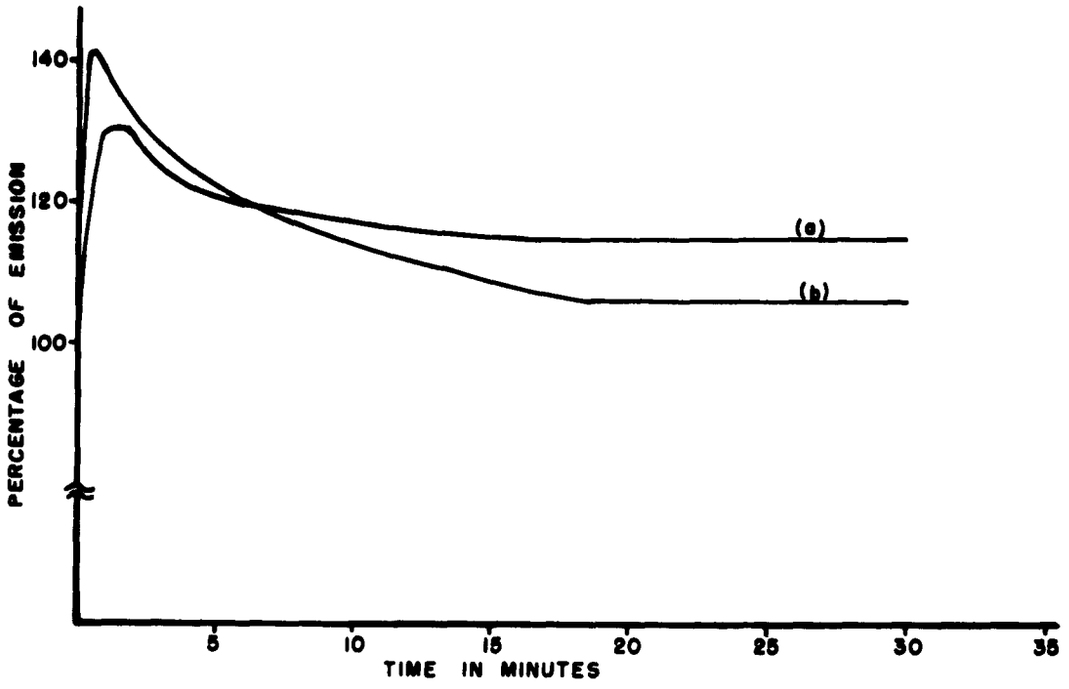

Figure 24. Effect of Carbon Dioxide on Emission (a) T_c 1250°C, (b) T_c = 1210°C, p = 2.2 x 10^{-6}.

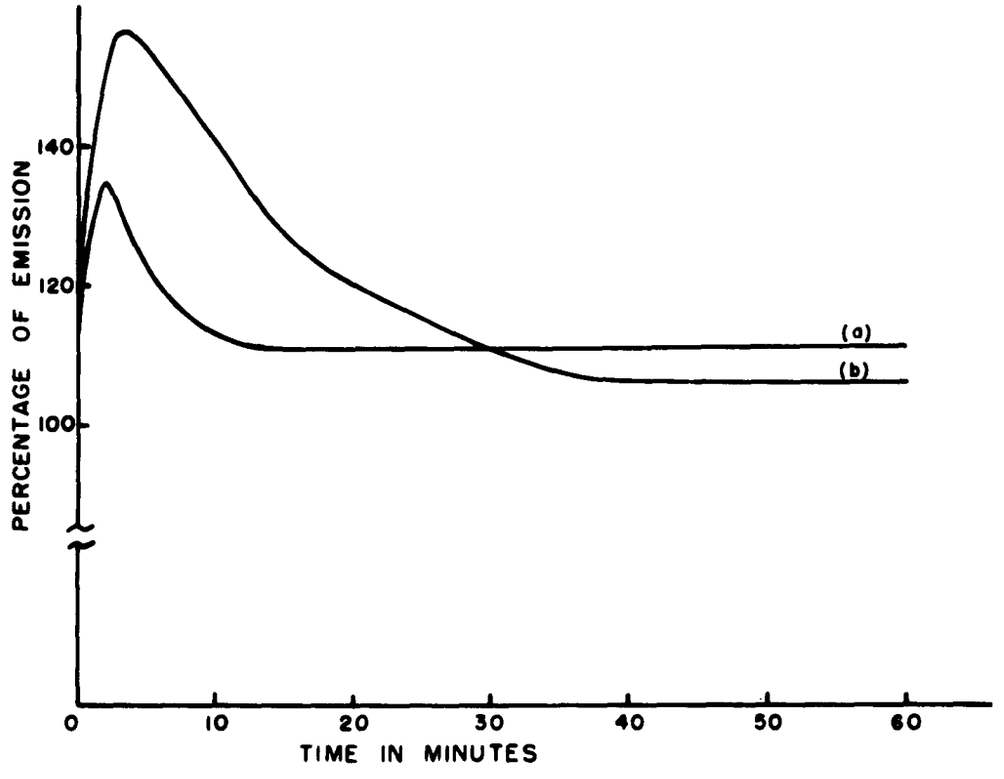

Figure 25. Recovery from Carbon Dioxide. (a) T_c = 1250°C, (b) T_c = 1210°C.

114.5 per cent of its original value at 1250°C and to 106 per cent at a cathode temperature of 1210°C. During this experiment the system pressure was kept constant at a value of 2.2×10^{-6} mm Hg.

When the valve was closed and the pressure was allowed to fall to the original value (3.0×10^{-7} mm Hg), the variation of emission with time is shown in Figure 25. It can be seen that the lower the cathode temperature the longer it took for emission to assume a constant value.

2. Effect of Hydrogen on Emission

The effect of hydrogen on the emission properties of an L cathode have been studied at various system pressures. Variation of emission with time for three different system pressures is shown in Figure 26.

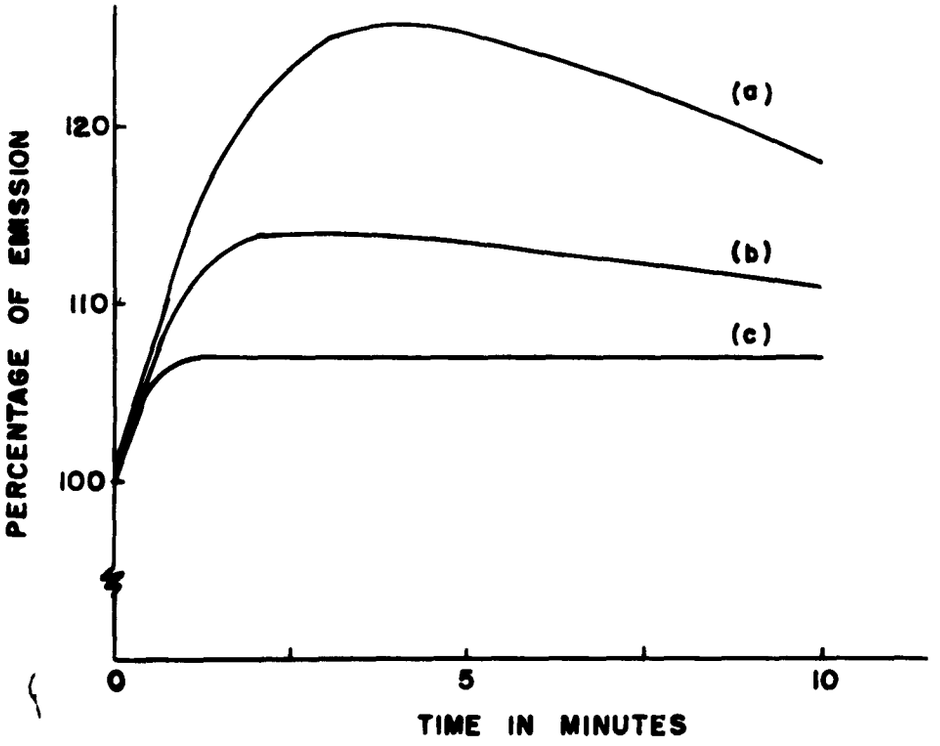

Figure 26. Effect of Hydrogen on Emission at Various System Pressures. (a) $p = 1.0 \times 10^{-6}$ mm Hg, (b) $p = 1.6 \times 10^{-6}$ mm Hg, (c) $p = 2.0 \times 10^{-6}$ mm Hg, $T_c = 1250°C$.

It is seen that the stability of emission increases with a decrease in system pressure. At a pressure of 1.0×10.6^{-6} mm Hg emission increases to 107 per cent of its initial value and is stable. As the pressure is increased by admitting more hydrogen into the system the initial increase in emission becomes higher. However, it gradually falls down and assumes a value which is less than the original value.

3. Effect of Oxygen on Electron Emission of L Cathode

The effect of oxygen on the emission activity of an L cathode have been studied. Variation of emission with time at various system pressures is shown in Figure 27. It can be seen that the initial rate of decrease in the emission increased with increase in pressure. After six minutes of poisoning, the emission decreases to 15 per cent at 0.8×10^{-6} mm Hg, to 4.5 per cent at 1.2×10^{-6} mm Hg, and to 2.0 per cent at 1.6×10^{-6} mm Hg system pressures.

When the high-vacuum valve was closed and the pressure was allowed to fall to the original value (3.0×10^{-7} mm Hg), full restoration of emission was observed. The renewal of emission after six minutes of poisoning at different system pressures is shown in Figure 28. It is seen that the higher the poisoning pressure, the longer it took for the emission to be fully restored. Cathode temperature was kept constant at 1250°C during this experiment.

The poisoning effect of oxygen at two cathode temperatures is shown by Figure 29. It can be seen that the initial rate of decrease in the emission increases with decrease in the cathode temperature. After six and a half minutes of poisoning the final values of emission were 14.5 per cent for 1250°C cathode temperature and 5.0 per cent for 1210°C

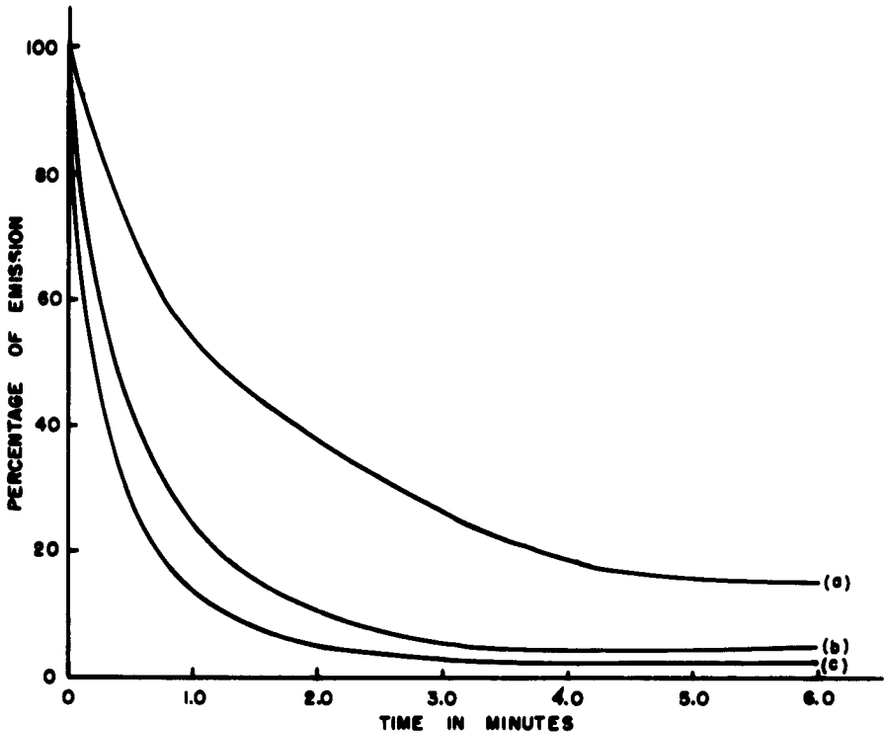

Figure 27. Oxygen Poisoning of L-Cathode at Various System Pressures.

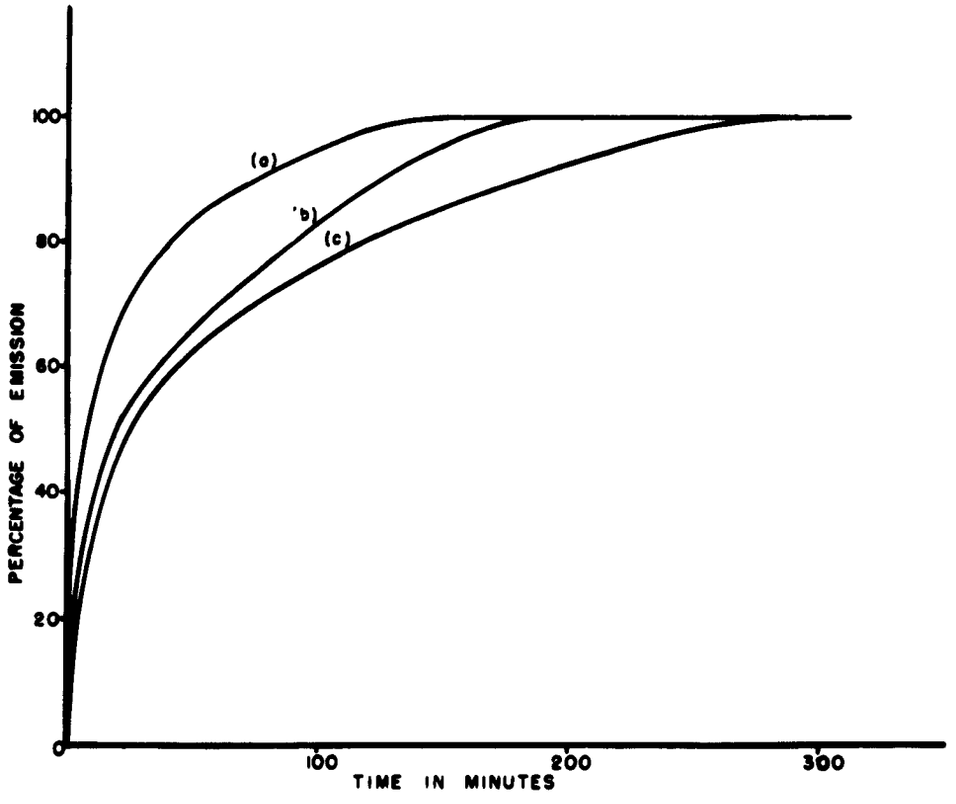

Figure 28. Recovery of Emission Poisoned at Various Oxygen Pressures.

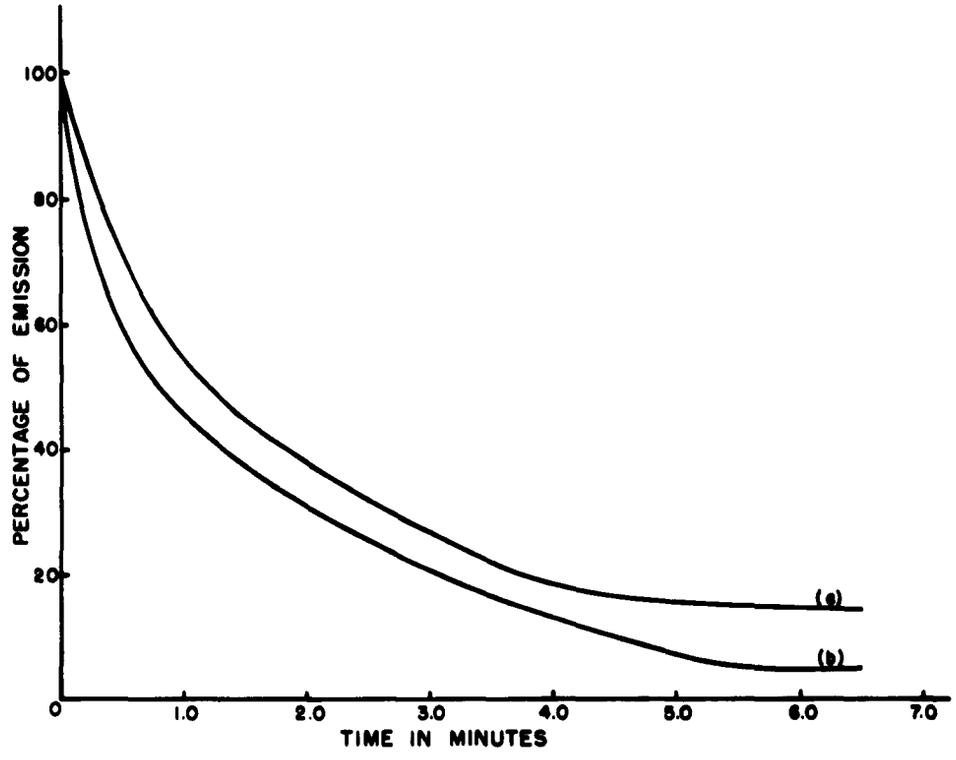

Figure 29. Oxygen Poisoning of L-Cathode at Various Cathode Temperatures. (a) 1250°C, (b) 1210°C, $p = 8 \times 10^{-7}$ mm Hg.

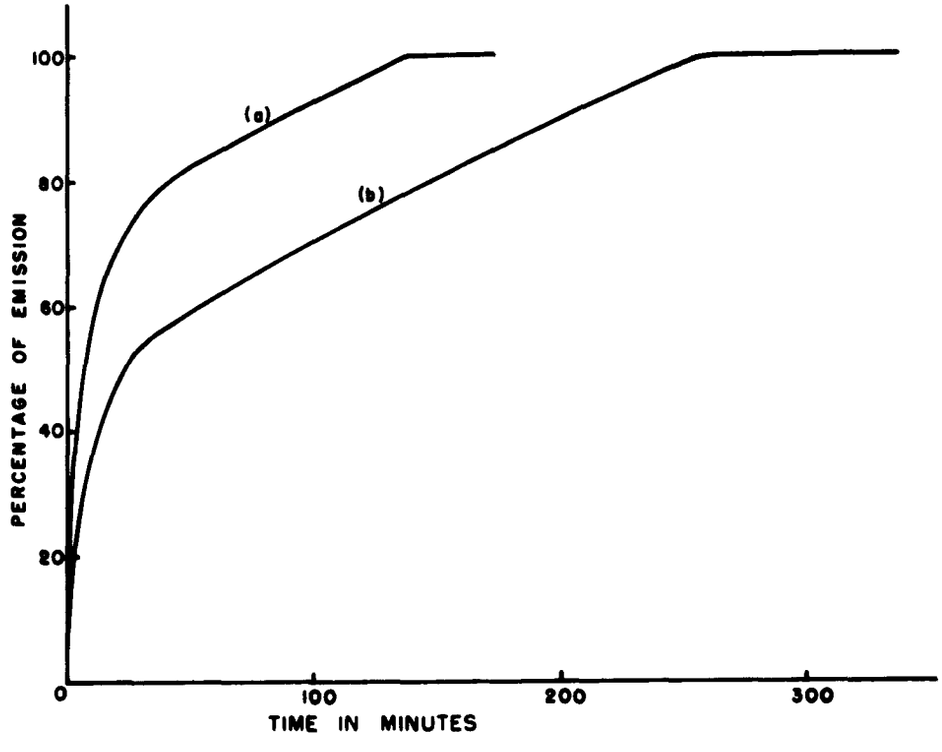

Figure 30. Recovery of L-Cathode Poisoned by Oxygen of Two Different Cathode Temperatures. (a) $T_c = 1250°C$, (b) $T_c = 1210°C$, $p = 8 \times 10^{-7}$ mm Hg.

cathode temperature. In both cases it was possible to keep the pressure at a constant value of 8.0×10^{-7} mm Hg by the manual adjustment of the high-vacuum valve.

When the valve was closed and the pressure was allowed to fall to its original value, the renewal of emission for the two cathode temperatures is shown by Figure 30. It can be seen that in this case the higher the cathode temperature the less time it takes for the full restoration of the emission.

The rate of reactivation depends also on the length of time that the heated cathode has been in the poisoning oxygen atmosphere. The renewal of emission for various poisoning periods is shown by Figure 31. It can be seen that the rate of activation is smaller, the longer the cathode remained in the oxygen atmosphere. The pressure of the system during each poisoning period was kept at a constant value of 1.2×10^{-6} mm Hg.

At the present time there are two points of view concerning the nature of the activity of an L cathode. According to D. L. Schaefer and I. E. White,[9] an L cathode represents a simple tungsten-barium film system, while F. K. DuPre and E. S. Rittner[10] consider a more complicated tungsten-oxygen-barium system. Also from the work of A. L. Reiman[11] it is known that the tungsten-oxygen-barium system has a higher emission activity than the tungsten barium system; therefore, if the L cathode under experimental conditions were a tungsten-barium system, it would be expected that at the start of work with oxygen the system would pass over into the tungsten-oxygen-barium system and an increase in the emission activity of the cathode would be observed. This type of activity was not observed, indicating that the initial state of the L cathode was

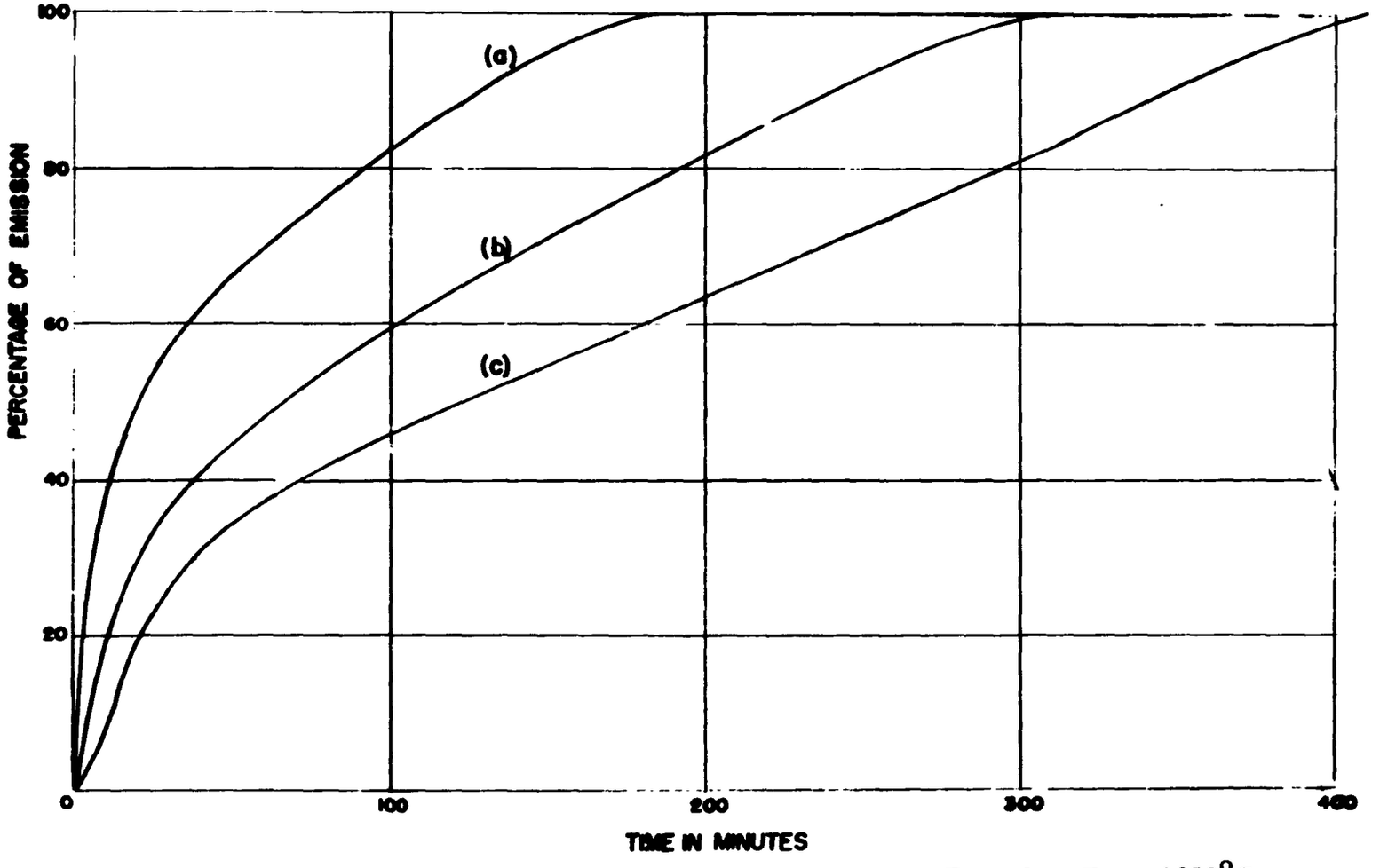

Figure 31. Recovery of Emission for Various Oxygen Poisoning Periods. T_c = 1250°C, (a) t = 4 min, (b) t = 10 min, (c) t = 15 min.

already a tungsten-oxygen-barium system.

From the consideration of the physical process that determines the emission activity of an L cathode, it can be assumed that the essence of oxygen poisoning is twofold: (1) partial binding of the barium layer on the surface of the tungsten sponge by oxygen, which causes a rise in the work functions, and (2) reduction of the stream of barium atoms from the cathode cavity, which is due to the oxidation of the barium in the tungsten pores and in the cathode cavity.

Evidently these two processes have different time constants; as a result their relative roles differ during the different stages of poisoning. Because of the low permeability of the tungsten sponge, the fundamental role at the beginning of oxygen poisoning should be played by the effect of binding of the barium layer. The second effect can be expected only when oxygen diffusion through the tungsten pores causes a substantial change in the barium vapor pressure.

From the curves of the variation of emission with time, it can be seen that they are distinguished by a sharp initial drop in emission and a slow change during further poisoning process. This observation justifies the above assumptions quite well.

V. CONCLUSION

A. THORIUM-TUNGSTEN CATHODE

1. It was found that the residual gases present in the tube were composed of carbon monoxide, carbon dioxide, atomic oxygen, and a trace of

hydrogen. Heating the cathode and drawing current, however, causes a progressive increase in the percentage of carbon monoxide and a decrease in the percentages of all other residual gas components.

2. The temperature-independent component of the work function determined from the Richardson plot resulted in ϕ_o being 2.39 ev. This agrees well with the given work function of 2.4 ev.

3. Carbon monoxide and carbon dioxide have an activating effect on the cathode, the amount of increase in emission being higher at higher cathode temperatures. Also, the higher the cathode temperature the less time it takes for emission to assume a constant value.

4. The thorium-tungsten cathode is very sensitive to oxygen poisoning. At a pressure of 2.0×10^{-6} mm Hg the emission decreased within less than a minute.

B. L CATHODE

1. During the breakdown of the carbonate the reactions were mainly

$$BaCO_3 \longrightarrow BaO + CO_2 \qquad (7)$$

$$3BaCO_3 + W \longrightarrow Ba_3WO_6 + 3CO \qquad (8)$$

As the cathode temperature was increased the percentage of carbon monoxide increased indicating an excess in reaction (8). However, reaction (8) which results from an oxygen-bearing poisoning agent is undesirable, therefore the breakdown of carbonates must be carried out at low temperatures.

2. The residual gases present in the tube were composed of carbon monoxide, carbon dioxide, atomic oxygen, and a trace of carbon. Heating

the cathode caused no change in the percentage of the residual gases. Drawing current, however, increased the percentage of carbon monoxide.

3. The temperature-independent component of the work function obtained from the Richardson plot resulted in ϕ_o being 1.67 ev. This agrees very well with the literature.[12]

4. Carbon monoxide and carbon dioxide activate the cathode. The amount of activation increases with increase in cathode temperature. Also, the higher the cathode temperature, the less time it takes for emission to assume a constant value.

5. Hydrogen has an activating effect on the emission activity of the cathode. As the system pressure was increased above 1.0×10^{-6} mm Hg, however, the emission drops after a sudden increase and assumes a value that is less than the original value.

6. Oxygen has a poisoning effect on the emission activity of the cathode. The rate of poisoning increases both with an increase in the pressure of oxygen in the atmosphere and with a decrease in the cathode temperature.

7. Full restoration of emission is possible. The rate of reactivation decreases, however, with an increase in poisoning pressure, an increase in poisoning time, and a decrease in the cathode temperature. These results agree well with the work of Y. P. Zingerman and V. Y. Soltyk.[13]

8. Data obtained from oxygen poisoning and from the reactivation supports the theory, that the cathode represents a tungsten-oxygen-barium system rather than a simple tungsten-barium film.

9. Oxygen poisoning consists of two processes: (a) the partial binding of the barium layer on the surface of the tungsten sponge by oxygen, (b) the reduction of the stream of barium atoms from the cathode cavity.

VI. BIBLIOGRAPHY

1. G. Pikus, Izv. Akad. Nauk. S.S.S.R., Ser. Phys. 20, 10 (1956), p. 1085.

2. N. Erdibil, "Mass-Spectrometric Study of 6CY5 Tetrode," Senior Project, Cornell University, June 1959.

3. Yu. G. Putushinskii and B. S. Chuikov, "Mass-Spectrographic Determination of Composition of Residual Gases in Electron Devices with Porous Metal-Film Cathodes," Inst. of Physics Akad., Nauk. Ukr. S. S. R., Kiev.

4. J. P. Sackinger and R. J. Foreman, "Thorium-Tungsten Cermet Cathodes," Military System Design, (Nov.-Dec. 1959).

5. A. Venema, "Dispenser Cathodes," Philips Technical Rev., 19 (December 1957), pp. 177-208.

6. I. Turkekul, "The Estimation of Total Cathode Emission from Shot-Noise Measurements," M.S. Thesis, Cornell University, February 1959.

7. G. C. Dalman and I. Turkekul, "Estimation of Cathode Emission from Noise Measurements," Res. Rep. EE 452, Cornell University, October 1959.

8. A. S. Gilmour, Jr., "Preliminary Studies on the Limitations of Radio-Frequency Mass Spectrometer," M.S. Thesis, Cornell Univ., February 1959.

9. D. L. Schaefer and I. E. White, "Physical Processes in the L-Cathode," Jour. Ap. Physics, 23 (1952), pp. 669.

10. F. K. DuPre and E. S. Rittner, "Mechanism of Operation of the L-Cathode," Physical Rev., 82 (1951), pp. 573.

11. A. L. Reimann, Thermionic Emission, New York: Wiley and Sons, 1934, Chapter 3, Section III.

12. A. S. Rittner, "Studies on the Mechanism of Operation of the L-Cathode," Jour. Ap. Physics, 28 (Jan.-June 1957).

13. Ya. P. Zingerman andV. Ya. Saltyk, "Chemical Effects of Oxygen on the Electron Emission of the Porous Metal-Film Cathode," Inst. of Physics Akad., Nauk Ukr. S.S.R., Kiev., (May 1957).

LONG-PULSE DIODE STUDY

H. Hollister

School of Electrical Engineering
CORNELL UNIVERSITY
Ithaca, New York

RESEARCH REPORT EE 430

LONG-PULSE DIODE STUDY

H. Hollister

THEORETICAL AND EXPERIMENTAL INVESTIGATION
OF LINEAR-BEAM MICROWAVE TUBES

Technical Report No. 4 29 May 1959

Published under Contract No. AF 30(602)-1696
Rome Air Development Center
Griffiss Air Force Base, New York

CONTENTS

ABSTRACT

A mass spectrometer examination was made of the gases given off by a high-power diode during cathode breakdown, tube processing, and sparking under pulsed operation. During the breakdown of the cathode, the main gases given off were carbon monoxide and carbon dioxide. During the processing of the tube tube main gases present were carbon monoxide and atomic hydrogen. Water vapor and molecular hydrogen were also given off in processing. The pressure rise accompanying sparking was found to be due almost solely to carbon monoxide with a small amount of molecular hydrogen also given off. The origin of this carbon monoxide was apparently the result of cathode breakdown.

INTRODUCTION

An important limitation on the power capabilities of present day high power radar transmitting tubes is the maximum current that can be drawn from the cathode. Such tubes are operated under pulsed conditions so that much higher currents can be drawn than by using direct current and the problem of increasing the energy per pulse becomes that of increasing either the peak current or the length of the pulse.

The peak current is limited by two phenomena, depending on the condition of the cathode: (1) the maximum emission of which the cathode is capable, and (2) the sparking phenomenon. In the laboratory maximum emission currents up to 100 amp/cm^2 have been obtained, but in practice an emission of 6 amp/cm^2 is considered very good. The problem of obtaining higher emission therefore seems to be that of minimizing the poisoning agents present in the tube and improving the processing of the tube so that high emissions can be obtained in practice. Even with the best cathodes, the emission is found ultimately to be limited by the sparking phenomenon.[1] Furthermore, this sparking threshold is found to be lower for longer pulse lengths, so that it imposes a limit on the maximum pulse length that can be used as well as on the amplitude of the pulse. In practice this sparking threshold as well as the maximum emission is found to be much lower than the maximum obtainable under ideal conditions.

As to what factors lower both the emission and sparking

threshold of cathodes of commercial tubes to values less than those obtained in the laboratory, the obvious answer seems to be contamination in some form or another. This contamination may arise from several sources: contamination always present, though only in small amounts, in the atmosphere of a manufacturing plant; contaminations introduced at various stages of the manufacturing process despite precautions; residue left by imperfect cathode breakdown; and especially by back poisoning of the cathode by materials given off during breakdown. It is believed that these contaminations must appear in the form of gases in the tube in order to reach the cathode to poison it, although some of them may be driven off directly from the anode to the cathode without ever appearing as gases.

If the rate of occurrence of sparking is observed throughout the life of a cathode, it is observed that there is a great deal of sparking initially, the rate of occurrence becoming much less as the tube is processed, and rising sharply towards the end of cathode life.[2] The initial sparking occurs at currents much lower than those which may be safely drawn with a well-processed tube and is accompanied by a large pressure rise in the tube. Comparison of the sparking current for well-activated cathodes with the resistance of the cathode shows that the lowest sparking current occurs for those cathodes having the highest coating resistance.[3] All this suggests that both the emission and the sparking problems are traceable to the poisoning agents present in the tubes.

For these reasons a mass spectroscopic examination of the gases present during the operation of a commercial tube seems

worthwhile. In the experiments described here, the main object was to study the gases given off by cathode sparking during the initial stages of operation when these gas bursts are plentiful and the quantities of gas given off are large. The reasons for this are that, with the instrumentation available, this is the period in which data is most readily obtained, and that the evidence seems to indicate that the same basic mechanism and poisoning agents are responsible for these gas bursts as for the emission limitation and sparking of a well-activated cathode. The immediate purpose of this work then, is to identify the gases given off by gas bursts and thus, assuming that these are the gases mainly responsible for the less than optimum state of the cathode, to obtain ideas on how better to prepare the tube.

For this study, a diode representing the electron gun of a high-power klystron was furnished by the Sperry Gyroscope Co.* This diode was incorporated in a vacuum system with a mass spectrometer and a flow rate meter inserted between it and the vacuum pump, so that both the species and quantity of gas given off could be determined. The gases given off by this diode were determined during breakdown, processing, and operation with gas bursts, so that after the damaging gases had been identified, their history throughout the preparation of the tube would be known.

---

* Acknowledgment is gratefully made to the Sperry Gyroscope Company of Great Neck, Long Island for their donation of this tube and to Mr. L. Anderson for his advice on its operation.

The instrumentation used in this experiment is first described, followed by a description of the procedure used and the results obtained in carrying out the experiment as outlined above. Lastly, some suggestions are given for improving the instrumentation in order both to obtain better data and to extend the experiment to very active cathodes operating in ultra-high vacuum.

EXPERIMENTAL APPARATUS

The layout of the whole vacuum system is shown in Figure 1. The part of the system inside the dashed rectangle was baked out at 410°C for 10 hours. After this was done, and before cathode breakdown was begun, the pressure at both ion gauges was $1.5\,(10)^{-8}$ mm Hg. Each unit of the apparatus was demountable and adjoining units were connected by knife edge flanges with OFHC copper blocks between them (not shown in Figure 1).

A three-stage glass oil diffusion pump was used, with a charcoal trap to prevent backstreaming of the oil. The charcoal in the charcoal trap could be heated and was thus outgassed both during bakeout and after cathode conversion. The efficiency of such a trap is not certain, however, and although there were no hydrocarbons detected by the mass spectrometer, they may still have been present in quantities large enough for cumulative poisoning of the cathode.

A photograph of the diode (extreme left), mass spectrometer, and flow rate meter is given in Figure 2. The monel bellows and loop in the copper pipe were necessary to allow for the strains involved in assembling the system, pumping down, and baking out.

A. Experimental Diode

Figure 3 is a photograph of the diode used in this experiment. This diode is essentially a high-power klystron with the drift space and cavities removed. Its perveance is $2(10)^{-6}$ so that at the operating voltage of 90 kv a space-charge limited current of 56 amperes is obtained.

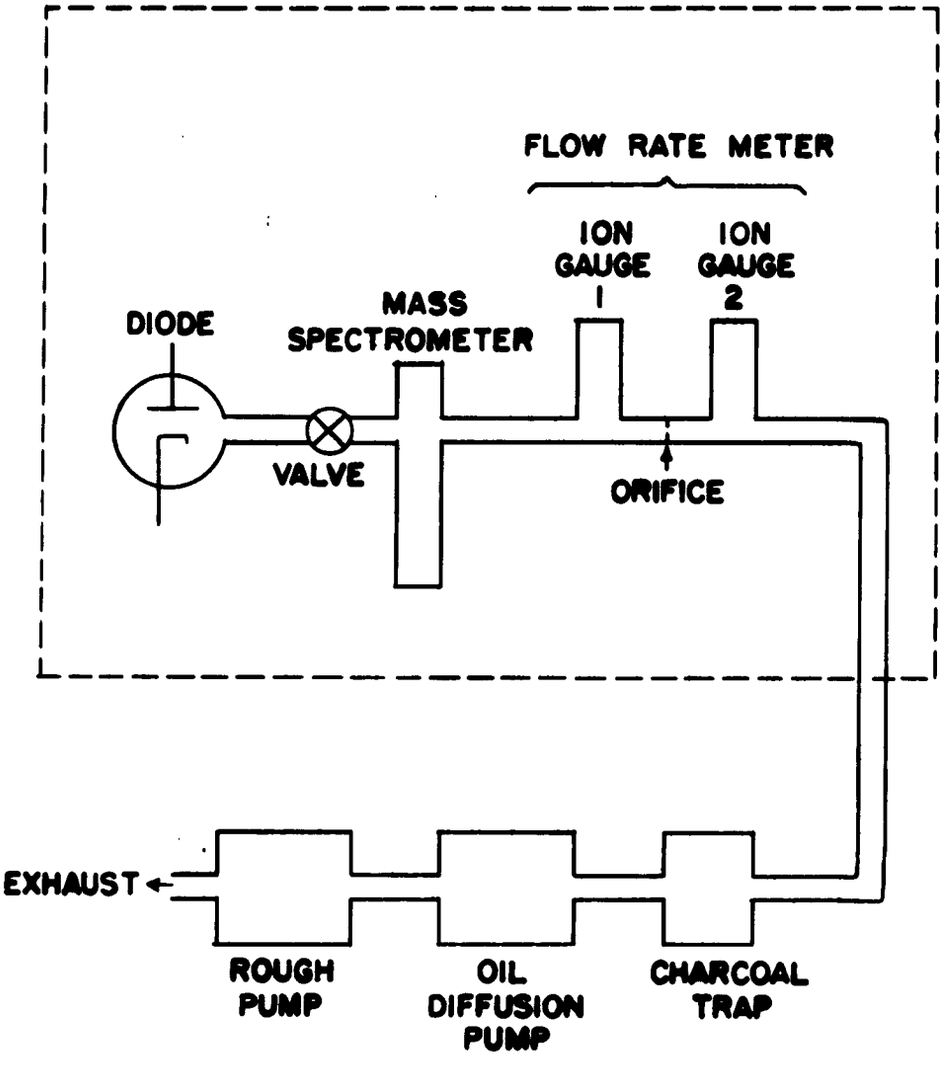

Figure 1. Vacuum System.

operation, since perturbations such as structural imperfections, and the tuners and antenna one invariably inserts in these cavities can easily excite nonsymmetrical modes. A first approximation to this nonsymmetrical operation is made in a later section, where a rather artificial technique is used to introduce the nonsymmetrical modes.

The assumptions made in the following derivation are quite usual, and are good approximations for the practical cavity which is either lightly loaded or symmetrically loaded. The conductivity of the metal walls of the cavity is assumed infinite and, most important, the gap edges are assumed to be square. The one further assumption (as mentioned above) is that perfect mechanical symmetry exists in the ϕ direction.

1. Cavity Admittance of Region 1

Since this region is to be treated as a short-circuited radial line, one need not begin with Maxwell's basic equations; instead a modal analysis can be used. These radial-line modes themselves have been derived from Maxwell's equations, so there is no loss of generality in applying them directly. *

The general expressions for the field components in a radial-line cavity for the H type modes are as follows:

* This derivation or its method may be found in any elementary textbook on electromagnetics.

The cathode of this diode is a thin (3 mg/cm^2) coating of RCA-33C-118 oxide on a base metal of electroetched 220 nickel, having an area of 17.6 cm^2. Its operating temperature is 805°C and it gives an emission current of about 3.2 amp/cm^2 during normal operation. The anode ring of the electron gun is stainless steel the electron beam collector is a copper cylinder. Prior to assembly all parts were cleaned by hydrogen firing for 10 to 20 minutes at 1100°C and then vacuum firing for one to two hours at 1100°C.

B. Mass Spectrometer

A linear beam radio frequency mass spectrometer was used. This type of instrument was developed by Redhead[4] and has been more thoroughly investigated by Gilmour.[5] The geometry of the linear beam radio frequency mass spectrometer is shown in Figure 4.

As is seen in Figure 4, the gas is ionized by 50-volt electrons and then accelerated into the analyzer structure through a potential of 50 volts. At a given frequency of the signal on the alternate grids of the analyzer, only those ions having the proper velocity will pass through the whole structure in synchronization with the signal and thus gain enough energy to get past the 100-volt grid and arrive at the collector. As one would expect, the higher the voltage of this final grid, the higher will be the resolution. However, the practical necessity of having an easily measurable ion current, sets an upper limit to the value of this voltage when working in high vacuum. Thus a compromise was made necessary which resulted in the mass spectrometer being operated with a resolution of about 12 during this experiment. At this resolution, H_2O (mass 18) and O (mass 16) are

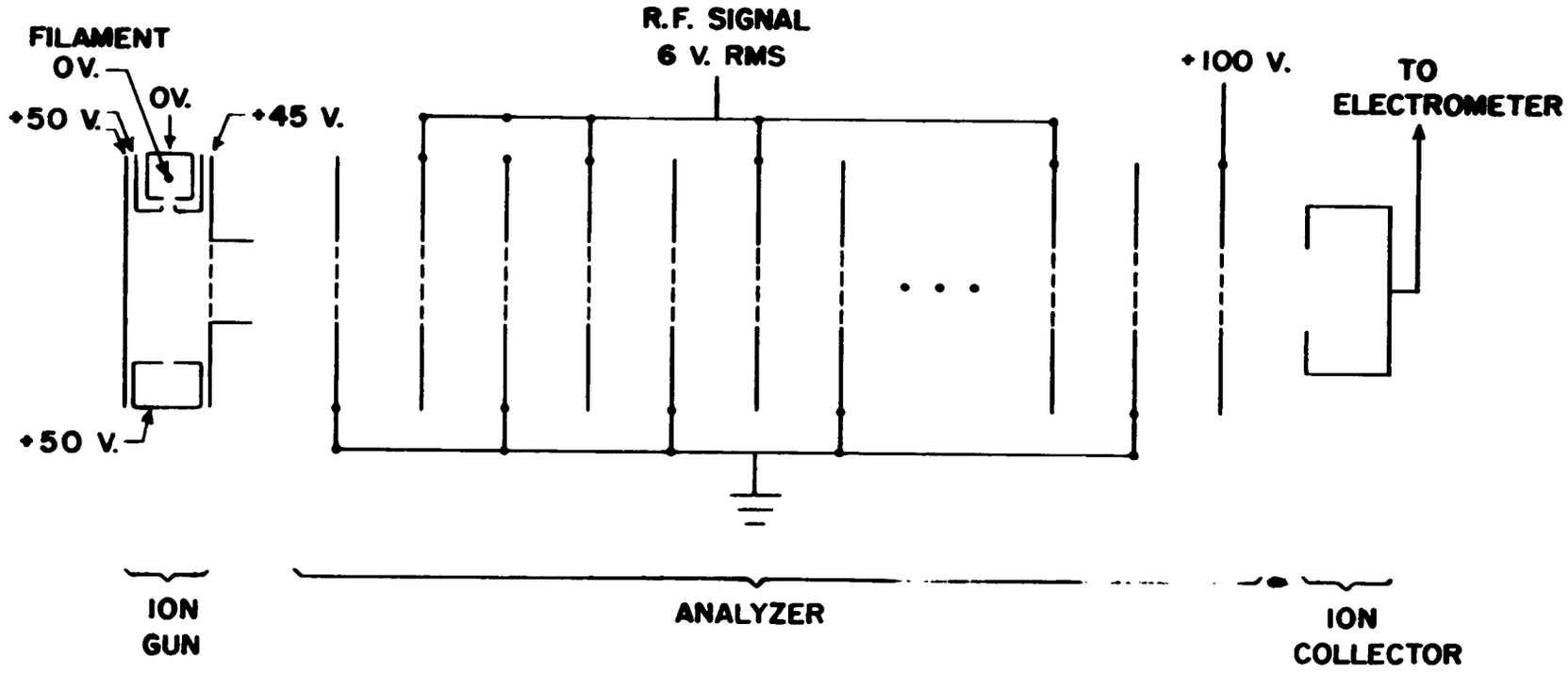

Figure 4. Details of the Mass Spectrometer.

barely distinguishable and an amount of one exceeding the amount of the other by a factor of 5 or so would completely mask the presence of the second. More will be said on this subject in the suggestions for improvement of the instrumentation.

The electron source in the ion gun is a tungsten filament, as are the filaments of the ion gauges. Tungsten filaments are undesirable since they are known to convert a very high percentage of the oxygen present in the system to carbon monoxide thus introducing some ambiguity as to the source of any carbon monoxide observed. Some auxiliary experiments were carried out in order to assess the importance of this effect.

C. Flow Rate Meter

The flow rate meter consists of a small orifice (.095 inches in diameter) with a standard Bayard-Alpert ionization gauge on each side. The quantity of gas flowing through such an orifice is:[6]

$$Q = F(P_1 - P_2) \quad \frac{\text{micron-litre}}{\text{sec}} \ ,$$

where $(P_1 - P_2)$ is the pressure drop across the orifice and F is the conductivity of the orifice, given by

$$F = \frac{A v_a}{4} \quad \frac{3}{4} \ (10)^{-3} \ ,$$

where

A = area of orifice

v_a = average molecular velocity = $14,551 \sqrt{\frac{T}{m}}$.

For the orifice used, and at room temperature

$$Q = 2.07 \frac{1}{\sqrt{M}} (P_1 - P_2) \frac{\text{micron-litre}}{\text{sec}}.$$

For example, if the gas is mostly carbon monoxide (M = 28) and the pressures are

$$P_1 = 5(10)^{-6} \text{ mm Hg} = 5(10)^{-3} \text{ micron} ,$$

$$P_2 = 3(10)^{-6} \text{ mm Hg} = 3(10)^{-3} \text{ micron} ,$$

the rate of gas flow is

$$Q = 2.07 \frac{1}{28} (5-3) (10)^{-3} \frac{\text{micron-litre}}{\text{sec}} ,$$

$$= .784 (10)^{-3} \frac{\text{micron-litre}}{\text{sec}} ,$$

$$= .784 (10)^{-3} \frac{\text{micron-litre}}{\text{sec}} \times 1.62 (10)^{-6} \frac{\text{gm}}{\text{micron-litre}} ,$$

$$= 1.27 (10)^{-9} \frac{\text{gm}}{\text{sec}} .$$

At this rate, in one hour, 4.57 micrograms of carbon monoxide will have flowed through.

A much more convenient approximate treatment is as follows. It is observed that over most of the pressure range used $P_2 = .6 P_1$ so that

$$P_1 - P_2 = .4 P_1 .$$

For carbon monoxide, therefore, the orifice can be considered as having a pumping speed of

$$s = \frac{2.07}{\sqrt{M}} (.4) = .155 \frac{\text{litre}}{\text{sec}} ,$$

and the gas flow rate is obtained simply from

$$Q = SP_1 = .155\ P_1 \quad \frac{\text{micron-litre}}{\text{sec}} \quad .$$

For gases other than carbon monoxide, this speed must be multiplied by the ratio $\frac{M_{CO}}{M_x}$ where M_x is the molar weight of the gas in question. It should be mentioned that the above analysis is only approximate since the pumping rates of the ion gauges have been neglected and are, in fact, different for different gases.

EXPERIMENTAL PROCEDURE AND RESULTS

A. Cathode Breakdown

The cathode breakdown schedule used was simply to increase the heater voltage gradually to a maximum of 5.5 v, keeping the pressure in the tube below $5(10)^{-4}$ mm Hg at all times. Because of the small orifice in the vacuum line, this was a very slow procedure, requiring three days. The cathode was then allowed to outgas for two days at this heater voltage, after which the heater voltage was increased to 6.5 v for five minutes. Then with the heater at 5.25 to 5.5 v, the cathode was outgassed for seven more days, the charcoal trap reactivated, and the cathode outgassed three more days. At this time the pressure was $1(10)^{-6}$ mm Hg with the heater at its operating voltage of 5.0 v.

Carbon monoxide and carbon dioxide were the only gases given off in large quantities during breakdown. During the initial stage of breakdown about twice as much CO as CO_2 was given off, the amounts becoming roughly equal at the middle stage when the most gas was given off. Then the amount of CO_2 decreased rapidly so that at outgassing and operating temperatures the principle gas present was CO. Only CO was given off during the five-minute operation at 6.5 v on the heater. Carbon and atomic oxygen were observed in small amounts, the quantities being roughly those expected from fractionation of the CO and CO_2.

These results are similar to those of Morgulius and Pikus[7] and are somewhat less similar to some observations of Varadi,[8] in

that he observed the CO_2 to peak at an earlier stage. On the other hand, Stier[9] found most of the gas given off his cathodes to be CO_2 which is significantly different from the breakdown observed here.

This comparison of the different results that are obtained using different cathodes and breakdown schedules shows that there can be a great deal of variation in the amounts of CO and CO_2 given off during breakdown and hence in the residues left behind in the cathode coating. These residues could then be expected to play an important part in the activation and emission properties of the cathode. At first glance the best breakdown schedule would seem to be that in which the most CO_2 is given off, since much oxygen left behind would leave the cathode hard to activate, but this may not be the case since the chemistry of the cathode is very complicated. For instance it may be that CO is much harder to get out of the cathode than is CO_2 and that the CO remaining in the cathode causes high resistance regions which are thus more susceptible to gas bursts. In this case the best breakdown procedure would be that which eliminates the most CO. The observations on gas bursts reported below tend to support this latter concept.

Therefore, the mass spectrometric monitoring of cathode breakdown appears to be a promising method for obtaining the optimum breakdown schedule for a given cathode. By using the observation of gases given off by cathode sparking as a probe for determining the condition of the cathode, and correlating this condition with the gases given off during breakdown, it should be possible to improve at least the sparking and maybe even the emission properties of the cathode.

Another factor to be taken into account is the fact that the ion gun of the mass spectrometer used in this experiment was not in line of sight with the cathode, so that any nonvolatile substances given off would have been greatly attenuated before being observed. For this reason it may be that the small amount of carbon observed actually represents only part of a larger amount given off the cathode; this would also have to be taken into account in arriving at the best breakdown schedule. This question can only be answered by conducting the experiment with the ion gun in line of sight with the cathode.

B. Processing

The processing of the tube was begun using 5 microsecond pulses with the voltage being slowly increased to 95 kv and the repetition rate to 500 pulses per second. During this phase of the processing the pressure rose to $3(10)^{-6}$ mm Hg, and eventually dropped to below $1(10)^{-6}$ mm Hg. Next the tube was operated with 15 microsecond pulses, the voltage being slowly increased to 85 kv and the repetition rate to 300 pulses per second. After this processing the pressure stayed in the 10^{-7} range during regular operation. This is a shorter processing schedule, and the resulting operating pressure is higher than recommended by Sperry. At this time the cathode gave a current density of about 2 amp/cm^2 at its operating temperature of 805°C and voltage of 100 kv.

The gases given off during an early stage of the processing are plotted in Figure 5 as a function of the voltage on the tube. At

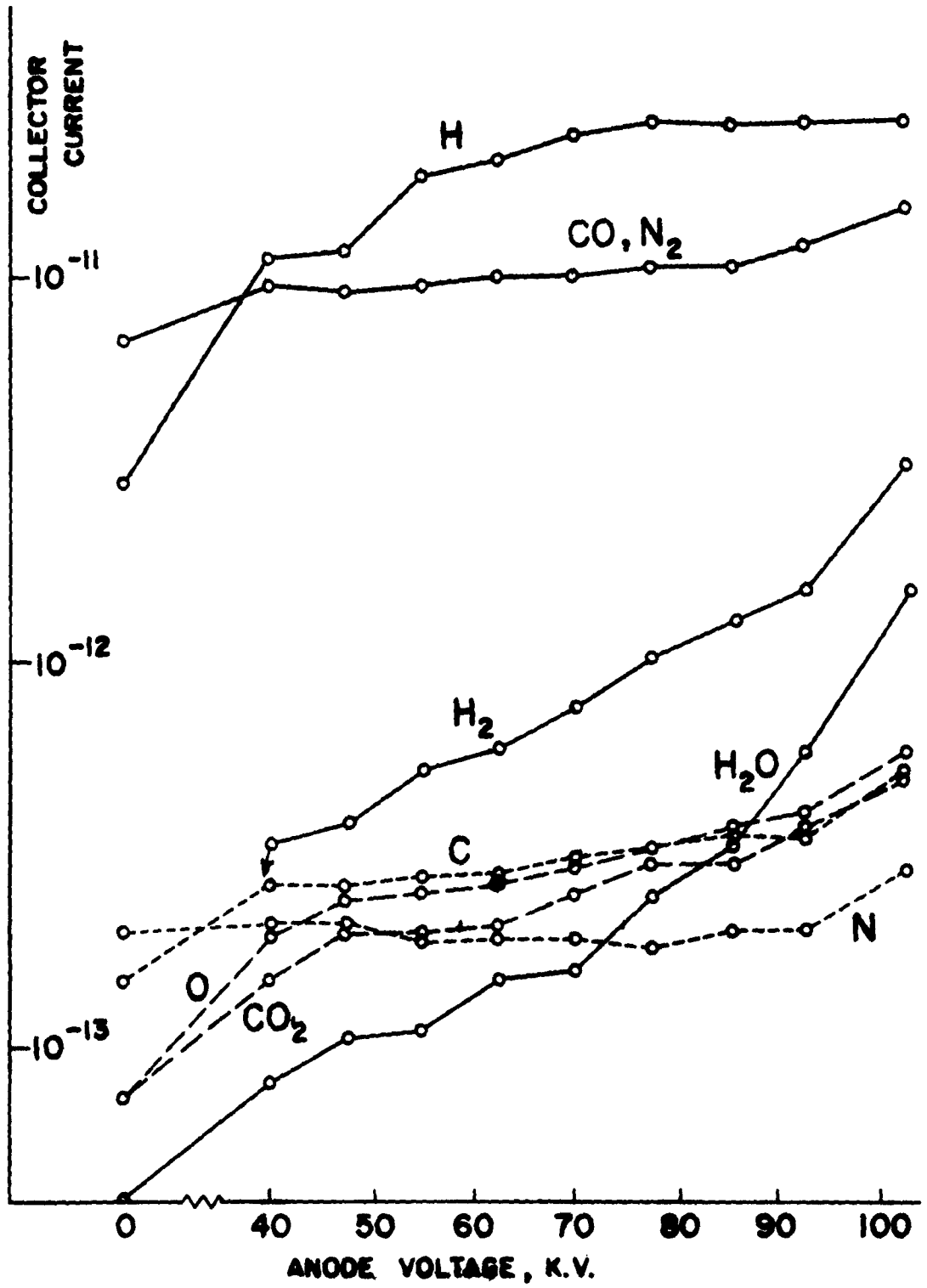

Figure 5. Gases Observed During Processing with 5 Microsecond Pulses at 300 Pulses Per Second.

this stage 5 microsecond pulses were being used at a repetition rate of 300 pulses per second. The tube was operated for 20 to 30 minutes at each voltage shown, so that the curves represent short-time equilibrium conditions.

As may be seen in Figure 5, most of the pressure in the tube is accounted for by gases of mass 1 and 28. The gas of mass 1 is believed to be atomic hydrogen which is actually given off from the tube in atomic form. This must be so, since if it were formed in the electron beam, either by double ionization or by fractionization of molecular hydrogen, there should be a strong correlation between the amount of atomic and of molecular hydrogen. Since large amounts of H_2 were observed at times and were completely independent of the amounts of H, it is concluded that the H is actually present in atomic form. The mass spectrometer reading for H is felt to be more indicative of its true partial pressure than is its pressure read from an ionization gauge. This is because although H and H_2 have very low ionization cross sections, thus giving a low reading on an ionization gauge, this factor is somewhat compensated for, in the RF mass spectrometer by a biasing towards lighter masses because of space charge effects. Further evidence for this is the fact that in certain cases, where the mass spectrometer reading of H was larger than all the other gases together, large variations in the level of the H peak were still accompanied by very little change in the ion gauge pressure.

This partial pressure of atomic hydrogen becomes even more significant when it is recalled that the pumping speed of the orifice,

being inversely proportional to the square root of the mass, is about four or five times as large for H as for the other gases present. The conclusion then is that very large quantities of H are given off by the tube during processing and their presence is due to all parts having been cleaned by hydrogen firing. This hydrogen is then desorbed in atomic form either because of heating up of the parts or directly due to electron bombardment. Since hydrogen is believed to be a good activating agent, this large amount is probably very beneficial to the activation of the cathode and might better be left in the tube.

The mass 28 peak could be due either to molecular nitrogen or to carbon monoxide. In this case, most of the mass 28 peak is apparently CO since N_2 is found to be accompanied by about 10 per cent N due to fractionization, and the amount of N observed is such that less than one fifth of the mass 28 peak can be due to N_2. A simple approach to the determination of the relative amounts of CO and N_2 in a mass 28 peak is to observe the fractionization patterns of both CO and N_2 and then to calculate their abundances from the relative amounts of the atomic species present. Such an approach is not very reliable where the atomic species may come from other sources, however, so that no great accuracy is claimed, and it is safest to use this method only to set an upper limit on the amount of a given component that can be present.

Once the mass 28 peak is acknowledged to be carbon monoxide, a further ambiguity remains as to its source. It is found[10] that hot tungsten filaments, such as those used in the mass spectrometer and ion gauges, convert oxygen to carbon monoxide in varying amounts.

In order to assess the possibility of this being the source of the CO observed here, an experiment was performed in which O_2 was allowed to flow through the mass spectrometer at a known rate. It was found that not only was about 10 per cent of the O_2 converted to CO, but that in addition roughly the same amount of CO_2 was formed. Since the flow rate in the above experiment was 1 litre per second as compared to 0.1 litre per second with the diode, it is concluded that most of the oxygen given off by the diode would be converted, but the comparable amounts of CO and CO_2 should be expected. Since, as can be seen from Figure 5, there is very little CO_2 observed during processing, it is concluded that the mass 28 peak actually does represent CO given off by the diode during processing. A further consideration brought up by these results is that care must be taken in the interpretation of the oxygen peak, i.e., that fact that no O_2 was observed does not conclusively indicate that none was given off. In order to remove these ambiguities definitely, a filament such as an iridium thorium-coated filament which probably does not interact with O_2, should be used in any further work. Further experimental work on the interaction of O_2 with the mass spectrometer is also being undertaken.

The other important feature shown in Figure 5 is the striking increase with voltage in the amounts of molecular hydrogen and of water. It seems unlikely that the water could be present as such on the walls of the tube, since it could not have remained there during bakeout and was not given off during breakdown. Thus it must either be given off by the activation of the cathode or else

formed by catalytic action of the surface of the collector at elevated temperatures. The latter suggests the interesting possibility that CO_2 deposited on the collector during bakeout is converted into CO plus H_2O due to the abundance of H and to the catalytic action of the surface. This has the advantage of accounting for the abundance of CO and H_2O and the lack of CO_2 even though large amounts of CO_2 are also deposited on the walls during bakeout.

C. Sparking

After this short processing, the tube was operated and the initial sparking observed at four different pulse lengths: 5, 10, 15, and about 30 microseconds with current densities up to 2 amp/cm^2. As the pulse lengths were increased this initial "cleaning up" sparking was found to increase in incidence and to occur at lower voltages, as has been observed for the ultimate current-limiting sparking. This supports the assumption that they are basically the same phenomenon. With the 5- and 10-microsecond pulses, there were very few initial sparks, and these were accompanied by very little pressure rise in the tube. The ultimate sparking limit in these cases was beyond the limit of the pulse modulator being used (about 100 kv). With the 15-microsecond pulse, the incidence of initial sparking was much higher and this sparking was accompanied by large amounts of gas. Using this pulse length, the ultimate sparking limitation seemed to be about the same as the limit of the modulator. At the longest pulse length used, the incidence of sparking was still greater than for the 15-microsecond pulse and occurred at lower voltages. The ultimate limitation in this case was at about 70 kv.

In order to determine what gases were given off by these gas bursts it was necessary to set the mass spectrometer at some gas, then cause a gas burst and record the increase in the amount of this gas. This process then had to be repeated for each of the gases present. Then to obtain the spectrum of gases given off, the results of all these different runs had to be compared. This comparison is complicated by several factors: 1) the amounts of gas given off by different gas bursts may vary by a factor of as much as 100, 2) the relative amounts of each gas may change both with the processing of the tube and with the intensity of the gas burst. Furthermore, this variation with processing is one of the factors of great interest in any attempt to improve the sparking limitation. Because of these complications, an attempt is made to obtain a quantitative comparison of the different gases by normalizing the increment of gas given off at each gas burst in Table I. This normalized increment is given by

$$\frac{\text{(peak gas reading)} - \text{(initial gas reading)}}{\text{(peak pressure)} - \text{(initial pressure)}} .$$

Such a normalization was necessary in order to obtain any comparison at all, since the pressure rise varied so much from one gas burst to another. Unfortunately, this method of comparison hides the effect of variations during the life of the tube. This drawback can be rectified by improved instrumentation in later studies.

Several important points are apparent from an examination of Table I: 1) The pressure rise during a gas burst can almost all be attributed to a gas of mass 28, probably carbon monoxide. 2) Atomic hydrogen, although present in the tube in large quantities

Table I.

Averages of Normalized Increments of Gases
Given off by All Gas Bursts Observed

Mass No.	Gas	Normalized Increment
44	CO_2	0
28	CO, N_2	1.20
18	H_2O	0
16	O	0.024
14	CO^{++}, N	0.04
12	C	0.04
2	H_2	0.03
1	H	0

plays no part whatsoever in the gas bursts. 3) Water vapor, which played a striking part in the processing of the tube, is not involved in the sparking. 4) Molecular hydrogen, which also plays an important part in the processing, is given off in moderate quantities by the gas bursts. 5) Carbon, nitrogen, and oxygen are present in amounts of the order of magnitude to be expected from fractionization of CO.

The total amount of CO given off by each gas burst was determined by means of the flow rate meter and was found to vary from less than 0.001 microgram for the mild gas bursts to about 0.1 microgram for the largest gas bursts.

Given that the pressure rise during a gas burst is due to carbon monoxide, it is of importance to determine its origin. The sparking is believed to be caused by a small part of the cathode being volatilized, either by heating or by dielectric breakdown,[3] and this volatilized cathode material ionizing and providing an easy conduction path. This path would presumably end in a very small area on the anode, which might thus be heated very high. Therefore, the gas probably comes both from the area of the cathode at which the spark originates and from the area of the anode at which it ends.

The fact that there is no water vapor or atomic hydrogen given off by the gas bursts can be explained by either of two reasons:

1) These gases originate at the copper beam collector, and hence out of the region in which gas bursts occur.
2) If these gases originate at the cathode or anode, then the point of origin does not contribute to the gas.

Since it seems that both the cathode and anode must contribute to the

gas, the conclusion is that both the atomic hydrogen and water vapor observed during processing originate at the copper collector and are driven off by the electron beam. In order to make a separate check of this, the collector was heated to 70° C without operating. It was observed that, although the pressure rose by only 6 per cent and none of the other gases rose, the amount of atomic hydrogen rose by 50 per cent. As mentioned before, this large difference is due to the fact that the mass spectrometer is much more sensitive to H than is the ion gauge.

If a significant part of the gas actually does come from the cathode, an analysis of its constitution as the condition of the cathode improves through processing should give important information as to exactly what is present in the cathode that enhances sparking. That is, an analysis of the gases given off by gas bursts can be used as a probe to study the condition of the cathode. Unfortunately, the method used in this experiment is not adequate for obtaining much quantitative information beyond the fact that it is quite possibly due to carbon monoxide dissolved in the oxide coating of the cathode or to something that can be released in the form of carbon monoxide, such as BaC and O in the oxide. In order to make a careful study of this, it will be necessary to have a complete mass spectrum during each gas burst and to have the ion gun of the mass spectrometer in line of sight with the cathode. Although a great deal of the variation of the normalized gas increments from the averages given in Table I is probably due to the nonlinearity of the ion current as a function of pressure, which is due both to space charge and mean free path effect, and to in-

accuracies in the technique of observation, there still seems to be some evidence of real variation in the constitution of different gas bursts.

On examining the cathode after completion of the above experiments, a large number of pits due to sparking were observed. These were mostly of the deep type in which the nickel base metal was exposed, and were especially numerous near the center of the cathode. The number of sparking pits per unit area fell off roughly as the distance from the center of the cathode. Due to the beam geometry of the electron gun the ion bombardment of the cathode is the most severe at the center, and falls off towards the edges. Thus, visual inspection of the cathode points to ion bombardment as an important factor in the production of gas bursts. There are two apparent ways in which this ion bombardment may enhance the sparking: 1) The ions deposited in the cathode may cause regions of high resistance or low breakdown strength that are then susceptible to sparking, 2) The heating and secondary emission effects of ion bombardment may be helping to initiate the sparking.

SUGGESTED IMPROVEMENTS IN INSTRUMENTATION

A. Increased Output from Spectrometer

The main practical hindrance in the use of the mass spectrometer at present is the low ion current. This causes difficulty in several respects. The chief difficulty is that in order to measure the low current without expensive vibrating reed electrometers, it is necessary to use large resistances with their accompanying long-time constants, or else to use a large d-c amplification with its accompanying high noise level. This causes the recording of the complete mass spectrum to be a time-consuming process and makes it impossible to monitor more than one gas during each gas burst. As already mentioned, this greatly reduces the information that can be obtained. Another drawback is that with ultra-high vacuum, such as that obtained after the tube has been well-processed, most of the gas readings are down in the noise region so that they cannot be monitored until they rise above the noise level. A third drawback is that the main limitation on the resolution of the mass spectrometer is the necessity of operating at a low enough repeller voltage that a usable ion current is obtained.[5] For these reasons, an improvement in the ion current by several orders of magnitude should be the first step in preparing for further experimental work.

The simplest and also apparently the best way to improve the ion current is by replacing the ion collector of the mass spectrometer by the electron multiplier assembly of a photomultiplier tube. This is rapidly becoming standard procedure in mass spectrometry. For best results this electron multiplier assembly should have beryllium-

copper dynodes so that it can be opened to air without damage and can be baked out to obtain high vacuum. To minimize the photo-noise, it should also be taken from the assembly line before mounting of the light-sensitive dynode, rather than merely having this dynode taken off. Glass-encased ceramic resistors capable of withstanding bakeout can be obtained for use as voltage dividers so that the whole assembly can be prepared as a unit and mounted in place of the ion collector on a spectrometer similar to that already in use. This should result in an ion current increased by a factor of $(10)^6$ and permit operation at a much higher repeller voltage with a corresponding improvement in resolution by an order of magnitude.

B. Sweep Provision on Mass Spectrometer

With the larger ion current available it will be possible to sweep the frequency of the mass spectrometer, amplify the ion current with an ordinary low-noise a-c amplifier, and observe the mass spectrum directly on an oscilloscope. The r-f oscillator used is a General Radio unit oscillator for which a voltage regulator and four-cycle-per-second sweep drive are available so that this provision can be readily added to the present setup.

The fast sweep, combined with the improved resolution will facilitate the taking of data at all stages of tube operation. It will be possible to monitor the gases given off during breakdown, even using the fastest breakdown schedules, in order to determine the best breakdown schedule. During processing it will be easier to monitor the gases given off, thus following the process more closely. The main improvement will be in obtaining gas burst data. Since a

complete and well-resolved spectrum will be obtained at each gas burst, the amounts of each gas given off will be absolutely determined, and it will be possible to study them as a function of the various parameters of interest.

C. Other Improvements

Some other changes in the system that will significantly improve the data obtained are as follows.

1. The ion gun of the mass spectrometer should be in a line of sight with the cathode and anode of the experimental diode in order to observe the nongaseous substances given off by breakdown and gas bursts.

2. The tungsten filament of the mass spectrometer should be replaced by a iridium thorium-coated one in order to eliminate the possibility that oxygen is being converted to carbon monoxide by it.

3. In order to extend the study to longer pulses and higher currents, it will be necessary to replace the diode used here by an experimental one having a higher perveance and hence capable of being operated directly from the modulator without the use of a pulse transformer.

4. Some of the gases observed may have been due to broken down oil from the diffusion pump, even though a charcoal trap was used. Oil poisoning may also introduce another unknown effect on the cathode. Therefore, either a mercury diffusion pump or an ion pump should be used.

The constriction in the vacuum line is necessary only in determining the amount of gas passing through over a long period

of time. For short bursts of gas the amount can be calculated from the volume of the tube and the pressure rise. Elimination of this constriction will result in a much better pumping speed and especially will allow the use of a faster cathode breakdown.

CONCLUSIONS AND RECOMMENDATIONS

It has been observed that during cathode breakdown the main gases given off are carbon monoxide and carbon dioxide, in varying quantities. Although at first glance one would expect only carbon dioxide according to the reaction $BaCO_3 \longrightarrow BaO + CO_2$, the actual situation in breakdown is a much more complicated reaction in which the chemical kinetics are determined by partial pressures of the various gases and by temperature. Therefore it is concluded that the relative amounts of gases given off, and hence the residues left behind in the cathode may be varied according to the breakdown schedule used.

Four gases were found to play an important part in the processing of the tube: atomic hydrogen, molecular hydrogen, water vapor, and carbon monoxide. From the fact that two of these gases, atomic hydrogen and water vapor are not given off at all by gas bursts, it is concluded that they must originate at the only other part of the tube that can be affected by processing, the beam collector. From the fact that although a great deal of CO_2 was given off by cathode breakdown, but not by processing, it is concluded that this gas when adsorbed on the walls is then converted to CO before being driven off, possibly by the reaction $CO_2 + 2H \longrightarrow CO + H_2O$ which may be catalyzed by the copper surface of the collector under action of the electron beam. In addition to this origin, the CO observed is probably also being given off by the cathode and anode during processing. The H_2 observed must come from the cathode or the anode, and in large quantities although it is difficult to understand why it is given off in molecular

rather than atomic form or why the two forms come from distinctly different sources.

It was found that the pressure rise in the tube during sparking was due almost entirely to carbon monoxide and its fragmentation products, the only other gas given off being molecular hydrogen. Therefore the tentative conclusion is that the areas of high resistance in the cathode which cause sparking are due to some condition with which CO is intimately involved. Examples of such a condition may be either areas with a great deal of CO dissolved in the oxide or areas of high concentration of BaC and excess oxygen. The amount of CO given off by each gas burst varied from a minimum of 0.001 microgram to a maximum of more than 0.1 microgram depending on the intensity of the gas burst.

In order to confirm this conclusion it will be necessary to determine the following: 1) whether at least enough of the gas does come from the cathode that this is indicative of the condition of the cathode, and 2) assuming that a considerable amount of the CO does actually come from the cathode, whether it is a residue from the breakdown or back poisoning from the anode.

It will be possible to determine how much of the gas observed during sparking originates at the cathode by repeating the experiment using a special diode with a "false anode" arrangement. By using a false anode to shield the true anode during breakdown and especially by making the true anode of tungsten with provision for flash cleaning, it will be certain that all gases given off originate at the cathode.

The false anode experiment can also be used to determine whether the carbon monoxide is present in the cathode as a residue

of breakdown or from back poisoning from the anode. By operating the tube a while using the contaminated anode and then causing gas bursts using the clean anode and comparing the gases given off with those given off before, when the tube was operated only with the clean anode, the extent of back poisoning can be measured.

It is proposed that, once it has definitely been established what part of the gas given off by gas bursts comes from the cathode, the observation of these gases during the initial sparking, when the contamination is mostly due to residue from breakdown, can be used to determine to what extent the breakdown is complete. Then, comparing this result with the gases observed during breakdown, the best breakdown schedule can be determined. Of special interest will be the matter of whether the amounts of C, CO^{++}, N, and O are in proportion to have come from fractionization of the CO or whether an excess of one of them is indicated. This should provide more specific information about the form in which the CO is present in the cathode.

The fact that the main gas involved in the gas bursts was also the main gas given off by cathode breakdown and thus absorbed on the walls of the tube, points to back poisoning as an important factor. Thus the findings of this experiment tend to support the importance of work being done to eliminate this back poisoning.

Visual inspection of the cathode indicates that ion bombardment is an important factor in the production of gas bursts. This ion bombardment may act either by ionic deposition of poisoning agents in the cathode coating or by initiating the gas burst itself. Further studies of the effect of ion bombardment are indicated.

REFERENCES

1. E. A. Coomes, "The Pulsed Properties of Oxide Cathodes," J. Ap. Physics, 17, (1946), p. 647.

2. J. B. Fisk, H. D. Hagstrum, P. L. Hartmann, "The Magnetron as a Generator of Centimeter Waves," Bell Syst. Tech. Jour., 25, (1946), p. 342.

3. W. E. Danforth and D. L. Goldwater, "Resistance of Oxide Cathode Coatings for High Values of Pulsed Emissions," J. Ap. Physics, 20, (1949), p. 163.

4. P. A. Redhead, "A Linear Radio-Frequency Mass Spectrometer," Can. J. Physics, 30, (1952), p. 1.

5. A. S. Gilmour, Jr., "A Study of the Limitations of the Radio-Frequency Mass Spectrometer," Res. Rep. EE 424, Cornell Univ., May 1959.

6. S. Dushmann, Scientific Foundations of Vacuum Technique, New York: John Wiley, 1949.

7. N. Morgulis and J. Pikus, "Application of the Mass Spectrometer for the Study of the Process of Activation of an Oxide Cathode," J. Tech. Physics, 26, (1956), p. 1174.

8. P. F. Varadi, "H. F. - Massenspektrometer und Seine Anwendung in der Vakuumtechnik," Telefunken Z., Report 57/3, 17 May 1957.

9. P. M. Stier, "A Mass Spectrometric Study of the Activation of Barium Oxide Cathodes," Unpublished Ph. D. Thesis, Cornell Univ., 1952.

10. R. E. Schlier, "Absorption of Oxygen and Carbon Monoxide on Tungsten," Jour. Ap. Physics, 29, (1958), pp. 1162.